



Automated Evaluation of One-Loop Six-Point Processes
for the LHC

Thomas Reiter

15 September 2008

Submitted in satisfaction of the requirements
for the degree of Doctor of Philosophy
in the University of Edinburgh
2008.

Declaration

I declare that this thesis has been composed by myself and that the work presented is my own. This work has not been submitted for any other degree or professional qualification.

Edinburgh, 15 September 2008

Abstract

In the very near future the first data from LHC will be available. The searches for the Higgs boson and for new physics will require precise predictions both for the signal and the background processes. Tree level calculations typically suffer from large renormalization scale uncertainties. I present an efficient implementation of an algorithm for the automated, Feynman diagram based calculation of one-loop corrections to processes with many external particles. This algorithm has been successfully applied to compute the virtual corrections of the process $u\bar{u} \rightarrow b\bar{b}b\bar{b}$ in massless QCD and can easily be adapted for other processes which are required for the LHC.

Contents

Declaration	iii
Abstract	v
Introduction	1
Chapter 1. Principles of QCD	9
Introduction	9
1. The LAGRANGIAN Density of QCD	9
2. The Effective Coupling and Asymptotic Freedom	12
3. Flavour Symmetry	13
Chapter 2. Representations of QCD Amplitudes	17
Introduction	17
1. Colour-Flow Decomposition	18
2. Irreducible Representations of $SU(N)$	27
3. The Spinor Helicity Projection Method	44
Chapter 3. QCD at One-Loop Precision	55
Introduction	55
1. QCD in Dimensional Regularisation	56
2. Reduction of the Scalar Integrals	66
3. Tensor Reduction by Subtraction	76
4. Representation of the Virtual Corrections	84
5. Renormalisation of Quantum Chromodynamics (QCD)	86
6. Real Emission Contribution	89
7. Dipole Subtraction	95
8. Phase Space Integration and Monte-Carlo Techniques	106
Chapter 4. Virtual NLO Corrections for $u\bar{u} \rightarrow b\bar{b}b\bar{b}$	113
Introduction	113
1. Performance and Accuracy	114
2. Exclusive Observables	117
Chapter 5. Conclusion	121
1. Summary	121
2. Outlook	122
Appendix A. Distributions	123
Introduction	123
1. The δ - Distribution	123
2. The Plus Distribution	124
Appendix B. The MOORE-PENROSE Inverse	125

Appendix C. Loop Integrals	127
1. Mathematical Prerequisites	127
2. An Axiomatic Approach	132
3. Evaluation of Loop Integrals	134
Appendix D. Integral Tables	137
1. Conventions	137
2. Relations for One- and Two-Point Functions	138
3. Massless Two- and Three-Point Integrals	139
4. Polynomial Loop Integrals	140
Appendix E. Implementation of Amplitude Computations	143
Introduction	143
1. Overview	153
2. Diagram Generation	156
3. Automatic Code Generation	159
4. Translation of Tensor Integrals into Form Factors	163
5. Algebraic Simplification	168
6. Numerical Evaluation	199
7. Index of Literate Programs	206
Acronyms	211
Bibliography	213
Acknowledgements	221
Index	223

Introduction

Awaiting the first results from the Large Hadron Collider (LHC), the current problems in particle physics, through the eyes of a broader public, are very often reduced to a single particle that is missing for the Standard Model (SM) to be consistent: the HIGGS boson. Although the physics programme of the LHC is much richer, the discovery of the HIGGS boson — or its exclusion — is one of the main physics motivations having lead to the construction of the LHC. In 1997, when the predecessor experiment LEP was still running¹, the main goals of the LHC were described as follows [**Wom**]:

The fundamental goal is to uncover and explore the physics behind electroweak symmetry breaking. This involves the following specific challenges:

- *Discover or exclude the Standard Model Higgs and/or the multiple Higgses of supersymmetry.*
- *Discover or exclude supersymmetry over the entire theoretically allowed mass range.*
- *Discover or exclude new dynamics at the electroweak scale.*

The HIGGS boson gives mass to the fermions and is responsible for electroweak symmetry breaking in the Standard Model (SM), which to our current understanding describes the physics of the smallest constituents of matter in terms of a LORENTZ invariant quantum field theory. Interactions are mediated through gauge fields of the group structure $SU(3)_C \times SU(2)_L \times U(1)$, which describe the strong, the weak and the electro-magnetic force².

The interactions resulting from the $SU(2)_L \times U(1)$ gauge symmetry describe the *Electroweak Standard Model* [**Gla61**, **Sal**, **Wei67**]. Since left-handed and right-handed fermions couple differently under the $SU(2)_L$ interaction, a mass-term for the fermions is forbidden. Furthermore, the observation of massive gauge bosons in the SM, i.e. the W^\pm and Z bosons³, requires that this symmetry group is broken. In 1964 HIGGS [**Hig64b**, **Hig64a**, **Hig66**] and independently BROUT and ENGLERT [**EB64**] introduced a mechanism for mass generation through spontaneous symmetry breaking. The model starts from a LAGRANGIAN density without fermion and gauge boson masses and introduces

¹In 1997 there were two particles missing in the SM, the HIGGS boson and the ν_τ . The latter one was found in 2000 [**DONUT01**].

²Gravitation, the fourth interaction is not included in the Standard Model. Compared to the coupling strengths of the other three interactions gravitation is very weak and therefore can be neglected for the concerns of collider physics at an energy scale of $\mathcal{O}(1 \text{ TeV})$

³see e.g. [**Eid04**]

a complex scalar SU(2) doublet Φ ,

$$(1) \quad \Phi = \begin{pmatrix} \Phi^+ \\ \Phi^0 \end{pmatrix}.$$

In addition to the LAGRANGIAN density of the pure gauge theory one has interactions between the HIGGS doublet and the SU(2) gauge fields through a covariant derivative, YUKAWA type interactions between the fermions and the scalar doublet, and the HIGGS potential

$$(2) \quad \mathcal{V}(\Phi) = -\mu^2 |\Phi|^2 + \lambda (|\Phi|^2)^2.$$

The crucial point here is the negative quadratic term $-\mu^2 |\Phi|^2$: the potential develops a minimum away from $|\Phi| = 0$ but for a non-vanishing vacuum expectation value

$$(3) \quad |\Phi| = \frac{v}{\sqrt{2}} = \sqrt{\frac{\mu^2}{2\lambda}}.$$

Rotational symmetry allows one to write the scalar doublet as

$$(4) \quad \Phi = \frac{1}{\sqrt{2}} e^{i\vec{T} \cdot \vec{\xi}/v} \begin{pmatrix} 0 \\ H + v \end{pmatrix},$$

requiring a perturbative expansion around the true minimum for the fields H and $\vec{\xi}$ to obtain the physical degrees of freedom. It turns out that the scalars in $\vec{\xi}$ are absorbed by the longitudinal modes of the (former massless, now massive) gauge bosons, and the HIGGS boson acquires a mass $M_H = \sqrt{2\lambda}v$. The fermion masses on the other hand are generated through the YUKAWA interactions and are of the form $m_f = g_f v / \sqrt{2}$, where g_f is the YUKAWA coupling constant of the considered fermion.⁴ This implies that within the SM one expects the HIGGS boson to couple predominantly to heavy particles.

The SU(3)_C gauge group gives rise to the strong interaction that binds the partons inside the nucleons; because the charge of the strong force is called *colour* [**FGML73**] the theory usually is referred to as Quantum Chromodynamics (QCD).

The SM to date has endured all experimental tests without showing significant deviations between the SM predictions and the experimental data [(**PDG08**), (**LHWG03**), (**ALEPH06**)] as can be seen from Figure 1 (a). It shows the results of a simultaneous fit of 18 observables to the SM predictions. The bar charts indicate the deviation of the fitted value from the measurement of the observable, weighted by the experimental uncertainty σ^{meas} ; all values are within a 3σ interval demonstrating the consistency of the SM.

Although direct evidence is still missing for a SM HIGGS boson, the precision of the LEP experiments allows not only to constrain the range for the HIGGS mass from below⁵ but also from above, one reason being the influence of the presence of HIGGS particles on the decay width of the Z boson. Figure 1 (b) shows the so-called *blue-band plot*, a fit of the HIGGS boson mass obtained from 18 input parameters. The LEP II experiment excluded the mass range of $M_H < 114.4 \text{ GeV}$ for a SM HIGGS boson at 95% CL [(**LHWG03**)]. The combined fit in [**ALEPH06**] yields an upper bound on the HIGGS boson mass of $M_H < 285 \text{ GeV}$ at 95% CL on $\log_{10}(M_H/1 \text{ GeV})$.

⁴See for example [**ESW96**, **BDJ01a**, **DGH94**, **BP99**].

⁵through lack of observation

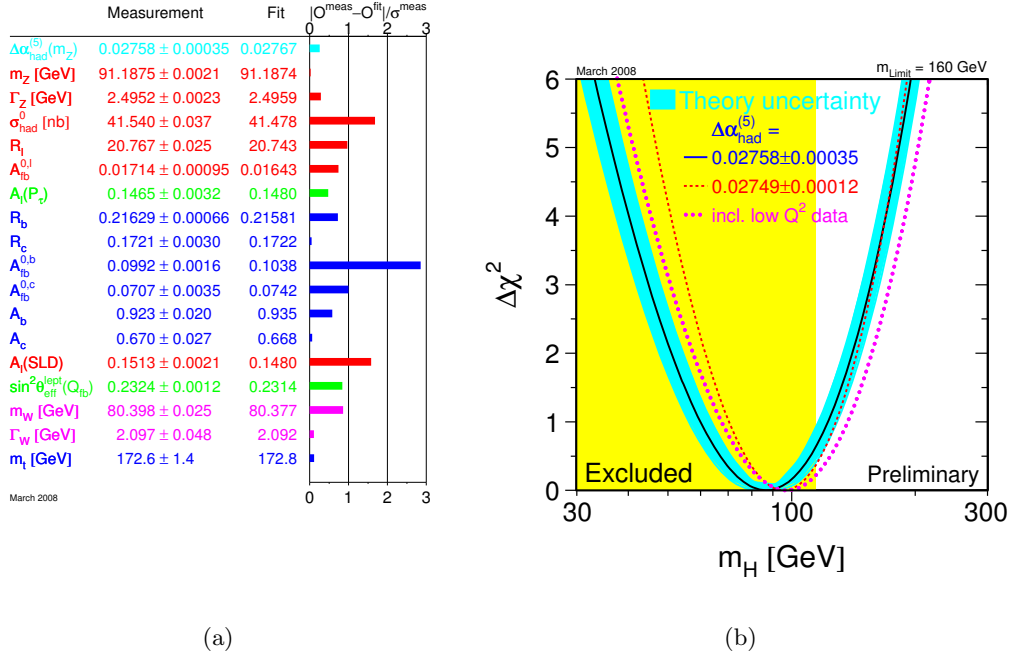


Figure 1: Results from the analysis of electro-weak precision data as of March 2008 [(LHWG)03, ALEPH06, EWW]. Left: global fit of 18 SM observables. Right: the current best fit for the mass of a SM HIGGS boson. The yellow area is experimentally excluded. Combined analysis of precision measurements predict a light SM HIGGS boson.

Figure 2 demonstrates that the at the LHC one will be able to claim a HIGGS discovery over the entire mass range that is allowed in the SM or to rule out the SM if no HIGGS particle is found. The LHC therefore will probe if the SM describes elementary particle physics at the energy scale of electro-weak symmetry breaking. However, one of the design goals of the LHC is also to be sensitive to new physics — Beyond Standard Model (BSM) physics — if it leaves signatures in the energy range below $O(10 \text{ TeV})$.

Despite its big success the SM can only be the low energy effective theory of another, more fundamental theory. The most obvious reason why the SM cannot be a fundamental theory is the fact that it does not incorporate gravity. Currently no renormalisable description of gravity as a gauge theory is known and the most promising approaches are based on local supersymmetry as an extension of the LORENTZ symmetry. Another issue which is not addressed by the SM is dark matter: the amount of matter in the universe predicted by cosmological observations cannot be explained by the amount of baryonic matter, neither can any of the lighter SM particles account for the matter content of the universe. Therefore the existence of new particles beyond the SM is well motivated and indicated experimentally [BHS05, WMAP03].

Other indications for the incompleteness of the SM are concerned with a certain lack of explanation rather than direct experimental motivation. The SM does not explain the hierarchy of masses and mixing angles, nor the presence of three generations, nor

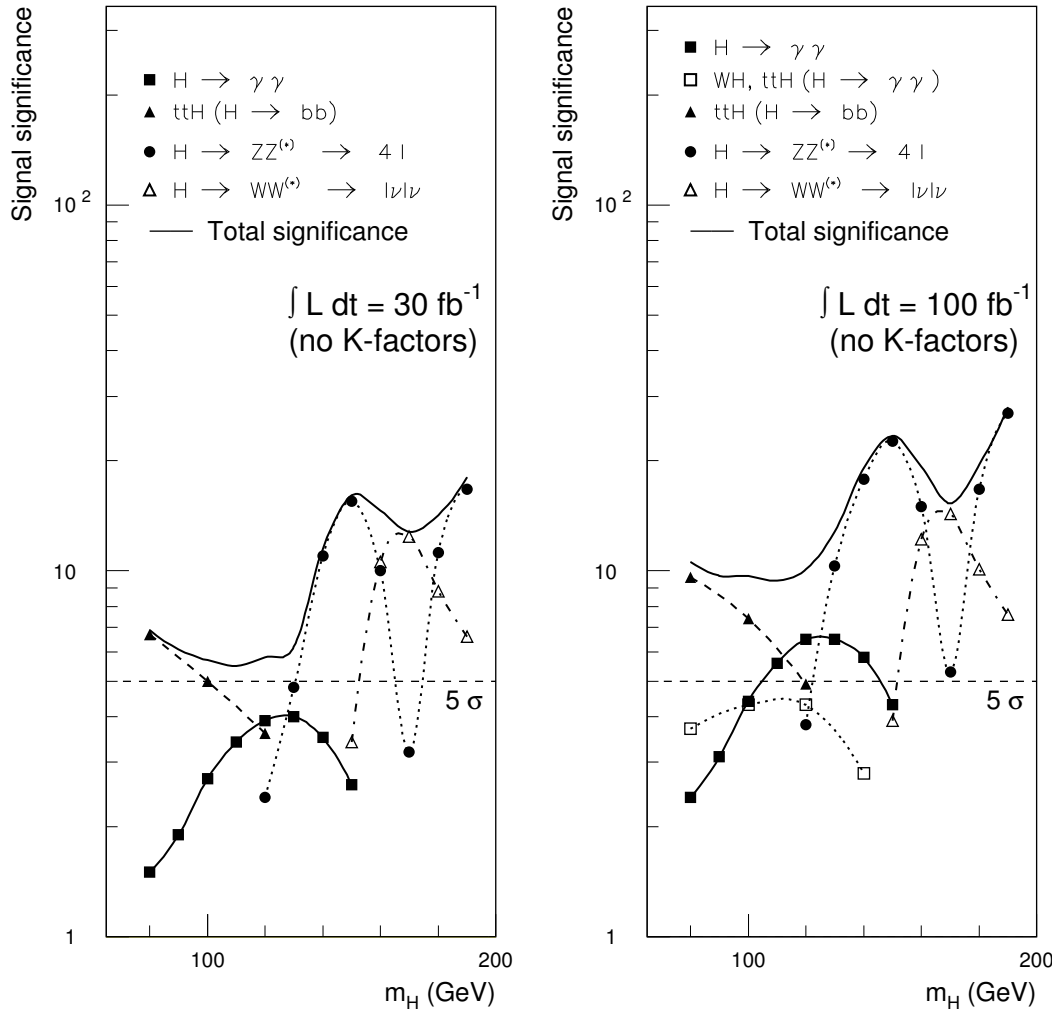


Figure 2: Sensitivity of the ATLAS experiment to the discovery of a SM HIGGS boson for an intermediate mass range for integrated luminosities of 30 fb^{-1} (left) and 100 fb^{-1} . The plots show S/\sqrt{B} where S is the number of signal events and B is the number of background events. [ATL]

the protection of the HIGGS mass from large radiative corrections, to name only a few. [Moh02]

The LHC will be able to explore energies of order 10 TeV, which is the energy range new physics is expected to set in for the above reasons. Therefore the investigation of different new physics models, their experimental signatures and their SM backgrounds is well motivated. One of the BSM candidates is a *supersymmetric* extension of the SM. The simplest of these models consistent with the current experimental data is the Minimal Supersymmetric Standard Model (MSSM)⁶. For each particle of the SM it introduces a corresponding super-partner, thus promoting each field to a super-field. To maintain holomorphy of the super-potential and in order to guarantee that the theory is free of anomalies one introduces a second HIGGS doublet, one coupling to the up-type

⁶See for example [Moh02]

quarks and the second doublet coupling to the down-type quarks. Since pure supersymmetry predicts equal masses for SM particles and their supersymmetric partners it cannot be an exact symmetry in nature but has to be broken by some mechanism, introducing a mass hierarchy between the new particles. In order to conform with the current bounds on the proton life time, usually only R -parity conserving models are considered, where R -parity of a particle can be defined as $R = (-1)^{2j+L+3B}$, j being its spin, L its lepton number and B its baryon number. The conservation of R -parity ensures that supersymmetric partners of the SM particles are always pair-produced and that the Lightest Supersymmetric Particle (LSP) is stable.

Although in the MSSM the HIGGS sector is richer than in the SM one usually obtains stronger bounds on the lightest HIGGS mass, which will be shown in this paragraph. The two HIGGS doublets, Φ_u and Φ_d , manifest themselves after symmetry breaking in five physical states: two \mathcal{CP} -even, neutral scalar bosons H^0 and h^0 with masses $M_{H^0} > M_{h^0}$, a \mathcal{CP} -odd scalar field A^0 , and two charged states H^\pm . The ratio of the vacuum expectation values of the two doublets is called $\tan \beta$,

$$(5) \quad \tan \beta = \frac{|\langle \Phi_d \rangle|}{|\langle \Phi_u \rangle|}.$$

At tree-level the mass spectrum of the HIGGS sector is described completely by the gauge boson masses m_Z and m_W , $\tan \beta$ and the mass of the \mathcal{CP} -odd scalar, m_{A^0} ,

$$(6a) \quad m_{H^\pm}^2 = m_{A^0}^2 + m_W^2,$$

$$(6b) \quad 2m_{H^0, h^0}^2 = m_{A^0}^2 + m_Z^2 \pm \sqrt{(m_{A^0}^2 + m_Z^2)^2 - 4m_Z^2 m_{A^0}^2 \cos^2 2\beta}.$$

The tree-level results imply that $M_{h^0} < M_Z$, a constraint which would have ruled out the MSSM already by the LEP experiment. However, radiative corrections to the masses are significant and have to be taken into account [Hab97] and in the one-loop leading logarithmic approximation one obtains the weaker bound [HH91, OYY91]

$$(7) \quad m_{h^0}^2 \lesssim m_Z^2 \cos^2 \beta + \frac{3g^2 m_t^4}{8\pi^2 m_W^2} \ln \left(\frac{M_{\tilde{t}_1} M_{\tilde{t}_2}}{m_t^2} \right)$$

with $M_{\tilde{t}_{1/2}}$ being the masses of the top-squark mass eigenstates. This implies that for a supersymmetry breaking scale at around 1 TeV one expects to find the lightest HIGGS boson to have a mass below 150 GeV [ADK⁺04, Djo08].

For large values of $\tan \beta$ the $H^0 b\bar{b}$ coupling is enhanced and one expects HIGGS signals predominantly in b -associated channels [RWF97, DGV95, DGV96]; therefore it is not surprising that “*at large $\tan \beta$ the $b\bar{b}\tau^+\tau^-$ and $b\bar{b}b\bar{b}$ final states may provide the only access to two of the three neutral MSSM HIGGS bosons.*” [DGV95].

Figure 3 shows the parameter regions in the $(M_{A^0}, \tan \beta)$ plane for which a 5σ discovery is possible at the LHC after both the experiments ATLAS and CMS have collected 30 fb^{-1} integrated luminosity, analysing events with three and four tagged b -jets in the final state [DGV96]⁷. In [DGV95] the lack of a full background study at Next to Leading Order (NLO) is accounted for by the use of a global K -factor of 2 which compromises the significance of the study, and hence the authors argue that “*explicit calculations of the actual K factors are needed*”. Also in SM studies for the LHC, missing higher order corrections to background processes are often limiting the precision

⁷ Further detailed studies of discovering MSSM HIGGS bosons in the $b\bar{b}b\bar{b}$ final state can for example be found in [D⁺00, Mah01].

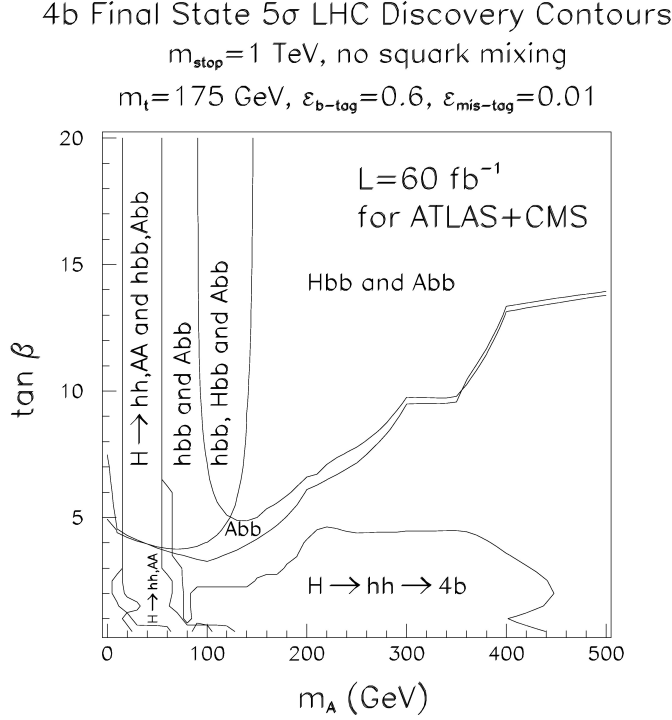


Figure 3: 5 σ discovery contours in the $(M_{A^0}, \tan \beta)$ parameter plane for the channels $gg \rightarrow b\bar{b}H \rightarrow b\bar{b}b\bar{b}$ ($H \in \{h^0, H^0, A^0\}$) and $gg \rightarrow H^0 \rightarrow (h^0 h^0)/(A^0 A^0) \rightarrow b\bar{b}b\bar{b}$ for an integrated luminosity of 30 fb $^{-1}$ for ATLAS and CMS individually, combining their statistic. [DGV96]

with which the measurements can be evaluated. The ATLAS sensitivity study for the discovery of a HIGGS boson (see Figure 2), for example, does not include higher order corrections for “these K -factors are generally not known for most background processes.” [ATL]

At hadron-hadron colliders such as the LHC providing a purely partonic initial state one expects most of the dynamics to be due to the strong interaction. Renormalisation introduces an unphysical scale μ_R which would drop out if all orders of the perturbative expansion were summed up. Realistically one computes cross-sections only to a fixed order in perturbation theory, which leaves a residual dependence on μ_R . The prediction only stabilises as higher-order corrections are added to the Leading Order (LO) result [ESW96]. The precision with which the LHC will measure the events requires the prediction of both signal and background processes to at least Next to Leading Order (NLO) in the strong coupling constant α_s for processes with up to four particles in the final state [(NLO/ML)08, ESW96, ATL, DKP02] — a limit dictated by what is computable with current techniques and technology rather than desired from an experimental point of view [B⁺06]. A list of processes which are well motivated for LHC phenomenology and seem computationally within reach has been compiled at the *Les Houches* conferences on *Physics at TeV Colliders* in recent years [B⁺06, (NLO/ML)08].

Although many important calculations have been accomplished in recent years⁸, there are still few $2 \rightarrow 4$ processes to be calculated which are crucial for HIGGS and BSM studies at the LHC [(NLO/ML)08], and the first years of the LHC's run time will probably lead to new requirements of precision predictions. The high demand for NLO calculations for the LHC induces the need for automated tools for the calculation cross-sections and other observables at the one-loop order.

This thesis presents an algorithm that automates the generation of the virtual corrections to NLO matrix elements. The current implementation is capable of generating Fortran90 code for the numerical evaluation of massless QCD amplitudes⁹.

As an application the $q\bar{q} \rightarrow b\bar{b}b\bar{b}$ amplitude at NLO in α_s has been calculated, which is part of the SM background to the $b\bar{b}b\bar{b}$ channels in MSSM HIGGS searches. Although mainly motivated by supersymmetry, the four- b final state also allows the study of other interesting BSM physics models such as hidden valley models, where decays of hadrons of an additional confining gauge group can produce high multiplicities of $b\bar{b}$ pairs [Kro08, (NLO/ML)08].

In Chapter 1 I introduce QCD with its LAGRANGIAN density and FEYNMAN rules. Chapter 2 describes the structure of QCD amplitudes and techniques for treating the colour algebra. Methods for calculating amplitudes at one-loop precision are discussed in Chapter 3. Results for the computation of the virtual corrections of the process $u\bar{u} \rightarrow b\bar{b}b\bar{b}$ are presented in Chapter 4. A more technical discussion of the underlying implementation that has been used for this calculation is attached in Appendix E.

⁸See [DKU08, CKEZ07, SK08, CEZ06, BDDP08, CDD08, CDD07, LMP07, HZ08, JOZ06a, JOZ06b, BJOZ07]

⁹The extension of the implementation to massive amplitudes is in preparation but beyond the scope of this thesis.

CHAPTER 1

Principles of QCD

The beauty of the basic laws of natural science, as revealed in the study of particles and of the cosmos, is allied to the liteness of a merganser diving in a pure Swedish lake, or the grace of a dolphin leaving shining trails at night in the Gulf of California, or the loveliness of the ladies assembled at this banquet. — MURRAY GELL-MANN

Introduction

Quantum Chromodynamics (QCD) is the non-ABELian gauge theory of the SU(3) group. Within the SM it describes the strong interaction. The aim of this thesis is the development of methods to calculate QCD amplitudes and to present results of one example calculation. The LAGRANGIAN density of QCD is introduced in Section 1 setting up the framework for the rest of this thesis. The FEYNMAN rules induced by the LAGRANGIAN density build one of the fundamental tools in our calculation. Section 2 describes in short *asymptotic freedom*: QCD, at low energies, is strongly coupled. The coupling strength only decreases for energy scales larger than about 1 GeV which justifies a perturbative expansion of QCD to be used as a description of a hard collision of partons in a hadron-hadron collider.

As a last general aspect the *flavour symmetry* of QCD is discussed in Section 3. The interactions of QCD do not distinguish between quark flavours which induces an additional, discrete symmetry to this theory. We exploit flavour symmetry in our calculation as it allows to reduce the number of different FEYNMAN diagrams to be calculated.

1. The Lagrangian Density of QCD

Throughout this document I follow the convention for the metric tensor¹

$$g^{\mu\nu} = \text{diag}(1, -1, -1, -1),$$

the LEVI-CIVITA tensor with $\epsilon_{0123} = +1$ and the DIRAC γ -matrices obey the anticommutation relation

$$(8) \quad \{\gamma^\mu, \gamma^\nu\} \equiv \gamma^\mu \gamma^\nu + \gamma^\nu \gamma^\mu = 2g^{\mu\nu}.$$

¹The extension to $n \neq 4$ dimensions is described separately in Section 1, Chapter 3.

Contractions of DIRAC matrices with LORENTZ vectors are denoted by the FEYNMAN-slash, $\not{p} \equiv \gamma^\mu p_\mu$. Summation over repeated indices is understood unless explicitly noted differently. This summation convention is applied not only to LORENTZ indices but also to Special Unitary Group (SU(N)) colour indices. The indices of the representation of the Dirac algebra are omitted where no ambiguities are possible. I work in natural units², $\hbar = c = 1$.

Historically, the concept of colour was introduced in the quark model to satisfy DIRAC statistics for hadrons with three identical quarks; the colour symmetry was a global SU(3) gauge symmetry. It was a real breakthrough in the success of the quark model when two main observations, confinement and asymptotic freedom, could be described by the gauge theory of a local SU(3) colour symmetry, i.e. Quantum Chromodynamics (QCD)³. QCD is a strongly coupled theory which in principle requires non-perturbative methods. Here, lattice QCD plays the most important role allowing the precise determination of the properties of QCD bound states.

Due to the running of the coupling constant for very high energies the coupling constant of QCD becomes small and a perturbative expansion becomes meaningful. Perturbative QCD therefore can be used as a predictive tool for collider experiments and is the main focus of this work.

The LAGRANGIAN density \mathcal{L}_{QCD} of QCD can be split into three parts: the classical density \mathcal{L}_{cl} , the gauge fixing term \mathcal{L}_{gf} and the ghost term \mathcal{L}_{gh} ,

$$(9) \quad \mathcal{L}_{\text{QCD}} = \mathcal{L}_{\text{cl}} + \mathcal{L}_{\text{gf}} + \mathcal{L}_{\text{gh}}.$$

The classical LAGRANGIAN density of a non-ABELIAN gauge theory coupled to fermionic matter reads

$$(10) \quad \mathcal{L}_{\text{cl}} = -\frac{1}{4}F_{\mu\nu}^A F^{\mu\nu,A} + \sum_{q \in \text{flav.}} \bar{q}_a (i\not{D}_{ab} - m_q \delta_{ab}) q_b.$$

The fermion fields are denoted by q_a , where the sum over the quark fields q runs over all different flavours (u , d , s , c , b and t) and m_q stands for the mass of a quark of the respective flavour. The field strength tensor $F_{\mu\nu}^A$ for the gluon field \mathcal{A}_μ^A is

$$(11) \quad F_{\mu\nu}^A = \partial_\mu \mathcal{A}_\nu^A - \partial_\nu \mathcal{A}_\mu^A - g_s f^{ABC} \mathcal{A}_\mu^B \mathcal{A}_\nu^C,$$

where g_s is the strong coupling constant and f^{ABC} is the structure constant of the gauge group. Capital Latin letters denote indices over the adjoint representation of the gauge group and lower case letters stand for indices in the fundamental representation. The properties of the colour algebra are described in detail in Chapter 2, Sections 1 and 2. I also use the symbol

$$(12) \quad \alpha_s = \frac{g_s^2}{4\pi}.$$

The covariant derivative has the form

$$(13a) \quad \mathcal{D}_{ab}^\mu = \partial^\mu \delta_{ab} + i g_s \mathcal{A}^{\mu,C} t_{ab}^C \quad \text{in the fundamental, and}$$

$$(13b) \quad \mathcal{D}_{AB}^\mu = \partial^\mu \delta_{AB} + i g_s \mathcal{A}^{\mu,C} T_{AB}^C \quad \text{in the adjoint representation,}$$

²This leads to the usual conversion factors $\hbar/1 \text{ GeV} \approx 6.58212 \cdot 10^{-25} \text{ s}$ and $\hbar c/1 \text{ GeV} \approx 1.97327 \cdot 10^{-16} \text{ m}$; the units for cross-sections therefore are $1 \text{ mb} \approx 2.56819 (\hbar c)^2/1 \text{ GeV}^2$.

³See for example [ESW96]

where t_{ab}^A (T_{AB}^C) are the generators of the fundamental (adjoint) representation of the gauge group.

Again following [ESW96], I describe two different families of gauge fixing terms. A covariant gauge fixing term is provided by

$$(14) \quad \mathcal{L}_{\text{gf}} = -\frac{1}{2\lambda} (\partial^\mu \mathcal{A}_\mu^A) (\partial^\nu \mathcal{A}_\nu^A)$$

with the gauge parameter λ . This approach requires the introduction of a ghost field via

$$(15) \quad \mathcal{L}_{\text{gh}} = (\partial_\mu \eta^A)^\dagger (\mathcal{D}_{AB}^\mu \eta^B)$$

to remove the remaining unphysical degree of freedom. The ghost field is a complex scalar field obeying fermionic statistics. Diagrams with external ghost fields can be avoided by an appropriate choice of the gluon polarisation vectors.

A second class of gauge fixing terms are the axial gauges, which involve an arbitrary four-vector q ,

$$(16) \quad \mathcal{L}_{\text{gf}} = -\frac{1}{2\lambda} (q^\mu \mathcal{A}_\mu^A) (q^\nu \mathcal{A}_\nu^A).$$

This gauge fixing term does not require the ghost sector but leads to a more complicated gluon propagator.

The two most prominent gauge choices of covariant gauges are $\lambda = 1$ (i.e. the FEYNMAN gauge) and $\lambda \rightarrow 0$ (i.e the LANDAU gauge). For practical calculations very often FEYNMAN gauge is chosen for it leads to a simpler numerator structure than an arbitrary choice of λ .

The LAGRANGIAN density (9) in covariant gauge leads to the following set of FEYNMAN rules, given in (17). Straight lines represent quarks, gluons are drawn as curly lines and ghosts as dotted lines. These FEYNMAN rules correspond to the ones given in [BDJ01b]; the corresponding rules in [ESW96] are obtained by the transformation $g_s \rightarrow -g_s$.

$$(17a) \quad \longrightarrow = i\delta_{ab} \frac{\not{p} + m}{p^2 - m^2 + i\delta}$$

$$(17b) \quad \text{curly line} = \delta^{AB} \frac{i}{p^2 + i\delta} \left(-g^{\mu\nu} + (1 - \lambda) \frac{p^\mu p^\nu}{p^2 + i\delta} \right)$$

$$(17c) \quad \cdots \cdots \blacktriangleright \cdots \cdots = \delta^{AB} \frac{i}{p^2 + i\delta}$$

$$(17d) \quad \begin{array}{c} \text{diagram: three gluon vertex} \end{array} = g_s f^{ABC} \left[\begin{array}{l} g^{\mu\nu}(p_1 - p_2)^\rho \\ + g^{\nu\rho}(p_2 - p_3)^\mu \\ + g^{\mu\rho}(p_3 - p_1)^\nu \end{array} \right]$$

$$(17e) \quad \begin{array}{c} \text{diagram: four gluon vertex} \end{array} = -ig_s^2 \left[\begin{array}{l} f^{ABE} f^{CDE} (g^{\mu\rho} g^{\nu\sigma} - g^{\mu\sigma} g^{\nu\rho}) \\ + f^{ACE} f^{BDE} (g^{\mu\nu} g^{\rho\sigma} - g^{\mu\sigma} g^{\nu\rho}) \\ + f^{ADE} f^{BCE} (g^{\mu\nu} g^{\rho\sigma} - g^{\mu\rho} g^{\nu\sigma}) \end{array} \right]$$

$$(17f) \quad \begin{array}{c} \text{diagram: quark-gluon vertex} \end{array} = ig_s t_{ba}^C \gamma^\mu$$

$$(17g) \quad \begin{array}{c} \text{diagram: ghost-gluon vertex} \end{array} = -g_s f^{ABC} p^\mu$$

These rules are valid in the covariant gauge, all momenta are ingoing at the vertices and following the arrow along propagators. In axial gauge the gluon propagator has to be replaced by

$$\delta^{AB} \frac{i}{p^2 + i\delta} \left(-g^{\mu\nu} + \frac{p^\mu q^\nu + q^\mu p^\nu}{q \cdot p} + \frac{(q^2 + \lambda p^2) p^\mu p^\nu}{(q \cdot p)^2} \right).$$

2. The Effective Coupling and Asymptotic Freedom

Calculating terms of higher order of $\alpha_s = g_s^2/(4\pi)$ in the perturbative expansion usually introduces ultraviolet divergences which have to be cured by renormalisation. One generic property of regularisation is the appearance of a new mass scale, which in dimensional regularisation usually is called μ . A physical observable R therefore not only depends on the energy scale Q of the process but also on the parameter μ . Since the

second dependency is unphysical — every choice of μ should lead to the same result — one may postulate this independence by the renormalisation group equation [ESW96]

$$(18) \quad \mu^2 \frac{d}{d\mu^2} R(Q^2/\mu^2, \alpha_s) = \left[\mu^2 \frac{\partial}{\partial \mu^2} + \mu^2 \frac{\partial \alpha_s}{\partial \mu^2} \frac{\partial}{\partial \alpha_s} \right] R(Q^2/\mu^2, \alpha_s) = 0.$$

The coefficient of the second term is called the β -function,

$$(19) \quad \beta(\alpha_s) \equiv \mu^2 \frac{\partial \alpha_s(\mu^2)}{\partial \mu^2} = Q^2 \frac{\partial \alpha_s(Q^2)}{\partial Q^2},$$

which implicitly defines a scale dependent coupling constant, the so called *running coupling constant* $\alpha_s(Q^2)$.

In the perturbative regime and for n_f flavours of massless quarks only we can express the β -function as

$$(20) \quad \beta(\alpha_s) = -b\alpha_s(Q^2) [1 + b'\alpha_s(Q^2) + \mathcal{O}(\alpha_s(Q^2)^2)],$$

with the coefficients

$$(21a) \quad b = \frac{33 - 2n_f}{12\pi} \quad \text{and}$$

$$(21b) \quad b' = \frac{153 - 19n_f}{24\pi^2 b}.$$

Neglecting b' and all higher order terms, the partial differential equation (19) can be solved leading to a relation between $\alpha_s(Q^2)$ and $\alpha_s(\mu^2)$,

$$(22) \quad \alpha_s(Q^2) = \frac{\alpha_s(\mu^2)}{1 + \alpha_s(\mu^2)b \ln(Q^2/\mu^2)}$$

and the behaviour of α_s depends on the number of flavours: b is positive as long as $n_f < 33/2$.

The scale at which the denominator of (22) vanishes is called the LANDAU pole $Q = \Lambda_{\text{QCD}}$. Setting μ to the Z-mass m_Z in this approximation and for $n_f = 5$ one obtains using $\alpha_s(m_Z^2)$ [Eid04]

$$(23) \quad \Lambda_{\text{QCD}} = m_Z \exp \left[-\frac{1}{b\alpha_s(m_Z^2)} \right] \approx 91 \text{ MeV}.$$

Better approximations yield values around 200 MeV. For large energies $\alpha_s(Q^2)$ decreases since the Standard Model contains $n_f = 6$ flavours, a fact that is known as *asymptotic freedom*. As low energies close to the LANDAU pole are reached, the coupling constant becomes large and a perturbative expansion is no longer valid. This strongly coupled regime leads to quark *confinement* and ensures that in nature no free coloured particles appear.

3. Flavour Symmetry

Under the interactions of QCD all quark flavours interact in the same way with the gluons. If in addition one considers the approximation of massless quarks the LAGRANGIAN density is invariant under the exchange of flavour and hence any amplitude calculated in massless QCD is invariant under the exchange of flavours. This is true only if the combinatorics of the configuration does not change.

In the following section I derive the relation between the two amplitudes $\mathcal{A}_{u\bar{u} \rightarrow b\bar{b}b\bar{b}}$ and $\mathcal{A}_{u\bar{u} \rightarrow b\bar{b}s\bar{s}}$. This relation is useful for the calculation of the first amplitude from the second one and has been exploited in our calculation of the former amplitude. Because of its higher symmetry $\mathcal{A}_{u\bar{u} \rightarrow b\bar{b}b\bar{b}}$ consists of more FEYNMAN diagrams than $\mathcal{A}_{u\bar{u} \rightarrow b\bar{b}s\bar{s}}$. Hence the second amplitude is easier to calculate and implement.

For the derivation of the relation between the amplitudes the following abstractions from QCD can be made: the only requirement of flavour symmetry is that the quarks couple equally to the other fields in the theory, which are represented by a single field Φ . We consider a theory with two quark fields Ψ and Ξ . If no contact interaction of two quark pairs is allowed the LAGRANGIAN density can be written as

$$(24) \quad \mathcal{L} = \bar{\Psi}Q\Psi + \bar{\Xi}Q\Xi + \mathcal{L}_B(\Phi, \partial\Phi) + \bar{\Psi}V(\Phi)\Psi + \bar{\Xi}V(\Phi)\Xi.$$

The operator Q stands for the kinetic part of the LAGRANGIAN density; usually $Q = (\not{\partial} + m)$, but the exact form is irrelevant for the discussion. The interaction between the quarks and Φ is denoted by $V(\Phi)$. \mathcal{L}_B contains the self interactions and the kinetic part of the LAGRANGIAN density for the field Φ .

The partition function Z is defined as

$$(25) \quad Z[\bar{\eta}, \eta, \bar{\xi}, \xi] = \int \mathcal{D}\bar{\Psi}\mathcal{D}\Psi\mathcal{D}\bar{\Xi}\mathcal{D}\Xi\mathcal{D}\Phi e^{i \int d^d x \mathcal{L} + \bar{\eta}\Psi - \bar{\Psi}\eta + \bar{\xi}\Xi - \bar{\Xi}\xi + \Phi J_\Phi}.$$

The functional integral can be separated from the sources by completing the square and introducing the GREEN's function S that fulfils

$$(26) \quad QS(x, x') = \delta^{(d)}(x - x')$$

as explained in standard textbooks about quantum field theory [PS95, BDJ01a]. Using the notation

$$(27) \quad \mathcal{L}_0[\bar{\Psi}, \Psi, \bar{\Xi}, \Xi] = \bar{\Psi}Q\Psi + \bar{\Xi}Q\Xi \quad \text{and}$$

$$(28) \quad \mathcal{L}_I[\bar{\Psi}, \Psi, \bar{\Xi}, \Xi, \Phi] = \bar{\Psi}V(\Phi)\Psi + \bar{\Xi}V(\Phi)\Xi + \mathcal{L}_B(\Phi, \partial\Phi)$$

one obtains

$$(29) \quad Z[\bar{\eta}, \eta, \bar{\xi}, \xi] = \exp \left\{ i \int d^d x \mathcal{L}_I \left[\frac{\delta}{i\delta\bar{\eta}(x)}, \frac{\delta}{i\delta\eta(x)}, \frac{\delta}{i\delta\bar{\xi}(x)}, \frac{\delta}{i\delta\xi(x)}, \frac{\delta}{i\delta J_\Phi(x)} \right] \right\} \times \\ \exp \left\{ i \int d^d x d^d y \bar{\eta}(x)S(x, y)\eta(y) + \bar{\xi}(x)S(x, y)\xi(y) \right\} \left(\int \mathcal{D}\bar{\Psi}\mathcal{D}\Psi\mathcal{D}\bar{\Xi}\mathcal{D}\Xi\mathcal{D}\Phi e^{i \int d^d x \mathcal{L}_0} \right).$$

The remaining functional integral is called Z_0 and is only a constant which does not carry any functional dependence.

Now, we can compare the correlation functions

$$(30) \quad \langle T\bar{\Psi}(x_1)\Psi(x_2)\bar{\Xi}(x_3)\Xi(x_4) \rangle = \frac{1}{Z_0} \frac{\delta^4 Z[\bar{\eta}, \eta, \bar{\xi}, \xi]}{\delta\bar{\eta}(x_1)\delta\eta(x_2)\delta\bar{\xi}(x_3)\delta\xi(x_4)} \bigg|_{\substack{\eta=\bar{\eta}=0 \\ \xi=\bar{\xi}=J_\Phi=0}} \quad \text{and}$$

$$(31) \quad \langle T\bar{\Psi}(x_1)\Psi(x_2)\bar{\Psi}(x_3)\Psi(x_4) \rangle = \frac{1}{Z_0} \frac{\delta^4 Z[\bar{\eta}, \eta, \bar{\xi}, \xi]}{\delta\bar{\eta}(x_1)\delta\eta(x_2)\delta\bar{\eta}(x_3)\delta\eta(x_4)} \bigg|_{\substack{\eta=\bar{\eta}=0 \\ \xi=\bar{\xi}=J_\Phi=0}}$$

by direct calculation. It is sufficient to compare both correlation functions for the term

$$-\frac{1}{2} \int d^d x V \left(\frac{\delta}{i\delta\Phi(x)} \right) \left(\frac{\delta}{i\delta\bar{\eta}(x)} \frac{\delta}{i\delta\eta(x)} + \frac{\delta}{i\delta\bar{\xi}(x)} \frac{\delta}{i\delta\xi(x)} \right) \times \\ \int d^d y V \left(\frac{\delta}{i\delta\Phi(y)} \right) \left(\frac{\delta}{i\delta\bar{\eta}(y)} \frac{\delta}{i\delta\eta(y)} + \frac{\delta}{i\delta\bar{\xi}(y)} \frac{\delta}{i\delta\xi(y)} \right)$$

from the expansion of $\exp(\int i\mathcal{L}_I)$. This expansion has been done with the computer algebra system FORM [Ver00, Ver02] and the result, written in terms of quarks and gluons is summarised below:

$$(32) \quad \mathcal{A}_{u\bar{u} \rightarrow b\bar{b}b\bar{b}}(a, b; 1, 2, 3, 4) = \mathcal{A}_{u\bar{u} \rightarrow b\bar{b}s\bar{s}}(a, b; 1, 2, 3, 4) - \mathcal{A}_{u\bar{u} \rightarrow b\bar{b}s\bar{s}}(a, b; 1, 4, 3, 2),$$

$$(33) \quad \mathcal{A}_{gg \rightarrow b\bar{b}b\bar{b}}(a, b; 1, 2, 3, 4) = \mathcal{A}_{gg \rightarrow b\bar{b}s\bar{s}}(a, b; 1, 2, 3, 4) - \mathcal{A}_{gg \rightarrow b\bar{b}s\bar{s}}(a, b; 1, 4, 3, 2).$$

The external fields are denoted simply by their indices ($a, b, 1, 2, \dots$); this notation implies that momenta, colour and helicity labels need to be swapped accordingly.

CHAPTER 2

Representations of QCD Amplitudes

It is the harmony of the diverse parts, their symmetry, their happy balance; in a word it is all that introduces order, all that gives unity, that permits us to see clearly and to comprehend at once both the ensemble and the details. — JULES HENRI POINCARÉ

Introduction

In order to make predictions for colliders at high energies one needs to relate observables with the underlying theory. In quantum mechanics this relation is given through the *scattering matrix*¹ S ; the S -matrix element $\langle f|S|i\rangle$ describes the transition from an initial state $|i\rangle$ to a final state $\langle f|$, where $|i\rangle$ is taken at time $t \rightarrow -\infty$ and $|f\rangle$ is a state at $t \rightarrow +\infty$. The operator S can be related to the interaction part of the LAGRANGian density²,

$$(34) \quad S = \mathbf{T} e^{i \int d^4x \mathcal{L}_I},$$

where \mathbf{T} denotes the time-ordered product. For momentum eigenstates of momenta p_i and p_f respectively the S -matrix elements can be written as

$$(35) \quad \langle f|S|i\rangle = \langle f|i\rangle + i(2\pi)^4 \delta^{(4)}(p_i - p_f) \mathcal{M}_{fi}.$$

The FEYNMAN rules give a prescription how to obtain an analytical expression for $i\mathcal{M}$ from a sum of FEYNMAN diagrams. In QCD each FEYNMAN diagram can be written as a product of a colour vector $|c\rangle$ and a kinematical coefficient. With a common choice of a colour basis \mathcal{B} for all diagrams, the invariant matrix element has the form

$$(36) \quad \mathcal{M}_{fi} = \sum_{|c\rangle \in \mathcal{B}} \mathcal{A}_c(p_a, p_b; p_1, \dots, p_N) |c\rangle,$$

where p_a and p_b denote the momenta of the incoming particles and p_1, \dots, p_N those of the final state particles. Different choices of bases \mathcal{B} are discussed in Sections 1 and 2. The coefficient function \mathcal{A}_c contains all dependencies on the momenta. Its calculation can be simplified through projections on the physical degrees of freedom for spinors and polarisation vectors, which leads to the formalism of spinor helicity projections described in Section 3.

¹In Section 1.4 of Chapter 3 I introduce a matrix S_{ij} that encodes the kinetic information of a FEYNMAN diagram at one-loop. Although the two matrices are unrelated objects, in the literature for both matrices S is the commonly used symbol.

²See for example [BDJ01a]

Observables measured at colliders can usually be expressed through a differential cross-section³,

$$(37) \quad d\sigma = \frac{1}{2|p_a + p_b|^2} \frac{1}{n_a n_b} d\Phi^{(N)}(p_a + p_b) \sum_{c, c' \in \mathcal{B}} \langle c' | \mathcal{A}_{c'}^* \mathcal{A}_c | c \rangle F_J^{(N)}(p_1, \dots, p_N).$$

The measurement function $F_J^{(N)}$ defines the observable and usually contains Θ -functions, defining the experimental cuts, the definition of jets in the case of jet-observables and, in the case of exclusive observables, the quantities of which distributions are to be obtained. The N -particle phase space can be parametrised as follows,

$$(38) \quad d\Phi^{(N)}(Q; p_1, \dots, p_N) = \prod_{j=1}^N \frac{d^4 p_j}{(2\pi)^3} \Theta(p_j^0) \delta(p_j^2 - m_j^2) \cdot (2\pi)^4 \delta^{(4)} \left(Q - \sum_{i=1}^N p_i \right)$$

and is discussed in more detail in Chapter 3 in Section 8. The factors n_a and n_b denote normalisations induced by spin and colour averages. A factor of $1/n!$ for has to be included for each set of n final state particles that are not distinguished in the observable.

1. Colour-Flow Decomposition

1.1. $SU(N)$ Diagrammatics. One part of amplitude calculations in non-ABELian gauge theories is the simplification and evaluation of the colour structure. In this section I will present a diagrammatic approach which is mainly motivated and introduced in [Cvi08]. The basic idea is to represent all indices by external lines and all tensors by vertices; KRONECKER delta symbols therefore appear as internal lines. I use dashed lines for the adjoint representation, fermion lines for the fundamental representation and dotted lines for the trivial representation. The dotted lines could be left out in most cases since they only represent a one; they are drawn here anyway to clarify the origin of the formulæ.

$$(39a) \quad \text{-----} = \delta^{AB}$$

$$(39b) \quad \text{--->} = \delta_b^a$$

$$(39c) \quad \text{.....} = 1$$

$$(39d) \quad \begin{array}{c} \text{--->} \\ | \\ \text{--->} \end{array} = t_{ba}^C$$

³As QCD partons cannot be observed as free particles in nature, one distinguishes between the partonic and the hadronic cross-section. The latter is obtained by the former through a convolution with parton distribution functions. Here, I describe the partonic cross-section. For a discussion of its hadronic equivalent see Section 7 in Chapter 3

$$(39e) \quad \begin{array}{c} \diagup \\ \bullet \\ \diagdown \end{array} \text{---} = if^{ABC}$$

In diagrammatic form the defining equation of the LIE algebra reads

$$(40) \quad \begin{array}{c} \text{---} \bullet \text{---} \bullet \text{---} \\ \text{---} \bullet \text{---} \bullet \text{---} \end{array} - \begin{array}{c} \text{---} \bullet \text{---} \bullet \text{---} \\ \text{---} \bullet \text{---} \bullet \text{---} \end{array} = \begin{array}{c} \text{---} \bullet \text{---} \bullet \text{---} \\ \text{---} \bullet \text{---} \bullet \text{---} \end{array}$$

Up to now no specific gauge group has been chosen. The only ingredient that depends on the gauge group is the completeness relation stating that the identity can be written as a sum of projections into all different irreducible representations. For a tensor product of the fundamental representation with its conjugate of $SU(N)$ this sum simplifies to two terms, a projection on the adjoint and a projection onto the trivial representation:

$$(41) \quad \begin{array}{c} \text{---} \bullet \text{---} \bullet \text{---} \\ \text{---} \bullet \text{---} \bullet \text{---} \end{array} = \frac{\text{---} \bullet \text{---} \bullet \text{---}}{\text{---} \bullet \text{---} \bullet \text{---}} + \frac{\text{---} \bullet \text{---} \bullet \text{---}}{\text{---} \bullet \text{---} \bullet \text{---}}$$

Diagrams with no external lines always represent scalar. A circle without a vertex is just the trace over the corresponding identity matrix and therefore the dimension of that representation. Lines of the trivial representation can be omitted and therefore the only unknown symbol is

$$(42) \quad \begin{array}{c} \text{---} \bullet \text{---} \bullet \text{---} \\ \text{---} \bullet \text{---} \bullet \text{---} \end{array} = \text{tr}\{T^A T^A\} \equiv T_R \delta^{AA}.$$

The quadratic CASIMIR operator T_R can be chosen as the normalisation of the generators; following common conventions, I use $T_R = 1/2$. In $SU(N_C)$, the dimensions of the representations are $\delta^{AA} = N_C^2 - 1$ and $\delta_a^a = N_C$. The completeness relation (41) can now be rearranged to

$$(43) \quad \begin{array}{c} \text{---} \bullet \text{---} \bullet \text{---} \\ \text{---} \bullet \text{---} \bullet \text{---} \end{array} = T_R \left(\begin{array}{c} \text{---} \bullet \text{---} \bullet \text{---} \\ \text{---} \bullet \text{---} \bullet \text{---} \end{array} - \frac{1}{N_C} \begin{array}{c} \text{---} \bullet \text{---} \bullet \text{---} \\ \text{---} \bullet \text{---} \bullet \text{---} \end{array} \right).$$

With the above relations one already can reduce simple two-point functions by using SCHUR's lemma, which allows the CASIMIR operators to be written in terms of multiples

of the identity matrix:

$$(44) \quad \begin{array}{c} \text{---} \bullet \text{---} \bullet \text{---} \\ \text{---} \bullet \text{---} \bullet \text{---} \end{array} = \frac{\begin{array}{c} \text{---} \bullet \text{---} \bullet \text{---} \\ \text{---} \bullet \text{---} \bullet \text{---} \end{array}}{\begin{array}{c} \text{---} \bullet \text{---} \bullet \text{---} \\ \text{---} \bullet \text{---} \bullet \text{---} \end{array}} = C_F \text{---}$$

$$(45) \quad \begin{array}{c} \text{---} \bullet \text{---} \bullet \text{---} \\ \text{---} \bullet \text{---} \bullet \text{---} \end{array} = \frac{\begin{array}{c} \text{---} \bullet \text{---} \bullet \text{---} \\ \text{---} \bullet \text{---} \bullet \text{---} \end{array}}{\begin{array}{c} \text{---} \bullet \text{---} \bullet \text{---} \\ \text{---} \bullet \text{---} \bullet \text{---} \end{array}} = T_R \text{---}$$

$$(46) \quad \begin{array}{c} \text{---} \bullet \text{---} \bullet \text{---} \\ \text{---} \bullet \text{---} \bullet \text{---} \end{array} = \frac{\begin{array}{c} \text{---} \bullet \text{---} \bullet \text{---} \\ \text{---} \bullet \text{---} \bullet \text{---} \end{array}}{\begin{array}{c} \text{---} \bullet \text{---} \bullet \text{---} \\ \text{---} \bullet \text{---} \bullet \text{---} \end{array}} = C_A \text{---}$$

The constant C_F can be read off directly,

$$(47) \quad C_F = \frac{T_R \delta^{AA}}{\delta_a^a} = \frac{N_C^2 - 1}{2N_C},$$

whereas for C_A another trick is needed.

One can obtain a relation to express the structure constants f^{ABC} in terms of generators in the fundamental representation by multiplying (40) with another generator,

$$(48) \quad \begin{array}{c} \text{---} \bullet \text{---} \bullet \text{---} \\ \text{---} \bullet \text{---} \bullet \text{---} \end{array} - \begin{array}{c} \text{---} \bullet \text{---} \bullet \text{---} \\ \text{---} \bullet \text{---} \bullet \text{---} \end{array} = \begin{array}{c} \text{---} \bullet \text{---} \bullet \text{---} \\ \text{---} \bullet \text{---} \bullet \text{---} \end{array} = T_R \begin{array}{c} \text{---} \bullet \text{---} \bullet \text{---} \\ \text{---} \bullet \text{---} \bullet \text{---} \end{array}$$

Together with (43) and (44) we obtain one of the so called *star-triangle relations*:

$$(49) \quad \begin{array}{c} \text{---} \bullet \text{---} \bullet \text{---} \\ \text{---} \bullet \text{---} \bullet \text{---} \end{array} = T_R N_C \begin{array}{c} \text{---} \bullet \text{---} \bullet \text{---} \\ \text{---} \bullet \text{---} \bullet \text{---} \end{array}$$

This result can be used to evaluate C_A replacing one structure constant using (48) and then applying the previous star triangle relation; using that f^{ABC} is antisymmetric one then finds

$$(50) \quad T_R \begin{array}{c} \text{---} \bullet \text{---} \bullet \text{---} \\ \text{---} \bullet \text{---} \bullet \text{---} \end{array} = 2T_R N_C \begin{array}{c} \text{---} \bullet \text{---} \bullet \text{---} \\ \text{---} \bullet \text{---} \bullet \text{---} \end{array} = 2N_C^2 C_F T_R,$$

and hence $C_A = N_C$. A second star triangle relation can be obtained in a similar way to this leading to

$$(51) \quad \begin{array}{c} \text{---} \bullet \text{---} \bullet \text{---} \\ \quad \diagdown \quad \diagup \\ \quad \bullet \\ \quad \text{---} \end{array} = T_R N_C \begin{array}{c} \text{---} \diagdown \diagup \text{---} \\ \quad \bullet \\ \quad \text{---} \end{array}$$

1.2. Colour Decomposition. One way of organising QCD amplitudes is to project onto a colour basis which separates the amplitude into gauge invariant subamplitudes⁴. It is therefore convenient to choose a common set of indices both for the quarks and the gluons. To achieve this common form every external gluon with the adjoint index A is multiplied by $(1/\sqrt{T_R})t_{ij}^A$ to satisfy and eliminate all external adjoint indices. When the amplitude is squared instead of carrying out a colour sum over the adjoint index A one has to run two colour sums over i and j . The advantage of this procedure is that the colour structure of the amplitude now is formed in terms of KRONECKER deltas and hence the amplitude splits into subamplitudes as follows

$$(52) \quad \mathcal{A}(q_{i_1}, \bar{q}^{j_1}, q_{i_2}, \bar{q}^{j_2}, \dots, g_{i_m}^{j_m}, \dots, g_{i_n}^{j_n}) = \sum_{\sigma \in \mathcal{S}_n} \delta_{i_{\sigma(1)}}^{j_1} \cdots \delta_{i_{\sigma(N)}}^{j_N} \mathcal{A}_\sigma,$$

where q (\bar{q}) and g represent the colour structure introduced by quarks and gluons, \mathcal{S}_n is the symmetric group⁵ and \mathcal{A}_σ is the respective subamplitude. Since all external adjoint indices have been replaced by a pair of fundamental ones, Algorithm 1 ensures that all colour structure is reduced to KRONECKER deltas and no contracted nor external adjoint indices are left over. Statements 1–3 in Algorithm 1 are optional, but they improve the performance for diagrams containing many gluon self couplings. An algorithm similar to Algorithm 1 has been described in [HK97].

Algorithm 1 Evaluation of the colour structure

- 1: Simplify repeating (51)
 - 2: Simplify repeating (49)
 - 3: Simplify repeating (46)
 - 4: **repeat**
 - 5: Eliminate f^{ABC} using (48)
 - 6: Eliminate t_{ab}^C using (43)
 - 7: **until** no more replacements possible
-

1.3. Other Colour Bases. In the approach I presented above, for an amplitude calculation the traditional QCD FEYNMAN rules, as given in Section 1 of Chapter 1, are used. Later the colour related objects are translated into a graphical notation. External gluons are multiplied by a generator of the fundamental $SU(N_C)$ representation to allow a unified treatment of quarks and gluons in the calculation of colour factors. Going on step further, one can rewrite the LAGRANGIAN density of QCD such that

$$(53) \quad \delta^{AB} = \frac{1}{T_R} \text{tr}\{t^A t^B\} = \left(\frac{1}{\sqrt{T_R}} (t^A)_i^j \right) \left(\frac{1}{\sqrt{T_R}} (t^B)_j^i \right)$$

⁴See for example [Dix96]

⁵ \mathcal{S}_n is the group of permutations of n elements.

and thus replacing all appearances of the gluon field by

$$(54) \quad \left(\frac{1}{\sqrt{T_R}} (t^A)_i^j \right) \mathcal{A}_\mu^A \rightarrow (A_\mu)_i^j$$

and treating the LAGRANGIAN density with respect to the new variable. This leads to a different representation of the FEYNMAN rules which are known as *double-line notation* [tH74, MPSW03]. Similarly, one could also introduce a double-line notation for the LORENTZ part of the amplitude by replacing

$$(55) \quad g^{\mu\nu} = \frac{1}{2} \sigma_{\alpha\dot{\alpha}}^\mu \bar{\sigma}^{\nu,\dot{\alpha}\alpha},$$

which replaces all LORENTZ indices by a pair of WEYL spinor indices [Wei06]. This representation of the spinorial indices is known as the WEYL-VAN DER WAERDEN representation and is discussed in detail in Section 3.7.

One of the disadvantages of this approach is the fact that one does not generate a true basis of the colour space but introduces spurious vectors: permutations containing a δ_j^i acting on a gluonic leg $(t^A)_i^j$ will project out the trace $\text{tr}\{t^A\} = 0$ and hence should be removed explicitly. From counting the number of possibilities of tracing single generators t^A one finds that such a basis has

$$(56) \quad \sum_{i=0}^G (-1)^i \binom{G}{i} (2Q + G - i)!$$


elements, when G is the number of external gluons and Q is the number of external quarks. For amplitudes with many external gluons this removal of zero-vectors can be cumbersome. This is one of the reasons why for these amplitudes usually colour ordering is considered a better solution; it is described, for example, in [Dix96]. Here the fact is used that purely gluonic amplitudes can be decomposed into the form

$$(57) \quad \mathcal{A}(g_{A_1}, g_{A_2}, \dots, g_{A_n}) = \sum_{\substack{\sigma \vec{\lambda} \vdash n \\ \lambda_i \geq 2}} \text{tr} \left\{ t^{A_{\sigma(1)}} t^{A_{\sigma(2)}} \dots t^{A_{\sigma(\lambda_1)}} \right\} \dots \text{tr} \left\{ t^{A_{\sigma(n-\lambda_p+1)}} \dots t^{A_{\sigma(n-1)}} t^{A_{\sigma(n)}} \right\} \mathcal{A}_{\sigma, \vec{\lambda}},$$

where only permutations $\sigma \in \mathcal{S}_n$ leading to distinguishable terms for the traces⁶ are summed over. The condition $\vec{\lambda} \vdash n$ denotes that the sum over $\vec{\lambda}$ traverses all integer partitions of n .

This construction of a basis can easily be extended to the mixed case of quarks and gluons and can be understood diagrammatically through a theory defined by the following FEYNMAN rules

$$\begin{array}{c} \text{---} \bullet \text{---} \\ \text{---} \bullet \text{---} \\ \text{---} \bullet \text{---} \end{array} = (t^A)_i^j \quad \text{and} \quad \text{---} \bullet \text{---} = \delta_i^j.$$

One then has to create all possibly disconnected diagrams removing tadpoles and empty traces , because they lead to additional linearly dependent vectors.

⁶i.e. all cyclic permutations of the elements of one trace and all permutations that reorder traces of the same length are factored out

As long as one works with a general number of colours N_C the dimension $d_{g,f}$ of such a basis for g gluons and f quark pairs can be derived from considering the number of possibilities of inserting an additional gluon; this is equivalent to inserting an additional quark pair and removing the singlet combination,

$$(58) \quad d_{g+1,f} = d_{g,f+1} - d_{g,f}.$$

In the purely fermionic case one has the $d_{0,f} = f!$ permutations of the fermion lines. One can prove by direct calculation that

$$(59) \quad d_{g,f} = \sum_{i=0}^g (-1)^i \binom{g}{i} (g+f-i)!.$$

fulfils the two properties. The closed form, however, suggests the equivalence with the basis described in Equations (53) to (56).

Further reductions of this basis can be achieved by considering the irreducible representations of the symmetric group permuting the $g+f$ lines in the fundamental representation. If one fixes N_C it is clear that no antisymmetrisation over more than N_C lines is possible and hence those combinations of permutations have to vanish. A systematic treatment of the symmetric group is given in Section 2. Table 1 shows the number of basis⁷ elements in the different representations for a number of different processes. The colour-basis of the amplitude is usually smaller than the ones presented because the BOSE symmetry of the amplitude allows the application of further symmetrisation of the colour vectors. However, helicity projections destroy some of the symmetries of the amplitude and hence one would have to work out a different basis for each helicity projection. This is important if one tries to achieve a compact analytical result; the trade-off in a numerical calculation is debatable.

1.4. Recoupling Relations. In this section I describe recoupling relations for QCD, which are useful for a quick reduction of large loops. The reader be reminded of two basic relations which have been introduced earlier for the special case of the fundamental and the adjoint representation. As a direct consequence of SCHUR's lemma any two-point birdtrack diagram must connect two lines of the same irreducible representation and hence be proportional to a KRONECKER delta,

$$(60) \quad \begin{array}{c} \text{---} \bullet \text{---} \text{---} \bullet \text{---} \\ \text{---} \bullet \text{---} \text{---} \bullet \text{---} \end{array} = \frac{\begin{array}{c} \text{---} \bullet \text{---} \text{---} \bullet \text{---} \\ \text{---} \bullet \text{---} \text{---} \bullet \text{---} \end{array}}{\begin{array}{c} \text{---} \bullet \text{---} \text{---} \bullet \text{---} \\ \text{---} \bullet \text{---} \text{---} \bullet \text{---} \end{array}} \longrightarrow \delta_{\lambda\lambda'}.$$

⁷The term *basis* should not be taken in the literal mathematical sense; the spirit of this section is to show that depending on different assumptions there are additional relations that render some of the vectors linearly dependent.

A second identity is the completeness relation,

$$(61) \quad \begin{array}{c} \longrightarrow \\ \longrightarrow \end{array} = \sum_{\lambda} \frac{\text{[Diagram: Two circles with arrows, one top and one bottom, connected by a horizontal line with an arrow pointing right]} }{\text{[Diagram: Two circles with arrows, one top and one bottom, connected by a horizontal line with an arrow pointing right]} } \text{[Diagram: A four-point vertex with two incoming lines from the left and two outgoing lines to the right]} ,$$

where the sum runs over all irreducible representations of the underlying LIE algebra with non-vanishing coupling to the representations μ and ν .

The starting point for the derivation of the recoupling relation is a four point tree graph with arbitrary, irreducible representations [Cvi08], as shown in (62); Equation (61) is used twice and the sum over λ' is evaluated using Equation (60).

$$(62) \quad \begin{array}{c} \nearrow \quad \searrow \\ \bullet \\ \searrow \quad \nearrow \\ \bullet \\ \nwarrow \quad \swarrow \end{array}$$

Both sides can then be multiplied by a \mathbb{I} expressed through the completeness relation. To obtain the final formula SCHUR's lemma is applied to the propagator:

$$(63) \quad \begin{array}{c} \nearrow \quad \searrow \\ \bullet \\ \searrow \quad \nearrow \\ \bullet \\ \nwarrow \quad \swarrow \end{array} = \sum_{\lambda} \sum_{\lambda'} \frac{\text{[Diagram: Two circles with arrows, one top and one bottom, connected by a horizontal line with an arrow pointing right]} }{\text{[Diagram: Two circles with arrows, one top and one bottom, connected by a horizontal line with an arrow pointing right]} } \text{[Diagram: A four-point vertex with two incoming lines from the left and two outgoing lines to the right]} \\ \Rightarrow \begin{array}{c} \nearrow \quad \searrow \\ \bullet \\ \searrow \quad \nearrow \\ \bullet \\ \nwarrow \quad \swarrow \end{array} = \sum_{\lambda} \frac{\text{[Diagram: A complex diagram with multiple loops and vertices]} }{\text{[Diagram: Two circles with arrows, one top and one bottom, connected by a horizontal line with an arrow pointing right]} } \text{[Diagram: A four-point vertex with two incoming lines from the left and two outgoing lines to the right]}$$

In literature the coefficients of this relation are referred as 3- j and 6- j symbols or Wigner coefficients.

The 3- j symbols already appeared earlier in the QCD self-energy graphs, and together with the 6- j symbols one can derive the general version of the star-triangle relations which were introduced in the special case of quarks and gluons. Starting from a general triangle $SU(N)$ -graph we can recouple one of its propagators, which reduces the triangle to a self-energy graph; the latter can be eliminated by SCHUR's lemma and hence

one gets

(64)

The recoupling relation provides a useful check for the calculation of $6-j$ coefficients when applied to two non-adjacent lines of a $6-j$ symbol:

(65)

Another useful application of the recoupling relations is the systematic reduction of large loops. The first step of such a reduction would be the projection on a basis of tree graphs, which in the simplest case could just be formed by KRONECKER delta symbols if the external legs are in the same representation. As a result one obtains tree graphs which have graphs without external legs, so-called bubble graphs, as coefficients. The bubbles evaluate to scalars and therefore represent the group-theoretical factor of the underlying diagram. The knowledge of all $6-j$ and $3-j$ symbols is enough to evaluate any given bubble diagram⁸: Any loop of size two can be reduced by SCHUR's lemma (60) and cycles of size three are eliminated by the star-triangle relation. Larger loops can always be split in half using the completeness relation (61).

The statistical run time for the reduction of a loop of size n is $\mathcal{O}(n^{\log_2 m})$, where m is the average number of irreducible representation that appear under the sum of the completeness relation⁹. This is no improvement over algorithm 1 for the SU(3) colour factors of QCD. However, there is no restriction to a special LIE group and therefore this approach also works for the orthogonal group. With few modifications one can include spinor representations and use the same algorithm for the evaluation of spinor traces, which I will discuss in Section 1 in Chapter 3. Another advantage is that one is free in the choice of the basis which the diagram is projected on; algorithm 1, however, restricts itself to the choice of a basis formed by KRONECKER symbols. As already mentioned above, this approach requires knowledge of all $3-j$ and $6-j$ symbols that might appear during the computation. Therefore efficient methods to calculate these factors should be investigated.

⁸In fact the dimensions of the representations and the $3-j$ symbols are just special cases of $6-j$ coefficients containing the fundamental representation in two (resp. one) of the lines.

⁹For $m = 1$ the run time reduces to $\mathcal{O}(\log_2 n)$.

process	$(g+f)!$	$d_{g,f}$	$\bar{d}_{g,f}(3)$
$q\bar{q} \rightarrow g$	2	1	1
$gg \rightarrow g$	6	2	2
$q\bar{q} \rightarrow q\bar{q}$	2	2	2
$gg \rightarrow q\bar{q}$	6	3	3
$gg \rightarrow gg$	24	9	8
$q\bar{q} \rightarrow gq\bar{q}$	6	4	4
$gg \rightarrow gq\bar{q}$	24	11	10
$gg \rightarrow ggg$	120	44	32
$q\bar{q} \rightarrow q\bar{q}q\bar{q}$	6	6	6
$gg \rightarrow q\bar{q}q\bar{q}$	24	14	13
$gg \rightarrow gq\bar{q}q\bar{q}$	120	53	40
$gg \rightarrow gggg$	720	265	145
$q\bar{q} \rightarrow gq\bar{q}q\bar{q}$	24	18	17
$gg \rightarrow gq\bar{q}q\bar{q}$	120	64	50
$gg \rightarrow gggq\bar{q}$	720	309	177
$gg \rightarrow ggggg$	5040	1854	702
$q\bar{q} \rightarrow q\bar{q}q\bar{q}q\bar{q}$	24	24	23
$gg \rightarrow q\bar{q}q\bar{q}q\bar{q}$	120	78	63
$gg \rightarrow gq\bar{q}q\bar{q}q\bar{q}$	720	362	217
$gg \rightarrow ggggq\bar{q}$	5040	2119	847
$gg \rightarrow gggggg$	40320	14833	3598

Table 1: For the different processes the number of basis elements in different representations of the colour structure is compared: $(g+f)!$ is the number of vectors obtained when all gluons are projected onto a quark-antiquark pair. $d_{g,f}$ is the number of vectors after subtracting all spurious vectors. $\bar{d}_{g,f}(3)$ counts the vectors if the \mathcal{S}_{g+f} structure considering $N_C = 3$ is taken into account and one works with irreducible representations only.

2. Irreducible Representations of $SU(N)$

Introduction. In the previous section I have presented an algorithm for the reduction of colour-tensors into an irreducible basis that relies on the knowledge of the $1-j$ (i.e. dimensions), $3-j$ and $6-j$ symbols of all appearing irreducible representations of the $SU(N)$. In this section I discuss, in a slightly more general context, how to obtain all irreducible representations of the General Linear Group ($GL(N)$) and an algorithm for the calculation of all relevant coefficients. One can then apply restrictions to the representations such that the irreducible representations of the $GL(N)$ reduce further down to the ones of its subgroups. For QCD one is interested in the $SU(N)$ only but the presented algorithm applies to other LIE groups as well once one knows how to construct the irreducible representation of those groups.

It is well known that the irreducible representations of the $GL(N)$ are described by the irreducible representations of the symmetric group \mathcal{S}_k , which are labelled by partitions or equivalently by Young diagrams [Wey39, Mur38, Ful97, Sag01]. In section 2.1 I briefly sketch the relevant properties of the symmetric group and establish a diagrammatic notation for permutations and vectors of the module $\mathbb{C}\mathcal{S}_k$ which allows us to construct irreducible matrix representations of \mathcal{S}_k . A matrix representation called YOUNG's Natural Representation is introduced in 2.2. In the following section, 2.3 these representations are used to calculate the $n-j$ symbols for the $SU(N)$. I conclude this section with the discussion of a complete diagram-based algorithm for the reduction of $GL(N)$ -tensors in 2.5.

2.1. Diagrammatics for the Symmetric Group. The Symmetric Group (\mathcal{S}_k) describes the set of bijective maps on a set with k elements. The concatenation of two elements $\sigma_1, \sigma_2 \in \mathcal{S}_k$ with $\sigma_{1,2} : x_j \mapsto x_{j'} = \sigma_{1,2}(x_j)$ defines a multiplication $\sigma_1 \cdot \sigma_2 : x_j \mapsto \sigma_1(\sigma_2(x_j))$. Several notations for the elements of \mathcal{S}_k are used in the literature: a permutation $\sigma : x_j \mapsto x_{j'} = \sigma(x_j)$ can be written in two rows as follows

$$(66) \quad \sigma = \begin{pmatrix} x_1 & x_2 & \dots & x_k \\ \sigma(x_1) & \sigma(x_2) & \dots & \sigma(x_k) \end{pmatrix}$$

Let, for instance, $\sigma_1, \sigma_2 \in \mathcal{S}_4$ be

$$(67) \quad \sigma_1 = \begin{pmatrix} a_1 & a_2 & a_3 & a_4 \\ a_3 & a_1 & a_2 & a_4 \end{pmatrix}, \quad \sigma_2 = \begin{pmatrix} a_1 & a_2 & a_3 & a_4 \\ a_4 & a_2 & a_3 & a_1 \end{pmatrix};$$

one can turn the rows into columns and connect the position of a_j with that of its image $a_{j'} = \sigma(a_j)$, i.e. if the elements on the left are ordered according to the indices j , connect the j -th row on the left with the j' -th row on the right. Multiplication is then carried out as denoted below; where unambiguous labels can be omitted:

$$(68) \quad \sigma_1 \cdot \sigma_2 = \begin{array}{c} \begin{array}{ccc} a_1 & a_2 & a_2 \\ a_2 & a_3 & a_3 \\ a_3 & a_1 & a_4 \\ a_4 & a_4 & a_1 \end{array} \cdot \begin{array}{ccc} a_1 & a_2 & a_2 \\ a_2 & a_3 & a_3 \\ a_3 & a_4 & a_1 \\ a_4 & a_1 & a_4 \end{array} \\ \hline \begin{array}{ccc} a_1 & a_2 & a_2 \\ a_2 & a_3 & a_3 \\ a_3 & a_4 & a_1 \\ a_4 & a_1 & a_4 \end{array} \end{array} = \begin{pmatrix} a_1 & a_2 & a_3 & a_4 \\ a_4 & a_1 & a_2 & a_3 \end{pmatrix}$$

Another notation is the so called cycle notation. This notation is useful to exhibit the cycle structure of a permutation and hence for finding the conjugacy classes. Since \mathcal{S}_n is a finite group, for any permutation $\sigma \in \mathcal{S}_n$ and every a_j there must be a positive integer $p \leq n$ with $\sigma^p(a_j) = a_j$. The cycle notation is obtained by writing down all

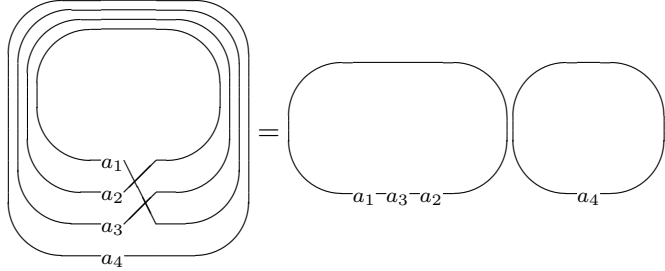
disjoint cycles $(a_j, \sigma(a_j), \dots, \sigma^{p-1}(a_j))$; cycles of length one can be omitted. For the above example one gets

$$(69a) \quad \sigma_1 = (a_1, a_3, a_2)(a_4) = (a_1, a_3, a_4)$$

$$(69b) \quad \sigma_2 = (a_1, a_4)(a_2)(a_3) = (a_1, a_4)$$

$$(69c) \quad \sigma_1 \sigma_2 = (a_1, a_2, a_3, a_4)$$

Graphically one can obtain this notation by closing the loops around the permutation and reading of the labels as one follows every loop. For example for σ_1 one has



As a corollary of the character orthogonality (cf. [Sag01]) the conjugacy classes of the symmetric group label its irreducible representations. This fact is used extensively to obtain a complete list of all irreducible representations, not only of \mathcal{S}_k but also of $\text{Gl}(N)$.

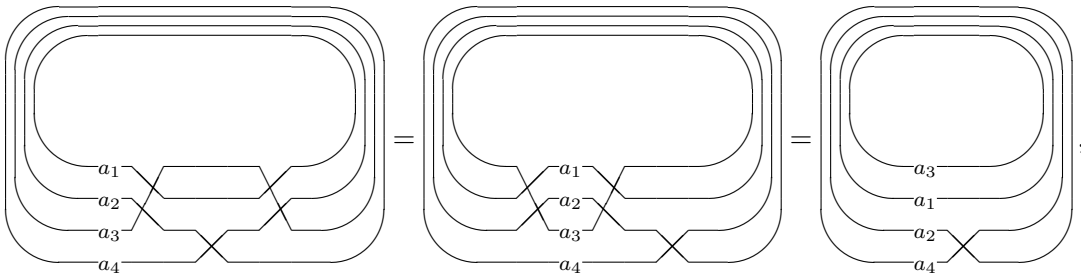
Whenever acting on a tensor, permutations denote a product of Kronecker deltas acting on the indices of a tensor:

$$(70) \quad (a_1, a_2)(a_3, a_4) T^{a_1 a_2 a_3 a_4} = \delta_{a_2}^{a_1} \delta_{a_1'}^{a_2} \delta_{a_4}^{a_3} \delta_{a_3'}^{a_4} T^{a_1' a_2' a_3' a_4'} = T^{a_2 a_1 a_4 a_3}$$

The conjugacy class of a group element $\sigma \in \mathcal{S}_k$ is defined as the set

$$(71) \quad \{\pi \sigma \pi^{-1} | \pi \in \mathcal{S}_k\}$$

One can see that the conjugacy classes of the symmetric group are determined by the cycle structure of each group element, since the extra pair of permutations π and π^{-1} can always be absorbed in a permutation of the labels a_1, \dots, a_k without changing the cycle structure of the permutation. Using σ_1 and σ_2 defined above one obtains:



and hence we have $\sigma_1 \cdot (a_1, a_4) \cdot \sigma_1^{-1} = (a_2, a_4)$. In the diagrammatic notation the decomposition into transpositions can be found by moving the crossings of lines such that all crossings are horizontally separated and therefore the signum of a permutation is just determined by the number line crossings. The signum is a group homomorphism and obeys multiplicativity, $\text{sgn}(\sigma\pi) = \text{sgn}(\sigma) \text{sgn}(\pi)$.

Each conjugacy class is determined by the cycle structure of its elements which in turn can be described by an integer partition denoting the lengths of the cycles. σ_1 contains a three-cycle and a one cycle, σ_2 contains one two-cycle and two one-cycles. One writes

$(1^1, 2^0, 3^1)$ and $(1^2, 2^1)$ respectively where the exponents denote the multiplicities of the different cycle lengths [Sag01]. Alternatively, YOUNG diagrams can be used for the same purpose where the length of each row corresponds to each cycle length,

$$(1^1, 2^0, 3^1) \equiv \begin{array}{|c|c|c|} \hline \square & \square & \square \\ \hline \square & & \\ \hline \end{array} \quad \text{and} \quad (1^2, 2^1) \equiv \begin{array}{|c|c|} \hline \square & \square \\ \hline \square & \square \\ \hline \square & \\ \hline \end{array}.$$

As one can see from the examples, a YOUNG diagram of shape λ is a system of square unit-boxes with λ_j boxes in each row aligned at the left with descending row lengths. The transposed diagram λ' is the diagram with rows and columns exchanged, e.g.

$$\left(\begin{array}{|c|c|c|c|c|} \hline \square & \square & \square & \square & \square \\ \hline \square & \square & \square & & \\ \hline \square & \square & \square & & \\ \hline \square & \square & & & \\ \hline \end{array} \right)' = \begin{array}{|c|c|c|c|} \hline \square & \square & \square & \square \\ \hline \square & \square & \square & \square \\ \hline \square & \square & \square & \\ \hline \square & \square & & \\ \hline \square & & & \\ \hline \end{array}.$$

Cycles of length two are called transpositions. It can be shown that every permutation has a decomposition into transpositions and one can assign an invariant

$$(72) \quad \text{sgn}(\pi) \equiv (-1)^{\text{number of transpositions in } \pi}$$

which does not depend on the way π is decomposed into transpositions. The permutation $(1234) = (34)(23)(12)$ and its signum is $\text{sgn}((1234)) = (-1)^3 = -1$. From this one can construct two one-dimensional and therefore irreducible representations: the trivial representation $\rho(\sigma) = 1$ and the alternating representation $\rho(\sigma) = \text{sgn}(\sigma)$.

For a complete treatment of all irreducible representations, however, one must extend the discussion to group modules. A module V is called a group module of the group G if there is a multiplication such that

$$(73a) \quad gv \in V,$$

$$(73b) \quad g(cv + dw) = c(gv) + d(gw),$$

$$(73c) \quad (gh)v = g(hv) \quad \text{and}$$

$$(73d) \quad \mathbb{I}v = v, \quad \text{where } \mathbb{I} \text{ is the identity in } G,$$

for all $g, h \in G$ and $v, w \in V$ together with¹⁰ $c, d \in \mathbb{C}$. Every group module defines a matrix representation of the group. Let \mathcal{B} be a basis of V and $\langle \cdot, \cdot \rangle$ be the canonical inner product which on two basis vectors $b_i, b_j \in \mathcal{B}$ is $\langle b_i, b_j \rangle = \delta_{ij}$ then the matrices $\rho(g)$,

$$(74) \quad \rho_{ij}(g) \equiv \langle b_i, gb_j \rangle$$

form a representation of the group because¹¹

$$(75) \quad [\rho(g)\rho(h)]_{ij} = \sum_k \langle b_i, gb_k \rangle \langle b_k, hb_j \rangle = \sum_{k', b_{k'} = gb_k} \langle b_i, b_{k'} \rangle \langle g^{-1}b_{k'}, hb_j \rangle = \langle g^{-1}b_i, hb_j \rangle = \langle b_i, ghb_j \rangle = \rho(gh)_{ij}.$$

¹⁰It is sufficient to restrict the discussion to modules over the field \mathbb{C} .

¹¹Note: $\langle g^{-1}b_i, hb_j \rangle = \delta_{g^{-1}b_i, hb_j} = \langle b_i, ghb_j \rangle$ because of the equivalence $g^{-1}b_i = hb_j \Leftrightarrow b_i = ghb_j$.

Two \mathcal{S}_k -modules play a special role: when \mathcal{S}_k acts on the set $\mathbf{S} = \{1, 2, \dots, k\}$ of k formal symbols the space $\mathbb{C}\mathbf{S}$ forms a group module with the action

$$\sigma \sum_{\mathbf{s} \in \mathbf{S}} c_{\mathbf{s}} \mathbf{s} = \sum_{\mathbf{s} \in \mathbf{S}} c_{\mathbf{s}} \sigma(\mathbf{s}), \quad \sigma \in \mathcal{S}_k.$$

This module induces the *defining representation* of the group.

The module $\mathbb{C}[\mathcal{S}_k]$, i.e. the space of all formal linear combinations $\sum_{\sigma \in \mathcal{S}_k} c_{\sigma} \cdot \sigma$ is called the *group algebra*, and the multiplication is defined by the usual group multiplication. The group algebra defines the *regular representation*.

Two particularly useful elements of $\mathbb{C}[\mathcal{S}_k]$ are the so-called symmetrisers and antisymmetrisers on k lines, as introduced in [Cvi08]. Symmetrisers are represented by empty boxes,

$$(76) \quad \begin{array}{|c|} \hline 1 \\ \vdots \\ k \\ \hline \end{array} = \frac{1}{k!} \sum_{\sigma \in \mathcal{S}_k} \sigma$$

and antisymmetrisers by filled boxes

$$(77) \quad \begin{array}{|c|} \hline 1 \\ \vdots \\ k \\ \hline \end{array} = \frac{1}{k!} \sum_{\sigma \in \mathcal{S}_k} \text{sgn}(\sigma) \cdot \sigma$$

As an example those two symbols are given below for \mathcal{S}_3 :

$$\begin{array}{|c|} \hline \\ \hline \end{array} = \frac{1}{3!} \left(\begin{array}{|c|} \hline \\ \hline \end{array} + \begin{array}{|c|} \hline \\ \hline \end{array} + \begin{array}{|c|} \hline \\ \hline \end{array} + \begin{array}{|c|} \hline \\ \hline \end{array} + \begin{array}{|c|} \hline \\ \hline \end{array} + \begin{array}{|c|} \hline \\ \hline \end{array} \right)$$

and the corresponding antisymmetriser is

$$\begin{array}{|c|} \hline \\ \hline \end{array} = \frac{1}{3!} \left(\begin{array}{|c|} \hline \\ \hline \end{array} - \begin{array}{|c|} \hline \\ \hline \end{array} + \begin{array}{|c|} \hline \\ \hline \end{array} - \begin{array}{|c|} \hline \\ \hline \end{array} + \begin{array}{|c|} \hline \\ \hline \end{array} - \begin{array}{|c|} \hline \\ \hline \end{array} \right).$$

These elements have the obvious properties: they are idempotent and they are eigenvectors of the permutations acting exclusively on the lines of the (anti-)symmetriser,

$$(78) \quad \begin{array}{|c|} \hline \times \\ \hline \end{array} = \begin{array}{|c|} \hline \times \\ \hline \end{array} = \begin{array}{|c|} \hline \\ \hline \end{array}, \quad \begin{array}{|c|} \hline \times \\ \hline \end{array} = (-1) \begin{array}{|c|} \hline \times \\ \hline \end{array} = (-1) \begin{array}{|c|} \hline \\ \hline \end{array}.$$

Hence symmetrisers and antisymmetrisers that overlap in more than one line annihilate each other because one can always find a permutation which has different eigenvalues under each of the two algebra elements,

$$(79) \quad (+1) \begin{array}{|c|} \hline \\ \hline \end{array} \begin{array}{|c|} \hline \times \\ \hline \end{array} = \left(\begin{array}{|c|} \hline \times \\ \hline \end{array} \right) \begin{array}{|c|} \hline \\ \hline \end{array} = \begin{array}{|c|} \hline \\ \hline \end{array} \left(\begin{array}{|c|} \hline \times \\ \hline \end{array} \right) = (-1) \begin{array}{|c|} \hline \\ \hline \end{array} \begin{array}{|c|} \hline \times \\ \hline \end{array} = 0.$$

The idempotence of the (anti-)symmetrisers is in fact only a special case of a more general absorption property of smaller (anti-)symmetrisers by bigger one if all lines of

the smaller one are connected to the other one:

$$(80) \quad \begin{array}{c} \text{---} \\ | \\ \text{---} \\ | \\ \text{---} \\ | \\ \text{---} \\ | \\ \text{---} \\ | \\ \text{---} \end{array} = \begin{array}{c} \text{---} \\ | \\ \text{---} \\ | \\ \text{---} \\ | \\ \text{---} \\ | \\ \text{---} \\ | \\ \text{---} \end{array}, \quad \begin{array}{c} \text{---} \\ | \\ \text{---} \\ | \\ \text{---} \\ | \\ \text{---} \\ | \\ \text{---} \\ | \\ \text{---} \end{array} = \begin{array}{c} \text{---} \\ | \\ \text{---} \\ | \\ \text{---} \\ | \\ \text{---} \\ | \\ \text{---} \\ | \\ \text{---} \end{array}.$$

For actual calculations an expansion of the (anti-)symmetrisers would lead to a spurious proliferation of terms and is therefore to avoid. Instead a recursive definition given in [Cvi08] can be used,

$$(81) \quad \begin{array}{c} 1 \\ | \\ 2 \\ | \\ \vdots \\ | \\ p \end{array} = \frac{1}{p} \left(\begin{array}{c} 1 \\ | \\ 2 \\ | \\ \vdots \\ | \\ p \end{array} + (p-1) \begin{array}{c} 1 \\ | \\ 2 \\ | \\ \vdots \\ | \\ p \end{array} \right)$$

and

$$(82) \quad \begin{array}{c} 1 \\ | \\ 2 \\ | \\ \vdots \\ | \\ p \end{array} = \frac{1}{p} \left(\begin{array}{c} 1 \\ | \\ 2 \\ | \\ \vdots \\ | \\ p \end{array} - (p-1) \begin{array}{c} 1 \\ | \\ 2 \\ | \\ \vdots \\ | \\ p \end{array} \right).$$

In this representation of the (anti-)symmetrisers the smaller elements can be reused in a computation which reduces the run time for the computation of a symmetriser to polynomial rather than factorial.

2.2. Garnir Relations and Young's Natural Representation. The goal of this section is to define a set of projectors P_λ into invariant subspaces $V^\lambda \subseteq \mathbb{C}\mathcal{S}_k$ for integer partitions (i.e. YOUNG diagrams) $\lambda \vdash k$ of k . The GARNIR relations then allow to construct irreducible matrix representations ρ_λ for each group element.

Before the construction of the projectors can be addressed, a couple of well known combinatorial facts about YOUNG diagrams have to be reviewed (see for example [Ful97, Sag01]). First of all, the notion of a *tableau* has to be introduced.

Definition 1 (YOUNG Tableau). *Let $\lambda = (\lambda_1, \lambda_2, \dots, \lambda_p) \vdash n$ be an integer partition, $\lambda_1 \geq \lambda_2 \geq \dots \geq \lambda_p$ and A be an alphabet ($\epsilon \in A$). The pair $Y = (\lambda, \rho)$ where ρ is a mapping $\rho : \mathbb{N} \times \mathbb{N} \mapsto A$ with $\rho(i, j) = \epsilon$ iff $i > p \vee j > \lambda_i$ defines a YOUNG tableau of shape λ over the alphabet A . If no alphabet is specified the positive integer numbers are understood. Tableaux are denoted by a YOUNG diagram with the values $\rho(i, j)$ filled into its boxes at the i -th row and j -th column.*

The filling of a tableau $Y = (\lambda, \rho)$ over the positive integer numbers is the integer partition built from all entries $\rho(i, j) \neq \epsilon$.

The shape of a diagram $Y = (\lambda, \rho)$ is also denoted as $\text{sh}(Y) = \lambda$.

Examples for YOUNG tableaux with the filling $(1^2, 2, 3^2)$ are

$$\begin{array}{|c|c|} \hline 1 & 1 \\ \hline 2 & 3 \\ \hline 3 & \\ \hline \end{array}, \begin{array}{|c|c|} \hline 1 & 2 \\ \hline 3 & 1 \\ \hline 3 & \\ \hline \end{array}, \begin{array}{|c|c|c|} \hline 1 & 1 & 3 \\ \hline 2 & 3 & \\ \hline \end{array}.$$

The first two diagrams have the same shape. Two properties of tableaux over alphabets with an ordering¹² are the following:

Definition 2 ((Semi)-Standard Tableau). A YOUNG tableau is called a *standard tableau* if for all elements inside the shape of the tableau have $\rho(i, j) < \rho(i, j+1)$ and $\rho(i, j) < \rho(i+1, j)$, i.e. the entries are strictly increasing along both the rows and the columns. A tableau is called *semi-standard* if the elements inside the shape of the tableau have $\rho(i, j) \leq \rho(i, j+1)$ and $\rho(i, j) < \rho(i+1, j)$, i.e. the entries are strictly increasing along the columns and non-decreasing along the rows.

In the above example the first and the last tableau are semi-standard. None of the three tableaux is a standard tableau because no filling with repeated elements gives a standard tableau.

One combinatorial quantity which appears in many of the later formulæ is the hook number $h_\lambda = \prod_{i,j} h_{ij}$: it is constructed by filling the entries $\rho(i, j)$ of a tableau by the hook length h_{ij} of each box, where the hook length is the number of boxes below and to the right of the box including the box itself. For example in the diagram below $h_{22} = 4$, and $h_\lambda = 537600$ because

$$h_{22} = \begin{array}{|c|c|c|c|} \hline & & & \\ \hline & \bullet & \bullet & \\ \hline & \bullet & & \\ \hline & \bullet & & \\ \hline \end{array} = 4, \quad h_\lambda = \prod \begin{array}{|c|c|c|c|c|} \hline 8 & 7 & 5 & 2 & 1 \\ \hline 5 & 4 & 2 & & \\ \hline 4 & 3 & 1 & & \\ \hline 2 & 1 & & & \\ \hline \end{array} = 8 \cdot 7 \cdot 5^2 \cdot 4^2 \cdot 3 \cdot 2^3 = 537600.$$

The number of standard tableaux (with the number $1 \dots k$ as filling) of a given shape $\lambda \vdash k$ is

$$(83) \quad f^\lambda = \frac{k!}{h_\lambda}.$$

A proof for this formula can be found in [Sag01].

The so-called YOUNG projectors can be defined as follows:

Definition 3 (YOUNG Projector). For a given standard tableau Y of shape $\lambda \vdash k$ where the entries of the boxes label a set of k lines, the product of symmetrisers on all lines according to the rows of the YOUNG diagram and antisymmetrisers (multiplied from the right) according to the columns of the same diagram together with the normalisation factor¹³

$$(84) \quad \alpha = \frac{\prod_j \lambda_j! \prod_i \lambda'_i!}{h_\lambda}$$

and an appropriate permutation between the symmetrisers and the antisymmetrisers is called the YOUNG projector P_Y of the standard tableau Y .

As an example $\lambda = \begin{array}{|c|c|c|} \hline & & \\ \hline & & \\ \hline \end{array}$ is chosen. The normalisation factor is

$$h_{\begin{array}{|c|c|c|} \hline & & \\ \hline & & \\ \hline \end{array}} = \frac{(3!2!2!)(3!3!1!)}{\prod \begin{array}{|c|c|c|} \hline 5 & 4 & 1 \\ \hline 3 & 2 & \\ \hline 2 & 1 & \\ \hline \end{array}} = \frac{9}{5}$$

¹²For the ease of notation one can assume $a < \epsilon \forall a \in A - \{\epsilon\}$.

¹³ λ' denotes the transposed YOUNG diagram, as defined on Page 29.

and hence the projector is

$$P \begin{array}{|c|c|c|} \hline 1 & 2 & 3 \\ \hline 4 & 5 & \\ \hline 6 & 7 & \\ \hline \end{array} = \frac{9}{5} \cdot \begin{array}{c} \text{Diagram of a projector with 7 lines and 3 columns. The first column has three boxes (symmetrisers) and the second column has three boxes (antisymmetrisers). Lines connect the boxes in a specific permutation pattern. The third column has three boxes (symmetrisers). The diagram is a Young diagram for the partition (3,3,1).} \end{array}.$$

The above definition seems somewhat arbitrary and it is neither clear that P_Y is in fact a projector nor if the definition specifies P_Y uniquely. The following theorems fix that shortcoming and their proofs follow mainly [ECK03].

Theorem 1 (Uniqueness of P_Y). *There is only one independent, non-vanishing choice of the permutation that connects the symmetrisers of a projector P_Y on their right to the antisymmetrisers on their left. Rearranging any non-vanishing choice of the internal lines of the projector to any other non-vanishing choice of that permutation leads to a global factor of ± 1 .*

The proof is done by induction over the number of columns [ECK03]. For only one column of length k the projector consists of k symmetrisers of one line each and one antisymmetriser of length k . In this case swapping two lines at the left leads to a factor (-1) by the definition of the antisymmetriser. Adding a column of length k at the left to a projector corresponding to a standard tableau Y of shape λ with $k' \leq k$ rows corresponds to adding another line to each existing symmetriser, adding an antisymmetriser of length k and possibly adding $(k - k')$ new symmetrisers of length 1 each. Now there are k symmetrisers of various lengths and at least one antisymmetriser of length k . Since one cannot connect two lines of that antisymmetriser to the same symmetriser there is essentially one way of connecting those k lines, and the different possibilities can be canonicalised by allowing a factor ± 1 and swapping legs at the single symmetrisers and antisymmetrisers. Connecting the remaining lines now reduces to connecting the lines of the tableau of the previous induction step.

Theorem 2 (Properties of P_λ). *The YOUNG projectors have the following properties:*

- (a) $P_Y P_Z = \delta_{YZ} P_Y$, where $\text{sh}(Y), \text{sh}(Z) \vdash k$
- (b) $\sum_Y P_Y = \mathbb{I}_k$, where the sum runs over all standard tableaux Y with $\text{sh}(Y) \vdash k$
- (c) $P_Y \sigma P_Y = m_Y(\sigma) P_Y$ and $m_Y(\sigma) \in \{0, \pm 1\}$ for any permutation $\sigma \in \mathcal{S}_k$, $\text{sh}(Y) \vdash k$.

Property (c) is the easiest to prove since the antisymmetrisers of the projector on the left and the symmetrisers of the projector on the right with σ in between can be read as a YOUNG projector from right to left. The uniqueness argument 1 holds and proves $m_Y(\sigma) \in \{0, \pm 1\}$.

If in property (a) the shapes of Y and Z are the same, the permutation between the antisymmetrisers of Y and the symmetrisers of Z is either equal to the inverse of the internal permutation in Z in which case $Y = Z$, or it is different (for $Y \neq Z$) in which case $P_Y P_Z = 0$ due to (c). For $\text{sh}(Y) \neq \text{sh}(Z)$ we consider the case where

some¹⁴ column of Y is longer than in Z . Then it is easy to see that at least two lines coming from the same antisymmetriser have to be connected to the same symmetriser at the second projector and hence the product vanishes. For the reverse case, i.e. one column in Z is longer than in Y , one can expand out the antisymmetrisers in Y and the symmetrisers in Z ; for every term in the sum one can apply the above argument and hence the product must vanish.

Only the completeness (b) and the idempotence $P_Y P_Y = P_Y$ remain to be shown. Using the uniqueness argument again one can again expand out the inner symmetrisers and antisymmetrisers of $P_Y P_Y$ and obtains idempotence up to a normalisation:

$$(85) \quad P_Y P_Y = P_Y \cdot \text{const}$$

and the sum runs over all permutations with their appropriate signs that appear in the expansion of the internal (anti-)symmetrisers.

In order to complete the proof one has to establish that the P_Y with Y running over all standard tableaux $\text{sh}(Y) \vdash k$ form a complete basis of \mathbb{CS}_k . The integer partitions of $\lambda \vdash k$ label the conjugacy classes, and the standard tableaux of shape λ form a basis of each subspace $V^\lambda \equiv P_\lambda \cdot \mathbb{CS}_k$. The latter statement is proved¹⁵ by the

Theorem 3 (GARNIR Relations). *The action of a permutation σ acting on a YOUNG projector P_Y in a way that σY corresponds to non-standard tableau can always be expressed in terms of a linear combination of YOUNG projectors*

$$\sigma P_Y = \sum_Z c_{\sigma,Z} P_Z$$

with complex numbers $c_{\sigma,Z}$ and the sum running over all standard tableaux $\text{sh}(Z) = \text{sh}(Y)$. The coefficients are generated by repeatedly applying the following algorithm, which terminates:

For two adjacent columns j and $(j+1)$ in πY with the elements $(a_1 < a_2 < \dots < a_p)$ and $(b_1 < b_2 < \dots < b_q)$ respectively find the smallest index r such that $a_r > b_r$. Let $A = \{a_r, a_{r+1}, \dots, a_p\}$ and $B = \{b_1, b_2, \dots, b_r\}$ and form the GARNIR element

$$(86) \quad g_{A,B} = \sum_{\pi} \text{sgn}(\pi) \pi$$

where the sum runs over all permutations $\pi \in \mathcal{S}_{A \cup B}$ which leave the ordering of each column-strip $\pi(a_r, \dots, a_p)$ and $\pi(b_1, \dots, b_r)$ intact. The GARNIR element annihilates σP_Y , and since the identity is always in the sum, one can replace

$$(87) \quad \sigma P_Y = \sum_{\pi \neq \text{id}} \text{sgn}(\pi) \pi \sigma P_Y.$$

To finish the proof of Theorem 2 it now is sufficient to show that α_Y is chosen such that $\sum P_Y = \mathbb{I}$. One can use the fact that in the expansion of P_Y the identity appears only once (see [ECK03]) and hence can write the completeness relation as

$$(88) \quad \mathbb{I} = \sum_Y \alpha_Y \frac{1}{\prod_{\lambda_i: \lambda = \text{sh}(Y)} \lambda_i! \prod_{\lambda'_j: \lambda = \text{sh}(Y)} \lambda'_j!} \mathbb{I}$$

¹⁴If necessary the same recursive argument as in Theorem 1 can be used.

¹⁵For a proof the reader is referred to [Ful97, Sag01].

we can now use that $\alpha_Y \equiv \alpha_\lambda$ in fact only depends on the shape $\lambda = \text{sh}(Y)$ and rewrite the sum as a sum over partitions:

$$(89) \quad 1 = \sum_{\lambda \vdash k} \frac{\alpha_\lambda f^\lambda}{\prod_{\lambda_i} \lambda_i! \prod_{\lambda'_j} \lambda'_j!} = k! \sum_{\lambda \vdash k} \frac{\alpha_\lambda / h_\lambda}{\prod_{\lambda_i} \lambda_i! \prod_{\lambda'_j} \lambda'_j!}.$$

Plugging in the expression for α_λ and the relation for the dimensions of the conjugacy classes $k! = \sum_\lambda (f^\lambda)^2$ one immediately proves everything because the idempotence can be obtained from multiplying $\mathbb{I} = \sum_Y P_Y$ by P_Z and using orthogonality.

Along the way we also proved that those representations are in fact the irreducible representations which is due to the fact that they are constructed from the conjugacy classes of the group.

Construction of the Representation Matrices. Before going on to the actual construction of the representation matrices the results of the first part of this section are summarised below: the projectors $\langle P_{Y_1}, P_{Y_2}, \dots, P_{Y_{f^\lambda}} \rangle$, Y_i being the standard tableaux of shape $\text{sh}(Y_i) = \lambda \vdash k$, form an orthogonal basis of the invariant subspaces $V^\lambda \subset \mathbb{C}\mathcal{S}_k$. The GARNIR relations establish a constructive proof and allow the calculation of the coefficients $\rho_{ij}(\sigma)$ as defined below:

$$(90) \quad \sigma P_{Y_i} = \sum_{j=1}^{f^\lambda} \rho_{ij}(\sigma) P_{Y_j}.$$

This notation suggests that the matrices

$$(91) \quad \rho(\sigma) = (\rho_{ij}(\sigma))_{i,j=1}^{f^\lambda}$$

form a f^λ -dimensional representation of the symmetric group, the caveat being that the matrices multiply from the right as one multiplies permutations to the left, as can be seen below,

$$(92) \quad \sigma_1 \sigma_2 P_{Y_i} = \sigma_1 \sum_{j=1}^{f^\lambda} \rho_{ij}(\sigma_2) P_{Y_j} = \sum_{j=1}^{f^\lambda} \rho_{ij}(\sigma_2) \sum_{k=1}^{f^\lambda} \rho_{jk}(\sigma_1) P_{Y_k} = \sum_{k=1}^{f^\lambda} (\rho(\sigma_2) \rho(\sigma_1))_{ik} P_{Y_k}.$$

The matrices satisfy $\rho(\sigma_1 \sigma_2) = \rho(\sigma_2) \rho(\sigma_1)$, so in fact $\rho(\sigma)^T$ would make a representation matrix in the ordinary sense. It is also clear from its definition that $\rho(\text{id}) = \mathbb{I}$ as required.

An explicit example for the representation $\lambda = \square$ is given below to clarify the construction of the representation matrices. The basis of this subspace consists of the five standard tableaux

$$Y_1 = \begin{array}{|c|c|} \hline 1 & 2 \\ \hline 3 & 4 \\ \hline 5 & \\ \hline \end{array}, \quad Y_2 = \begin{array}{|c|c|} \hline 1 & 3 \\ \hline 2 & 4 \\ \hline 5 & \\ \hline \end{array}, \quad Y_3 = \begin{array}{|c|c|} \hline 1 & 2 \\ \hline 3 & 5 \\ \hline 4 & \\ \hline \end{array}, \quad Y_4 = \begin{array}{|c|c|} \hline 1 & 3 \\ \hline 2 & 5 \\ \hline 4 & \\ \hline \end{array}, \quad Y_5 = \begin{array}{|c|c|} \hline 1 & 4 \\ \hline 2 & 5 \\ \hline 3 & \\ \hline \end{array}.$$

The corresponding projectors are, up to a common normalisation factor,

$$P_{Y_1} = \text{diagram}, P_{Y_2} = \text{diagram}, P_{Y_3} = \text{diagram}, P_{Y_4} = \text{diagram}, P_{Y_5} = \text{diagram}.$$

Applying the permutation $\sigma = (354)$ to P_{Y_1} leads to a non-standard ordering of the lines,

$$(93) \quad \sigma P_{Y_1} = \text{diagram}$$

whereas on P_{Y_3} the action of σ is trivial,

$$(94) \quad \sigma P_{Y_3} = \text{diagram} = \text{diagram} = \text{diagram} = P_{Y_1}.$$

To reduce (93) one has to apply the GARNIR relations, which as a diagrammatic analogue can be represented by applying a symmetriser on the left to the legs according to the set $A \cup B$ in Theorem 3:

$$(95) \quad 0 = \text{diagram} = \frac{2}{3!} \left(\text{diagram} + \text{diagram} + \text{diagram} \right) = \frac{2}{3!} (P_{Y_1} + \sigma P_{Y_1} + P_{Y_3})$$

The action of σ on V^λ can summarise in a system of equations,

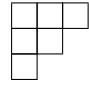
$$(96) \quad \sigma \begin{pmatrix} P_{Y_1} \\ P_{Y_2} \\ P_{Y_3} \\ P_{Y_4} \\ P_{Y_5} \end{pmatrix}^\top = \begin{pmatrix} -P_{Y_1} - P_{Y_3} \\ P_{Y_5} \\ P_{Y_1} \\ -P_{Y_1} - P_{Y_2} \\ -P_{Y_3} - P_{Y_4} \end{pmatrix}^\top = \begin{pmatrix} P_{Y_1} \\ P_{Y_2} \\ P_{Y_3} \\ P_{Y_4} \\ P_{Y_5} \end{pmatrix}^\top \cdot \begin{pmatrix} -1 & 0 & 1 & -1 & 0 \\ 0 & 0 & 0 & -1 & 0 \\ -1 & 0 & 0 & 0 & -1 \\ 0 & 0 & 0 & 0 & -1 \\ 0 & 1 & 0 & 0 & 0 \end{pmatrix}$$

$\text{Gl}(N)$ -Dimensions. So far the only representations of the symmetric group have been considered. It is well known that by acting with the appropriate \mathcal{S}_k -projectors on the direct product of k copies of vectors in the fundamental representation of $\text{Gl}(N)$, one generates the irreducible representations of $\text{Gl}(N)$. The dimensions of these $\text{Gl}(N)$ -representations is calculated as follows: Let Y be one of the standard tableaux¹⁶ of shape λ . The $\text{Gl}(N)$ -dimension of the irreducible representation constructed from the projectors P_Y is

$$(97) \quad \dim_{\text{Gl}(N)} P_Y = \text{tr}\{P_Y\} = \frac{h_\lambda(n)}{h_\lambda},$$

where $h_\lambda(n)$ is the modified hook number constructed as follows: the top-left box of the diagram λ is filled with the symbol n , all other boxes are filled increasing by one

¹⁶ The representations are labelled by the integer partitions, not by individual tableaux. I have chosen an arbitrary basis-element Y only in order to remain consistent in the notation P_Y , where Y has to be a standard tableau.

along the rows and decreasing along the columns. For $\lambda =$  one gets

$$\dim_{\text{Gl}(N)} P_{\begin{smallmatrix} \square & \square & \square \\ \square & \square \\ \square \end{smallmatrix}} = \frac{\prod_{\begin{smallmatrix} \square & \square & \square \\ \square & \square \\ \square \end{smallmatrix}} \begin{matrix} n & n+1 & n+2 \\ n-1 & n \\ n-2 \end{matrix}}{\prod_{\begin{smallmatrix} \square & \square & \square \\ \square & \square \\ \square \end{smallmatrix}} \begin{matrix} 5 & 3 & 1 \\ 3 & 1 \\ 1 \end{matrix}} = \frac{n^2(n^2-1)(n^2-4)}{45}.$$

Amongst other proofs a diagrammatic version of the proof based on a colouring algorithm has been presented by the authors of [ECK03]. Since every index of the tensor runs over the value $1, \dots, n$ and the indices are symmetrised along the rows and anti-symmetrised along the columns of the YOUNG diagram λ , the semi-standard tableaux of shape λ over the alphabet $\{1, \dots, n\}$ enumerate the independent components of the tensor which is the same as the number in (97).

With respect of the irreducible representations, the only difference between $\text{Gl}(N)$ and its subgroups, such as $SU(N)$ and $SO(N)$, are the appearance of additional invariant tensors that can reduce irreducible representations of $\text{Gl}(N)$ further. For $SU(N)$ the new tensor is the totally antisymmetric LEVI-CIVITA tensor which diagrammatically can be represented by half an antisymmetriser over n lines [Cvi08]:

$$(98a) \quad \epsilon^{a_1 a_2 \dots a_n} = i^{-n(n-1)/2} \sqrt{n!} \begin{array}{c} \text{---} a_1 \\ \text{---} a_2 \\ \vdots \\ \text{---} a_n \end{array}$$

$$(98b) \quad \epsilon_{a_1 a_2 \dots a_n} = i^{n(n-1)/2} \sqrt{n!} \begin{array}{c} a_1 \text{---} \\ a_2 \text{---} \\ \vdots \\ a_n \text{---} \end{array}$$

The normalisation in front of the tensor has been chosen such that

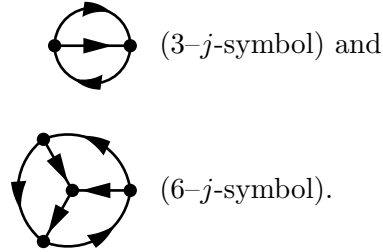
$$(99) \quad \begin{array}{c} \text{---} \\ \text{---} \\ \text{---} \end{array} \begin{array}{c} \text{---} \\ \text{---} \\ \text{---} \end{array} = \begin{array}{c} \text{---} \\ \text{---} \\ \text{---} \end{array} \quad \text{and} \quad \begin{array}{c} \text{---} \\ \text{---} \\ \text{---} \end{array} \begin{array}{c} \text{---} \\ \text{---} \\ \text{---} \end{array} = 1.$$

For the representations the existence of this invariant tensor implies that any projector that contains a column of length n can be decomposed and is no longer irreducible. Hence, in $SU(N)$ representations with extra columns of length n have to be regarded equivalent to those with the columns of length n being stripped off, for $n = 3$ for example one has

$$\begin{array}{|c|c|c|c|} \hline \bullet & \bullet & & \\ \hline \bullet & \bullet & & \\ \hline \bullet & \bullet & & \\ \hline \end{array} \equiv \begin{array}{|c|c|c|} \hline \bullet & & \\ \hline \bullet & & \\ \hline \bullet & & \\ \hline \end{array} \equiv \begin{array}{|c|c|} \hline & \\ \hline & \\ \hline \end{array}.$$

Similarly, one obtains the representations of the orthogonal group by removing all traces, since in $SO(N)$ the metric g_{ν}^{μ} forms another invariant tensor. As a consequence the treatment of $SO(N)$ is more complicated since the number of boxes is not conserved anymore and therefore this work is restricted to the treatment of the unitary group.

2.3. Calculation of n - j Symbols in $SU(N)$. In Section 1.4 it has been shown that only three kinds of numeric invariants are enough to calculate any vacuum-bubble diagram, i.e. a diagram with no external indices and therefore corresponds to a scalar. They are the $Gl(N)$ -dimension (1 - j -symbols),



In terms of projectors, the CLEBSH-GORDAN vertices are up to a phase,

$$(100) \quad \begin{array}{c} \nearrow \\ \bullet \\ \nwarrow \end{array} \rightarrow \begin{array}{c} \text{---} \text{---} \text{---} \\ \boxed{X} \\ \text{---} \text{---} \text{---} \\ \text{---} \text{---} \text{---} \\ \boxed{Y} \\ \text{---} \text{---} \text{---} \\ \text{---} \text{---} \text{---} \\ \boxed{Z} \\ \text{---} \text{---} \text{---} \end{array}$$

where the boxes represent the appropriate projectors.

Therefore the n - j -symbols are

$$\begin{aligned} \text{Triangle} &= \text{tr}\{P_X P_Y P_Z\} = \text{tr} \left\{ \begin{array}{c} \text{---} \text{---} \text{---} \\ \boxed{Z} \\ \text{---} \text{---} \text{---} \\ \text{---} \text{---} \text{---} \\ \boxed{X} \\ \text{---} \text{---} \text{---} \\ \text{---} \text{---} \text{---} \\ \boxed{Y} \\ \text{---} \text{---} \text{---} \\ \text{---} \text{---} \text{---} \end{array} \right\} \\ \text{Hexagon} &= \text{tr}\{P_\xi P_\nu P_\mu P_\beta P_\gamma P_\chi\} = \text{tr} \left\{ \begin{array}{c} \text{---} \text{---} \text{---} \text{---} \text{---} \text{---} \\ \boxed{\xi} \\ \text{---} \text{---} \text{---} \text{---} \text{---} \text{---} \\ \text{---} \text{---} \text{---} \text{---} \text{---} \text{---} \\ \boxed{\nu} \\ \text{---} \text{---} \text{---} \text{---} \text{---} \text{---} \\ \text{---} \text{---} \text{---} \text{---} \text{---} \text{---} \\ \boxed{\mu} \\ \text{---} \text{---} \text{---} \text{---} \text{---} \text{---} \\ \text{---} \text{---} \text{---} \text{---} \text{---} \text{---} \\ \boxed{\beta} \\ \text{---} \text{---} \text{---} \text{---} \text{---} \text{---} \\ \text{---} \text{---} \text{---} \text{---} \text{---} \text{---} \\ \boxed{\gamma} \\ \text{---} \text{---} \text{---} \text{---} \text{---} \text{---} \\ \text{---} \text{---} \text{---} \text{---} \text{---} \text{---} \\ \boxed{\chi} \\ \text{---} \text{---} \text{---} \text{---} \text{---} \text{---} \\ \text{---} \text{---} \text{---} \text{---} \text{---} \text{---} \\ \boxed{\xi} \end{array} \right\} \end{aligned}$$

In the second step the idempotence of the largest projector and the cyclicity of the trace have been used. It is clear that the n -dependence only comes in through the dimension $\dim_{Gl(N)}(P_Z)$ ($\dim_{Gl(N)}(P_\xi)$ resp.) of the highest weight representation occurring in the diagram: the smaller projectors sandwiched in between the largest can be expanded leading only to a sum of permutations σ of which the contribution to the result is $m_Z(\sigma)$ ($m_\xi(\sigma)$ resp.). Hence, the 3- j - and 6- j -symbols can be evaluated as a trace of \mathcal{S}_k -representation matrices times the $Gl(N)$ -dimension of the highest weight

representation,

$$\begin{aligned}
 \text{Diagram 1: A circle with two horizontal arrows pointing right.} &= \dim_{\text{Gl}(N)}(P_Z) \alpha_X \alpha_Y \alpha_Z \text{tr}\{\rho_Z(P_X) \rho_Z(P_Y) \rho_Z(Z)\} \quad \text{and} \\
 \text{Diagram 2: A circle with four arrows forming a cycle: top-left to top-right, top-right to bottom-right, bottom-right to bottom-left, bottom-left to top-left.} &= \dim_{\text{Gl}(N)}(P_\xi) \alpha_\xi \alpha_\mu \alpha_\nu \alpha_\beta \alpha_\gamma \alpha_\chi \text{tr}\{\rho_\xi(P_\xi) \rho_\xi(P_\nu) \rho_\xi(P_\mu) \rho_\xi(P_\beta) \rho_\xi(P_\gamma) \rho_\xi(P_\chi)\}.
 \end{aligned}$$

In the calculation one can make use of the fact that $\rho_Z(Z) = vw^\top$, where $v_j = \delta_{ZY_j}$, $w_i = m_Z(\sigma_{Y_i})$, and σ_{Y_i} is the permutation that has to be applied to the canonical projector¹⁷ to obtain P_{Y_i} . The representation matrices of the permutations are constructed in YOUNG's natural representation as explained in Section 2.2, the matrices for the antisymmetrisers and symmetrisers are built recursively using Equations (81) and (82).

2.4. The Littlewood-Richardson Rule. One of the remaining problems for an actual implementation of an algorithm, using a reduction of the $SU(N)$ -group structure of a FEYNMAN diagram into irreducible pieces, is the determination of the representations λ occurring in the completeness relation (61) together with their multiplicities. The second problem to be solved is fixing the freedom of having additional permutations between μ , ν and λ in the equation above; especially in the case where the multiplicity $c_{\mu\nu}^\lambda$ of a representation λ is larger than one, one has to find $c_{\mu\nu}^\lambda$ independent permutations which span the subspace concerned.

In 1934 LITTLEWOOD and RICHARDSON [LR34] formulated a rule to calculate the multiplicities, that is the LITTLEWOOD-RICHARDSON (LR) coefficients $c_{\mu\nu}^\lambda$ in the decomposition

$$(101) \quad V^\mu \otimes V^\nu = \bigoplus_{\lambda} c_{\mu\nu}^\lambda V^\lambda$$

The formulation of the LR rule requires us to introduce the concept of skew-tableaux:

Definition 4 (Skew Tableau). *The skew tableau λ/μ ($\lambda_i \geq \mu_i, \forall i$) is obtained from a YOUNG tableau of shape λ by removing all boxes of the partition μ from the top left corner. The shape of the remaining boxes is preserved, i.e. the boxes are not aligned at the left. Skew tableaux are denoted as follows:*

$$\lambda = \begin{array}{|c|c|c|c|} \hline \square & \square & \square & \square \\ \hline \square & \square & \square & \square \\ \hline \square & & & \\ \hline \end{array}, \mu = \begin{array}{|c|c|} \hline \square & \square \\ \hline \square & \square \\ \hline \end{array} \Rightarrow \lambda/\mu = \begin{array}{|c|c|c|c|} \hline \blacksquare & \blacksquare & \square & \square \\ \hline \blacksquare & \square & \square & \square \\ \hline \square & & & \\ \hline \end{array}$$

The LR rule counts skew tableaux of which the row words are *reverse lattice words*.

Definition 5 (Lattice word). *A lattice word (also lattice permutation, ballot sequence or YAMANOUCI word) is a word $x_1 x_2 \dots x_p$ of positive integers such that at each*

¹⁷i.e. the projector corresponding to the tableau which is filled by $1, 2, \dots, k$ when the rows are read line-wise left to right and top to bottom

position $i \leq p$ for each x , $1 < x \leq \max_{j \leq i}(x_j)$ the number $x - 1$ occurs at least as often as x .

A reverse lattice word is a word $x_1 x_2 \dots x_p$ such that the reverse word $x_p x_{p-1} \dots x_1$ is a lattice word.

The LR rule then states the following.

Theorem 4 (LITTLEWOOD-RICHARDSON rule). *The value of the coefficient $c_{\mu\nu}^\lambda$ in the decomposition*

$$V^\mu \otimes V^\nu = \bigoplus_{\lambda} c_{\mu\nu}^\lambda V^\lambda$$

is the number of skew semi-standard tableaux of shape λ/μ filled with the numbers of the partition $(1^{\nu_1}, 2^{\nu_2} \dots)$ such that its row word is a reverse lattice word. The row word is obtained by reading the rows of the skew tableau from left-to right, bottom to top.

As an example we consider the multiplication of

$$\mu = \begin{array}{|c|c|} \hline & \\ \hline & \\ \hline \end{array} \quad \text{and} \quad \nu = \begin{array}{|c|c|} \hline & \\ \hline & \\ \hline \end{array}$$

The only non-zero coefficients stem from those partitions λ where the number of boxes is the same on both sides of the equation¹⁸.

As a first step we have to generate all integer partitions $\lambda \vdash k$, where k is the sum of the number of boxes in μ and ν . Only those partitions contribute to the result where $\lambda_i \geq \mu_i$ for all rows; the authors of [ZS98] present an algorithm which generates integer partitions in lexicographic order such that one can stop the iteration when the first partition is lexicographically smaller than μ .¹⁹ For generating the ballot sequences we can use the algorithm given in [NW78]. For the example we get the skew tableaux

Hence the partition $\begin{array}{|c|c|} \hline & \\ \hline & \\ \hline \end{array}$ has a multiplicity $c_{\mu\nu}^\lambda = 2$ whereas the other partitions appear only once in the decomposition.

One can check that no representations are missing and all LR coefficients are correct by ensuring that the dimensions on both sides add up

$$(102) \quad d_{\text{Gl}(N)}(\mu) \cdot d_{\text{Gl}(N)}(\nu) = \sum_{\lambda} c_{\mu\nu}^\lambda d_{\text{Gl}(N)}(\lambda).$$

As mentioned at the beginning of this section, for our algorithm in addition to the multiplicities one also needs according permutations that span the subspace V^λ . This can be achieved by the observation [Ful97] that one can construct a standard tableau Y_w of shape ν from the skew tableau λ/μ as constructed above: for each lattice word $w = x_1 x_2 \dots x_p$ occurring in the LR rule, put the number i in the x_i -th row, filling the rows from left to right. The permutation between the tableau Y_w and the canonical

¹⁸This is an obvious corollary of the LR rule.

¹⁹If a partition λ is lexicographically smaller than μ it implies that $\lambda_i \geq \mu_i$ fails.

The remainder of this section describes graph algorithms to determine the topological properties of the diagram. Algorithm 2 summarises the steps that are required for the tensor reduction, after one has projected on the irreducible basis of trees.

Algorithm 2 GRAPH REDUCTION(G). Returns the value associated with a bubble graph as a function in n .

Require: a bubble graph G as an array of tuples (i, j, λ) .

```

 $L \leftarrow \text{FIND LOOPS}(G)$ .
 $S \leftarrow \text{SHORTEST LOOP}(L)$ .
if LENGTH( $S$ )  $\geq 4$  then
    Select a pair of edges  $X, Y$  from  $S$ .
    return  $\sum_Z c_Z^{X,Y} \cdot \text{GRAPH REDUCTION}(G')$ , where  $G'$  is the Graph that is generated by inserting  $Z$  according to Equation (61).
else if LENGTH( $S$ ) = 3 then
    return  $c \cdot \text{GRAPH REDUCTION}(G')$ , where  $G'$  is generated by Equation (64) and  $c$  is the appropriate coefficient.
else if LENGTH( $S$ ) = 2 then
    return  $c \cdot \text{GRAPH REDUCTION}(G')$ , where  $G'$  is generated by Equation (60) and  $c$  is the appropriate coefficient.
else
    return the dimension  $\dim(\lambda)$  of the representation  $\lambda$  corresponding to this line.
end if

```

If one allows for disconnected graphs Algorithm 2 has to be run on every connected component of the graph. Efficient algorithms for finding connected components as well as finding cycles can be, found for example, in [GF64, Knu97, KBR07]: Algorithm 3 enumerates the connected components of a graph and Algorithm 4 returns a list of all cycles.

All array indices are assumed to be 1-based, and the symbols V_G denotes the number of vertices in a graph G and E_G the number of edges. The ancestor function A is defined as [KBR07],

$$(104) \quad A(i, F) = \begin{cases} i, & F[i] = 0 \text{ or } F[i] = i, \\ A(F[i], F), & \text{else.} \end{cases}$$

A vector of the space $(\mathbb{Z}_3)^{E_G}$ is called a \mathbb{Z}_3 -chain. Let $z = \langle z_1, \dots, z_{E_G} \rangle \in (\mathbb{Z}_3)^{E_G}$ describe a cycle in the graph G , and $G[k] = (i, j, \lambda)$. z_k is therefore zero if the edge of index k is not an element of the cycle, $z_k = +1$ if $G[k]$ is an element and $z_k = -1$ if the cycle contains $G[k]$ against its orientation, i.e. the cycle contains (j, i, λ) . Similarly to A one can define a function A_R that keeps also track of the path between two vertices,

$$(105) \quad A_R(i, F) = \begin{cases} (i, \langle 0 \dots 0 \rangle), & F[i] = 0 \text{ or } F[i] = i, \\ (i', r' + R[i]), & \text{else, where } (i', r') = A_R(F[i], F). \end{cases}$$

For the reduction algorithm the selection of the shortest cycle is not essential: for the the algorithm to terminate any random selection of a edge pairs (X, Y) that reduces the length of a cycle²¹ is sufficient. On the other hand the order in which the reduction

²¹and does not increase the length of all other cycles

Algorithm 3 FIND CONNECTED COMPONENTS(G). Returns a partition of the indices of the edges into their connected components.

Require: a bubble graph G as an array of tuples (i, j, λ) .

```

 $P \leftarrow \emptyset; F[i] \leftarrow i \quad \forall i \in 1 \dots V_G.$ 
for all  $(i, j, \lambda) \in G$  do
  if  $A(i, F) \neq A(j, F)$  then
     $F[A(i, F)] \leftarrow A(j, F).$ 
  end if
end for
 $R \leftarrow \{A(i, F) | i = 1 \dots V_G\}.$ 
for all  $r \in R$  do
   $P \leftarrow P \cup \{i \in 1 \dots V_G | A(i, F) = r\}.$ 
end for
return  $P$ 

```

Algorithm 4 FIND LOOPS(G). Returns a set of \mathbb{Z}_3 -chains constituting the cycles of the graph G .

Require: a bubble graph G as an array of tuples (i, j, λ) .

```

 $L \leftarrow \emptyset; F[i] \leftarrow i \quad \forall i \in 1 \dots V_G; R[i] \leftarrow \langle 0, \dots, 0 \rangle \quad \forall i \in 1 \dots V_G.$ 
for all  $g_k = (i, j, \lambda) \in G$  do
   $(a_i, p_i) \leftarrow A_R(i, F); (a_j, p_j) \leftarrow A_R(j, F).$ 
   $p_{ij} \leftarrow -p_i + p_j + \langle \delta_{kl} | l = 1 \dots E_G \rangle.$ 
  if  $a_i \neq a_j$  then
     $F[a_i] \leftarrow a_j; R[a_i] \leftarrow p_{ij}.$ 
  else
     $L \leftarrow L \cup \{p_{ij}\}.$ 
  end if
end for
return  $L$ 

```

is done can well influence the performance of the algorithm which has not been studied in detail.

3. The Spinor Helicity Projection Method

3.1. Introduction. The *Spinor Helicity Formalism* has proved to be very convenient for calculation within the framework of massless QCD. Massless fermions and massless gauge bosons have only two physical degrees of freedom but are represented by objects with four components, DIRAC spinors and polarisation vectors, respectively. This mismatch is cured by projecting on helicity states leading to more compact expressions than traditional approaches.

Intrinsically this formalism is designed for the four dimensional case. Therefore, a prescription has to be defined how to extend helicity amplitudes to $n = 4 - 2\varepsilon$ dimension for to embed them into the Dimensional Regularization (DReg) scheme; this will be an issue of Section 1 in Chapter 3. The extension to massive particles is described at the end of this Chapter in Sections 3.4 and 3.5.

The equations of motion for a spin- $\frac{1}{2}$ field with mass m are given by the DIRAC equations

$$(106) \quad (\not{p} - m)u(p) = (\not{p} + m)v(p) = 0 \quad \text{and}$$

$$(107) \quad \bar{u}(p)(\not{p} - m) = \bar{v}(p)(\not{p} + m) = 0.$$

In the massless case, solutions of positive and negative energy are degenerate²² which can be seen from the operators $(\not{p} - m)$ and $(\not{p} + m)$ becoming the same, i.e. (\not{p}) ; hence the solutions

$$(108a) \quad u_{\pm}(p) = \Pi_{\pm}u(p) \quad \text{and}$$

$$(108b) \quad v_{\mp}(p) = \Pi_{\mp}v(p)$$

can be identified, where I use the helicity projection operators

$$(109) \quad \Pi_{\pm} \equiv \frac{1}{2} (\mathbb{I} \pm \gamma_5).$$

I use the common bracket notation [XZC87]

$$(110a) \quad |p_{\pm}\rangle \equiv u_{\pm}(p) = v_{\mp}(p) \quad \text{and}$$

$$(110b) \quad \langle p_{\pm}| \equiv \bar{u}_{\pm}(p) = \bar{v}_{\mp}(p) \quad \text{together with}$$

$$(110c) \quad \langle pq| \equiv \langle p_-|q_+ \rangle \quad \text{and}$$

$$(110d) \quad [pq] \equiv \langle p_+|q_- \rangle = \text{sgn}(p \cdot q) \langle qp \rangle^*$$

In the literature the extra sign in the last equation is usually omitted since it becomes essential only for non-physical kinematics.

The orthogonality of the projectors Π_{\pm} leads to the annihilation of all other products

$$(111) \quad \langle p_+|q_+ \rangle = \langle p_-|q_- \rangle = 0;$$

the completeness relation reads in this notation as

$$(112) \quad |p_+\rangle \langle p_+| + |p_-\rangle \langle p_-| = \not{p},$$

and hence

$$(113) \quad |p_{\pm}\rangle \langle p_{\pm}| = \Pi_{\pm} \not{p}.$$

²²See for example [Dix96].

One can conclude that

$$(114) \quad \langle pq \rangle [qp] = \langle p_- | q_+ \rangle \langle q_+ | p_- \rangle = \bar{u}(p) \Pi_+ \Pi_+ \not{q} \Pi_- u(p) = \text{tr} \{ \not{p} \Pi_+ \Pi_+ \not{q} \Pi_- \} = \text{tr}^+ \{ \not{p} \not{q} \} = 2 p \cdot q.$$

Here I make use of the notation

$$(115) \quad \text{tr}^\pm \{ \Gamma \} = \text{tr} \{ \Pi_\pm \Gamma \}.$$

Equations (110d) and (114) determine the spinor product $\langle pq \rangle$ up to a phase; hence, after a certain phase choice these products, which evaluate to a complex number, can be computed numerically.

3.2. Choosing a Representation. Not only for numerical calculations but also to find a proper fixing of the phase ϕ_{pq} in the defining equation

$$(116) \quad \langle pq \rangle = \sqrt{|(pq)|} e^{i\phi_{pq}}$$

a certain basis choice is very convenient.

Following [KS85, JWW01], a pair of *basic spinors* is introduced: two four-vectors ζ and η are chosen such that²³

$$(117) \quad \zeta^2 = 0, \quad \eta^2 = -1 \quad \text{and} \quad \zeta \cdot \eta = 0.$$

Once the spinor $|\zeta_- \rangle$ is defined and obeys

$$(118) \quad |\zeta_- \rangle \langle \zeta_-| = \Pi_- \not{\zeta}$$

it is easy to show that for the positive-helicity state $|\zeta_+ \rangle$ the definition

$$(119) \quad |\zeta_+ \rangle = \not{\eta} |\zeta_- \rangle$$

suffices the DIRAC equation and (113).

Hence, for all lightlike four-vectors p with $p \cdot \zeta \neq 0$ one can define the corresponding spinors as

$$(120) \quad |p_\pm \rangle = \frac{\not{p}}{\sqrt{2p \cdot \zeta}} |\zeta_\mp \rangle \quad \text{and} \quad \langle p_\pm| = \langle \zeta_\mp| \frac{\not{p}}{\sqrt{2p \cdot \zeta}}.$$

The important detail about the definition is that the bra- and ket-spinors are not exactly conjugates of each other because for negative $p \cdot \zeta$ the denominator becomes imaginary; this feature, however, is important in order to preserve (114).

The representation in terms of the reference vectors ζ and η now can be used to give an expression for the spinor products $[pq]$ and $\langle pq \rangle$ of two lightlike vectors p and q .

$$(121) \quad [pq] = \langle p_+ | q_- \rangle = \frac{\langle \zeta_- | \not{p} \not{q} | \zeta_+ \rangle}{\sqrt{2p \cdot \zeta} \sqrt{2q \cdot \zeta}} = \frac{\text{tr}^- \{ \not{\zeta} \not{p} \not{q} \not{\eta} \}}{2\sqrt{p \cdot \zeta} \sqrt{q \cdot \zeta}} = \frac{1}{\sqrt{p \cdot \zeta} \sqrt{q \cdot \zeta}} ((p \cdot \zeta)(q \cdot \eta) - (p \cdot \eta)(q \cdot \zeta) - i\epsilon_{\mu\nu\rho\sigma} \zeta^\mu p^\nu q^\rho \eta^\sigma) = -[qp],$$

²³In the original paper ζ and η are called k^0 and k^1 respectively.

and in analogy we obtain

$$(122) \quad \langle qp \rangle = \frac{1}{\sqrt{q \cdot \zeta} \sqrt{p \cdot \zeta}} ((p \cdot \zeta)(q \cdot \eta) - (p \cdot \eta)(q \cdot \zeta) + i \epsilon_{\mu\nu\rho\sigma} \zeta^\mu p^\nu q^\rho \eta^\sigma) = \\ = -\langle pq \rangle = \text{sgn}(p \cdot \zeta) \text{sgn}(q \cdot \zeta) [pq]^* .$$

The signum functions arise from the ratio

$$(123) \quad \frac{\sqrt{p \cdot \zeta}^*}{\sqrt{p \cdot \zeta}} = \left\{ \begin{array}{ll} \sqrt{|p \cdot \zeta|} / \sqrt{|p \cdot \zeta|} & = 1 \quad \text{if } p \cdot \zeta > 0 \\ -i \sqrt{|p \cdot \zeta|} / i \sqrt{|p \cdot \zeta|} & = -1 \quad \text{if } p \cdot \zeta < 0 \end{array} \right\} = \text{sgn}(p \cdot \zeta)$$

The product of signs in the last line of (122) can be rewritten²⁴ as

$$(124) \quad \text{sgn}(p \cdot \zeta) \text{sgn}(q \cdot \zeta) = \text{sgn}(p \cdot q)$$

since we can represent

$$\zeta = \frac{\zeta^0}{|\vec{\zeta}|} (|\vec{\zeta}|, \vec{\zeta})$$

and analogously p and q . One can work out all dot products and apply the CAUCHY-SCHWARZ inequality on the three-dimensional scalar products to obtain Equation (124) above in terms of the zero components only. Similarly, it follows from Equations (121) and (122) that

$$(125) \quad \langle -p, q \rangle = \langle p, -q \rangle = i \langle pq \rangle \quad \text{and} \quad [-p, q] = [p, -q] = i [pq] .$$

For a numerical evaluation it is helpful to relate these expressions directly to the components of the vectors p and q . To achieve this any choice of ζ and η subjected to (117) can be used:

$$(126a) \quad \zeta^\mu = (1, 0, 0, 1)$$

$$(126b) \quad \eta^\mu = (0, 1, 0, 0)$$

To allow for a compact notation, the abbreviations $p_\pm = p^0 \pm p^3$ and $p_\perp = p^1 + ip^2$ are used, leading to

$$(127) \quad \langle pq \rangle = \sqrt{\frac{q_-}{p_-}} p_\perp^* - \sqrt{\frac{p_-}{q_-}} q_\perp^* = \sqrt{2|p \cdot q|} e^{i\phi_{pq}}$$

with a phase $e^{i\phi_{pq}}$ which is characterised by

$$(128a) \quad \cos \phi_{pq} = \frac{q_- p^1 - p_- q^1}{\sqrt{2|p \cdot q| p_- q_-}} \quad \text{and}$$

$$(128b) \quad \sin \phi_{pq} = \frac{q_- p^2 - p_- q^2}{\sqrt{2|p \cdot q| p_- q_-}} .$$

It should be noted that this phase is not LORENTZ invariant. This can be seen, for example, from a rotation round the z -axis by an angle α , which leads to an additional phase

$$(129) \quad \langle p' q' \rangle = \sqrt{|(pq)|} e^{i\phi_{pq}} e^{-i\alpha} = e^{-i\alpha} \langle pq \rangle .$$

²⁴ It is assumed that none of the products vanish.

3.3. External Massless Gauge Bosons. The method of Spinor Helicity Projections (SHPs) has been introduced to provide a compact representation of amplitudes. So far we have only regarded external fermions. In general however, amplitudes containing external gauge bosons are needed as well. This requires an appropriate representation of the polarisation vectors $\varepsilon_{\pm}^{\mu}(k)$ belonging to a gauge boson of momentum k , which is introduced according to [XZC87]. The definition

$$(130a) \quad \varepsilon_{+}^{\mu}(q, k) = \frac{\langle q_{-} | \gamma^{\mu} | k_{-} \rangle}{\sqrt{2} \langle qk \rangle},$$

$$(130b) \quad \varepsilon_{-}^{\mu}(q, k) = \frac{\langle q_{+} | \gamma^{\mu} | k_{+} \rangle}{\sqrt{2} [kq]}$$

with q being lightlike represents a polarisation vector in an axial gauge and hence the completeness relation

$$(131) \quad \varepsilon_{+}^{\mu}(q, k) (\varepsilon_{+}^{\nu}(q, k))^{*} + \varepsilon_{-}^{\mu}(q, k) (\varepsilon_{-}^{\nu}(q, k))^{*} = -g^{\mu\nu} + \frac{k^{\mu} q^{\nu} + q^{\mu} k^{\nu}}{k \cdot q}$$

must hold²⁵.

To show that (130) is a valid definition of a polarisation vector a few auxiliary relations are needed. The GORDON identity

$$(132) \quad \langle p_{\pm} | \gamma^{\mu} | p_{\pm} \rangle = \text{tr}^{\pm} \{ \gamma^{\mu} \not{p} \} = 2 p^{\mu}$$

can be used to express lightlike vectors in terms of spinor strings.

The second required ingredient is a FIERZ rearrangement formula,

$$(133) \quad \langle p_{+} | \gamma^{\mu} | q_{+} \rangle \langle r_{+} | \gamma_{\mu} | s_{+} \rangle = 2 [pr] \langle sq \rangle,$$

where p, q, r and s are lightlike vectors. To show this identity the left hand side can be completed to a single trace by insertion of

$$(134) \quad 1 = \frac{\langle q_{+} | \not{m} | r_{+} \rangle \langle s_{+} | \not{n} | p_{+} \rangle}{[qm] \langle mr \rangle [sn] \langle np \rangle},$$

where again m and n are arbitrary, lightlike momenta. Here I use the fact that

$$(135) \quad \langle q_{+} | \not{m} | r_{+} \rangle = \langle q_{+} | (|m_{+}\rangle \langle m_{+}| + |m_{-}\rangle \langle m_{-}|) | r_{+} \rangle = \\ \langle q_{+} | m_{-} \rangle \langle m_{-} | r_{+} \rangle = [qm] \langle mr \rangle$$

and for any string Γ of DIRAC matrices

$$(136) \quad \langle q_{\pm} | \Gamma | q_{\pm} \rangle = \text{tr} \{ \langle q_{\pm} | \Gamma | q_{\pm} \rangle \} = \text{tr} \{ \Gamma | q_{\pm} \rangle \langle q_{\pm} | \} = \text{tr} \{ \Gamma \Pi_{\pm} \not{q} \} = \text{tr}^{\pm} \{ \not{q} \Gamma \}.$$

The left hand side of (134) now reads

$$(137) \quad \frac{\langle p_{+} | \gamma^{\mu} | q_{+} \rangle \langle q_{+} | \not{m} | r_{+} \rangle \langle r_{+} | \gamma_{\mu} | s_{+} \rangle \langle s_{+} | \not{n} | p_{+} \rangle}{[qm] \langle mr \rangle [sn] \langle np \rangle} = \frac{\text{tr}^{+} \{ \not{p} \gamma^{\mu} \not{q} \not{m} \not{r} \gamma_{\mu} \not{s} \not{n} \}}{[qm] \langle mr \rangle [sn] \langle np \rangle} = \\ \frac{-2 \text{tr}^{+} \{ \not{p} \not{r} \not{m} \not{q} \not{s} \not{n} \}}{[qm] \langle mr \rangle [sn] \langle np \rangle} = \frac{-2 [sn] \langle np \rangle [pr] \langle rm \rangle [mq] \langle qs \rangle}{[qm] \langle mr \rangle [sn] \langle np \rangle} = \\ -2 [pr] \langle qs \rangle = 2 [pr] \langle sq \rangle.$$

In this derivation I made use of the relation $\gamma^{\mu} \gamma^{\nu} \gamma^{\rho} \gamma^{\sigma} \gamma_{\mu} = -2 \gamma^{\sigma} \gamma^{\rho} \gamma^{\nu}$, which is only valid in four dimensions. In n dimensions the additional term $(4 - n) \gamma^{\nu} \gamma^{\rho} \gamma^{\sigma}$ arises,

²⁵See for example [Dix96]

which changes the right hand side of Equation (137) to $(4 - n) [rs] \langle pq \rangle$. Similarly²⁶, the analog of (133) with different signs can be proved,

$$(138) \quad \langle p_+ | \gamma^\mu | q_+ \rangle \langle r_- | \gamma_\mu | s_- \rangle = 2 [ps] \langle rq \rangle.$$

Equations (132) and (133) together prove the orthogonality condition

$$(139) \quad \varepsilon_\pm^\mu(q, k) k_\mu \propto \langle q_\mp | \gamma^\mu | k_\mp \rangle \langle k_\mp | \gamma_\mu | k_\mp \rangle = -2 [qk] \langle kk \rangle = 0$$

and by similar arguments $(\varepsilon_\pm)^2 = \varepsilon_\pm \cdot q = 0$ can be shown.

Finally, equation (131) has to be proved. From the definition of $\varepsilon_\pm^\mu(q, k)$ one can read off immediately that $(\varepsilon_\pm^\mu)^* = \varepsilon_\mp^\mu$, and hence the left hand side of (131) reads

$$\varepsilon_+^\mu(q, k) \varepsilon_-^\nu(q, k) + \varepsilon_-^\mu(q, k) \varepsilon_+^\nu(q, k).$$

Substituting the definition of ε into Equation (130) and using the charge conjugation relation for vector currents, $\langle q_\mp | \gamma^\mu | k_\mp \rangle = \langle k_\pm | \gamma^\mu | q_\pm \rangle$, both terms can be rewritten as traces, which evaluate to

$$(140) \quad \varepsilon_+^\mu(q, k) \varepsilon_-^\nu(q, k) = \frac{1}{2} \left(-g^{\mu\nu} + \frac{k^\mu q^\nu + q^\mu k^\nu}{k \cdot q} \right) - \frac{i}{2} \varepsilon^{\rho\mu\sigma\nu} k_\rho q_\sigma$$

and the respective term with μ and ν exchanged. Adding both terms up one reproduces Equation (131).

As a further result one can show that for any LORENTZ contractions of polarisation vectors of same helicity one can always find a gauge choice such that the dot product reduces to a pure phase. Using a suitable choice for the auxiliary vectors together with the FIERZ identity (133), one achieves the form

$$(141) \quad \varepsilon_\pm(k_i, q_i = k_j) \cdot \varepsilon_\pm(k_j, q_j = k_i) = \left(\frac{\langle k_i k_j \rangle}{[k_i k_j]} \right)^{\pm 1} = e^{2i\phi_{ij}}.$$

For the case of mixed helicities in this gauge choice the product vanishes, that is

$$(142) \quad \varepsilon_\pm(k_i, q_i = k_j) \cdot \varepsilon_\mp(k_j, q_j = k_i) = 0.$$

3.4. Massive Fermions. For massive fermions the fields obey the massive DIRAC equation and the spinors $u(p)$ and $v(p)$ have to be distinguished. A common notation for both can be achieved, following [Tan90], by introducing an additional index $\rho = \pm 1$ to distinguish the solutions of the equations:

$$(143) \quad (\not{p} - \rho m) |p_\lambda^\rho\rangle = 0 \quad \text{and} \quad \langle p_\lambda^\rho | (\not{p} - \rho m) = 0.$$

The construction

$$(144a) \quad |p_\lambda^\rho\rangle = \frac{1}{\sqrt{2p \cdot \zeta}} (\not{p} + \rho m) |\zeta_{-\lambda}\rangle \quad \text{and}$$

$$(144b) \quad \langle p_\lambda^\rho | = \frac{1}{\sqrt{2p \cdot \zeta}} \langle \zeta_{-\lambda} | (\not{p} + \rho m)$$

clearly obeys (143) and hence it remains to be shown that the solutions form a complete set. From direct calculation one gets

$$(145) \quad |p_\lambda^\rho\rangle \langle p_\lambda^\rho| = \frac{1}{2} (\mathbb{I} + \lambda \rho \gamma_5 \not{\zeta}) (\not{p} + \rho m),$$

²⁶In fact the prove is simpler since an insertion of $[qr] \langle sp \rangle$ already completes the trace

where

$$(146) \quad s^\mu = \frac{1}{m}p^\mu - \frac{m}{p \cdot \zeta}\zeta^\mu, \quad s^2 = -1,$$

and hence summing up the helicities $\lambda = \pm 1$ leads to the required result.

Another way of constructing massive spinors is by decomposing p into a sum of two lightlike vectors $p = p_1 + p_2$, $p_1^2 = p_2^2 = 0$. Given an arbitrary lightlike vector ζ this can always be achieved by choosing

$$(147) \quad p_1 = \frac{m^2}{2p \cdot \zeta}\zeta \quad \text{and} \quad p_2 = p - p_1.$$

Then $p_1 \cdot p_2 = p \cdot p_1 = p \cdot p_2 = m^2/2$ and one can rewrite (144a) as

$$(148) \quad |p_\lambda^\rho\rangle = \frac{1}{\sqrt{2p \cdot p_1}}(\not{p} + \rho m) |p_{1-\lambda}\rangle = \frac{1}{\sqrt{2p \cdot p_1}}(\not{p}_1 + \not{p}_2 + \rho m) |p_{1-\lambda}\rangle = \\ \frac{1}{\sqrt{2p \cdot p_1}}\not{p}_1 |p_{1-\lambda}\rangle + \frac{1}{\sqrt{2p \cdot p_2}}\not{p}_2 |p_{1-\lambda}\rangle + \rho |p_{1-\lambda}\rangle = |p_{2\lambda}\rangle + \rho |p_{1-\lambda}\rangle.$$

3.5. Massive Gauge Bosons. Although the treatment of massive gauge bosons is not part of my thesis I want to describe two extensions of the massless spinor helicity formalism for these cases.

The authors of [KS85] also describe a formalism that deals with massive vector bosons by turning the helicity sum into a Monte-Carlo integral. The idea is, similar to the case of fermions, to split the massive momentum q into a sum of lightlike four-vectors $q = q_1 + q_2$ and to introduce the polarisation vector

$$(149) \quad a^\mu = \frac{\langle q_{1-} | \gamma^\mu | q_{2-} \rangle}{\sqrt{2m}}$$

without further constraints. The cross section is still reproduced correctly if one replaces the spin sum by the integral

$$(150) \quad \sum \epsilon^\mu (\epsilon^\nu)^* \rightarrow \int \frac{d^2\Omega}{4\pi/3} a^\mu (a^\nu)^* = -g^{\mu\nu} + \frac{q^\mu q^\nu}{m^2}.$$

While this approach is very well suited for a direct numerical evaluation of unpolarised amplitudes, for an analytical result another technique should be used where the polarisations become accessible directly. Formula for such an approach are given in [Nan03] but should also be proved in what follows.

The candidates for the polarisation vectors for a massive gauge boson of momentum $q^\mu = q_1^\mu + q_2^\mu$, $q^2 = m^2$ and $q_1^2 = q_2^2 = 0$ are as follows

$$(151a) \quad \varepsilon_\pm^\mu(q, m) = \frac{\langle q_{1\pm} | \gamma^\mu | q_{2\pm} \rangle}{\sqrt{2m}},$$

$$(151b) \quad \varepsilon_0^\mu(q, m) = \frac{\langle q_{1+} | \gamma^\mu | q_{1+} \rangle}{2m} - \frac{\langle q_{2+} | \gamma^\mu | q_{2+} \rangle}{2m} = \frac{q_1^\mu - q_2^\mu}{m}.$$

The structure of ε_\pm is very similar to the case of massless bosons, and hence the proves for $\varepsilon_\pm \cdot q = \varepsilon_\pm \cdot \varepsilon_p m = 0$ and $(\varepsilon_\pm)^* = \varepsilon_\mp$ are just as above. Hence we need to show that

$$(152a) \quad \varepsilon_0 \cdot q = 0,$$

$$(152b) \quad \varepsilon_\pm \cdot \varepsilon_\mp = -1,$$

$$(152c) \quad \varepsilon_0 \cdot \varepsilon_0 = -1 \quad \text{and}$$

$$(152d) \quad \varepsilon_\pm \cdot \varepsilon_0 = 0.$$

For the first equation it suffices to split q into q_1 and q_2 ; half of the terms vanish due to $\not{q}_i |q_{i+}\rangle = 0$. For the remaining terms we get

$$(153) \quad 2m\varepsilon_0 \cdot q = \langle q_{1+} | \not{q}_2 | q_{1+} \rangle - \langle q_{2+} | \not{q}_1 | q_{2+} \rangle = \\ [q_2 q_1] \langle q_1 q_2 \rangle - [q_1 q_2] \langle q_1 q_2 \rangle = 2q_1 \cdot q_2 - 2q_1 \cdot q_2 = 0.$$

To prove (152d) one can use the FIERZ identity, which in this case for each term yields one factor of the form $\langle q_i q_i \rangle$ or $[q_i q_i]$. Similarly, in (152c) after applying the FIERZ identity all but two terms cancel, and one finds

$$(154) \quad \varepsilon_0 \cdot \varepsilon_0 = -2 \frac{[q_1 q_2] \langle q_1 q_2 \rangle}{4m^2} = -1$$

since $2q_1 \cdot q_2 = m^2$. In the same spirit one can evaluate (152b) by applying (138).

Finally we have to establish that the spin sum is complete. We can expand out

$$(155) \quad \varepsilon_+^\mu (\varepsilon_+^\nu)^* = \frac{1}{2m^2} \langle q_{1+} | \gamma^\mu | q_{2+} \rangle \langle q_{2+} | \gamma^\nu | q_{1+} \rangle = \frac{1}{2m^2} \text{tr}^+ \{ \not{q}_1 \gamma^\mu \not{q}_2 \gamma^\nu \} = \\ \frac{2}{2m^2} \left(q_1^\mu q_2^\nu + q_1^\nu q_2^\mu - \frac{m^2}{2} g^{\mu\nu} \right) = \varepsilon_-^\mu (\varepsilon_-^\nu)^*$$

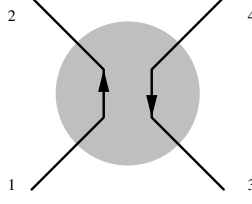
and do the same for

$$(156) \quad \varepsilon_0^\mu (\varepsilon_0^\nu)^* = \frac{1}{4m^2} (\langle q_{1+} | \gamma^\mu | q_{1+} \rangle \langle q_{1+} | \gamma^\nu | q_{1+} \rangle \\ + \langle q_{2+} | \gamma^\mu | q_{2+} \rangle \langle q_{2+} | \gamma^\nu | q_{2+} \rangle - \langle q_{1+} | \gamma^\mu | q_{1+} \rangle \langle q_{2+} | \gamma^\nu | q_{2+} \rangle \\ - \langle q_{2+} | \gamma^\mu | q_{2+} \rangle \langle q_{1+} | \gamma^\nu | q_{1+} \rangle) \\ = \frac{1}{4m^2} (\text{tr}^+ \{ \not{q}_1 \gamma^\mu \not{q}_1 \gamma^\nu \} + \text{tr}^+ \{ \not{q}_2 \gamma^\mu \not{q}_2 \gamma^\nu \} - \text{tr}^+ \{ \not{q}_1 \gamma^\mu \} \text{tr}^+ \{ \not{q}_2 \gamma^\nu \} \\ - \text{tr}^+ \{ \not{q}_2 \gamma^\mu \} \text{tr}^+ \{ \not{q}_1 \gamma^\nu \}) = \frac{1}{m^2} (q_1^\mu q_1^\nu + q_2^\mu q_2^\nu - q_1^\mu q_2^\nu - q_2^\mu q_1^\nu).$$

Gathering all terms the completeness comes out as expected

$$(157) \quad \varepsilon_+^\mu (\varepsilon_+^\nu)^* + \varepsilon_-^\mu (\varepsilon_-^\nu)^* + \varepsilon_0^\mu (\varepsilon_0^\nu)^* = -g^{\mu\nu} + \frac{q^\mu q^\nu}{m^2}.$$

3.6. Amplitude Representation. The formalism of SHPs is a very powerful technique for the calculation of matrix elements because it splits every amplitude in a natural way into gauge invariant pieces. In principle these subamplitudes are observable in an experiment where all helicities of the initial particles can be prepared and those of the final state particles are measured. One generates the subamplitudes by inserting helicity projection operators in every spinor line. As example we shall have a look at the $q\bar{q} \rightarrow q'\bar{q}'$ amplitude, of which a sketch is shown in figure 1. The expression for the

Figure 1: Schematic picture of the amplitude $q\bar{q} \rightarrow q'\bar{q}'$.

amplitude $\mathcal{A}(1, 2, 3, 4)$ has the generic form²⁷

$$(158) \quad \mathcal{A}(1, 2, 3, 4) = \bar{v}(p_2)\Gamma_{12}u(p_1) \otimes \tau \otimes \bar{u}(p_3)\Gamma_{34}v(p_4).$$

I abbreviate the momenta by their indices where this is unambiguous. We split this expression into subamplitudes by the help of $\mathbb{I} = \Pi_+ + \Pi_-$,

$$(159) \quad \begin{aligned} \mathcal{A}(1, 2, 3, 4) &= \bar{v}(p_2)\Gamma_{12}\Pi_+u(p_1) \otimes \tau \otimes \bar{u}(p_3)\Gamma_{34}\Pi_+v(p_4) \\ &\quad + \bar{v}(p_2)\Gamma_{12}\Pi_-u(p_1) \otimes \tau \otimes \bar{u}(p_3)\Gamma_{34}\Pi_+v(p_4) \\ &\quad + \bar{v}(p_2)\Gamma_{12}\Pi_+u(p_1) \otimes \tau \otimes \bar{u}(p_3)\Gamma_{34}\Pi_-v(p_4) \\ &\quad + \bar{v}(p_2)\Gamma_{12}\Pi_-u(p_1) \otimes \tau \otimes \bar{u}(p_3)\Gamma_{34}\Pi_-v(p_4) \\ &= \langle p_2^+ | \Gamma_{12} | p_1^+ \rangle \otimes \tau \otimes \langle p_3^+ | \Gamma_{34} | p_4^+ \rangle + \langle p_2^- | \Gamma_{12} | p_1^- \rangle \otimes \tau \otimes \langle p_3^+ | \Gamma_{34} | p_4^+ \rangle \\ &\quad + \langle p_2^+ | \Gamma_{12} | p_1^+ \rangle \otimes \tau \otimes \langle p_3^- | \Gamma_{34} | p_4^- \rangle + \langle p_2^- | \Gamma_{12} | p_1^- \rangle \otimes \tau \otimes \langle p_3^- | \Gamma_{34} | p_4^- \rangle \\ &\equiv \mathcal{A}^{++++}(1, 2, 3, 4) + \mathcal{A}^{--++}(1, 2, 3, 4) + \mathcal{A}^{++--}(1, 2, 3, 4) + \mathcal{A}^{----}(1, 2, 3, 4). \end{aligned}$$

The signs in this notation correspond to the signs of the helicity projectors; for antifermions the sign is different from the physical helicity. Further simplifications can be achieved by parity invariance: for any helicity subamplitude in QCD, the action of the parity operator \mathcal{P} is

$$(160) \quad \mathcal{A}^{\lambda_1, \lambda_2, \dots}(1, 2, \dots) = \mathcal{P}\mathcal{A}^{\lambda_1, \lambda_2, \dots}(1, 2, \dots) = \mathcal{A}^{-\lambda_1, -\lambda_2, \dots}(\mathcal{P}1, \mathcal{P}2, \dots),$$

where $\mathcal{P}i = \mathcal{P}p_i = (p_i^0, -p_i^1, -p_i^2, -p_i^3)$ is the parity conjugated of the momentum vector p_i . This allows the computation of the whole amplitude from the knowledge of just two helicity amplitudes, \mathcal{A}^{++++} and \mathcal{A}^{++--} :

$$(161) \quad \begin{aligned} \mathcal{A}(1, 2, 3, 4) &= \mathcal{A}^{++++}(1, 2, 3, 4) + \mathcal{A}^{++--}(\mathcal{P}1, \mathcal{P}2, \mathcal{P}3, \mathcal{P}4) \\ &\quad + \mathcal{A}^{++--}(1, 2, 3, 4) + \mathcal{A}^{++++}(\mathcal{P}1, \mathcal{P}2, \mathcal{P}3, \mathcal{P}4). \end{aligned}$$

For an algebraic treatment of the amplitude one might want to work with traces, i.e. with polynomials in the MANDELSTAM variables rather than spinor products; this can be achieved using a lightlike auxiliary vector m when applying (135) and (136) to

$$(162) \quad \langle p_2^+ | \Gamma_{12} | p_1^+ \rangle = \frac{\langle p_1^+ | \not{m} | p_2^+ \rangle}{[p_1 m] \langle m p_2 \rangle} \langle p_2^+ | \Gamma_{12} | p_1^+ \rangle = \frac{\text{tr}^+ \{ \not{p}_1 \not{m} \not{p}_2 \Gamma_{12} \}}{2\sqrt{|p_1 \cdot m|} \sqrt{|p_2 \cdot m|} e^{i\phi_{mp_2}} e^{-i\phi_{mp_1}}}.$$

The advantage of this method is the simpler treatment of the resulting expressions where the coefficients of the integrals are expressed in terms of MANDELSTAM variables

²⁷ The complete tensor structure is represented by the direct product \otimes . Γ_{12} and Γ_{34} are two strings of DIRAC gamma matrices, and τ is the remaining, momentum dependent part of the amplitude.

only. An alternative approach is based on the use of spinor products instead of MANDELSTAM variables [Pit97]: every appearance of an integration momentum q_a in the numerator can be extracted from the spinor line by the use of

$$(163) \quad q_a = \frac{1}{2k_i \cdot k_j} (2q_a \cdot k_i \not{k}_j + 2q_a \cdot k_j \not{k}_i - \not{k}_i q_a \not{k}_j - \not{k}_j q_a \not{k}_i)$$

with the two lightlike momenta k_i and k_j .²⁸ If there are not enough lightlike vectors in the amplitude there is an easy way of constructing a pair of massless momenta from two massive ones, by starting from the ansatz $l_1 = k_1 + \eta_1 k_2$ and $l_2 = k_2 + \eta_2 k_1$ and imposing $l_1^2 = l_2^2 = 0$. Equation (163) allows all appearances of q_a to be rewritten in terms of dot-products $q_a \cdot k_i$, $q_a \cdot k_j$ and simple spinor products $\langle k_{i,\pm} | q_a | k_{j,\pm} \rangle$. In the end one can always achieve having only one such spinor product left because²⁹

$$(164) \quad \langle k_{i,\pm} | \not{p} | k_{j,\pm} \rangle \langle k_{j,\pm} | \not{p} | k_{i,\pm} \rangle = \text{tr} \{ \Pi^\pm \not{k}_i \not{p} \Pi^\pm \not{k}_j \not{p} \} = 4(k_i \cdot \hat{p})(k_j \cdot \hat{p}) - 2(k_i \cdot k_j) \hat{p}^2.$$

3.7. The Weyl-van der Waerden Representation. The spinor helicity projections as described above on the one hand are a tool for structuring an amplitude into orthogonal pieces on a symbolical level, so-called helicity amplitudes. These are easier to handle than the full amplitude and allow for much more compact expressions. However, the fact that one projects from the 4 by 4 DIRAC matrices onto two-dimensional subspaces also allows for a different notation of the CLIFFORD algebra on these subspaces and also a more efficient, numerical computation of the traces and spinor products.

WEYL [Wey31] and VAN DER WAERDEN [Wae32] originally developed the representation theory of the LORENTZ group in a way that later lead into spinorial methods in quantum field theory. The basic idea behind the WEYL-VAN DER WAERDEN (WvdW) representation is the fact that the matrices

$$(165) \quad \gamma^\mu = \begin{pmatrix} 0_{2 \times 2} & \sigma^\mu \\ \bar{\sigma}^\mu & 0_{2 \times 2} \end{pmatrix} \quad \text{with } \sigma^\mu = (\sigma_0, \vec{\sigma}) \quad \text{and } \bar{\sigma}^\mu = (\sigma_0, -\vec{\sigma}),$$

where $\sigma_0 = \mathbb{I}_{2 \times 2}$ and $\vec{\sigma}$ are the PAULI matrices

$$(166) \quad \sigma^1 = \begin{pmatrix} 0 & 1 \\ 1 & 0 \end{pmatrix}, \quad \sigma^2 = \begin{pmatrix} 0 & -i \\ i & 0 \end{pmatrix}, \quad \sigma^3 = \begin{pmatrix} 1 & 0 \\ 0 & -1 \end{pmatrix},$$

form a representation of the CLIFFORD algebra

$$(167) \quad \{\gamma^\mu, \gamma^\nu\} = 2g^{\mu\nu} \otimes \mathbb{I}_{4 \times 4} \quad \text{because} \quad \sigma_{\alpha\dot{\beta}}^\mu \bar{\sigma}^{\nu\dot{\beta}\gamma} + \sigma_{\alpha\dot{\beta}}^\nu \bar{\sigma}^{\mu\dot{\beta}\gamma} = 2g^{\mu\nu} \delta_\alpha^\gamma.$$

In this representation the helicity projectors are

$$(168) \quad \Pi_+ = \begin{pmatrix} \mathbb{I} & 0 \\ 0 & 0 \end{pmatrix} \quad \text{and } \Pi_- = \begin{pmatrix} 0 & 0 \\ 0 & \mathbb{I} \end{pmatrix}.$$

Tracing both sides of Equation (167) and using the HERMITICITY of the PAULI matrices yields a decomposition of the metric tensor $g^{\mu\nu}$ into σ and $\bar{\sigma}$:

$$(169) \quad g^{\mu\nu} = \frac{1}{2} \sigma_{\alpha\dot{\beta}}^\mu \bar{\sigma}^{\nu\dot{\beta}\alpha}$$

It should be noted that α and $\dot{\alpha}$ denote distinct indices; the dot distinguishes the spin- $\frac{1}{2}$ representation and its conjugate.

²⁸The application of this equation allows to separate q_a from an adjacent γ^μ if one wants to apply FIERZ identities before carrying out the integrals because one can split the spinor lines using $\not{k}_i q_a \not{k}_j = |k_{i,\lambda}\rangle \langle k_{i,\lambda}| q_a |k_{j,\lambda}\rangle \langle k_{j,\lambda}|$.

²⁹ k_i and k_j are assumed to be four-dimensional vectors.

The above relation allows to define a bijective mapping between four-vectors k^μ and matrices $k_{\alpha\dot{\alpha}}$.

$$(170a) \quad k_{\alpha\dot{\alpha}} = k_\mu \sigma_{\alpha\dot{\alpha}}^\mu \Leftrightarrow k^\mu = \frac{1}{2} k_{\alpha\dot{\alpha}} \bar{\sigma}^{\mu\dot{\alpha}\alpha}$$

and similarly

$$(170b) \quad \bar{k}^{\dot{\alpha}\alpha} = k_\mu \bar{\sigma}^{\mu\dot{\alpha}\alpha} \Leftrightarrow k^\mu = \frac{1}{2} \bar{k}^{\dot{\alpha}\alpha} \sigma_{\alpha\dot{\alpha}}^\mu.$$

With the abbreviations $p_\pm = p^0 \pm p^3$ and $p_\perp = p^1 + ip^2$ one obtains in components

$$(171) \quad p_{\alpha\dot{\alpha}} = \begin{pmatrix} p_- & -p_\perp^* \\ -p_\perp & p_+ \end{pmatrix} \quad \text{and} \quad \bar{p}^{\dot{\alpha}\alpha} = \begin{pmatrix} p_+ & p_\perp^* \\ p_\perp & p_- \end{pmatrix}.$$

Since $k_{\alpha\dot{\alpha}}$ is a HERMITIAN two by two matrix one can use the spectral theorem to decompose it into its eigenvectors,

$$(172) \quad k_{\alpha\dot{\alpha}} = \lambda_+ |k_\alpha^+\rangle \langle k_{\dot{\alpha}}^+| + \lambda_- |k_\alpha^-\rangle \langle k_{\dot{\alpha}}^-|$$

where the inner product is defined by the antisymmetric spinor-metrics $\varepsilon^{\alpha\beta}$ with $\varepsilon^{12} = \varepsilon_{21} = 1$ and $\varepsilon^{\dot{1}\dot{2}} = \varepsilon_{\dot{2}\dot{1}} = 1$ following the convention of [WB92], raising and lowering is done by $|p^\alpha\rangle = \varepsilon^{\alpha\beta} |p_\beta\rangle$ and $|p_\alpha\rangle = \varepsilon_{\alpha\beta} |p^\beta\rangle$. The dotted and undotted spinors are related by complex conjugation: $\langle p_{\dot{\alpha}}| = \delta_{\dot{\alpha}}^\alpha (|p^\alpha\rangle)^*$ and $\langle p^\alpha| = \delta_\alpha^{\dot{\alpha}} (|p_{\dot{\alpha}}\rangle)^*$. Hence $\langle p_\alpha|q^\alpha\rangle = |p_1\rangle|q_2\rangle - |p_2\rangle|q_1\rangle$.

The eigenvalues can be derived easily from the components of (171) as $\lambda_\pm = p^0 \pm |\vec{p}|$; the eigenvectors have a compact representation if one chooses spherical coordinates for the space like components of $k^\mu = (k^0, |\vec{k}| \cos \phi \sin \vartheta, |\vec{k}| \sin \phi \sin \vartheta, |\vec{k}| \cos \vartheta)$ as for example in [Dit99]

$$(173) \quad |k_\alpha^+\rangle = \begin{pmatrix} e^{-i\phi} \cos \frac{\vartheta}{2} \\ \sin \frac{\vartheta}{2} \end{pmatrix} \quad \text{and} \quad |k_\alpha^-\rangle = \begin{pmatrix} \sin \frac{\vartheta}{2} \\ -e^{+i\phi} \cos \frac{\vartheta}{2} \end{pmatrix}.$$

Complex conjugation relates therefore the eigenvectors as $\langle k_\alpha^+| = \delta_\alpha^{\dot{\alpha}} \varepsilon^{\dot{\alpha}\beta} |k_{\dot{\beta}}^- \rangle$.

For lightlike vectors $\lambda_- = 0$ and hence with the redefinition

$$(174) \quad |k_\alpha\rangle = \sqrt{2k^0} |k_\alpha^+\rangle$$

one is back to the usual spinors as defined in the section before when $k_{\alpha\dot{\alpha}}$ and $\bar{k}^{\dot{\alpha}\alpha}$ are identified with the projections $\Pi_\pm \not{k}$.

Another useful identity on the PAULI matrices which can be used for symbolic calculations can be simply derived by inspection:

$$(175) \quad \sigma_{\alpha\dot{\alpha}}^\mu \bar{\sigma}_{\dot{\mu}}^{\dot{\beta}\beta} = 2\delta_\alpha^\beta \delta_{\dot{\alpha}}^{\dot{\beta}}.$$

This allows to either cut or sew together traces with contracted LORENTZ indices similar to the CHISHOLM identities for DIRAC matrices.

An interesting numerical application of the WvdW representation is the efficient evaluation of traces. As has been shown in the previous section any trace of contracted DIRAC matrices $\Gamma = \not{p}_1 \not{p}_2 \cdots \not{p}_{2n}$ can be written as a sum of traces of the form $\text{tr}^+ \{\Gamma'\}$,

where Γ' is a cyclic permutation of Γ . We can now introduce projectors, according to the commutation relation $\Pi_{\pm}\not{p} = \not{p}\Pi_{\mp}$,

$$(176) \quad \text{tr}^+\{\Gamma\} = \text{tr}\{(\Pi_+\not{p}_1\Pi_-)(\Pi_-\not{p}_2\Pi_+)\cdots(\Pi_-\not{p}_{2n}\Pi_+)\} = p_{1\alpha\dot{\beta}}\bar{p}_2^{\dot{\beta}\gamma}\cdots\bar{p}_{2n}^{\dot{\omega}\alpha}$$

because

$$\Pi_+\not{p}\Pi_- = \begin{pmatrix} \mathbb{I} & 0 \\ 0 & 0 \end{pmatrix} \begin{pmatrix} 0 & p_{\alpha\dot{\alpha}} \\ \bar{p}^{\dot{\alpha}\alpha} & 0 \end{pmatrix} \begin{pmatrix} 0 & 0 \\ 0 & \mathbb{I} \end{pmatrix} = \begin{pmatrix} 0 & p_{\alpha\dot{\alpha}} \\ 0 & 0 \end{pmatrix}$$

and

$$\Pi_-\not{p}\Pi_+ = \begin{pmatrix} 0 & 0 \\ 0 & \mathbb{I} \end{pmatrix} \begin{pmatrix} 0 & p_{\beta\dot{\beta}} \\ \bar{p}^{\dot{\beta}\beta} & 0 \end{pmatrix} \begin{pmatrix} \mathbb{I} & 0 \\ 0 & 0 \end{pmatrix} = \begin{pmatrix} 0 & 0 \\ \bar{p}^{\dot{\beta}\beta} & 0 \end{pmatrix}.$$

This shows that once one uses helicity projections one can evaluate traces of two by two matrices instead of four by four, which reduces the number of multiplications involved significantly.

The possible applications of the WvdW representation go beyond what has been described here, and for a more complete treatment the reader is referred to [Dit99, Wei06].

CHAPTER 3

QCD at One-Loop Precision

An expert is someone who knows some of the worst mistakes that can be made in his subject and who manages to avoid them.

— WERNER HEISENBERG

Introduction

At the lowest order in the perturbative expansion of a scattering amplitude one obtains only tree-like diagrams and various automated tools exist to generate and evaluate LO matrix elements numerically [**KKS02**, **MOR01**, **MS03**, **Y⁺00**, **Hah01**, **Hah05**, **CompHEP04**, **MMP⁺03**]. At NLO a cross-section for a $2 \rightarrow N$ process consists of three different terms:

$$(177) \quad \sigma = \sigma^{\mathcal{B}} + (\sigma^{\mathcal{R}} + \sigma^{\mathcal{V}}) + \mathcal{O}(\alpha_s^{N+2}).$$

The first term, $\sigma^{\mathcal{B}}$, corresponds to the LO result which in QCD is of order $\mathcal{O}(\alpha_s^N)$. The corrections of order $\mathcal{O}(\alpha_s^{N+1})$ are given in parenthesis: the real emission corrections $\sigma^{\mathcal{R}}$, that is the emission of an additional parton, correspond to a $2 \rightarrow (N+1)$ tree-level process whereas the virtual corrections $\sigma^{\mathcal{V}}$ are described by a $2 \rightarrow N$ process containing one loop in the FEYNMAN diagrams.

In four dimensions, both $\sigma^{\mathcal{V}}$ and $\sigma^{\mathcal{R}}$ are divergent and need to be regularised in order to lead to a meaningful physical result. As a regularisation method we choose Dimensional Regularization (DReg), where one replaces the number of dimensions by $n = 4 - 2\epsilon$. Section 1.1 reviews the most important implications of this regularisation scheme. In the virtual correction, working in an d -dimensional space requires to solve integrals of the type

$$\int \frac{d^d k}{i\pi^{d/2}} \frac{k^{\mu_1} \dots k^{\mu_r}}{\prod_{j=1}^N ((k + r_j)^2 - m_j^2 + i\delta)},$$

where the divergences show up in poles of $1/\epsilon$ and $1/\epsilon^2$. For our calculation we use a systematic reduction of these integrals in order to express them in terms of simpler building blocks. This reduction method is presented in Sections 2 and 3. A more fundamental introduction to one-loop integrals can be found in Appendix C.

The divergencies in the real emission part $\sigma^{\mathcal{R}}$ of the cross-section are discussed in 6. Applying DReg to the real emission contributions requires to integrate the unobserved particle over an n -dimensional phase space. In practise, however, one carries out the phase space integration by Monte Carlo techniques, as described in Section 8 and hence working in fractional-dimensional spaces appears to be impractical. Instead, we use a subtraction method as described in Section 7, that subtracts the terms leading to

singularities from the integrand of $\sigma^{\mathcal{R}}$, rendering it finite. The subtracted terms can be integrated analytically over the one-particle subspace, leading to poles in $1/\varepsilon$ and $1/\varepsilon^2$; this integrated subtraction terms are added back to the virtual amplitude, cancelling the so-called infrared (IR) poles of the amplitude. The remaining singularities are due to ultraviolet (UV) poles and are cured by renormalisation as shown in Section 5.

For the calculation of NLO corrections to cross-sections the level of automisation in current computer programs is far more limited as for LO calculations. The computation of the real corrections has recently been automated by different groups [GK08, FGG08, ST08]. The automated computation of the virtual corrections, although having received much effort, have not reached the same degree of automisation and current implementations are limited to $2 \rightarrow 2$ [K⁺06] or $2 \rightarrow 3$ [HR06] processes. Therefore, NLO corrections for QCD processes with more than two partons in the final state still remain a computational challenge, mainly due to the combinatorial complexity of the problem.

1. QCD in Dimensional Regularisation

1.1. Introduction. Higher order calculation in four dimensional, continuous field theories lead to singularities which have to be systematically removed by a renormalisation procedure. In order to handle these singularities in a consistent way a regularisation of the loop integrals is needed. The so called Dimensional Regularization (DReg) scheme as proposed by 't HOOFT and VELTMAN [tHV72] is one of the most widely used regularisation schemes and has led to many successful SM calculations over last decades. According to the Modified Minimal Subtraction ($\overline{\text{MS}}$) scheme I use the subtraction term¹

$$(178) \quad \Delta = \frac{1}{\varepsilon} - \gamma_E + \ln(4\pi)$$

It is well known² that in presence of gauge anomalies, a consistent continuation of γ_5 to $D \neq 4$ dimensions is not possible while preserving gauge invariance.

As the QCD is invariant under space reflections it is free of those anomalies [BDJ01b, Bar69]. Hence calculations in this work can be treated using the 't HOOFT-VELTMAN algebra, which extends the four dimensional DIRAC algebra to general $\text{SO}(1, D-1)$ vectors using the relation

$$(179) \quad \{\gamma^\mu, \gamma_5\} = \begin{cases} 0, & \mu \in \{0, 1, 2, 3\}, \\ 2\bar{\gamma}^\mu \gamma_5, & \text{otherwise.} \end{cases}$$

Here the symbol $\bar{\gamma}^\mu = \bar{g}_\nu^\mu \gamma^\nu$ has been used, where the metric is split up into

$$(180) \quad g^{\mu\nu} = \hat{g}^{\mu\nu} + \bar{g}^{\mu\nu},$$

and \hat{g}_ν^μ is a projector on the physical subspace,

$$(181) \quad \hat{g}_\nu^\mu \equiv \begin{cases} \delta_\nu^\mu, & \mu \in \{0, 1, 2, 3\}, \\ 0, & \text{otherwise.} \end{cases}$$

¹ $\gamma_E = -\Gamma'(1)$ is the EULER constant.

²See for example [Jeg01].

This notation is applied to all vectors, i.e. $\bar{p}^\mu = \bar{g}_\nu^\mu p^\nu$ and $\hat{p}^\mu = \hat{g}_\nu^\mu p^\nu$, and since $\hat{g}_\rho^\mu \bar{g}_\nu^\rho = 0$ one obtains for the modulus of an arbitrary vector $k^2 = \bar{k}^2 + \hat{k}^2$.

Equation (179) can also be read as

$$[\gamma_5, \bar{\gamma}^\mu] = 0,$$

which can be interpreted as γ_5 acting trivial in the non-physical dimensions. This behaviour becomes manifest through the definition

$$(182) \quad \gamma_5 \equiv \frac{i}{4!} \epsilon_{\mu\nu\rho\sigma} \hat{\gamma}^\mu \hat{\gamma}^\nu \hat{\gamma}^\rho \hat{\gamma}^\sigma.$$

1.2. Spinor Traces in D Dimensions. An important issue for practical calculations is how to calculate spinor traces within DReg. In this section I show an algorithm (Algorithm 5) that separates $\hat{\gamma}^\mu$ and γ_5 matrices from $\bar{\gamma}^\mu$ and allows the separate evaluation of a purely four dimensional trace and a trace consisting of $\bar{\gamma}^\mu$ -objects only. We will see that the latter trace leads to $\mathcal{O}(\varepsilon)$ -terms in $n = 4 - 2\varepsilon$ dimensions.

Algorithm 5 Carry Out Traces

- 1: $\text{tr}\{\dots \gamma^\mu \dots\} \rightarrow \text{tr}\{\dots \bar{\gamma}^\mu \dots\} + \text{tr}\{\dots \hat{\gamma}^\mu \dots\}$
 - 2: **while** replacements left **do**
 - 3: $\text{tr}\{\dots \bar{\gamma}^\mu \hat{\gamma}^\nu \dots\} \rightarrow -\text{tr}\{\dots \hat{\gamma}^\nu \bar{\gamma}^\mu \dots\}$
 - 4: $\text{tr}\{\dots \bar{\gamma}^\mu \gamma_5 \dots\} \rightarrow +\text{tr}\{\dots \gamma_5 \bar{\gamma}^\mu \dots\}$
 - 5: $\text{tr}\{\dots \hat{\gamma}^\mu \gamma_5 \dots\} \rightarrow -\text{tr}\{\dots \gamma_5 \hat{\gamma}^\mu \dots\}$
 - 6: $\text{tr}\{\dots \gamma_5 \gamma_5 \dots\} \rightarrow +\text{tr}\{\dots \mathbb{I} \dots\}$
 - 7: **end while**
 - 8: */* All traces now have the form $\text{tr}\{\hat{\Gamma} \bar{\Gamma}\}$ or $\text{tr}\{\gamma_5 \hat{\Gamma} \bar{\Gamma}\}$ */*
 - 9: $\text{tr}\{\gamma_5 \bar{\gamma}^\mu \dots\} \rightarrow 0$ */* see Eq. (184) and (182) */*
 - 10: $\text{tr}\{\dots \hat{\gamma}^\mu \bar{\gamma}^\nu \dots\} \rightarrow \text{tr}\{\dots \hat{\gamma}^\mu\} \text{tr}\{\bar{\gamma}^\nu \dots\} / \text{tr}\{\mathbb{I}\}$
 - 11: Evaluate traces separately.
-

It is obvious that Algorithm 5 is confluent and terminating for it shuffles all $\bar{\gamma}^\mu$ to the right and all γ_5 to the left³. Rule 3 is valid as the anticommutator

$$(183) \quad \{\hat{\gamma}^\mu, \bar{\gamma}^\nu\} = \hat{g}_\rho^\mu \bar{g}_\sigma^\nu \{\gamma^\rho, \gamma^\sigma\} = 2\hat{g}_\rho^\mu \bar{g}_\sigma^\nu g^{\rho\sigma} = 2\hat{g}^{\mu\rho} \bar{g}_\rho^\nu = 0$$

vanishes. The rewriting rules 4–6 follow directly from the definition of the algebra (179). Step 9 is just a special case of step 10.

The missing bit in the proof of algorithm 5 is the equation

$$(184) \quad \text{tr}\{\mathbb{I}\} \text{tr}\{\hat{\Gamma} \bar{\Gamma}\} = \text{tr}\{\hat{\Gamma}\} \text{tr}\{\bar{\Gamma}\},$$

³A rigorous proof is easily done by introducing the lexicographic ordering $\mathbb{I} < \gamma_5 < \hat{\gamma}^0 < \dots < \hat{\gamma}^3 < \bar{\gamma}^0 < \dots < \bar{\gamma}^3$; for there exists a least element (\mathbb{I}) and the algorithm produces a (lexicographic) descending chain of expression termination is guaranteed by the generalised induction principle. The validity of comment 9 is guaranteed since, including the possibilities for either $\hat{\Gamma}$ and $\bar{\Gamma}$ being \mathbb{I} , not being in the given form would include at least one of the replacements 3–6 being applicable. To show the confluence of the algorithm one has to prove that all rewriting rules commute, which can be easily done.

where $\hat{\Gamma} = \hat{\gamma}^{\mu_1} \dots \hat{\gamma}^{\mu_m}$ and $\bar{\Gamma} = \bar{\gamma}^{\nu_1} \dots \bar{\gamma}^{\nu_n}$ for all non-negative integers m and n . This also covers the cases involving γ_5 being a product of four-dimensional DIRAC matrices, which can be seen from Equation (182).

The proof is done by complete induction over n , where $n = 0$ can be read off from (184). Since the trace is cyclic and due to (183) one obtains

$$(185) \quad \text{tr}\{\mathbb{I}\} \text{tr}\left\{\hat{\Gamma}\bar{\Gamma}\right\} = (-1)^m \text{tr}\{\mathbb{I}\} \text{tr}\left\{\hat{\Gamma}\bar{\gamma}^{\nu_n}\bar{\gamma}^{\nu_1}\dots\bar{\gamma}^{\nu_{n-1}}\right\} = \\ (-1)^m \sum_{i=1}^{n-1} (-1)^{i+1} \cdot 2\bar{g}^{\nu_i\nu_n} \text{tr}\{\mathbb{I}\} \text{tr}\left\{\hat{\Gamma}\bar{\gamma}^{\nu_1}\dots\bar{\gamma}^{\nu_{i-1}}\bar{\gamma}^{\nu_{i+1}}\dots\bar{\gamma}^{\nu_{n-1}}\right\} \\ + (-1)^{m+n-1} \text{tr}\{\mathbb{I}\} \text{tr}\left\{\hat{\Gamma}\bar{\Gamma}\right\}.$$

For the traces inside the sum we can substitute the induction step which leads to

$$(186) \quad (-1)^m \cdot (1 + (-1)^{m+n}) \text{tr}\{\mathbb{I}\} \text{tr}\left\{\hat{\Gamma}\bar{\Gamma}\right\} = \\ \text{tr}\left\{\hat{\Gamma}\right\} \sum_{i=1}^{n-1} (-1)^{i+1} \cdot 2\bar{g}^{\nu_i\nu_n} \text{tr}\{\bar{\gamma}^{\nu_1}\dots\bar{\gamma}^{\nu_{i-1}}\bar{\gamma}^{\nu_{i+1}}\dots\bar{\gamma}^{\nu_{n-1}}\} = 2 \text{tr}\left\{\hat{\Gamma}\right\} \text{tr}\left\{\bar{\Gamma}\right\}.$$

It remains to investigate the cases for the numbers m and n being even or odd. If m is odd, one obtains

$$(187) \quad \text{tr}\left\{\hat{\Gamma}\mathbb{I}\bar{\Gamma}\right\} = \text{tr}\left\{\hat{\Gamma}\gamma_5\gamma_5\bar{\Gamma}\right\} = -\text{tr}\left\{\gamma_5\hat{\Gamma}\gamma_5\bar{\Gamma}\right\} = \\ -\text{tr}\left\{\hat{\Gamma}\gamma_5\bar{\Gamma}\gamma_5\right\} = -\text{tr}\left\{\hat{\Gamma}\gamma_5\gamma_5\bar{\Gamma}\right\} = -\text{tr}\left\{\hat{\Gamma}\bar{\Gamma}\right\} = 0.$$

On the other hand, both sides vanish if n is odd. For the left, non-vanishing case the result agrees with the conjecture, and everything is proved.

It should be noted that the intermediate step in (186) already shows that the evaluation of the trace $\text{tr}\{\bar{\Gamma}\}$ yields products of $\bar{g}^{\mu\nu}$ tensors. In amplitude calculations these terms vanish unless they are traced or contracted with integration momenta; as external momenta in the 't HOOFT-VELTMAN ('tHo) scheme are kept in four dimensions their projection on the $(D-4)$ dimensional subspace vanishes. The trace $\bar{g}_\mu^\mu = (D-4)$ as well as the terms proportional to \bar{k}^2 lead to $\mathcal{O}(\varepsilon)$ -terms, giving rise to polynomial terms in the amplitude if they are multiplied to a $1/\varepsilon$ pole from the loop integrals. The evaluation of $\text{tr}\{\bar{\Gamma}\}$ can be implemented straightforward: we have already seen that only two kinds of non-vanishing terms can arise from these traces, i.e. $(D-4)$ and \bar{k}^2 and therefore no additional care needs to be taken in order to keep the number of terms low. The most naïve reduction formula

$$(188) \quad \text{tr}\{\bar{\gamma}^{\nu_1}\dots\bar{\gamma}^{\nu_n}\} = \sum_{i=2}^n (-1)^i \bar{g}^{\nu_1\nu_i} \text{tr}\{\bar{\gamma}^{\nu_2}\dots\bar{\gamma}^{\nu_{i-1}}\bar{\gamma}^{\nu_{i+1}}\bar{\gamma}^{\nu_n}\}$$

is sufficient.

For the four dimensional trace $\text{tr}\{\hat{\Gamma}\}$ we can use another tool: the CHISHOLM identity, which is valid in four dimensions only, allows the evaluation of traces regardless if they include a γ_5 or not. For an algebraic reduction shorter results are achieved by algorithms that include other relations as well [Ver02]; on the other hand one can use

the CHISHOLM identity to write a numerical evaluation of traces having all LORENTZ indices contracted with external momenta and avoiding explicit summation over indices.

The CHISHOLM identity can be derived following the proof in [KS85]. The initial point of the proof is the fact that in the four dimensional MINKOWSKI space for the generators of the CLIFFORD algebra a finite basis exists, and every product S consisting of an odd number of DIRAC matrices therefore can be expressed as

$$(189) \quad S = V_\mu \hat{\gamma}^\mu + A_\mu \gamma_5 \hat{\gamma}^\mu,$$

where V^μ and A^μ are the two coefficient vectors. Now one considers the expression

$$(190) \quad \text{tr}\{S\hat{\gamma}^\mu\} \hat{\gamma}_\mu = \text{tr}\{V_\nu \hat{\gamma}^\nu \hat{\gamma}^\mu + A_\nu \gamma_5 \hat{\gamma}^\nu \hat{\gamma}^\mu\} \hat{\gamma}_\mu = 4V_\mu \hat{\gamma}^\mu.$$

The right hand side can also stem from

$$(191) \quad 2(S + S^R) = 2(2V_\mu \hat{\gamma}^\mu + A_\mu \{\gamma_5, \hat{\gamma}^\mu\}) = 4V_\mu \hat{\gamma}^\mu,$$

where S^R denotes the reverse of the spinor line. Equating (190) and (191) leads to the desired identity,

$$(192) \quad \text{tr}\{S\hat{\gamma}^\mu\} \hat{\gamma}_\mu = 2(S + S^R).$$

The analogous formula for a string T of an even number of γ -matrices⁴ comes from the representation

$$(193) \quad T = T_{\mu\nu} [\hat{\gamma}^\mu, \hat{\gamma}^\nu] + P\gamma_5 + S\mathbb{I};$$

the same logic as above applies and leads to

$$(194) \quad \text{tr}\{T\gamma_5\} \gamma_5 + \text{tr}\{T\} \mathbb{I} = 2(T + T^R)$$

The identity (192) can be made twofold use of. It leads to a reduction formula for DIRAC traces on one hand, on the other hand it can be used to eliminate LORENTZ indices that are contracted between two traces since

$$(195) \quad \text{tr}\{S\hat{\gamma}^\mu\} \text{tr}\{S'\hat{\gamma}_\mu\} = \text{tr}\{S' \text{tr}\{S\hat{\gamma}^\mu\} \hat{\gamma}_\mu\} = 2 \text{tr}\{S'S\} + 2 \text{tr}\{S'S^R\}.$$

To get rid of pairs of contracted indices inside one trace we can apply (194) to a string $\hat{\gamma}^\mu S \hat{\gamma}_\mu$ of odd length, revealing

$$(196) \quad \hat{\gamma}^\mu S \hat{\gamma}_\mu = -2S^R.$$

Without loss of generality strings of even length can be treated through the case $\hat{\gamma}^\mu S \hat{\gamma}^\nu \hat{\gamma}_\mu$, where S has odd length and one finds

$$(197) \quad \hat{\gamma}^\mu S \hat{\gamma}^\nu \hat{\gamma}_\mu = 2(\hat{\gamma}^\nu S + S^R \hat{\gamma}^\nu).$$

For obtaining a reduction formula for traces one starts from the specific choice $S = -(i/4)\gamma_5\gamma^\mu\gamma^\nu\gamma^\rho$. This implies for (192)

$$(198) \quad \text{tr}\{S\hat{\gamma}^\sigma\} \hat{\gamma}_\sigma = \epsilon^{\mu\nu\rho\sigma} \hat{\gamma}_\sigma$$

Here I used, as an implication of (182), that

$$(199) \quad -\frac{i}{4} \text{tr}\{\gamma_5 \hat{\gamma}^\mu \hat{\gamma}^\nu \hat{\gamma}^\rho \hat{\gamma}^\sigma\} \hat{\gamma}_\sigma = \epsilon^{\mu\nu\rho\sigma} \hat{\gamma}_\sigma = -\frac{i}{2} (\gamma_5 \hat{\gamma}^\mu \hat{\gamma}^\nu \hat{\gamma}^\rho + \hat{\gamma}^\rho \hat{\gamma}^\nu \hat{\gamma}^\mu \gamma_5).$$

⁴If a γ_5 appears in a string of DIRAC matrices it counts as an even number of matrices.

Rearranging the terms of (198) this leads to

$$(200) \quad \text{tr} \left\{ \gamma_5 \hat{p}_1 \hat{p}_2 \hat{p}_3 \hat{p}_4 \cdots \hat{p}_n \right\} = \\ \hat{p}_1 \cdot \hat{p}_2 \text{tr} \left\{ \gamma_5 \hat{p}_3 \hat{p}_4 \cdots \hat{p}_n \right\} - \hat{p}_1 \cdot \hat{p}_3 \text{tr} \left\{ \gamma_5 \hat{p}_2 \hat{p}_4 \cdots \hat{p}_n \right\} \\ + \hat{p}_2 \cdot \hat{p}_3 \text{tr} \left\{ \gamma_5 \hat{p}_1 \hat{p}_4 \cdots \hat{p}_n \right\} + i \epsilon^{p_1 p_2 p_3 \mu} \text{tr} \left\{ \gamma_\mu \hat{p}_4 \cdots \hat{p}_n \right\}.$$

The notation $\epsilon^{p_1 \cdots}$ is a shorthand notation for $\epsilon^{\mu \cdots} p_{1,\mu}$. Using the pendant to (188),

$$(201) \quad \text{tr} \{ \hat{\gamma}^{\nu_1} \cdots \hat{\gamma}^{\nu_n} \} = \sum_{i=2}^n (-1)^i \hat{g}^{\nu_1 \nu_i} \text{tr} \{ \hat{\gamma}^{\nu_2} \cdots \hat{\gamma}^{\nu_{i-1}} \hat{\gamma}^{\nu_{i+1}} \hat{\gamma}^{\nu_n} \}$$

one can eliminate also the explicit index μ in the last term of (200), and hence ends up in a formula suitable for numerical evaluation, provided numerical implementations of $p_i \cdot p_j$ and $\epsilon^{p_i p_j p_m p_n}$ exist,

$$(202) \quad \text{tr} \left\{ \gamma_5 \hat{p}_1 \hat{p}_2 \hat{p}_3 \hat{p}_4 \cdots \hat{p}_n \right\} = \hat{p}_1 \cdot \hat{p}_2 \text{tr} \left\{ \gamma_5 \hat{p}_3 \hat{p}_4 \cdots \hat{p}_n \right\} \\ - \hat{p}_1 \cdot \hat{p}_3 \text{tr} \left\{ \gamma_5 \hat{p}_2 \hat{p}_4 \cdots \hat{p}_n \right\} + \hat{p}_2 \cdot \hat{p}_3 \text{tr} \left\{ \gamma_5 \hat{p}_1 \hat{p}_4 \cdots \hat{p}_n \right\} \\ + i \sum_{j=4}^n (-1)^j \epsilon^{p_1 p_2 p_3 p_j} \text{tr} \left\{ \hat{p}_4 \cdots \hat{p}_{j-1} \hat{p}_{j+1} \cdots \hat{p}_n \right\}.$$

We can complete algorithm 5 by specifying its last step, which leads to algorithm 6.

Algorithm 6 Evaluate traces separately

```

Evaluate  $\text{tr}\{\bar{\Gamma}\}$  using (188)
if numeric evaluation then
  while LORENTZ indices left do
    Apply (197) or (196)
5:   Apply (195)
    while applicable do
       $\text{tr}\{\dots \hat{\gamma}^\mu \gamma_5 \dots\} \rightarrow -\text{tr}\{\dots \gamma_5 \hat{\gamma}^\mu \dots\}$ 
    end while
  end while
10:   $\text{/\star All } \hat{\gamma} \text{ matrices are contracted with momenta now. \star/}$ 
    Evaluate traces via (202) and (201) numerically.
  else  $\text{/\star algebraic evaluation \star/}$ 
    Use FORM to evaluate  $\text{tr}\{\hat{\Gamma}\}$  algebraically.
  end if

```

The assertion 10 can be made for QCD where all epsilon tensors stem from the evaluation of traces and therefore no contractions of the form $\epsilon^{\mu \cdots} \text{tr}\{\hat{\gamma}_\mu \dots\}$ are possible here. However, this case would be easy to handle as well, since all epsilon tensors can be eliminated earlier via reverse application of (199). The steps up to line 13 are required for a numerical evaluation of the traces in order to remove all explicit LORENTZ indices; the matrices \hat{p} can be calculated, multiplied and traced numerically⁵.

⁵Line 13 suggests an alternative implementation.

1.3. Gluons in DReg. In Section 3 of Chapter 2 we have already seen that in $D = 4$ dimensions both the quarks and the gluons have two degrees of freedom and therefore introduced the spinors $|p_{\pm}\rangle$ for the quarks and the polarisation vectors ϵ_{\pm}^{μ} for the gluons. In the *Naïve Dimensional Reduction (NDR)* scheme one finds the number of polarisations to be $(n - 2)$ [SvN05]; in the 'tHo scheme scheme, which I use, all external particles are strictly kept four dimensional and therefore the number of polarisations is 2. Table 1 summarises the comparison between NDR, the 'tHo scheme and Dimensional Reduction (DR) [SvN05, Jeg01].

	NDR	'tHo	DR
$\{\gamma_5, \gamma^{\mu}\}$	$\gamma^{\mu} = \hat{\gamma}^{\mu} + \bar{\gamma}^{\mu}$	$\gamma^{\mu} = \hat{\gamma}^{\mu} + \bar{\gamma}^{\mu}$	$\gamma^{\mu} = \hat{\gamma}^{\mu}, \quad \bar{\gamma}^{\mu} \equiv 0$
internal momenta	0	eq. (179)	0
external momenta	$k = \hat{k} + \bar{k}$	$k = \hat{k} + \bar{k}$	$k = \hat{k} + \bar{k}$
int. gluon pol. ^a	$p_i = \hat{p}_i + \bar{p}_i$	$p_i = \hat{p}_i, \quad \bar{p}_i = 0$	$p_i = \hat{p}_i, \quad \bar{p}_i = 0$
ext. gluon pol. ^b	$n - 2$	$n - 2$	2
	$n - 2$	2	2

^anumber of polarisations of internal gluons

^bnumber of polarisations of external gluons

Table 1: Comparison of different regularisation prescriptions

1.4. Loop Integrals. As discussed in the introduction of this chapter, integration over an unobserved, virtual particle in the amplitude gives rise to tensor integrals like

$$\int \frac{d^n k}{i\pi^{n/2}} \frac{k^{\mu}}{[(k + r_1)^2 + i\delta][(k + r_2)^2 + i\delta][k^2 + i\delta]}.$$

These integrals can be evaluated by the traditional approach by projections of the tensor integral onto the vectors r_1^{μ} and r_2^{μ} and by rewriting it in terms of scalar integrals. The form factors, i.e. the coefficients of r_1^{μ} and r_2^{μ} , then contain the inverse of a GRAM determinant⁶

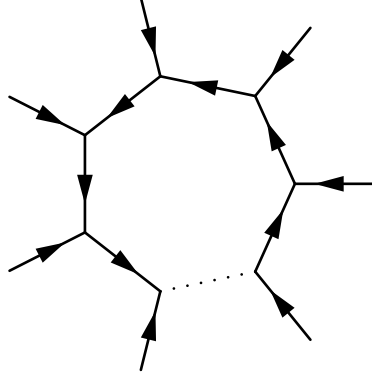
$$\det G = 4(r_1^2 r_2^2 - (r_1 \cdot r_2)^2).$$

This determinant vanishes for certain kinematic configurations; this kind of divergences is unphysical and must cancel in the full calculation. If not treated algebraically, these inverse GRAM determinants can spoil the numerical stability of an amplitude calculation and therefore have to be avoided.

Given an arbitrary loop amplitude we now concentrate on the one-particle irreducible part of the diagram, which always can be sketched as shown in figure 1. The notation is always chosen such that the external momentum flow of $p_i, i \in \{1, \dots, N\}$ is ingoing, and the indices are understood modulo N , i.e. $p_{N+1} \equiv p_1$. The momenta through the propagators are

$$(203) \quad q_i = k + r_i, \quad \text{where} \quad r_i - r_{i-1} = p_i,$$

⁶The related GRAM matrix would be defined via $G_{ij} = 2r_i \cdot r_j$. Later I will use a more convenient definition for the GRAM matrix, i.e. (247b); both definitions are equal up to a common shift of the momenta r_i .

Figure 1: Definition of the momenta at an arbitrary N -point integral

and the masses of the particles in the propagators are m_i . The definition of the vectors r_i resembles the invariance of the loop integral under shifts of the integration momentum. In the most general case one has to deal with integrals of the form

$$(204) \quad I_N^{d,\alpha;\mu_1\ldots\mu_r}(a_1,\ldots,a_r;S) \equiv \int \frac{d^d k}{i\pi^{d/2}} \frac{(\bar{k}^2)^\alpha \hat{q}_{a_1}^{\mu_1} \cdots \hat{q}_{a_r}^{\mu_r}}{\prod_{j=1}^N (q_j^2 - m_j^2 + i\delta)}.$$

It should be noted that in the following discussion I will always suppress a factor of $(4\pi\mu^2)^{2-n/2}$, which would naturally arise from the fact that the LAGRANGIAN density has to be kept dimensionless and therefore is multiplied by powers of an arbitrary mass scale μ . Furthermore, all logarithms of dimensionful quantities (e.g. $\ln(s)$) are understood to be regulated by powers of the same mass scale μ (i.e. $\ln(s/\mu^2)$); hence in these expressions the scale dependence on μ becomes explicit.

Integrals with $\alpha \neq 0$ stem from the evaluation of $\text{tr}\{\bar{\Gamma}\}$; only a limited number of them appear to be non-vanishing, and those left result in very simple expressions which are presented in Chapter 3, Section 1.5. For $\alpha = 0$, I will omit the superscript α .

Contrary to most existing approaches this definition of the tensor integrals has the propagator momenta q_i in the numerator instead of the integration momentum k . This generalisation takes into account the origin of the tensor integrals in the appropriate FEYNMAN rules. The way back to standard form is easy enough: one has to break shift invariance by choosing one $r_{a_\lambda} = 0, a_\lambda \in \{1, \ldots, N\}$ and only considering the integral $I_N^{d,\alpha;\mu_1\ldots\mu_r}(a_\lambda, \ldots, a_\lambda; S)$. Another generalisation is to also take into account integrals with dimensions $d \neq n$, where $n = 4 - 2\epsilon$. In the reduction formalism described in Sections 2 and 3, the basis integrals include the use of dimensions n , $n + 2$ and $n + 4$. It should also be noted that the momenta in the numerator are the four dimensional parts in this definition. Usually the definition with \hat{q}_a^μ cannot be distinguished from a definition with q_a^μ as long as the tensor integrals are contracted with external momenta which project onto the four-dimensional subspace. Care has to be taken if the contraction $k \cdot k = \hat{g}_{\mu\nu} \hat{k}^\mu \hat{k}^\nu + (\bar{k})^2$ appears in the calculation.

The matrix S contains the kinematic invariants in the following form

$$(205) \quad S_{ij} = (\Delta_{ij})^2 - m_i^2 - m_j^2, \quad \text{with} \quad \Delta_{ij}^\mu = r_i^\mu - r_j^\mu = q_i^\mu - q_j^\mu$$

The importance of the kinematic matrix S becomes clear if one writes down the loop integrals in FEYNMAN parameter space,

$$(206a) \quad I_N^d(l_1, \dots, l_r; S) = (-1)^N \Gamma(N - d/2) \int_0^1 d^N z \delta_z \frac{z_{l_1} \cdots z_{l_r}}{\left(-\frac{1}{2} z^T S z - i\delta\right)^{N-d/2}}.$$

The abbreviations I introduced are

$$(206b) \quad \delta_z = \delta \left(1 - \sum_{j=1}^N z_j\right),$$

$$(206c) \quad \int_0^1 d^N z = \int_{-\infty}^{\infty} \prod_{j=1}^N (dz_j \Theta(z_j)) \quad \text{and}$$

$$(206d) \quad z^T S z = \sum_{i,j=1}^N z_i S_{ij} z_j.$$

The relation between (204) and (204) can be found by the usual procedure, introducing FEYNMAN parameters and substituting $k \rightarrow k - \sum_{j=1}^N z_j r_j$ one obtains⁷

$$(207) \quad I_N^{d,\alpha;\mu_1 \dots \mu_r}(a_1, \dots, a_r; S) = \Gamma(N) \int_0^1 d^N z \delta_z \int \frac{d^4 \hat{k}}{i\pi^2} \frac{d^{d-4} \bar{k}}{\pi^{d/2-2}} \frac{(\bar{k}^2)^\alpha \prod_{\nu=1}^r (\hat{k}^{\mu_\nu} - \sum_{i=1}^N z_i \Delta_{ia_\nu}^{\mu_\nu})}{\left[\hat{k}^2 + \bar{k}^2 + \frac{1}{2} z^T S z + i\delta\right]^N}.$$

The momentum integration in the $(d-4)$ -dimensional subspace can be carried out immediately. Before one can treat the four-dimensional subspace as well the numerator needs some further investigation. First one observes that when the numerator is expanded all terms with an odd number of \hat{k} vectors vanishes under symmetric integration. Any even number $2l$ of \hat{k} can be reduced to

$$(208) \quad \hat{k}^{\nu_1} \dots \hat{k}^{\nu_{2l}} = \frac{\overbrace{[\hat{g}^{\dots} \dots \hat{g}^{\dots}]^{\nu_1 \dots \nu_{2l}}}^l}{\prod_{j=0}^{l-1} (4+2j)} (\hat{k}^2)^l = \frac{[\hat{g}^{\dots} \dots \hat{g}^{\dots}]^{\nu_1 \dots \nu_{2l}}}{2^l \Gamma(l+2)} (\hat{k}^2)^l.$$

The square brackets with trailing indices denote the distribution of the indices over the elements inside the brackets. The combinatorial factor can be obtained from considering all possibilities of connecting the endpoints of l lines where every closed line counts as factor $4 = \hat{g}_\mu^\mu$. The $(j+1)$ -th line is added by either connecting its two endpoints to each other and building an extra circle or by stitching itself to one of the $2j$ existing endpoints, which explains the factor $(4+2j)$. The second relation is then proved by induction.

⁷It must be considered that $\bar{k}^2 = -|\bar{k}|^2$.

Now the four-dimensional momentum integration can be carried out as well and the whole formula reads

$$(209) \quad I_N^{d,\alpha;\mu_1\ldots\mu_r}(a_1,\ldots,a_r;S) = (-1)^{r+\alpha} \frac{\Gamma(\alpha + d/2 - 2)}{\Gamma(d/2 - 2)} \sum_{l=0}^{\lfloor r/2 \rfloor} \left(-\frac{1}{2}\right)^l \times \\ \sum_{j_1,\ldots,j_{r-2l}=1}^N \underbrace{[\hat{g}^{\bullet\bullet} \cdots \hat{g}^{\bullet\bullet}]_l}_{\substack{\text{ } \\ \text{ } }} \Delta_{j_1}^{\bullet} \cdots \Delta_{j_{r-2l}}^{\bullet}]_{a_1\ldots a_r}^{\mu_1\ldots\mu_r} I_N^{d+2\alpha+2l}(j_1,\ldots,j_{r-2l};S).$$

1.5. Polynomial Loop Integrals. As mentioned earlier only a limited number of integrals with $\alpha > 0$ are non-zero. The reason therefore is the factor

$$(210) \quad c_\alpha^d = (-1)^\alpha \frac{\Gamma(\alpha + d/2 - 2)}{\Gamma(d/2 - 2)}.$$

For $\alpha = 0$ this factor is $c_0^d = 1$. In the case $\alpha > 0$ we only need to consider $d = n$ and get the result

$$(211) \quad c_\alpha^n = (-1)^{\alpha-1} \varepsilon \frac{\Gamma(\alpha - \varepsilon)}{\Gamma(1 - \varepsilon)} = (-1)^{\alpha-1} (\alpha - 1)! \varepsilon + \mathcal{O}(\varepsilon^2).$$

This coefficient has to be combined with the integral $I_N^{n+2\alpha+2l}$ from Equation (209). For phenomenological applications terms of order $\mathcal{O}(\varepsilon)$ are irrelevant, therefore one needs to consider only integrals that contain divergences. The dimension of the integral is always strictly larger than⁸ n and hence the integrals are free of IR singularities, which will be proved in Section 2.2. Hence the integrals leading to a finite contribution in the final result must contain a UV divergence coming from the Γ function,

$$(212) \quad \Gamma\left(N - \frac{n + 2\alpha + 2l}{2}\right) = \Gamma(N - 2 - \alpha - l + \varepsilon) \equiv \Gamma(\varepsilon - \eta).$$

In order to produce a UV divergence, the integer part of the argument needs to fulfil $\eta \geq 0$. Taking into account the ε stemming from c_α^n one obtains

$$(213) \quad \varepsilon I_N^{n+2l+2\alpha}(l_1,\ldots,l_r;S) = \begin{cases} \mathcal{O}(\varepsilon), & -\eta > 0, \\ (-1)^N \frac{1}{2^\eta \eta!} \int_0^N d^N z \delta_z \prod_{j=1}^r z_{l_j} [z^\top S z]^\eta + \mathcal{O}(\varepsilon), & \eta \geq 0. \end{cases}$$

Finally, the FEYNMAN parameter integral

$$(214) \quad P_{\alpha_1,\alpha_2,\ldots,\alpha_N} = \int d^N z \delta_z \prod_{j=1}^N z_j^{\alpha_j}, \quad \text{with } \forall j \in \{1,\ldots,N\} : \alpha_j \geq 0$$

can be solved and the solution is given below.

We start from the equation

$$(215) \quad f_p(r,s) = \int_0^p dx x^r (p-x)^s = \frac{r!s!}{(r+s+1)!} p^{r+s+1},$$

which is shown by induction and using integration by parts. Now we go back to (214), where the integration over z_N is carried out over the δ -function. What remains is the

⁸We only consider the case $\alpha \neq 0$.

integral

$$(216) \quad P_{\alpha_1, \alpha_2, \dots, \alpha_N} = \prod_{j=1}^{N-1} \left(\int_0^{p_{N-j}} dz_{N-j} z_{N-j}^{\alpha_{N-j}} \right) (p_1 - z_1)^{\alpha_N}$$

with the upper bounds $p_{i-1} = p_i - z_i$ and $p_{N-1} = 1$. The rightmost integral is recognised as

$$(217) \quad \int_0^{p_1} dz_1 z_1^{\alpha_1} (p_1 - z_1)^{\alpha_N} = f_{p_1}(\alpha_1, \alpha_N) = \frac{\alpha_1! \alpha_N!}{(\alpha_1 + \alpha_N + 1)!} (p_2 - z_2)^{\alpha_1 + \alpha_N + 1}$$

and analogously one iterates through all the integrals to the left. After the left integration the result is

$$(218) \quad P_{\alpha_1, \alpha_2, \dots, \alpha_N} = \frac{\prod_{j=1}^N (\alpha_j!)}{(N-1 + \sum_{i=1}^N \alpha_i)!}.$$

Finally the symbol $P_N(j_1, \dots, j_s)$ is introduced, which counts the indices in a expression:

$$(219) \quad P_N(j_1, \dots, j_s) = P_{(\sum_{i=1}^s \delta_{1,j_i}), \dots, (\sum_{i=1}^s \delta_{N,j_i})}.$$

Substituted back into (213), for the case $\eta \geq 0$ one obtains

$$(220) \quad \varepsilon I_N^{n-4+2(N+\eta)}(l_1, \dots, l_r; S) = \frac{(-1)^N}{2^\eta \eta!} \sum_{j_1, \dots, j_{2\eta}=1}^N S_{j_1 j_2} \cdots S_{j_{2\eta-1} j_{2\eta}} P_N(l_1, \dots, l_r, j_1, \dots, j_{2\eta}).$$

Working in the FEYNMAN gauge in QCD one can put a limit on the degree of the numerator, as the FEYNMAN rules in this case ensure that the tensorial rank of the integral never exceeds the number N of loop propagators,

$$(221) \quad 2l + 2\alpha \leq N.$$

Using the definition of $\eta = l + \alpha + 2 - N$ one obtains

$$(222) \quad 0 \leq 2\eta \leq 4 - N \quad \Rightarrow \quad N \leq 4 \quad \Rightarrow \quad l + \alpha \leq 2.$$

Taking all these formulæ together reveals that one does not need to know any integral with $\eta \geq 2$. On the other hand for $0 \leq \eta \leq 1$ the formulæ become very simple: for $\eta = 0$ one has $n + 2l + 2\alpha = n - 4 + N$ and hence

$$(223) \quad \varepsilon I_N^{n-4+2N}(l_1, \dots, l_r; S) = (-1)^N P_N(l_1, \dots, l_r).$$

For $\eta = 1$ one can replace $n + 2l + 2\alpha = n + 2(N+1)$ which yields

$$(224) \quad \varepsilon I_N^{n-4+2(N+1)}(l_1, \dots, l_r; S) = \frac{(-1)^N}{2} \sum_{j_1, j_2=1}^N S_{j_1 j_2} P_N(j_1, j_2, l_1, \dots, l_r).$$

Explicit formulæ for the required cases are given in Appendix D, Section 4.

In this context a caveat of DReg should be addressed: the order of different limits can have important consequences and therefore has to be treated with special care. Let us therefore refer back to the definition of the tensor integrals (204) and compare it to an equally valid definition, where the \hat{q}^μ in the numerator are replaced by q^μ :

$$(225) \quad \check{I}_N^{d, \alpha; \mu_1 \dots \mu_r}(a_1, \dots, a_r; S) \equiv \int \frac{d^d k}{i\pi^{n/2}} \frac{(\bar{k}^2)^\alpha q_{a_1}^{\mu_1} \cdots q_{a_r}^{\mu_r}}{\prod_{j=1}^N (q_j^2 - m_j^2 + i\delta)}$$

After a short calculation one finds for example

$$(226a) \quad I_4^{n,1;\mu\nu}(a_1, a_2; S) = -\left(\frac{1}{12} + \mathcal{O}(\varepsilon)\right) \hat{g}^{\mu\nu} \quad \text{versus}$$

$$(226b) \quad \check{I}_4^{n,1;\mu\nu}(a_1, a_2; S) = -\left(\frac{1}{8} + \mathcal{O}(\varepsilon)\right) g^{\mu\nu} \quad .$$

Since external vectors were assumed as four-dimensional from naïve treatment of the limits one would expect that for a vector p with $p^2 \neq 0$ the expressions $p_\mu p_\nu I_4^{n,1;\mu\nu}$ and $p_\mu p_\nu \check{I}_4^{n,1;\mu\nu}$ should be the same but they apparently are not. The reason can be seen if one splits the second expression into

$$(227) \quad \check{I}_4^{n,1;\mu\nu}(a_1, a_2; S) = A g^{\mu\nu} = \hat{A} \hat{g}^{\mu\nu} + \bar{A} \bar{g}^{\mu\nu},$$

where one obtains the values

$$(228a) \quad A = -\frac{1}{8} + \mathcal{O}(\varepsilon),$$

$$(228b) \quad \hat{A} = -\frac{1}{12} + \mathcal{O}(\varepsilon),$$

$$(228c) \quad \bar{A} = \frac{1}{12\varepsilon} + \mathcal{O}(1).$$

Contracting both sides of (227) with $g_{\mu\nu}$ leads to the correct result but the projections on the subspaces by contracting with $\hat{g}_{\mu\nu}$ and $\bar{g}_{\mu\nu}$ are different. Multiplying the equation with $p_\mu p_\nu$ reveals that

$$(229) \quad \left(-\frac{1}{8} + \mathcal{O}(\varepsilon)\right) p^2 \neq -\left(\frac{1}{12} + \mathcal{O}(\varepsilon)\right) \hat{p}^2 + \left(\frac{1}{12\varepsilon} + \mathcal{O}(1)\right) \bar{p}^2,$$

and hence, when using dimension splitting⁹ the above integral cannot be decomposed into a $g^{\mu\nu}$ component only but must be treated as a linear combination of $\hat{g}^{\mu\nu}$ and $\bar{g}^{\mu\nu}$ instead.

2. Reduction of the Scalar Integrals

2.1. Introduction. In the previous section one-loop integrals have been introduced and discussed in their general form, and a translation into FEYNMAN parameter integrals has been given. In the following section relations between scalar integrals are established that lead to a reduction algorithm which allows any one-loop tensor integral to be expressed in terms of a limited set of standard scalar integrals.

The observation of relations between scalar integrals [Mel65] has been a key development for the first computations of higher order corrections, e.g. for $e^+ + e^- \rightarrow \mu^+ + \mu^-$ [PV79] and later $e^+ + e^- \rightarrow e^+ + e^- + X$ with a pseudoscalar X in the final state [vNV84], and the techniques used for these early computations led into the systematic development of reduction techniques for one-loop integrals [Dav91, FJT00]. A systematic treatment of critical phase-space regions has been addressed by different approaches [BGH00, DD03, BGH⁺05, DD06]

⁹Conversely, in NDR this type of integrals with powers of \bar{k}^2 in the numerator do not appear.

In my present calculation the reduction method proposed in [BGH⁺05] is used. This chapter describes the foundation of this method; for a full list of form factors one should refer to the original paper. A complete list of the scalar one-loop integrals that are required as a basis has been compiled in [EZ08] and is provided as a numerical implementation by the same authors [EZ].

2.2. Infrared Divergences. It has been mentioned already that the reduction formalisms, both for scalar integrals and for tensor integrals separates infrared poles in the integrals and groups them such that cancellations can be carried out easily. While ultraviolet poles in dimensional regularisation stem from singularities of the Γ -function and are removed systematically by renormalisation, infrared divergences appear when massless particles propagate through the loop. These singularities usually are kept during the calculation and have to cancel in the end.

Two classes of infrared divergences have to be distinguished: A *soft divergence* arises when the integration momentum k becomes soft, i.e. $k^\mu \rightarrow 0$. Let all masses m_i be zero and all external particles be lightlike. Using shift invariance the integral $I_N^{d;\mu_1 \dots \mu_r}(S)$ under $k \rightarrow \lambda k - r_a$, where λ denotes an arbitrary real variable, becomes¹⁰

$$(230) \quad I_N^{d;\mu_1 \dots \mu_r}(a_1, \dots, a_r; S) = \int \frac{\lambda^d d^d k}{i\pi^{n/2}} \frac{(\lambda k^{\mu_1} + \Delta_{a_1 a}^{\mu_1}) \dots (\lambda k^{\mu_r} + \Delta_{a_r a}^{\mu_r})}{\lambda^2 k^2 \prod_{j \in S \setminus \{a\}} ((\lambda k + \Delta_{ja})^2 + i\delta)}.$$

Now the soft limit is taken by $\lambda \rightarrow 0$. Therefore the soft infrared behaviour of the integral is determined by the overall power of lambda. Hence a non-trivial numerator can improve the infrared behaviour, i.e. increase power of λ , but never generate singularities. In this respect the scalar functions are the worst case to be studied. In a scalar function there are three sources for λ^{-l} with negative exponent ($-l$). Obviously the k^2 term in the denominator contributes λ^{-1} but also two more propagators,

$$(231) \quad (\lambda k + \Delta_{(a\pm 1)a})^2 = \lambda^2 k^2 + 2\lambda k \cdot \Delta_{(a\pm 1)a} + \Delta_{(a\pm 1)a}^2 = 2\lambda k \cdot \Delta_{(a\pm 1)a} + \mathcal{O}(\lambda^2)$$

cause problems. Here I used the fact that $\Delta_{(a\pm 1)a}^2 = p_{a\pm 1}^2 = 0$. Including also the differential which yields a λ^d the overall degree of divergence is $(d-4)$. This is negative for $d = n = 4 - 2\varepsilon$ but always positive for any $d > 4$. Therefore all higher dimensional scalar integrals are free of soft divergences.

The second class of divergences is called *soft collinear infrared singularities*. They arise when two partons become collinear. The singularities can be exposed by the following procedure: the integration momentum is replaced by $k \rightarrow \lambda_\parallel k_\parallel + \lambda_\perp k_\perp - r_a$, where $k_\perp \cdot p_a = k_\perp \cdot k_\parallel = 0$ and k_\parallel lies in the one dimensional subspace of the d -dimensional MINKOWSKI space that is spanned by $\langle p_a \rangle$.

Now one can examine the collinear behaviour of scalar an arbitrary scalar integral,

$$(232) \quad I_N^d(S) = \int \frac{\lambda_\perp^{d-1} \lambda_\parallel d^{d-1} k_\perp dk_\parallel}{i\pi^{n/2}} \frac{1}{\prod_{j \in S} ((\lambda k + \Delta_{ja})^2 + i\delta)}.$$

¹⁰I do not distinguish between four and n -dimensional vectors here. It should be clear from former definitions where to use \hat{q} instead of q . For the discussion of infrared singularities this difference, however, is irrelevant.

The dangerous propagators in that case are

$$(233a) \quad (k + \Delta_{aa})^2 = \lambda_\perp^2 k_\perp^2,$$

$$(233b) \quad (k + \Delta_{(a-1)a})^2 = \lambda_\perp^2 k_\perp^2 \quad \text{and}$$

$$(233c) \quad (k + \Delta_{(a+1)a})^2 = \lambda_\perp^2 k_\perp^2 + 2\lambda_\parallel k_\parallel \cdot p_{a+1} + \lambda_\perp k_\perp \cdot p_{a+1}.$$

Now first the collinear limit is taken, i.e. $\lambda_\perp \rightarrow 0$; this limit causes no poles for $d > 5$. Performing $\lambda_\parallel \rightarrow 0$ in addition is safe as well since the λ_\parallel in numerator and denominator cancel exactly. This proves that all integrals in $d \geq 6 - 2\epsilon$ are infrared safe. Similar techniques can be applied to reveal infrared divergences in the real emission part of the amplitude.

2.3. Subtraction Method for Scalar Integrals. In this section I consider only integrals of the type

$$(234) \quad I_N^d(S) = \int \frac{d^N k}{i\pi^{n/2}} \frac{1}{\prod_{j \in S_\#} (q_j^2 - m_j^2 + i\delta)} = (-1)^N \Gamma(N - d/2) \int_0^1 d^N z \delta_z \frac{1}{(-\frac{1}{2} z^\top S z - i\delta)^{N-d/2}}.$$

With $S_\#$ I denote the support of the matrix $S \in \mathbb{R}^{N \times N}$,

$$(235) \quad S_\# \equiv \{i \in \{1, \dots, N\} \mid \exists j \in \{1, \dots, N\} : S_{ij} \neq 0\}.$$

This notation will become important because pinches of the matrix S , which are defined by

$$(236) \quad S_{ij}^{\{l_1, l_2, \dots, l_m\}} = \begin{cases} S_{ij}, & \{i, j\} \cap \{l_1, l_2, \dots, l_m\} = \emptyset, \\ 0, & \text{otherwise,} \end{cases}$$

play a central role in the formulation of the reduction algorithm¹¹. For example, starting from a non-singular matrix S , $S_\#^{\{j_1, j_2\}} = \{1, \dots, N\} - \{j_1, j_2\}$. All pinched matrices, that is all matrices where $\{l_1, l_2, \dots\} \neq \emptyset$, are singular by definition. As a proper way to treat them will use the MOORE-PENROSE pseudoinverse¹² $\tilde{S}^{\{l_1, \dots, l_m\}}$ of the pinched matrix $S^{\{l_1, \dots, l_m\}}$. In the presence of pinched matrices some of the previous definitions need to be slightly changed,

$$\delta_z = \delta \left(1 - \sum_{j \in S_\#} z_j \right),$$

$$z^\top S z = \sum_{i, j \in S_\#} z_i S_{ij} z_j$$

and

$$\int_0^1 d^N z = \int_{-\infty}^{\infty} \prod_{j \in S_\#}^N (dz_j \Theta(z_j)).$$

The aim of the reduction is to split the integral into an infrared safe part and a remainder that contains all possible sources for infrared singularities,

$$(237) \quad I_N^n(S) = I_{\text{div}} + I_{\text{fin}}.$$

¹¹ Alternatively, the algorithm could be written down in terms of matrices of different sizes.

¹² A detailed definition of the MOORE-PENROSE pseudoinverse can be found in Appendix B.

We will see that at the end of each reduction chain the infrared poles are always contained in the three-point functions.

To obtain a form like (237) the numerator of the integral is rewritten as a linear combination of the propagators,

$$(238) \quad I_N^n(S) = \sum_{j \in S_\#} b_j(S) \int \frac{d^n k}{i\pi^{n/2}} \frac{(q_j^2 - m_j^2)}{\prod_{j \in S_\#} (q_j^2 - m_j^2 + i\delta)} \\ + \int \frac{d^n k}{i\pi^{n/2}} \frac{1 - \sum_{j \in S_\#} b_j(S)(q_j^2 - m_j^2)}{\prod_{j \in S_\#} (q_j^2 - m_j^2 + i\delta)}.$$

The first term of the expression (238) is the sum of pinched integrals

$$(239) \quad I_{\text{div}} = \sum_{j \in S_\#} b_j(S) I_{N-1}^n(S^{\{j\}})$$

In the second term, analogous to the procedure in section 1.4, we introduce FEYNMAN parameters and shift the origin of the integration momentum by $k \rightarrow k - \sum_{i \in S_\#} z_i r_i$. The denominator can be written, as usual, in quadratic form; the numerator becomes

$$(240) \quad 1 - \sum_{j \in S_\#} b_j(S) \left((k - \sum_{i \in S_\#} z_i \Delta_{ij})^2 - m_j^2 \right) = \\ - \left(\sum_{j \in S_\#} b_j \right) \left(k^2 - \frac{1}{2} z^\top S z \right) + \left[1 - \sum_{j, k \in S_\#} z_k (b_j S_{jk} - 2\Delta_{kj} \cdot k) \right].$$

To obtain that result one needs the relation $2\Delta_{ij} \cdot \Delta_{kl} = S_{il} + S_{jk} - S_{ik} - S_{jl}$. The term linear in the integration momentum vanishes under symmetric integration. Now we can choose the $b_j(S)$, which are still undetermined, such that the square bracket vanishes. Once more we use the fact that $\sum_{k \in S_\#} z_k = 1$ and hence find the condition

$$(241) \quad \sum_{j \in S_\#} S_{ij} b_j(S) = 1$$

for the bracket to vanish. Before finding the solution of the above equation the remaining integral shall be brought back into standard form. Therefore I introduce the symbol $B(S) = \sum_{j \in S_\#} b_j(S)$, and hence

$$(242) \quad I_{\text{fin}} = -B(S) \Gamma(N) \int_0^N dz \delta_z \int \frac{d^n k}{i\pi^{n/2}} \frac{(k^2 - \frac{1}{2} z^\top S z)}{[k^2 + \frac{1}{2} z^\top S z + i\delta]^N}$$

Carrying out the momentum integration leaves us with

$$(243) \quad I_{\text{fin}} = -B(S) \Gamma(N) \int_0^N dz \delta_z \frac{(-1)^{N+1} \Gamma(N)}{\Gamma(\frac{n}{2}) [-\frac{1}{2} z^\top S z - i\delta]^{N - \frac{n+2}{2}}} \int_0^\infty dx \frac{x-1}{(x+1)^N} x^{\frac{n-2}{2}}.$$

The integral over x is a difference of beta-functions,

$$(244) \quad \int_0^\infty dx \frac{x-1}{(x+1)^N} x^{\frac{n-2}{2}} = \frac{\Gamma(\frac{n+2}{2}) \Gamma(N - \frac{n+2}{2})}{\Gamma(N)} - \frac{\Gamma(\frac{n}{2}) \Gamma(N - \frac{n}{2})}{\Gamma(N)} = \\ \frac{\Gamma(\frac{n}{2}) \Gamma(N - \frac{n+2}{2})}{\Gamma(N)} \left(\frac{n+2}{2} - N + \frac{n}{2} + 1 \right),$$

and therefore the whole integral is

$$(245) \quad I_{\text{fin}} = -B(S)(N - n - 1)I_N^{n+2}(S).$$

In the remaining part of this section I will review the result of [BGH⁺05], that (241) for any case can be solved using the pseudoinverse \tilde{S} ,

$$(246) \quad b_j(S) = \sum_{i \in S_{\#}} \tilde{S}_{ij}.$$

One always can rewrite S in terms of the GRAM matrix $G^{(a)}$ and a remainder,

$$(247a) \quad S = -G^{(a)} + v^{(a)}\eta^{\text{T}} + \eta v^{(a)\text{T}}, \quad \text{with}$$

$$(247b) \quad G_{ij}^{(a)} = 2\Delta_{ia} \cdot \Delta_{ja},$$

$$(247c) \quad v_i^{(a)} = \Delta_{ia}^2 - m_i^2 \quad \text{and}$$

$$(247d) \quad \eta_i = 1, \quad \forall i \in S_{\#}.$$

The vectors η and $v^{(a)}$ are column vectors; all (explicit and implicit) sums are understood over the support $S_{\#}$ of S . In what follows the index a is kept constant and therefore the superscript $^{(a)}$ is omitted. The definition of $G^{(a)}$ exposes that $G_{ia}^{(a)} = G_{ai}^{(a)} = 0, \forall i \in S_{\#}$.

In this notation equation (241) reads

$$(248) \quad -Gb + v\eta^{\text{T}}b + \eta v^{\text{T}}b = \eta,$$

and can equally be written as a set of two equations,

$$(249a) \quad Gb = (\eta^{\text{T}}b)v - Bv_a\eta = B(v - v_a\eta),$$

$$(249b) \quad (v^{\text{T}}b)\eta = (1 - Bv_a)\eta \quad \Leftrightarrow v^{\text{T}}b = 1 - Bv_a.$$

In the case $\det S \neq 0$, the matrix S is regular and the pseudoinverse is equal to the normal inverse S^{-1} . The required condition¹³

$$(250) \quad \sum_{j \in S_{\#}} S_{ij} b_j(S) = \sum_{j \in S_{\#}} \sum_{k \in S_{\#}} S_{ij} S_{ik}^{-1} = \sum_{k \in S_{\#}} \delta_{ik} = 1$$

trivially holds. If, however, $\det S = 0$ one has to ensure that

$$(251) \quad S\tilde{S}\eta = \eta$$

is fulfilled. According to theorem 5 constructing a solution to the linear system (249) implicitly proves equation (251).

First the GRAM matrix G is represented in an orthonormal basis $e_1^{\mu}, \dots, e_r^{\mu}$ of the subspace $\langle \Delta_{ia}^{\mu} | i \in S_{\#} \rangle$, where r is the rank of G , $r = \text{rk } G$. Since the physical MINKOWSKI space has dimension 4 there are never more than 4 linear independent external momenta, or equally one always has $\text{rk } G \leq \min(N - 1, 4)$. Now one can write

$$(252) \quad \Delta_{ia}^{\mu} = \sum_{m=1}^r R_{mi}^{(a)} e_m^{\mu}, \quad \hat{G}_{ij}^{(a)} = 2e_i \cdot e_j = 2\delta_{ij}, \quad R_{ij}^{(a)} = e_i \cdot \Delta_{ja}.$$

¹³ $S = S^{\text{T}}$ is used.

Hence one has $R \in \mathbb{R}^{r \times N}$, $\hat{G}, RR^\top \in \mathbb{R}^{r \times r}$ and $G, R^\top R \in \mathbb{R}^{N \times N}$, and G and \hat{G} are related by $G = R^\top \hat{G} R$. The matrix R has full line rank and therefore RR^\top is invertible. This allows to construct the pseudoinverse of G explicitly,

$$(253) \quad \tilde{G} = R^\top (RR^\top)^{-1} \hat{G}^{-1} (RR^\top)^{-1} R$$

To invert (249a) the consistency condition from theorem 5 has to be fulfilled,

$$(254) \quad B(\mathbb{I} - G\tilde{G})(v - v_a \eta) = 0.$$

Clearly, for $\text{rk } G < N - 1$ and general v this equation can only be satisfied¹⁴ when $B = 0$, since $(\mathbb{I} - G\tilde{G})$ projects on $\text{Ker } G$, and $\dim(\text{Ker } G) \geq 2$. For the case $\text{rk } G = N - 1$ and $\det S \neq 0$ the solution has been given before, and hence only the case $B = 0$ is given further investigation. The problematic regions where $\text{rk } G = N - 1$ but at the same time $\det S = 0$ are discussed separately in section 2.5.

The system (249) now simplifies to

$$(255) \quad Gb = 0, \quad v^\top b = 1, \quad B = \eta^\top b = 0.$$

With the abbreviations $\delta v = v - v_a \eta$ and $K_G = \mathbb{I} - \tilde{G}G$, which is the projector on $\text{Ker } G$, the solution is easily constructed:

$$(256a) \quad b_i = \frac{(K_G \delta v)_i}{\delta v^\top K_G \delta v} + \sum_{j=1}^{N-\text{rk } G-2} \beta_j u_i^{(j)}, \quad \text{if } i \in S_{\#}^{\{a\}},$$

$$(256b) \quad b_a = - \sum_{j \in S_{\#}^{\{a\}}} b_j,$$

where $u^{(j)}$ form a basis of $\text{Ker } G \cap \langle \delta v, \delta_a \rangle^\perp$, and $\langle \delta v, \delta_a \rangle^\perp$ is the space orthogonal to δv and δ_a , where $(\delta_a)_i = \delta_{ai}$. The vector δ_a has to be projected out because in the solution $b(S)$ the remnant of δ_a is the null-vector. The upper bound in the sum is the dimension of the solution space,

$$(257) \quad \dim(\text{Ker } G \cap \langle \delta v, \delta_a \rangle^\perp) = \dim(\text{Ker } G) - \dim(\langle \delta v, \delta_a \rangle) = N - \text{rk } G - 2.$$

The real constants β_j parametrise the solution $b(S)$. This allows to determine the rank of S for the dimension of the solution space of $Sb = \eta$ is $N - \text{rk } G - 2$; hence

$$(258) \quad \text{rk } S = \text{rk } G + 2, \quad \text{for } \text{rk } G \leq N - 2.$$

Though the solvability of $Sb = \eta$ has already been shown, the result can be exploited further. We have seen that the rank of G distinguishes two kinematic situations: the case $\text{rk } G = \min(4, N - 1)$ is called *non-exceptional kinematics*, conversely $\text{rk } G < \min(4, N - 1)$ is called *exceptional kinematic*. For non-exceptional kinematics relation (258) can be expressed as

$$(259) \quad \text{rk } S = \min(N, 6).$$

¹⁴Still a special v could be such that $(\mathbb{I} - G\tilde{G})(v - v_a \eta) = 0$. In that case theorem 5 also holds for $B \neq 0$ and the solution is given by the theorem through the pseudoinverse, i.e. $b = B\tilde{G}(v - v_a \eta) + (\mathbb{I} - \tilde{G}G)u$, where one always can choose u such that the two remaining constraints $\eta^\top b = B$ and $v^\top b = 1 + Bv_a$ are met.

Since S can be split through (247a) one finds another interpretation of (258). The matrix

$$(260) \quad M \equiv v\eta^\top + \eta v^\top$$

is of rank 2 as I will show now.

The eigenvectors of M are

$$(261) \quad x_\pm = \alpha_\pm \left(v \pm \sqrt{\frac{v^\top v}{N}} \eta \right)$$

with the eigenvalues $\lambda_\pm = v^\top \eta \pm \sqrt{N v^\top v}$ and the normalisation constants α_\pm such that $x_\pm^\top x_\pm = 1$, and an orthonormal basis x_i , $i = 1, \dots, N-2$ of the eigenspace for the eigenvalue 0,

$$(262) \quad \langle x_1, \dots, x_{N-2} \rangle = \langle v, \eta \rangle^\perp.$$

The orthogonal transformation matrix $O = (x_1, \dots, x_{N-2}, x_+, x_-)$ diagonalises M ,

$$(263) \quad M = O^\top \text{diag}(0, \dots, 0, \lambda_+, \lambda_-) O$$

and hence the rank of M is 2. The pseudoinverse of M is given by

$$(264) \quad \tilde{M} = O^\top \text{diag}(0, \dots, 0, 1/\lambda_+, 1/\lambda_-) O.$$

This proves the rank formula

$$(265) \quad \text{rk } S = \text{rk}(-G + M) = \text{rk } G + \text{rk } M$$

for exceptional kinematics. The fact that (265) is fulfilled allows to use explicit formulæ for the pseudoinverse \tilde{S} which are given in [HS81, FF00]. However, for a numerical implementation an appropriate choice is the GREVILLE algorithm [UK97].

To conclude this section I briefly review what one has gained so far. The reduction algorithm for scalar integrals splits the integrals into a infrared finite, higher dimensional part and a sum of pinched integrals containing the infrared divergences:

$$(266) \quad I_N^n(S) = \sum_{k \in S_\#} b_k(S) I_{N-1}^n(S^{\{k\}}) - B(S)(N-n-1) I_N^{n+2}(S)$$

The solutions $b_k(S)$ are constructed such that $B(S)$ generally vanishes for $N \geq 6$; in exceptional kinematics $B(S)$ vanishes for arbitrary N . In the case $N = 5$ the coefficient $(N-n-1) = \mathcal{O}(\varepsilon)$ and can be dropped in phenomenological applications since $I_5^{n+2}(S)$ is both, ultraviolet and infrared finite.

2.4. A Determinant Relation. In [BGH00, BDK94] a relation between the GRAM determinant and $\det S$ is given,

$$(267) \quad \det G^\phi = (-1)^{N-1} B \det S,$$

where G^ϕ refers to the matrix constructed from $G^{(a)}$ by eliminating the a -th row and column; analogously I call δv^ϕ the result of leaving out the a -th row from $\delta v^{(a)}$.

This equation reveals that the term proportional to I_N^{d+2} must vanish in (266) for $N \geq 6$ where $\det G = 0$ is generally true. On the other hand this relation proves, that in 3.4 the application of (266) introduces inverse GRAM determinants through the $1/B$ terms.

The proof is given for invertible G^ϕ . We have seen in the previous section that for $\det G^\phi = 0$ the b_j can always be chosen such that $B = 0$, which satisfies (267) trivially. It is

$$(268) \quad B \det S = B \det(-G^{(a)} + v\eta^\top + \eta v^\top),$$

and by standard determinant manipulations one can rewrite this determinant in block matrix form,

$$(269) \quad B \det S = B \det \begin{pmatrix} -G^\phi & \delta v^\phi \\ (\delta v^\phi)^\top & 2v_a^{(a)} \end{pmatrix}.$$

For $\det G^\phi \neq 0$ a proper inverse of G^ϕ exists, and therefore one can write

$$(270) \quad B \det S = B \det(-G^\phi) \cdot \det(2v_a^{(a)} + (\delta v^\phi)^\top (G^\phi)^{-1} \delta v^\phi) = \\ (-1)^{N-1} \det(G^\phi) \cdot (2Bv_a^{(a)} + (\delta v^\phi)^\top (G^\phi)^{-1} B \delta v^\phi).$$

The bracket simplifies to one because (249) can be expressed as

$$(271a) \quad B \delta v^\phi = G^\phi b \quad \text{and}$$

$$(271b) \quad (\delta v^\phi)^\top b = 1 - 2Bv_a^{(a)},$$

and hence leads to

$$(272) \quad 2Bv_a^{(a)} + (\delta v^\phi)^\top (G^\phi)^{-1} B \delta v^\phi = \\ 2Bv_a^{(a)} + (\delta v^\phi)^\top (G^\phi)^{-1} G^\phi b = 2Bv_a^{(a)} + 1 - 2Bv_a^{(a)} = 1.$$

2.5. Problematic Phase Space Regions. The previous sections reveal clearly that the reduction for scalar integrals as described above is unproblematic in all except one cases: as can be seen from the determinant relation (267), no solution for B can be found when $\det S$ vanishes while $\det G^\phi$ remains non-zero.

Due to the complexity of the full problem¹⁵ I restrict the discussion to the case of $2 \rightarrow (N-2)$ scattering, with $N \leq 6$, where all the external and internal particles are massless.

The conjecture to be shown in this section is that all problematic phase space regions, i.e. $\det S = 0 \wedge \det G^\phi \neq 0$, in fully massless $2 \rightarrow (N-2)$ -processes for $N \leq 6$ lie only on the soft and collinear phase space boundaries. On the other hand, N is also bounded from below: since triangles are the endpoint of the reduction only (sub-)determinants down to size four are considered.¹⁶

In the case $N = 4$ according to Figure 2a the determinant of S is just the product

$$(273) \quad \det S = s_{12}^2 s_{23}^2.$$

¹⁵ In general there are $N(N-1)/2$ MANDELSTAM variables plus N propagator masses which have to be considered when finding the roots of $\det S$

¹⁶ The tensor reduction of three-point functions is described in section 3.5 and does not involve $\det S$.

The MANDELSTAM variables are defined as

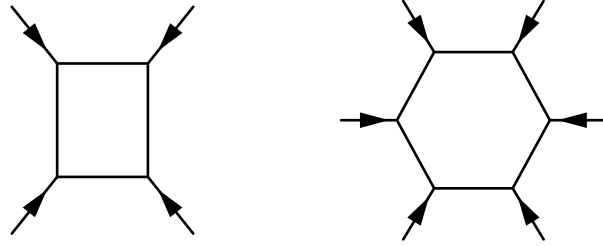
$$(274a) \quad s_i = k_i^2,$$

$$(274b) \quad s_{ij} = (k_i + k_j)^2,$$

$$(274c) \quad s_{ijl} = (k_i + k_j + k_l)^2,$$

...

where the k_i are the external momenta, defined as all ingoing. Where appropriate I identify $s_{12} \equiv s$, the centre of mass energy of the colliding partons.



(a) A box topology

(b) A hexagon topology

Figure 2: The topologies used in the discussion.

Hence the determinant only is zero when either s_{12} or s_{23} vanishes. By choosing an appropriate explicit representation of the kinematics the vanishing of a MANDELSTAM variable can be related to an infrared situation. Therefore I consider the centre of mass system of the ingoing particles, in which the four-vectors read

$$(275a) \quad k_1 = \sqrt{s}/2(1, 0, 0, 1),$$

$$(275b) \quad k_2 = \sqrt{s}/2(1, 0, 0, -1),$$

$$(275c) \quad k_3 = E_3(-1, 0, \sin \varphi, \cos \varphi),$$

$$(275d) \quad k_4 = -(k_1 + k_2 + k_3).$$

In this parametrisation we have $s_{12} = s$ and $s_{23} = -\sqrt{s}E_3(1 + \cos \varphi)$. The roots of $\det S$ lie where one of the energies vanishes and where the outgoing particles become collinear with the beam axis, both of which are infrared situations. On the other hand the point $\cos \varphi = -1$ can be related directly to vanishing transverse momentum $p_{3,T} = E_3 \sin \varphi = 0$.

Analogous treatment to the four-particle case is sufficient for $N = 5$. The determinant is $\det S = 2s_{12}s_{23}s_{34}s_{45}s_{51}$, and hence the roots of the determinant clearly lie on the phase space boundaries.

Next, I consider the situation for $N = 6$ kinematics (s. Figure 2b). The corresponding S -matrix is

$$(276) \quad S = \begin{pmatrix} 0 & 0 & s_{23} & s_{234} & s_{61} & 0 \\ 0 & 0 & 0 & s_{34} & s_{345} & s_{12} \\ s_{23} & 0 & 0 & 0 & s_{45} & s_{123} \\ s_{234} & s_{34} & 0 & 0 & 0 & s_{56} \\ s_{61} & s_{345} & s_{45} & 0 & 0 & 0 \\ 0 & s_{12} & s_{123} & s_{56} & 0 & 0 \end{pmatrix}$$

The interest is only to the subdeterminants of sizes 4 and 5. There are only three types of pinches from a hexagon down to boxes, which are shown in Figure 3: the one-mass box, the adjacent box and the opposite box. The one-mass box and the adjacent

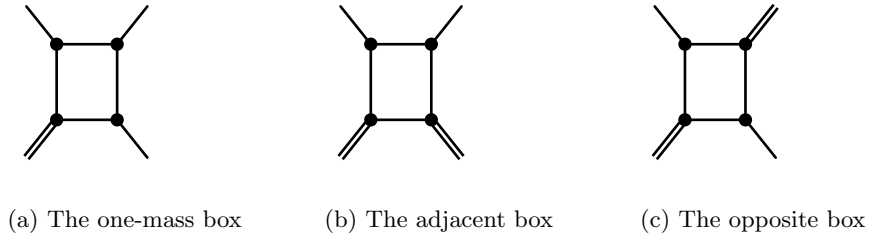


Figure 3: The three different types of pinched boxes that can arise from the reduction of a six-point diagram. Only one representative permutation of external legs is considered.

box lead to S -matrices of which the determinant is simply a product of MANDELSTAM variables. However, the opposite boxes is accompanied by the determinant

$$(277) \quad \det S^{\{3,6\}} = \left(\begin{vmatrix} s_{234} & s_{61} \\ s_{34} & s_{345} \end{vmatrix} \right)^2 \equiv D_3^2$$

and cyclic permutations of the indices of the MANDELSTAM variables respectively. The determinants D_1 , D_2 and D_3 are semi-definite and vanish only at the phase space boundary. This, again, can be shown by introducing an appropriate parametrisation of the kinematics. To do the prove for E_3 one can choose the reference frame where k_2 and $(-k_5)$ are back to back¹⁷:

$$(278a) \quad k_{61} = k_6 + k_1 = -k_2 - k_{34} - k_5,$$

$$(278b) \quad k_2 = \sqrt{s}/2(1, 0, 0, 1),$$

$$(278c) \quad k_{34} = k_3 + k_4 = (-E_{45}, 0, p \sin \varphi, p \cos \varphi) \quad \text{and}$$

$$(278d) \quad k_5 = E_5(-1, 0, 0, 1).$$

With the additional definition of the transverse momentum $p_T = p \sin \varphi$ one can write D_3 as

$$(279) \quad D_3 = -2\sqrt{s}E_5p_T^2 \leq 0,$$

which shows the proposed conjecture. Similar expressions one can derive for D_1 and D_2 , and in fact for all corresponding determinants for non-trivial permutations of the external legs, which also shows the semi-definiteness of these expressions. In particular,

¹⁷Consider that $(-k_5)$ is the physical, outgoing momentum, whereas k_5 itself is defined as the ingoing vector.

one finds $D_1 \geq 0$ and $D_2 \leq 0$ for any physical $2 \rightarrow 4$ kinematics. The same arguments apply to determinants with one pinched propagator because one obtains a very similar structure as one can see from

$$(280) \quad \det S^{\{3\}} = s_{23}s_{34}s_{45}D_3 \geq 0.$$

The case of $D_3 \rightarrow 0$ can be understood as a LANDAU singularity and is discussed for the six-photon amplitude in [BG08]. Equation (279) shows that the only non-trivial limit for $D_3 \rightarrow 0$ is caused by the collinear situation $p_T \rightarrow 0$, in which case one can write $k_{34} = -xk_5 - yk_2$ for x and y being uniquely defined by E_{45} and p . Equation (278a) implies $k_{61} = -(1-x)k_5 - (1-y)k_2$. In other words, the propagators of the loop carry momenta

$$(281a) \quad q_1 = -(1-y)k_2,$$

$$(281b) \quad q_2 = yk_2,$$

$$(281c) \quad q_4 = -xk_5 \quad \text{and}$$

$$(281d) \quad q_5 = (1-x)k_5.$$

This kinematical situation corresponds to a *double parton scattering* situation, where each of the partons 2 and 5 split into pairs of partons and each of the internal particles is collinear with either k_2 or k_5 , $q_1 \sim q_2 \sim k_2$ and $q_4 \sim q_5 \sim k_5$. Therefore all four internal propagators are on-shell and obey the LANDAU equations [Lan59],

$$(282) \quad q_1^2 = q_2^2 = q_4^2 = q_5^2 = 0.$$

3. Tensor Reduction by Subtraction

3.1. Form Factor Representation for Tensor Integrals. Before discussing the reduction of tensor integrals I introduce a form factor representation of the tensor integrals according to [BGH⁺05]. Equation (209) already suggests to write tensor integrals as a tensor product of a structure carrying the LORENTZ structure with a LORENTZ invariant form factor,

$$(283) \quad \begin{aligned} I_N^{n;\mu_1 \dots \mu_r}(a_1, \dots, a_r; S) = & \sum_{j_1, \dots, j_r \in S_{\#}} [\Delta_{j_1}^{\bullet} \dots \Delta_{j_r}^{\bullet}]_{a_1 \dots a_r}^{\mu_1 \dots \mu_r} A_{j_1 \dots j_r}^{N,r}(S) \\ & + \sum_{j_1, \dots, j_{r-2} \in S_{\#}} [g^{\bullet} \Delta_{j_1}^{\bullet} \dots \Delta_{j_{r-2}}^{\bullet}]_{a_1 \dots a_r}^{\mu_1 \dots \mu_r} B_{j_1 \dots j_{r-2}}^{N,r}(S) \\ & + \sum_{j_1, \dots, j_{r-4} \in S_{\#}} [g^{\bullet} g^{\bullet} \Delta_{j_1}^{\bullet} \dots \Delta_{j_{r-4}}^{\bullet}]_{a_1 \dots a_r}^{\mu_1 \dots \mu_r} C_{j_1 \dots j_{r-4}}^{N,r}(S). \end{aligned}$$

The square brackets are interpreted as follows:

$$(284a) \quad [\Delta_{j_1}^{\bullet} \dots \Delta_{j_r}^{\bullet}]_{a_1 \dots a_r}^{\mu_1 \dots \mu_r} = \Delta_{j_1 a_1}^{\mu_1} \dots \Delta_{j_r a_r}^{\mu_r},$$

$$(284b) \quad [\underbrace{g^{\bullet} \dots g^{\bullet}}_l \Delta_{j_1}^{\bullet} \dots \Delta_{j_{r-2l}}^{\bullet}]_{a_1 \dots a_r}^{\mu_1 \dots \mu_r} = \sum_{\substack{A \uplus B = \{1, \dots, r\} \\ |A|=2l}} [g^{\bullet} \dots g^{\bullet}]^{(\mu_i)_{i \in A}} \cdot \prod_{k \in B} \Delta_{j_k a_k}^{\mu_k}$$

and $[g^{\bullet} \dots g^{\bullet}]^{\mu_1 \dots \mu_{2l}}$ the sum of all distinguishable distributions of the indices, as explained earlier; the notation $A \uplus B$ denotes the union of two sets A and B where

$A \cap B = \emptyset$. No more than two metric tensors arise in the tensors on the right hand side of the form factor representation for calculations in the FEYNMAN gauge where the rank of an integral is never greater than N ; this is a result of (304) as shown in the following section.

3.2. Tensor Reduction by Subtraction. The same logic of the section about the reduction of scalar integrals can be applied to tensor integrals [BGH⁺05]. Starting from definition (204) one can split the tensor integral into¹⁸

$$(285) \quad I_N^{d;\mu_1 \dots \mu_r}(a_1, \dots, a_r; S) = \int \frac{d^d k}{i\pi^{n/2}} \frac{\left[q_{a_1}^{\mu_1} + \sum_{j \in S_{\#}} C_{ja_1}^{\mu_1} (q_j^2 - m_j^2) \right] q_{a_2}^{\mu_2} \dots q_{a_r}^{\mu_r}}{\prod_{j=1}^N (q_j^2 - m_j^2 + i\delta)} \\ - \sum_{j \in S_{\#}} C_{ja_1}^{\mu_1} \int \frac{d^d k}{i\pi^{n/2}} \frac{(q_j^2 - m_j^2) q_{a_2}^{\mu_2} \dots q_{a_r}^{\mu_r}}{\prod_{j=1}^N (q_j^2 - m_j^2 + i\delta)}.$$

This corresponds to the splitting in the scalar case, and one can write

$$(286) \quad I_N^{d;\mu_1 \dots \mu_r}(a_1, \dots, a_r; S) = I_{\text{div}} + I_{\text{fin}}, \text{ with}$$

$$(287) \quad I_{\text{div}} = - \sum_{j \in S_{\#}} C_{ja_1}^{\mu_1} I_{N-1}^{n;\mu_2 \dots \mu_r}(a_2, \dots, a_r; S^{\{j\}}) \quad \text{and}$$

$$(288) \quad I_{\text{fin}} = \int \frac{d^d k}{i\pi^{n/2}} \frac{A_{a_1}^{\mu_1} q_{a_2}^{\mu_2} \dots q_{a_r}^{\mu_r}}{\prod_{j=1}^N (q_j^2 - m_j^2 + i\delta)}.$$

I introduced the vector

$$(289) \quad A_{a_1}^{\mu_1} \equiv q_{a_1}^{\mu_1} + \sum_{j \in S_{\#}} C_{ja_1}^{\mu_1} (q_j^2 - m_j^2)$$

which must be brought in a form that ensures that I_{fin} is infrared safe. Therefore one proceeds exactly as in the scalar case by introducing FEYNMAN parameters and shifting the integration momentum $k \rightarrow k - \sum_{i \in S_{\#}} z_i r_i$. From

$$(290) \quad A_b^{\mu} = k^{\mu} + \left(\sum_{j \in S_{\#}} C_{jb}^{\mu} \right) \left(k^2 - \frac{1}{2} z^{\text{T}} S z \right) \\ + \sum_{k \in S_{\#}} z_k \left[\sum_{j \in S_{\#}} C_{jb}^{\mu} (S_{jk} + 2k \cdot \Delta_{jk}) - \Delta_{kb}^{\mu} \right]$$

one obtains a infrared safe integral if

$$(291) \quad \sum_{j \in S_{\#}} S_{kj} C_{jb}^{\mu} = \Delta_{kb}^{\mu}$$

in analogy to (241); this numerator makes the integral infrared safe because all terms are either proportional to k or to $(k^2 - 1/2 z^{\text{T}} S z)$, the first yielding an additional λ when referring to Section 2.2, the second leading to a higher dimensional integral.

¹⁸The derivation is written down for $\alpha = 0$ since it is more convenient to write. No changes have to be made for $\alpha \neq 0$.

It remains to show the solubility of (291). For invertible S the solution is

$$(292) \quad C_{ib}^\mu = \sum_{j \in S_\#} (S^{-1})_{ij} \Delta_{jb}^\mu.$$

For singular S the result can be given in terms of the pseudoinverse, if and only if the consistency condition

$$(293) \quad (\mathbb{I} - S\tilde{S}) \cdot C_b^\mu = 0$$

holds. Again the reverse way is chosen and the solution is constructed explicitly to prove (293).

The matrix S is split into its components $-G + \eta v^\top + v \eta^\top$, introducing a natural splitting on (291), where the abbreviation

$$(294) \quad \mathcal{V}_b^\mu \equiv \sum_{j \in S_\#} C_{jb}^\mu$$

becomes helpful:

$$(295a) \quad \sum_{j \in S_\#} G_{ij}^{(a)} C_{jb}^\mu = \delta v_i \mathcal{V}_b^\mu - \Delta_{ib}^\mu,$$

$$(295b) \quad \sum_{j \in S_\#} \delta v_j C_{jb}^\mu = \Delta_{ab}^\mu - 2v_a \mathcal{V}_b^\mu.$$

The system (295a) admits solutions if and only if

$$(296) \quad \sum_{j \in S_\#} K_{G,ij} (\Delta_{jb}^\mu - \delta v_j \mathcal{V}_b^\mu) = 0.$$

we have seen earlier that for general δv , $K_G \delta v \neq v$. On the other hand using (252) for Δ_{jb}^μ and $K_G = \mathbb{I} - R^\top (R R^\top)^{-1} R$ proves that

$$(297) \quad \sum_{j \in S_\#} K_{G,ij} \Delta_{jb}^\mu = 0,$$

and hence for $\mathcal{V}_b^\mu = 0$ solutions are constructable. Up to the choice of the parametrisation of $\text{Ker } G$ the solution is defined by theorem 5,

$$(298a) \quad C_{ib}^\mu = - \sum_{j \in S_\#} \tilde{G}_{ij} \Delta_{jb}^\mu + W_i^\mu, \quad i \in S_\#^{\{a\}},$$

$$(298b) \quad C_{ab}^\mu = - \sum_{j \in S_\#^{\{a\}}} C_{jb}^\mu, \quad \text{where}$$

$$(298c) \quad W_i^\mu = \frac{(K_G \delta v)_i}{\delta v^\top K_G \delta v} \left(\Delta_{ab}^\mu + \sum_{j,k \in S_\#^{\{a\}}} \delta v_j \tilde{G}_{jk} \Delta_{kb}^\mu \right) + \sum_{j=1}^{N-\text{rk } G-2} \beta_j^\mu u_i^{(j)}$$

As already in Section 2, $u^{(j)}$ form a basis of $\text{Ker } G \cap \langle \delta v, \delta_a \rangle^\perp$.

This solution is now regarded only for $N \geq 6$; in this case one always has $\mathcal{V}_b^\mu = 0$. Equation (298a) can now be plugged in back into the expression for A_b^μ ,

$$(299) \quad A_b^\mu = (\hat{g}^{\mu\nu} + 2 \sum_{j,k \in S_\#} z_k C_{jb}^\mu \Delta_{jk}^\nu) \hat{k}_\nu.$$

Using (252) and the fact $W^\mu \in \text{Ker } G$ — which implies

$$\sum_{j \in S_\#} \Delta_{jb}^\nu W_j^\mu = \sum_{j \in S_\#} \Delta_{jb}^\nu (K_G W^\mu)_j = \sum_{j,k \in S_\#} (K_{G,jk} \Delta_{kb}^\nu) W_j^\mu = 0 \quad —$$

it follows that

$$(300) \quad \sum_{j \in S_\#} C_{jb}^\mu \Delta_{jk}^\nu = - \sum_{ij \in S_\#} \Delta_{ib}^\mu \tilde{G}_{ij} \Delta_{jk}^\nu = -\frac{1}{2} \sum_{m=1}^{\text{rk } G} e_m^\mu e_m^\nu.$$

Since for non-exceptional kinematics¹⁹ we have $\text{rk } G = 4$ and therefore the right hand side of the above equation fulfils the completeness relation,

$$(301) \quad \sum_{j \in S_\#} C_{jb}^\mu \Delta_{jk}^\nu = -\frac{1}{2} g^{\mu\nu}.$$

and hence A_b^μ vanishes, which implies that for $N \geq 6$ only the pinched integrals survive. In phenomenological applications the remnant of A_b^μ can only be contracted with $\Delta_{ij}^\mu = \Delta_{ia}^\mu + \Delta_{ja}^\mu$, and one is left with

$$(302) \quad \Delta_{ia}^\mu A_{b,\mu} = \hat{k}_\nu \left(\Delta_{ia}^\nu - \sum_{m=1}^{\text{rk } G} e_m^\nu (e_m \cdot \Delta_{ia}) \right),$$

which simplifies by the help of

$$(303) \quad \sum_{m=1}^{\text{rk } G} e_m^\nu (e_m \cdot \Delta_{ia}) = \sum_{m=1}^{\text{rk } G} e_m^\nu R_{mi}^{(a)} = \Delta_{ia}^\nu$$

to $\Delta_{ij}^\mu A_{b,\mu} = 0$. Therefore, for phenomenology it is safe to conclude that

$$(304) \quad I_N^{n;\mu_1 \dots \mu_r}(a_1, \dots, a_r; S) = - \sum_{j \in S_\#} C_{ja_1}^{\mu_1} I_{N-1}^{n;\mu_2 \dots \mu_r}(a_2, \dots, a_r; S^{\{j\}}), \quad \text{for } N \geq 6.$$

3.3. Reduction of Non-Trivial Numerators in Integrals. The previous approach to tensor reduction leads to an integral basis that contains integrals with non-trivial polynomials of $\{z_i\}_{i=1}^N$ in their numerators. For a full reduction to simple scalar integrals I follow the approach of [BGH00]. This approach is based on the fact that the FEYNMAN parameter integrals are of the common form

$$(305) \quad I_N^d(l_1, \dots, l_r; S) = \int_{-\infty}^{\infty} dz_i \int_{-\infty}^{\infty} dz_j \delta(C - z_i - z_j) g(z_i, z_j).$$

On the other hand it is clear that

$$(306) \quad \int_{-\infty}^{\infty} dz_i \int_{-\infty}^{\infty} dz_j \frac{\partial}{\partial z_i} [\delta(C - z_i - z_j) g(z_i, z_j)] = 0.$$

Now one can integrate out the δ -function through the z_j -integration and apply the chain rule to the differentiation and reintroduce the δ -function after:

$$(307) \quad \int_{-\infty}^{\infty} dz_i \int_{-\infty}^{\infty} dz_j \frac{\partial}{\partial z_i} [\delta(C - z_i - z_j) g(z_i, z_j)] = \int_{-\infty}^{\infty} dz_i \frac{\partial}{\partial z_i} g(z_i, C - z_i) = \int_{-\infty}^{\infty} dz_i \left(\frac{\partial g(z_i, z_j)}{\partial z_i} - \frac{\partial g(z_i, z_j)}{\partial z_j} \right) \Big|_{z_j=C-z_i}.$$

¹⁹Still the constraint $N \geq 6$ is assumed.

Up to the integration over all z_l with $l \neq i, l \neq j$ and the respective Θ -functions for $I_N^d(l_1, \dots, l_r; S)$ the actual form of $g(z_i, z_j)$ is

$$(308) \quad g(z_i, z_j) = c_{ij} (-1)^N \Gamma(N - d/2) \Theta(z_i) \Theta(z_j) \left(\prod_{k=1}^r z_{l_k} \right) \left[-\frac{1}{2} z^\top S z \right]^{-(N-d/2)}$$

Based on (247a) one can write

$$(309) \quad z^\top S z = -z^\top G^{(a)} z + 2(z \cdot \delta v^{(a)})(z \cdot \eta) + 2v_a^{(a)}(z \cdot \eta)^2$$

where $z \cdot \eta = 1$ under the integral due to the δ -function. The required differentiation for the denominator then is

$$(310) \quad \frac{\partial}{\partial z_j} \left[-\frac{1}{2} z^\top S z \right] = \left(G^{(a)} \cdot z - \delta v^{(a)} \right)_j.$$

We will also use that pinched integrals can always be rewritten as integrals with an additional δ -function,

$$(311) \quad I_{N-1}^d(l_1, \dots, l_r; S^{\{a\}}) = (-1)^{N-1} \Gamma(N-1-d/2) \int_0^N dz \delta_z \frac{\delta(z_a) \prod_{k=1}^r z_{l_k}}{\left[-\frac{1}{2} z^\top S z - i\delta \right]^{N-1-d/2}}.$$

Now one index can be chosen to be a , such that $G_{ak}^{(a)}$ and $\delta v_a^{(a)}$ vanish; by the help of (307) one can relate integrals with a different number of FEYNMAN parameters in the numerator,

$$(312) \quad -I_{N-1}^{d-2}(l_1, \dots, l_r; S^{\{i\}}) + \sum_{k=1}^r \delta_{il_k} I_N^d(l_1, \dots, l_{k-1}, l_{k+1}, l_r; S) \\ - \sum_{l_0 \in S_\#} G_{il_0}^{(a)} I_N^{d-2}(l_0, \dots, l_r; S) + \delta v_i^{(a)} I_N^{d-2}(l_1, \dots, l_r; S) \\ = -I_{N-1}^{d-2}(l_1, \dots, l_r; S^{\{a\}}) + \sum_{k=1}^r \delta_{al_k} I_N^d(l_1, \dots, l_{k-1}, l_{k+1}, l_r; S).$$

S can be introduced back again while shifting the dimension $d \rightarrow d+2$. The term containing δ_{al_0} since the z_a -integration is used to eliminate the δ -function and therefore no z_a appears in the numerator²⁰

$$(313) \quad \sum_{l_0 \in S_\#} S_{il_0} I_N^d(l_0, \dots, l_r; S) + \sum_{k=1}^r \delta_{il_k} I_N^{d+2}(l_1, \dots, l_{k-1}, l_{k+1}, \dots, l_r; S) \\ - I_{N-1}^d(l_1, \dots, l_r; S^{\{i\}}) - 2v_a^{(a)} I_N^d(l_1, \dots, l_r; S) \\ - \sum_{l_0 \in S_\#} \delta v_{l_0}^{(a)} I_N^d(l_0, \dots, l_r; S) = -I_{N-1}^d(l_1, \dots, l_r; S^{\{a\}}).$$

²⁰However, the second term on the right hand side survives, since the corresponding θ -function appears either on the left or on the right hand side of the expression.

A crucial simplification can be achieved by eliminating $I_{N-1}^d(l_1, \dots, l_r; S^{\{a\}})$ through an auxiliary relation:

$$(314) \quad I_{N-1}^d(l_1, \dots, l_r; S^{\{a\}}) = (N - d - r - 1)I_N^{d+2}(l_1, \dots, l_r; S) \\ + \sum_{l_0 \in S_{\#}} \delta v_{l_0}^{(a)} I_N^d(l_0, \dots, l_r; S) + 2v_a^{(a)} I_N^d(l_1, \dots, l_r; S)$$

The prove is done via induction over r . For $p = 0$ one finds, applying Formulæ (242) and (245),

$$(315) \quad I_{N-1}^d(S^{\{a\}}) = \int \frac{d^d k}{i\pi^{d/2}} \frac{q_a^2 - m_a^2}{\prod_{j \in S_{\#}} (q_j^2 - m_j^2 + i\delta)} = \\ (N - d - 1)I_N^{d+2}(S) + \sum_{l \in S_{\#}} \delta v_l^{(a)} I_N^d(l; S) + 2v_a^{(a)} I_N^d(S).$$

This result is achieved by manipulating the numerator after introducing FEYNMAN parameter and completing the square in the denominator,

$$(316) \quad \left(k - \sum_{j \in S_{\#}} z_j \Delta_{ja} \right)^2 - m_a^2 = k^2 - 2 \sum_{j \in S_{\#}} z_j k \cdot \Delta_{ja} + \sum_{j_1, j_2 \in S_{\#}} z_{j_1} z_{j_2} \Delta_{j_1 a} \Delta_{j_2 a} - m_a^2.$$

The linear term vanishes under symmetric integration. Furthermore relations (247), (242) and (245) are used to achieve the above result.

The induction step can be carried out, regarding $\delta v_j^{(a)}$ as independent variables, by partial differentiation with respect to $\delta v_j^{(a)}$, because

$$(317) \quad \frac{\partial}{\partial \delta v_j^{(a)}} \left[-\frac{1}{2} z^T S z \right] = -z_j$$

allows the introduction of additional FEYNMAN parameters in the numerator,

$$(318) \quad \frac{\partial}{\partial \delta v_{l_{p+1}}^{(a)}} I_N^d(l_1, \dots, l_r; S) = I_N^{d-2}(l_1, \dots, l_{p+1}; S).$$

This result, substituted into equation (313) reads

$$(319) \quad \sum_{l_0 \in S_{\#}} S_{il_0} I_N^d(l_0, \dots, l_r; S) = +I_{N-1}^d(l_1, \dots, l_r; S^{\{i\}}) \\ - \sum_{k=1}^r \delta_{il_k} I_N^{d+2}(l_1, \dots, l_{k-1}, l_{k+1}, \dots, l_r; S) - (N - d - r - 1)I_N^{d+2}(l_1, \dots, l_r; S).$$

For $N \leq 6$ one can invert this equation, obtaining the desired result,

$$(320) \quad I_N^d(l_0, \dots, l_r; S) = - \sum_{k=1}^r S_{l_0 l_k}^{-1} I_N^{d+2}(l_1, \dots, l_{k-1}, l_{k+1}, \dots, l_r; S) \\ + \sum_{i \in S_{\#}} S_{l_0 i}^{-1} I_{N-1}^d(l_1, \dots, l_r; S^{\{i\}}) - b_{l_0} (N - d - r - 1) I_N^{d+2}(l_1, \dots, l_r; S).$$

For the case $N = 1$ the result can be obtained by explicit calculation²¹:

$$(321) \quad I_1^{n+2\alpha}(m^2) = I_1^{n+2\alpha}(l; m^2) = \frac{(-1)^\alpha (m^2)^{\alpha+1}}{2^\alpha (\alpha+1)!} \left[\Delta - \ln \left(\frac{m^2 - i\delta}{\mu^2} \right) + 1 + \sum_{\nu=1}^{\alpha} \left(\frac{1}{1+\nu} \right) \right] = \frac{(-1)^\alpha (m^2)^{\alpha+1}}{2^\alpha (\alpha+1)!} \left[I_2^n(0; 0, m^2) + \sum_{\nu=1}^{\alpha} \left(\frac{1}{1+\nu} \right) \right]$$

This result is valid for integer values $\alpha \geq 0$.

3.4. Tensor Reduction through Integration by Parts. Together with (209) and (266), the recurrence relation (320) provides a self-contained scheme for tensor reduction. By recursively applying (320) the highest dimension that appears in an integral is increased by two in each reduction step. These integrals then can be brought back to the standard basis by reverse application of (266). The only exception is the integral I_5^{n+2} where the inversion of (266) would lead to terms $\propto \varepsilon^{-1}$; however, terms containing that integral have been found to cancel in all practical cases. It should be noticed that the reduction involving the inverse of (266) is the only source for $1/B$ terms, i.e. for inverse GRAM determinants.

3.5. Reduction of Three-Point Tensor Integrals. In certain kinematical cases the S -matrix of the three-point functions can become singular while $\det G^\phi$ does not. While it was shown earlier in section 2.5 that these cases for $N \geq 4$ in the massless limit arise only on the infrared phase-space boundaries, for $N = 3$ the situation is worse due to a number of pinched matrices $S^{\{i,j,k\}}$ stemming from six-particle cases, where $\det S^{\{i,j,k\}}$ vanishes identically.

It turns out, however, that the GRAM matrix is the better choice for a tensor reduction in the three-particle case. The GRAM determinant in three-point kinematics is the KÄLLEN function

$$(322) \quad \det G^\phi = -\lambda(s_1, s_2, s_3) = -(s_1^2 + s_2^2 + s_3^2 - 2s_1s_2 - 2s_1s_3 - 2s_2s_3)$$

Solving the equation $\det G^\phi = 0$ only allows for the solutions

$$(323a) \quad s_1^\pm = (\sqrt{s_2} \pm \sqrt{s_3})^2, \quad s_2, s_3 \geq 0,$$

$$(323b) \quad s_1^\pm = -(\sqrt{|s_2|} \pm \sqrt{|s_3|})^2, \quad s_2, s_3 \leq 0.$$

The second solution cannot appear at one-loop for any physical $2 \rightarrow N$ kinematics. For the solutions (323a) also s_1 must be non-negative and hence one can derive the kinematical constraint

$$(324) \quad s_1 \geq (\sqrt{s_2} + \sqrt{s_3})^2 = s_1^+.$$

This means that singularities in $1/\det G^\phi$ lie only on the border of the phase space and correspond to physical thresholds.

The three-point functions therefore cannot be treated by the standard approach as introduced in 3.3. Explicit formulæ for the required integrals can be obtained from (207) by applying a PASSARINO-VELTMAN like tensor-reduction. By multiplying the equation

²¹The result is given only up to $\mathcal{O}(\varepsilon)$

by products of $2\Delta_{la_i}^{\mu_i}$ one generates products of $G_{ij}^{(a)}$ on the right hand side, while the numerators in the tensor integrals can be completed to propagators which partly cancel the denominators. One finds

$$(325) \quad 2\Delta_{ia} \cdot q_a = S_{aa} - S_{ia} + [q_i^2 - m_i^2] - [q_a^2 - m_a^2] \quad \text{and}$$

$$(326) \quad 2q_a \cdot q_b = -S_{ab} + [q_a^2 - m_a^2] + [q_b^2 - m_b^2].$$

Since G^ϕ is invertible, the integrals $I_3^d(l_0, \dots, l_r; S)$ can be extracted by solving a linear system of equations; however the inversion is only possible for $l_j \neq a$. No formula can be derived directly for the integral $I_3^d(l_1, l_2, l_3; S)$ for l_1, l_2, l_3 being mutually different since a cannot be chosen different from each of the l_i simultaneously. This problem can be circumvented applying the fact that the FEYNMAN parameters have to sum up to one and therefore the problematic integral can be replaced via

$$(327) \quad \sum_{l_r \in S_\#} I_N^d(l_1, \dots, l_{r-1}, l_r; S) = I_3^d(l_1, \dots, l_{r-1}; S)$$

The reduction formulæ are given below. It should be noted that the reduction of the higher dimensional scalar integrals down to four dimensions can be done using the standard approach, because of

$$(328) \quad I_3^{d+2}(S) = \frac{1}{B(d-2)} \left[I_3^d(S) - \sum_{j \in S_\#} b_j I_2^d(S^{\{j\}}) \right],$$

where only $1/B$ and b_j/B appear, which contain no factors of $1/\det S$.

In (329) the constraint $a \notin \{l_1, l_2, l_3\}$ is assumed. The inverse of $G^{(a)}$ is understood in terms of the pseudoinverse.

$$(329a) \quad I_3^d(l_1; S) = \left[\sum_{i \in S_\#} G_{l_1 i}^{(a)-1} (S_{ia} - S_{aa}) \right] I_3^d(S) - \sum_{i \in S_\#} G_{l_1 i}^{(a)-1} \left[I_2^d(S^{\{i\}}) - I_2^d(S^{\{a\}}) \right]$$

$$(329b) \quad I_3^d(l_1, l_2; S) = G_{l_1 l_2}^{(a)-1} I_3^{d+2}(S) - \left[\sum_{i \in S_\#} G_{l_1 i}^{(a)-1} (S_{aa} - S_{ia}) \right] I_3^d(l_2; S) - \sum_{i \in S_\#} G_{l_1 i}^{(a)-1} \left[I_2^d(l_2; S^{\{i\}}) - I_2^d(l_2; S^{\{a\}}) \right]$$

$$\begin{aligned}
(329c) \quad I_3^d(l_1, l_2, l_3; S) = & G_{l_1 l_2}^{(a)-1} I_3^{d+2}(l_3; S) + G_{l_1 l_3}^{(a)-1} I_3^{d+2}(l_2; S) + G_{l_2 l_3}^{(a)-1} I_3^{d+2}(l_1; S) \\
& - \left[\sum_{i \in S_{\#}} G_{l_1 i}^{(a)-1} (S_{ia} - S_{aa}) \right] \left(I_3^d(l_2, l_3; S) - G_{l_2 l_3}^{(a)-1} I_3^{d+2}(S) \right) \\
& - \sum_{i \in S_{\#}} G_{l_1 i}^{(a)-1} \left[I_2^d(l_2, l_3; S^{\{i\}}) - G_{l_2 l_3}^{(a)-1} I_2^{d+2}(S^{\{i\}}) \right] \\
& + \left(\sum_{i \in S_{\#}} G_{l_1 i}^{(a)-1} \right) \left[I_2^d(l_2, l_3; S^{\{a\}}) - G_{l_2 l_3}^{(a)-1} I_2^{d+2}(S^{\{a\}}) \right]
\end{aligned}$$

4. Representation of the Virtual Corrections

4.1. Basis Integrals. In Sections 2 and 3 it is shown that all one-loop integrals can be mapped onto a set of basis integrals using a set of reduction relations. One set of functions to represent an arbitrary amplitude [BGH00] consists of scalar integrals with FEYNMAN parameters in the numerators,

$$\begin{aligned}
(330a) \quad \mathcal{I}_{\mathcal{N}} = & \{I_2^n(S), I_2^n(l_1; S), I_2^n(l_1, l_2; S), \\
& I_3^n(S), I_3^n(l_1; S), I_3^n(l_1, l_2; S), I_3^n(l_1, l_2, l_3; S), I_3^{n+2}(S), \\
& I_4^{n+2}(S), I_4^{n+2}(l_1; S), I_4^{n+2}(l_1, l_2; S), I_4^{n+2}(l_1, l_2, l_3; S), I_4^{n+4}(S), I_4^{n+4}(l_1; S)\}.
\end{aligned}$$

In another step these integrals can be reduced further to scalar integrals with trivial numerators,

$$(330b) \quad \mathcal{I}_{\mathcal{S}} = \{I_2^n(S), I_3^n(S), I_4^6(S)\}.$$

However, this reduction step introduces inverse GRAM determinants, whereas while working with the set $\mathcal{I}_{\mathcal{N}}$ only determinants of S can arise in the denominator. Although higher-dimensional pentagons ($I_5^{n+2}, I_5^{n+4}, \dots$) formally appear in the reduction, too, it has been shown in [BGH⁺05] that the coefficients of these integrals are always of order $\mathcal{O}(\varepsilon)$ and therefore drop out in phenomenological calculations.

Hence we can write each diagram as

$$(331) \quad \mathcal{D}(S) = \sum_{I(S') \in \mathcal{I}_{\mathcal{N}}} \frac{\mathcal{P}_I}{\mathcal{Q}_I} I(S').$$

\mathcal{P}_I is a polynomial in the MANDELSTAM variables and contractions of the external momenta with the LEVI-CIVITA tensor; \mathcal{Q}_I is a product of determinants $\det S^{\{\dots\}}$, which arise from the reduction of the integrals. The S' represents the pinched submatrices of S .

Similarly, one could use the second set of integrals,

$$(332) \quad \mathcal{D}(S) = \sum_{I(S') \in \mathcal{I}_{\mathcal{S}}} \frac{\mathcal{P}_I}{\mathcal{Q}_I} I(S').$$

The only principal difference is, that now the polynomials \mathcal{Q}_I can also contain GRAM determinants, which should cancel against the numerator \mathcal{P}_I .

4.2. Mandelstam Variables. In this short section I want to present a way of finding an independent set of MANDELSTAM variables for an arbitrary number N of external legs. It can be easily implemented as an algorithm that carries out the substitution of dot products $k_i \cdot k_j$ by MANDELSTAM variables. The number of dot-products in an N -particle scattering problem is $N(N-1)/2$ as one of the momenta can be eliminated by momentum conservation. This number of independent variables can be achieved by considering all possible cuts through a generic N -particle diagram, as shown in Figure 4. Every cut through the diagram corresponds to a partition of the

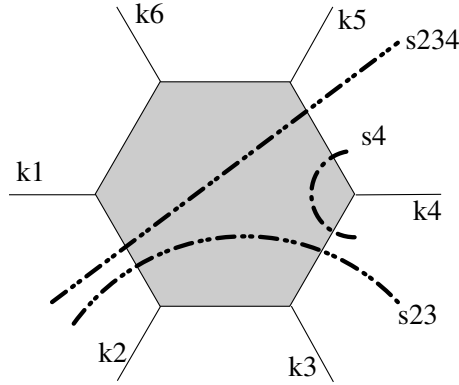


Figure 4: Three out of the fifteen possible cuts of a six-particle amplitude.

set of external momenta and hence to a MANDELSTAM variable, which is obtained from the square of the sum of all momenta in one subset of the partition. The cuts in the diagram of Figure 4 are

$$(333a) \quad s_4 = (k_4)^2 = (k_5 + k_6 + k_1 + k_2 + k_3)^2,$$

$$(333b) \quad s_{23} = (k_2 + k_3)^2 = (k_4 + k_5 + k_6 + k_1)^2 \quad \text{and}$$

$$(333c) \quad s_{234} = (k_2 + k_3 + k_4)^2 = (k_5 + k_6 + k_1)^2.$$

To get a unique naming scheme I always choose the smaller of both subsets and, if both are of equal size, the one starting, in a cyclical sense, with the smaller index. This means for the case $N = 6$ that I always use s_{23} instead of s_{4561} and s_{234} instead of s_{561} . Indices are always understood modulo N in generic expressions like $s_{i,i+1}$.

To show that all dot-products can be mapped onto this set of MANDELSTAM variables, I calculate $k_i \cdot k_{i+d}$ from $s_{i,i+1,\dots,i+d}$,

$$(334) \quad s_{i,\dots,i+d} = (k_i + \dots + k_{i+d})^2 = k_i^2 + k_{i+d}^2 + 2k_i \cdot k_{i+d} + \\ (k_{i+1} + \dots + k_{i+d-1})^2 + 2(k_i + k_{i+d}) \cdot (k_{i+1} + \dots + k_{i+d-1}) = \\ 2k_i \cdot k_{i+d} + s_{i,\dots,i+d-1} + s_{i+1,\dots,i+d} - s_{i+1,\dots,i+d-1},$$

and hence one finds

$$(335) \quad 2k_i \cdot k_{i+d} = s_{i,\dots,i+d} + s_{i+1,\dots,i+d-1} - s_{i,\dots,i+d-1} - s_{i+1,\dots,i+d}.$$

The other kind of LORENTZ-invariant contractions of the external vectors are the contractions with the LEVI-CIVITA symbol. These, however, always appear linear, since products of two ϵ -tensors can be expressed in a determinant of KRONECKER δ -symbols, and therefore in contraction with external momenta one ends up in a polynomial of MANDELSTAM variables again. The number of distinctive contractions is $(N-1)!/[4!(N-1-4)!]$ due to the antisymmetric character of the ϵ -tensor.

5. Renormalisation of QCD

5.1. Introduction. After having introduced the tools to evaluate integrals and DIRAC traces in a dimensionally regularised theory, we are in the position to calculate the counterterms which are necessary in order to obtain finite answers from the calculation of any observables in QCD.

Equation (9) gives the LAGRANGIAN density of QCD. In order to renormalise the theory one replaces the quantities in the original LAGRANGIAN by their bare counterparts which are related to each other by a multiplicative factor

$$(336) \quad \mathcal{L}_0 = \mathcal{L}_{\text{QCD}}(g \rightarrow g_0, q_a \rightarrow q_{a,0}, \mathcal{A} \rightarrow \mathcal{A}_0, \dots) = \mathcal{L}_{\text{QCD}}(Z_1 g, \sqrt{Z_2} q_a, \sqrt{Z_3} \mathcal{A}, \dots).$$

As described in Section 2 of Chapter 1, in dimensional regularisation one introduces an arbitrary energy scale μ in order to continue the dimension of the LAGRANGIAN density consistently to $n \neq 4$ dimensions. This leads to a redefinition of the coupling constant $g \rightarrow \mu^\epsilon g$, which is not discussed in the following. For a more detailed discussion the reader is referred to the conventions in Appendix D and, for example, to [Mut87].

The renormalisation constants Z_1, Z_2, \dots can be expanded in a power series in α_s ,

$$(337) \quad Z_i = 1 + \delta_i + \mathcal{O}(\alpha_s^2),$$

where one assumes that $\delta_i = \mathcal{O}(\alpha_s)$. Usually these terms in the LAGRANGIAN are split into a renormalised LAGRANGIAN \mathcal{L}_{ren} and a counterterm LAGRANGIAN \mathcal{L}_{ct} that contains all terms proportional to δ_i ,

$$(338) \quad \mathcal{L}_{\text{QCD}} = \mathcal{L}_{\text{ren}} + \mathcal{L}_{\text{ct}}.$$

This procedure allows for some freedom as to which terms, in addition to the poles, are taken into account in the calculation of δ_i . In order to fix this ambiguity I work in the $\overline{\text{MS}}$ scheme. This is a prescription according to which the counterterms contain only terms proportional to $\Delta = 1/\epsilon - \gamma_E + \ln(4\pi)$.

5.2. Renormalisation of the Gluon Propagator. The gluon propagator at NLO receives corrections from quark, gluon and ghost loops:

$$(339) \quad \Pi^{AB,\mu\nu}(p^2) = \text{diagram 1} = \text{diagram 2} + \text{diagram 3} + \text{diagram 4} + \text{diagram 5} + \text{diagram 6} + \text{diagram 7} = G_1 + G_2 + G_2 + G_3 + G_4 + G_5.$$

Gauge invariance requires²²

$$(340) \quad p_\mu \Pi^{AB,\mu\nu}(p^2) = 0$$

and hence imposes the tensor structure

$$(341) \quad \Pi^{AB,\mu\nu} = [p^\mu p^\nu - p^2 \hat{g}^{\mu\nu}] \delta^{AB} \Pi(p^2).$$

The diagram G_1 is the only contribution that involves a fermion loop and therefore, in contrast to all other contributions, depends on the number of flavours n_F . Since gauge invariance must not depend on the flavours, this contribution must be gauge invariant on its own, whereas it turns out that only the sum of the diagrams $G_2 + G_3 + G_4$ is gauge invariant. Direct calculation of the diagrams shows

$$(342a) \quad G_1 = n_F T_R \frac{\alpha_s}{4\pi} \frac{1-\varepsilon}{1-\frac{2}{3}\varepsilon} I_2^n(p^2) \cdot \frac{4}{3} [p^\mu p^\nu - p^2 \hat{g}^{\mu\nu}] \delta^{AB},$$

$$(342b) \quad G_2 = 0,$$

$$(342c) \quad G_3 = \frac{1}{2} C_A \frac{\alpha_s}{4\pi} \frac{1}{1-\frac{2}{3}\varepsilon} I_2^n(p^2) \times \left[\left(-\frac{11}{3} + \frac{7}{3}\varepsilon \right) p^\mu p^\nu + \left(\frac{19}{6} - 2\varepsilon \right) p^2 \hat{g}^{\mu\nu} \right] \delta^{AB},$$

$$(342d) \quad G_4 = C_A \frac{\alpha_s}{4\pi} \frac{1}{1-\frac{2}{3}\varepsilon} I_2^n(p^2) \times \left[\left(\frac{1}{6} - \frac{1}{6}\varepsilon \right) p^\mu p^\nu + \frac{1}{12} p^2 \hat{g}^{\mu\nu} \right] \delta^{AB},$$

$$(342e) \quad G_5 = (Z_3 - 1) [p^\mu p^\nu - p^2 \hat{g}^{\mu\nu}].$$

One can expand the diagrams in epsilon to extract the pole part, which determines Z_3 as

$$(343) \quad Z_3 = 1 + \frac{\alpha_s}{4\pi} \left(\frac{5}{3} C_A - \frac{4}{3} n_F T_R \right) \Delta$$

This result is gauge dependent and only true for $\lambda = 1$. In general gauge the coefficient of C_A in (343) is [PS95]

$$(344) \quad \frac{13}{6} - \frac{\lambda}{2} \xrightarrow{\lambda \rightarrow 1} \frac{5}{3}$$

²²I calculate the graphs for a four-dimensional gluon, which is sufficient for one-loop renormalisation.

Finally, the full expression for $\Pi(p^2)$ in F_{EY}NMAN gauge and $\overline{\text{MS}}$ is

$$(345) \quad \Pi(p^2) = \frac{\alpha_s}{4\pi} \left[\frac{4}{3} n_F T_R (1 - \varepsilon) - \left(\frac{5}{3} - \varepsilon \right) C_A \right] \frac{1}{1 - \frac{2}{3}\varepsilon} (I_2^n(p^2) - \Delta) + \frac{\alpha_s}{4\pi} \left[\frac{5}{3} C_A - \frac{4}{3} n_F T_R \right] \Delta.$$

5.3. Renormalisation of the Fermion Propagator. The renormalisation of the fermion propagator consists of a field strength renormalisation and a mass renormalisation [Gro07]. The term of interest from the LAGRANGIAN density is

$$(346) \quad \bar{q}_0(i\not{\partial} - m_0)q_0 = Z_2 \bar{q}(i\not{\partial} - Z_m m)q.$$

The bare propagator therefore reads

$$(347) \quad S_0(p) = \frac{\not{p} + m_0}{p^2 - m_0^2},$$

and summing up all 1PI corrections $\Sigma(p)$ one obtains the full propagator $S(p)$ which can be written recursively as

$$(348) \quad S(p) = S_0(p) + S_0(p)\Sigma(p)S(p)$$

or by solving the above equation as

$$(349) \quad S(p) = (S_0(p)^{-1} - \Sigma(p))^{-1}.$$

Since the two-point function only involves one external vector p the tensor structure of $\Sigma(p)$ has only two components

$$(350) \quad \Sigma(p) = \not{p}\Sigma_V(p) + m_0\Sigma_S(p).$$

Therefore the full propagator can be written as

$$(351) \quad S(p) = \frac{1}{1 - \Sigma_V(p)} \left(\not{p} - \frac{1 + \Sigma_S(p)}{1 - \Sigma_V(p)} m_0 \right)^{-1}$$

Comparing with equation (346) one can read off the two renormalisation conditions

$$(352) \quad (1 - \Sigma_V(p))Z_2 = \text{finite} \quad \text{and} \quad \frac{1 + \Sigma_S(p)}{1 - \Sigma_V(p)} Z_m = \text{finite}.$$

The only diagram that contributes to $\Sigma(p)$ is

$$(353) \quad i\Sigma(p) = \text{diagram} = \frac{\alpha_s}{4\pi} C_F \left\{ \frac{3}{2} \not{p} - m \right\} \Delta + \mathcal{O}(\varepsilon^0).$$

From this we can read off the conditions in order to satisfy (352),

$$(354a) \quad Z_2 = 1 + \frac{3}{2} \frac{\alpha_s}{4\pi} C_F \Delta + \mathcal{O}(\varepsilon) \quad \text{and}$$

$$(354b) \quad Z_m = 1 - \frac{\alpha_s}{4\pi} C_F \Delta + \mathcal{O}(\varepsilon).$$

5.4. Renormalisation of the Coupling Constant. Similarly, one can calculate the renormalisation constant Z_1 from the one-loop corrections to the gluon-quark vertex. The requirement of finiteness of the renormalised vertex in the $\overline{\text{MS}}$ scheme leads to the equation²³

$$(355) \quad \delta_1 + \delta_2 + \frac{1}{2}\delta_3 = -(C_A + C_F)\frac{\alpha_s}{4\pi}\Delta,$$

which can be solved for Z_1 ,

$$(356) \quad Z_1 = 1 + \left(\frac{2}{3}T_R N_F - \frac{11}{6}C_A \right) \frac{\alpha_s}{4\pi}\Delta.$$

It should be noted that the counter terms of the gluon self-interaction vertices and the ghost-sector are fixed by Z_1 , Z_2 and Z_3 through gauge invariance.

6. Real Emission Contribution

6.1. Introduction. For a systematic expansion of the scattering amplitude in α_s one has to consider not only loop diagrams but also diagrams belonging to the process which includes the emission of one extra, unresolved parton. The cross section up to NLO in α_s for a process with N final state partons and I partons in the initial state therefore has the form[CS97]

$$(357) \quad \sigma = \sigma^{\mathcal{B}} + (\sigma^{\mathcal{R}} + \sigma^{\mathcal{V}}) + \mathcal{O}(\alpha_s^{N+I}).$$

The leading term $\sigma^{\mathcal{B}}$ is the tree level contribution to the process and can be written as

$$(358) \quad \sigma^{\mathcal{B}} = \int d\Phi^{(N)} |\mathcal{M}^{\mathcal{B}}|^2 F_{\text{J}}^{(N)},$$

where $d\Phi^{(N)}$ denotes a N -particle phase space, $\mathcal{M}^{\mathcal{B}}$ is the BORN matrix element and $F_{\text{J}}^{(N)}$ is the jet measurement function. In order to result in a meaningful matching with the experiment the measurement function has to be IR safe, i.e. the function has to be defined such that in the collinear and soft limits one obtains

$$(359) \quad F_{\text{J}}^{(N+1)} \rightarrow F_{\text{J}}^{(N)}.$$

The terms $\sigma^{\mathcal{V}}$ and $\sigma^{\mathcal{R}}$ are the NLO corrections to the process; $\sigma^{\mathcal{V}}$ contains the one-loop diagrams whereas $\sigma^{\mathcal{R}}$ is the tree level process with $N + 1$ final state particles:

$$(360) \quad \sigma^{\mathcal{V}} = \int d\Phi^{(N)} (\mathcal{M}^{\mathcal{V}} \mathcal{M}^{\mathcal{B}*} + \mathcal{M}^{\mathcal{V}*} \mathcal{M}^{\mathcal{B}}) F_{\text{J}}^{(N)}$$

$$(361) \quad \sigma^{\mathcal{R}} = \int d\Phi^{(N+1)} |\mathcal{M}^{\mathcal{R}}|^2 F_{\text{J}}^{(N+1)}$$

Although this looks as if one could simply do a phase space integration over $d\Phi^{(N+1)}$ for the real corrections and separately integrate the other contributions over $d\Phi^{(N)}$ this naive approach derails due to IR singularities. These singularities cancel in inclusive cross-sections between $\sigma^{\mathcal{V}}$ and $\sigma^{\mathcal{R}}$ [BN37, Kin62, LN64, Cut60].

In the virtual correction the IR singularities can be extracted explicitly and usually are regularised and expressed as poles in ϵ . For the real corrections one has to choose

²³See for example [BDJ01a]

a different approach: in order to obtain an amplitude that is finite at every point in phase space one subtracts a term that contains the collinear and soft approximation of the matrix element $\mathcal{M}^{\mathcal{R}}$. In order to account for the subtraction a corresponding term has to be added to the virtual correction. Equation (357) then turns into

$$(362) \quad \sigma = \sigma^{\mathcal{B}} + \int d\Phi^{(N+1)} \left(|\mathcal{M}^{\mathcal{B}}|^2 F_J^{(N+1)} - d\sigma^{\mathcal{A}} \right)_{\varepsilon=0} \\ + \int d\Phi^{(N)} \left((\mathcal{M}^{\nu} \mathcal{M}^{\mathcal{B}*} + \mathcal{M}^{\nu*} \mathcal{M}^{\mathcal{B}}) F_J^{(N)} + \int d\Phi^{(1)} d\sigma^{\mathcal{A}} \right)_{\varepsilon=0} + \mathcal{O}(\alpha_s^{N+I}).$$

The calculation of the IR counterterm $d\sigma^{\mathcal{A}}$ relies on the fact that in the collinear limit the amplitude factorises into a hard subprocess and a soft part. Explicit expressions of counterterms have been derived in [ERT81]; in this work the fully process independent approach of Reference [CS97] is used.

6.2. A Complete Example: $e^+e^- \rightarrow q\bar{q}$. In this chapter the calculation of $e^+e^- \rightarrow q\bar{q}$ is reviewed in great detail [ERT81] to explicitly show the cancellation of IR poles and to motivate the use of the dipole subtraction method [CS97].

In the following example the amplitude of the process

$$(363) \quad e^+(p_1) + e^-(p_2) \rightarrow \gamma^*(p_1 + p_2) \rightarrow q(k_1) + \bar{q}(k_2)$$

is considered at NLO in α_s . In the real correction an additional gluon $g(k_3)$ is radiated off the quarks in the final state.

Since the initial state is not partonic this example avoids the discussion of initial state radiation which has been devoted a later section to.

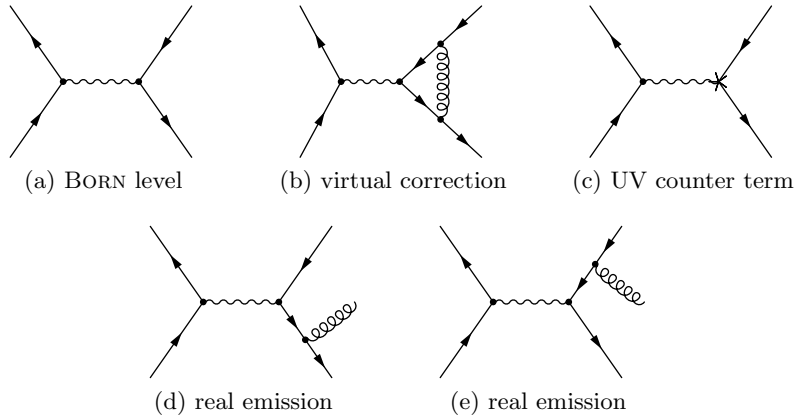


Figure 5: Diagrams contributing to the process $e^+e^- \rightarrow q\bar{q}$.

6.2.1. The Tree Level Contribution. The tree level contribution consists of only one FEYNMAN diagram, an s -channel photon exchange between the electrons and the quarks. I use physical, i.e. $p_1 + p_2 = k_1 + k_3$ resp. $p_1 + p_2 = k_1 + k_2 + k_3$ in the real emission. I use the MANDELSTAM variables $t_{ij} = (p_i - k_j)^2$, $s_{ij} = (k_i + k_j)^2$

and $s = (p_1 + p_2)^2$. Since all particles are assumed to be on-shell and massless these definitions boil down to $t_{ij} = -2p_i \cdot k_j$, $s_{ij} = 2k_i \cdot k_j$ and $s = 2p_1 \cdot p_2$.

The squared matrix element averaged over initial state spins and summed over final state spins and colours is

$$(364) \quad \overline{|\mathcal{M}^{\mathcal{B}}|^2} = 2(4\pi\alpha)^2 Q_f^2 N_C \left(\frac{t_{11}^2 + t_{21}^2}{s^2} - \varepsilon \right).$$

Here Q_f is the electrical charge of the quark flavour and N_C the number of $\text{SU}(N_C)$ colours.

6.2.2. *The Virtual Corrections.* Next we determine the virtual correction to this process. The squared amplitude that stems from Figure 5 (b) is

$$(365) \quad \overline{|\mathcal{M}^{\mathcal{V}}|^2} = \text{[Diagram 1]} + \text{[Diagram 2]} =$$

$$\frac{(4\pi\alpha)^2 Q_f^2 (4\pi\alpha_s) \text{tr}\{t^A t^A\}}{4s^2 \cdot 2^n \pi^{\frac{n}{2}}} \int \frac{d^n k}{i\pi^{\frac{n}{2}}} \frac{\text{tr}\{\not{p}_1 \gamma^\mu \not{p}_2 \gamma^\nu\} \text{tr}\{\not{k}_2 \gamma^\rho (\not{k} - \not{k}_2) \gamma_\mu (\not{k} + \not{k}_1) \gamma_\rho \not{k}_1 \gamma_\nu\}}{[k^2 + i\delta][(k + k_1)^2 + i\delta][(k - k_2)^2 + i\delta]} + \text{h.c.},$$

which can be simplified to the form given in [CS97]:

$$(366) \quad \overline{|\mathcal{M}^{\mathcal{V}}|^2} = \overline{|\mathcal{M}^{\mathcal{B}}|^2} \cdot \frac{C_F \alpha_s}{2\pi} \left(\frac{4\pi\mu^2}{s} \right)^\varepsilon \frac{1}{\Gamma(1-\varepsilon)} \left(-\frac{2}{\varepsilon^2} - \frac{3}{\varepsilon} - 8 + \pi^2 + \mathcal{O}(\varepsilon) \right).$$

It should be noted that the factor $s^{-\varepsilon}/\Gamma(1-\varepsilon)$ must be considered for a full expansion in ε ; however, for the purpose of the subtraction the given form is more convenient. Furthermore one should be aware that the expression contains IR poles only; UV renormalisation is trivial in this example since the counterterm from the vertex correction Figure 5 (c) is cancelled by the wave function renormalisation.

6.2.3. *The Real Emission.* We now consider the the real emission diagrams [Bin05] in Figure 5 (d) and (e),

$$(367) \quad \overline{|\mathcal{M}^{\mathcal{R}}|^2} = \text{[Diagram 3]} + \text{[Diagram 4]} + \text{IR finite diagrams} =$$

$$\begin{aligned}
& \frac{1}{4}(4\pi\alpha)^2(4\pi\alpha_s)Q_f^2 \operatorname{tr}\{t^a t^a\} \frac{1}{s^2} \operatorname{tr}\{\not{p}_2 \gamma_\mu \not{p}_1 \gamma_\nu\} \times \\
& \left\{ + \frac{1}{s_{13}^2} \operatorname{tr}\{k_2 \gamma^\nu (k_1 + k_3) \gamma^\rho k_1 \gamma^\sigma (k_1 + k_3) \gamma^\mu\} \right. \\
& - \frac{1}{s_{13}s_{23}} \operatorname{tr}\{k_2 \gamma^\nu (k_1 + k_3) \gamma^\rho k_1 \gamma^\mu (k_2 + k_3) \gamma^\sigma\} \\
& - \frac{1}{s_{13}s_{23}} \operatorname{tr}\{k_2 \gamma^\rho (k_2 + k_3) \gamma^\nu k_1 \gamma^\sigma (k_1 + k_3) \gamma^\mu\} \\
& \left. + \frac{1}{s_{23}^2} \operatorname{tr}\{k_2 \gamma^\rho (k_2 + k_3) \gamma^\nu k_1 \gamma^\mu (k_2 + k_3) \gamma^\sigma\} \right\} d_{\rho\sigma}(k_3) = \\
& 8\pi\alpha_s C_F \frac{1}{s_{13}s_{23}s} \left\{ 2(4\pi\alpha)^2 Q_f^2 N_C [t_{11}^2 + t_{21}^2 + t_{12}^2 + t_{22}^2 \right. \\
& \left. - \varepsilon(t_{11} - t_{22})^2 - \varepsilon(t_{12} - t_{21})^2 - \varepsilon s^2 - \varepsilon s_{12}^2 + \varepsilon^2(s - s_{12})^2] \right\}
\end{aligned}$$

The tensor $d_{\mu\nu}(k_3)$ stems from the polarisation sum

$$(368) \quad d_{\mu\nu}(k) = \sum_{\text{pol.}} \epsilon_\mu(k) \epsilon_\nu^*(k) = -g_{\mu\nu} + \frac{k_\mu r_\nu + k_\nu r_\mu}{k \cdot r},$$

using axial gauge with an arbitrary lightlike vector r .

By integrating over the phase space one runs into singularities whenever k_3 becomes soft or if it is in the collinear region with either k_1 or k_2 , which induces s_{13} and (or) s_{23} to tend to zero.

6.2.4. The Collinear Limit. In the collinear limit the amplitude factorises into a splitting function, a IR divergence and the tree level amplitude. To carry out the limit in a controlled manner one introduces a SUDAKOV parametrisation [CS97]:

$$(369a) \quad k_i^\mu = z p^\mu + k_\perp^\mu - \frac{k_\perp^2}{2(p \cdot n)z} n^\mu \quad \text{and}$$

$$(369b) \quad k_3^\mu = (1 - z) p^\mu - k_\perp^\mu - \frac{k_\perp^2}{2(p \cdot n)(1 - z)} n^\mu$$

where p is the common collinear direction of k_3 and k_i ($i = 1, 2$), k_\perp is the transverse direction and n is an auxiliary lightlike vector. The vectors p , k_\perp and n are obeying $p^2 = n^2 = 0$, $k_\perp^2 < 0$ and $k_\perp \cdot n = k_\perp \cdot p = 0$. The limit $k_\perp^2 \rightarrow 0$ represents the collinear case and $z \rightarrow 1$ leads to the soft case. It is easy to show that this parametrisation preserves $k_i^2 = k_3^2 = 0$ and with $j = 3 - i$ in the limit $k_\perp^2 \rightarrow 0$ the MANDELSTAM variables read

$$(370a) \quad s_{i3} = -\frac{k_\perp^2}{z(1 - z)} \rightarrow 0,$$

$$(370b) \quad s_{j3} = (1 - z)s,$$

$$(370c) \quad s_{12} = zs,$$

$$(370d) \quad t_{1i} = z t_{2j} \quad \text{and}$$

$$(370e) \quad t_{2i} = z t_{1j}.$$

The real emission part (367) in the collinear limit hence becomes

$$(371) \quad |\overline{\mathcal{M}^{\mathcal{R}}}|^2 \xrightarrow{k_\perp^2 \rightarrow 0} 8\pi\alpha_s \frac{1}{s_{i3}} C_F \left(\frac{1 + z^2}{1 - z} - \varepsilon(1 - z) \right) |\overline{\mathcal{M}^{\mathcal{B}}}|^2 = 8\pi\alpha_s \frac{1}{s_{i3}} P_{qq}(z) |\overline{\mathcal{M}^{\mathcal{B}}}|^2.$$

Here I introduced the ALTARELLI-PARISI splitting function $P_{qq}(z)$ which is a process independent function that only depends on the two particles involved in the soft subprocess²⁴.

In order to use the achieved result as a IR counter term one needs a momentum mapping from the $(N + 1)$ to the N -particle final state, i.e. one needs to express the quantities p , k_\perp , n and z in terms of the momenta k_i , k_j and k_3 such that the following properties are preserved:

$$(372a) \quad k_i + k_j + k_3 = \tilde{k}_i + \tilde{k}_j \quad (\text{momentum conservation})$$

$$(372b) \quad \tilde{k}_i^2 = \tilde{k}_j^2 = 0 \quad (\text{on-shell condition}),$$

where the momenta of the N -particle final state are denoted with a tilde. The mapping

$$(373a) \quad \tilde{k}_i = k_i + k_3 - \frac{y}{1-y} k_j$$

$$(373b) \quad \tilde{k}_j = \frac{1}{1-y} k_j$$

with the parameter

$$(373c) \quad y = \frac{s_{i3}}{s_{12} + s_{i3} + s_{j3}} \Leftrightarrow \frac{1}{1-y} = 1 + \frac{y}{1-y} = 1 + \frac{s_{i3}}{s_{12} + s_{j3}}$$

clearly obeys the conditions (372a) and (372b). Furthermore one introduces

$$(374) \quad \tilde{z}_3 = \frac{s_{j3}}{s_{12} + s_{j3}}.$$

Since in the collinear limit $\tilde{z}_3 \rightarrow z$ and $y \rightarrow 0$ the expression

$$(375) \quad d\sigma^A = \sum_{i=1}^2 8\pi\alpha_s \frac{1}{s_{i3}} P_{qq}(\tilde{z}_3) |\overline{\mathcal{M}^B(\tilde{k}_1, \tilde{k}_2)}|^2 F_J^{(N)}(\tilde{k}_1, \tilde{k}_2) d\Phi^{(3)}(k_i, k_j, k_3)$$

has the same IR behaviour as the real correction Equation (375) defines a valid counter term. It should be noted that one has the freedom to add any IR safe terms to the counter term. Here one makes use of the IR property (359) of the measurement function which is crucial for the definition of the counter term.

6.2.5. Phase Space Factorisation. In order to add the subtraction term back to the virtual contribution one must integrate over the one particle phase space of the extra parton. This requires to factorise the phase space $d\Phi^{(3)}(k_i, k_j, k_3)$ into $d\Phi^{(2)}(\tilde{k}_i, \tilde{k}_j) d\Phi^{(1)}(k_3)$,

$$(376) \quad d\Phi^{(3)}(k_i, k_j, k_3) = \frac{d^n k_3}{(2\pi)^{n-1}} \delta(k_3^2) \Theta(k_3^0) \times d\Phi^{(2)}(\tilde{k}_i, \tilde{k}_j) \left(\frac{\partial(\tilde{k}_i, \tilde{k}_j)}{\partial(k_i, k_j)} \right)_{k_3=\text{const}}^{-1}$$

with the JACOBIAN factor

$$(377) \quad \mathcal{J} = \left(\frac{\partial(\tilde{k}_i, \tilde{k}_j)}{\partial(k_i, k_j)} \right)_{k_3=\text{const}} = \det \begin{pmatrix} \frac{\partial \tilde{k}_i^\mu}{\partial k_i^\mu} & \frac{\partial \tilde{k}_j^\mu}{\partial k_i^\mu} \\ \frac{\partial \tilde{k}_i^\mu}{\partial k_j^\mu} & \frac{\partial \tilde{k}_j^\mu}{\partial k_j^\mu} \end{pmatrix}.$$

²⁴Here the soft subprocess is a gluon splitting off a quark.

The matrix in the determinant has dimension $(2n) \times (2n)$. For convenience the scale $Q = k_i k_j + k_3 k_j$ is introduced, and one gets

$$\begin{aligned}
 (378) \quad \mathcal{J} &= \det \begin{pmatrix} \delta_\nu^\mu - \frac{1}{Q} k_j^\mu \left(k_{3\nu} - \frac{y}{1-y} k_{j\nu} \right) & \frac{1}{Q} k_j^\mu \left(k_{3\nu} - \frac{y}{1-y} k_{j\nu} \right) \\ -\frac{y}{1-y} \left(\delta_\nu^\mu - \frac{1}{Q} k_j^\mu (k_i^\nu + k_3^\nu) \right) & \frac{1}{1-y} \delta_\nu^\mu - \frac{y}{1-y} \frac{1}{Q} k_j^\mu (k_{i\nu} + k_{3\nu}) \end{pmatrix} = \\
 &\det \begin{pmatrix} \delta_\nu^\mu & \frac{1}{Q} k_j^\mu \left(k_{3\nu} - \frac{y}{1-y} k_{j\nu} \right) \\ 0 & \frac{1}{1-y} \left(\delta_\nu^\mu - \frac{1}{Q} k_j^\mu (y k_{i\nu} - y k_{j\nu} + k_{3\nu}) \right) \end{pmatrix} = \\
 &(1-y)^{-n} \det \left(\delta_\nu^\mu - \frac{1}{Q} k_j^\mu (y k_{i\nu} - y k_{j\nu} + k_{3\nu}) \right) = (1-y)^{1-n} (1 - \tilde{z}_3).
 \end{aligned}$$

In the last line the identity $\det(\mathbb{I} + uv^\top) = 1 + v^\top u$ has been used. Another factor is introduced by the replacement $\delta(k_j^2) = (1-y)^2 \delta(\tilde{k}_j^2)$, and hence the factorisation reads

$$\begin{aligned}
 (379) \quad d\Phi^{(3)}(k_i, k_j, k_3) &= d\Phi^{(2)}(\tilde{k}_i, \tilde{k}_j) \frac{d^n k_3}{(2\pi)^{n-1}} \delta(k_3^2) \Theta(k_3^0) \frac{(1-y)^{n-3}}{(1-\tilde{z}_3)} \\
 &= d\Phi^{(2)}(\tilde{k}_i, \tilde{k}_j) \frac{d^{n-1} \mathbf{k}_3}{(2\pi)^{n-1} (2E_3)} \frac{(1-y)^{n-3}}{(1-\tilde{z}_3)}.
 \end{aligned}$$

In the centre of mass system of \tilde{k}_i and \tilde{k}_j ,

$$(380a) \quad \tilde{k}_i = \sqrt{\frac{\tilde{k}_i \cdot \tilde{k}_j}{2}} (1, \mathbf{0}^{(n-2)}, 1),$$

$$(380b) \quad \tilde{k}_j = \sqrt{\frac{\tilde{k}_i \cdot \tilde{k}_j}{2}} (1, \mathbf{0}^{(n-2)}, -1),$$

$$(380c) \quad k_3 = E_3 (1, \mathbf{k}_\perp^{(n-2)}(\theta), \cos(\theta))$$

one can express $d^{n-1} k_3$ in terms of spherical coordinates relative to the axis defined by $\tilde{\mathbf{k}}_i$, and Equation (379) becomes

$$(381) \quad d\Phi^{(3)}(k_i, k_j, k_3) = d\Phi^{(2)}(\tilde{k}_i, \tilde{k}_j) \frac{dE_3 E_3^{n-2}}{2E_3 (2\pi)^{n-1}} d(\cos \theta) (\sin \theta)^{n-4} d\Omega_{n-2} \frac{(1-y)^{n-3}}{(1-\tilde{z}_3)},$$

where $d\Omega_{n-2}$ describes the subspace orthogonal to the other integration directions as in (539). In terms of these coordinates, the variables \tilde{z}_3 and y have the form

$$(382) \quad \tilde{z}_3 = \frac{\tilde{k}_j \cdot k_3}{\tilde{k}_i \tilde{k}_j} = \frac{E_3}{\sqrt{2\tilde{k}_i \tilde{k}_j}} (1 + \cos \theta),$$

$$(383) \quad y = \frac{\tilde{k}_i \cdot k_3}{\tilde{k}_i \tilde{k}_j - \tilde{k}_j k_3} = -\frac{E_3 (1 - \cos \theta)}{E_3 (1 + \cos \theta) - \sqrt{2\tilde{k}_i \tilde{k}_j}}.$$

Another variable transform allows to replace E_3 and $\cos \theta$ by y and \tilde{z}_3 ,

$$(384) \quad E_3 = \frac{\sqrt{(2\tilde{k}_i \cdot \tilde{k}_j) y z (1 - \tilde{z}_3)}}{\sin \theta} \quad \text{and} \quad \frac{\partial(E_3, \cos \theta)}{\partial(y, z)} = \frac{(2\tilde{k}_i \cdot \tilde{k}_j)(1 - \tilde{z}_3)}{2E_3},$$

and hence

$$(385) \quad d\Phi^{(3)}(k_i, k_j, k_3) = d\Phi^{(2)}(\tilde{k}_i, \tilde{k}_j) dy d\tilde{z}_3 d\Omega_{n-2} \frac{(2\tilde{k}_i \cdot \tilde{k}_j)}{16\pi^2 (2\pi)^{1-2\varepsilon}} (E_3 \sin \theta)^{n-4} (1-y)^{n-3} \\ = d\Phi^{(2)}(\tilde{k}_i, \tilde{k}_j) (2\tilde{k}_i \cdot \tilde{k}_j)^{1-\varepsilon} d\Omega_{n-2} \frac{dy y^{-\varepsilon} (1-y)^{1-2\varepsilon}}{16\pi^2 (2\pi)^{1-2\varepsilon}} d\tilde{z}_3 (\tilde{z}_3 (1-\tilde{z}_3))^{-\varepsilon}.$$

Together with the limits on the integration variables, $\Theta(y(1-y))\Theta(\tilde{z}_3(1-\tilde{z}_3))$ one obtains the form given in [CS97].

We can now carry out the one-particle subspace $d\Phi^{(1)}(k_3)$ in Equation (375) by using $s_{i3} = y(2\tilde{k}_i \cdot \tilde{k}_j)$:

$$(386) \quad \int_{k_3} d\sigma^{\mathcal{A}} = \frac{\alpha_s \mu^\varepsilon}{2\pi} \sum_{i=1}^2 d\Phi^{(2)}(\tilde{k}_i, \tilde{k}_j) \overline{|\mathcal{M}^{\mathcal{B}}(\tilde{k}_1, \tilde{k}_2)|^2} F_J^{(N)}(\tilde{k}_1, \tilde{k}_2) (2\tilde{k}_i \cdot \tilde{k}_j)^{-\varepsilon} \\ \times \frac{\Omega_{n-2}}{(2\pi)^{1-2\varepsilon}} \int_0^1 dy y^{-1-\varepsilon} (1-y)^{1-2\varepsilon} \int_0^1 d\tilde{z}_3 (\tilde{z}_3 (1-\tilde{z}_3))^{-\varepsilon} P_{qq}(\tilde{z}_3; y).$$

Naively one might want to use $P_{qq}(\tilde{z})$ instead of

$$(387) \quad P_{qq}(z; y) = C_F \left[\frac{2}{1-z(1-y)} - (1+z) - \varepsilon(1-z) \right].$$

However, only the latter form takes care of overlapping singularities, and using $P_{qq}(z)$ would not reproduce the correct poles to cancel the ones in the virtual part of the amplitude. $P_{qq}(z; y)$ maps smoothly on the original function $P_{qq}(z)$ in the soft and collinear limit.

The second line of (386) can be evaluated using the trick in Equation (523),

$$(388) \quad C_F \frac{2\pi^{1-\varepsilon}}{\Gamma(1-\varepsilon)(2\pi)^{1-2\varepsilon}} \int_0^1 d\tilde{z}_3 \int_0^1 dy \tilde{z}_3^{-\varepsilon} (1-\tilde{z}_3)^{-\varepsilon} y^{-1-\varepsilon} (1-y)^{1-2\varepsilon} \\ \times \left(\frac{2}{1-\tilde{z}_3(1-y)} - (1+\tilde{z}_3) - \varepsilon(1-\tilde{z}_3) \right) \\ = \frac{C_F (4\pi)^\varepsilon}{\Gamma(1-\varepsilon)} \left(\frac{2}{\varepsilon^2} + \frac{3}{\varepsilon} + 10 - \pi^2 + \mathcal{O}(\varepsilon) \right).$$

The poles cancel with those in the virtual part of the amplitude, and one can write down the modified differential cross-section in the limit $\varepsilon \rightarrow 0$, which is suitable for direct numerical integration:

$$(389) \quad d\sigma^\nu + \int_1 d\sigma^{\mathcal{A}} = \frac{\alpha_s C_F}{2\pi} \cdot 2 \overline{|\mathcal{M}^{\mathcal{B}}|^2} F_J^{(N)}$$

7. Dipole Subtraction

7.1. Introduction. In the previous section it has been shown that for a complete NLO calculation, both the virtual one-loop corrections and the real emission of an additional particle have to be calculated to achieve a physically meaningful result.

Moreover, both parts of the calculation are divergent on their own but the divergences cancel when the parts are put together.

Although other methods are available as well [HO02, ELPW02] I will focus only on a method developed by CATANI and SEYMOUR [CS97] that works with local counter terms, so-called *dipoles*, that cancel the poles of both parts independently. This method has been extended also for the massive case [CDST02] and proves to be suitable for automation [GK08, FGG08, ST08].

In the previous section some of the subtleties of such a subtraction procedure have been neglected since they are discussed in detail in the original literature [CS97]; instead, I will give two examples of how to apply the original formulæ to actual processes, the amplitudes $u\bar{u} \rightarrow b\bar{b}s\bar{s}$ and $gg \rightarrow b\bar{b}s\bar{s}$. These two amplitudes are the basic ingredients for the calculation of the physical process $pp \rightarrow b\bar{b}b\bar{b}$. Although for the real emission besides an additional gluon one also has to consider the processes with one gluon in the initial state like $gq \rightarrow b\bar{b}s\bar{s}q$ these subprocesses do not contribute to the cancellation of the poles in the virtual amplitude and therefore are not needed to be included in the dipole subtraction.

In the following the notation of [CS97] is adapted and only massless partons are considered. For a $2 \rightarrow N$ process at a proton-proton collider an inclusive cross section can be calculated as a convolution of a partonic cross section σ_{ab} and the parton distribution functions $f_a(x)$ and $f_b(x)$,

$$(390) \quad \sigma_{\text{tot.}} = \int_0^1 dx_1 \int_0^1 dx_2 \sum_{a,b} f_a(x_1) f_b(x_2) \sigma_{ab}(x_1 P_1, x_2 P_2)$$

where the sum over a and b runs over all contributing parton flavours²⁵. The proton momenta are P_1 and P_2 . Here only jet cross sections are discussed and therefore the topic of fragmentation is neglected.

For the partonic cross section one has

$$(391) \quad \sigma_{ab}(p_a, p_b) = \sigma_{ab}^{\mathcal{B}}(p_a, p_b) + \sigma_{ab}^{\text{NLO}}(p_a, p_b) = \\ \sigma_{ab}^{\mathcal{B}}(p_a, p_b) + \sigma_{ab}^{\text{NLO}\{N+1\}}(p_a, p_b) + \sigma_{ab}^{\text{NLO}\{N\}}(p_a, p_b) + \sigma_{ab}^{\text{C}\{N\}}(p_a, p_b).$$

As before, $\sigma^{\mathcal{B}}$ is the leading order cross-section. It can be written as

$$(392) \quad \sigma_{ab}^{\mathcal{B}}(p_a, p_b) = \frac{1}{2|p_a + p_b|^2} \frac{1}{n_a n_b} \sum_{\lambda_i} \int d\Phi^{(N)}(Q) F_j^{(N)}(p_1, \dots, p_N) \\ \times \langle c' | \mathcal{A}_{c'}^{\mathcal{B}}(p_a^{\lambda_a}, p_b^{\lambda_b}; p_1^{\lambda_1}, \dots, p_N^{\lambda_N})^* \mathcal{A}_c^{\mathcal{B}}(p_a^{\lambda_a}, p_b^{\lambda_b}; p_1^{\lambda_1}, \dots, p_N^{\lambda_N}) | c \rangle.$$

In an appropriate colour basis there is one helicity amplitude $\mathcal{A} = \mathcal{A}^{\mathcal{B}}$ for each colour vector $|c\rangle$; the basis is not necessarily orthogonal and hence one has to take the correlation matrix $\langle c'|c\rangle$ into account. The normalisation constants n_a and n_b denote the additional constants for spin and colour average and only depend on the types of the incoming particles. The total incoming parton momentum is $Q = p_a + p_b$

²⁵ *Flavour* includes quark flavours as well as the possibility of an initial state gluon.

The second term in Equation (391) contains the real emission and an appropriate counter term such that the term is finite:

$$(393) \quad \sigma_{ab}^{\text{NLO}\{N+1\}}(p_a, p_b) = \int d\Phi^{(N+1)}(Q) \left[\left(\frac{d\sigma^{\mathcal{R}}}{d\Phi^{(N+1)}} \right)_{\varepsilon=0} - \left(\frac{d\sigma^{\mathcal{A}}}{d\Phi^{(N+1)}} \right)_{\varepsilon=0} \right].$$

Similar to the BORN cross section the real emission is

$$(394) \quad \frac{d\sigma^{\mathcal{R}}}{d\Phi^{(N+1)}} = \frac{1}{n_a n_b} \sum_{\lambda_i} F_J^{(N+1)}(p_1, \dots, p_{N+1}) \\ \times \langle c' | \mathcal{A}_{c'}^{\mathcal{R}}(p_a^{\lambda_a}, p_b^{\lambda_b}; p_1^{\lambda_1}, \dots, p_{N+1}^{\lambda_{N+1}})^* \mathcal{A}_c^{\mathcal{R}}(p_a^{\lambda_a}, p_b^{\lambda_b}; p_1^{\lambda_1}, \dots, p_{N+1}^{\lambda_{N+1}}) | c \rangle$$

with a corresponding colour basis that includes the extra parton.

The subtraction term is a sum over all dipoles,

$$(395) \quad \frac{d\sigma^{\mathcal{A}}}{d\Phi^{(N+1)}} = \frac{1}{n_a n_b} \frac{1}{S} \times \\ \left[\sum_{\{i,j\}=1}^{N+1} \sum_{\substack{k=1 \\ k \neq i,j}}^{N+1} \mathcal{D}_{ij,k}(p_a, p_b; p_1, \dots, p_{N+1}) F_J^{(N)}(p_a, p_b; p_1, \dots, \tilde{p}_{ij}, \tilde{p}_k, \dots, p_{N+1}) \right. \\ + \sum_{\{i,j\}=1}^{N+1} \mathcal{D}_{ij}^a(p_a, p_b; p_1, \dots, p_{N+1}) F_J^{(N)}(\tilde{p}_a, p_b; p_1, \dots, \tilde{p}_{ij}, \dots, p_{N+1}) \\ + \sum_{\{i,j\}=1}^{N+1} \mathcal{D}_{ij}^b(p_a, p_b; p_1, \dots, p_{N+1}) F_J^{(N)}(p_a, \tilde{p}_b; p_1, \dots, \tilde{p}_{ij}, \dots, p_{N+1}) \\ + \sum_{i=1}^{N+1} \sum_{\substack{k=1 \\ k \neq i}}^{N+1} \mathcal{D}_k^{ia}(p_a, p_b; p_1, \dots, p_{N+1}) F_J^{(N)}(\tilde{p}_{ai}, p_b; p_1, \dots, \tilde{p}_k, \dots, p_{N+1}) \\ + \sum_{i=1}^{N+1} \sum_{\substack{k=1 \\ k \neq i}}^{N+1} \mathcal{D}_k^{ib}(p_a, p_b; p_1, \dots, p_{N+1}) F_J^{(N)}(p_a, \tilde{p}_{bi}; p_1, \dots, \tilde{p}_k, \dots, p_{N+1}) \\ + \sum_{i=1}^{N+1} \mathcal{D}^{ai,b}(p_a, p_b; p_1, \dots, p_{N+1}) F_J^{(N)}(\tilde{p}_{ai}, \tilde{p}_b; p_1, \dots, p_{N+1}) \\ \left. + \sum_{i=1}^{N+1} \mathcal{D}^{bi,a}(p_a, p_b; p_1, \dots, p_{N+1}) F_J^{(N)}(\tilde{p}_a, \tilde{p}_{bi}; p_1, \dots, p_{N+1}) \right]$$

Formally there would be an additional sum over all $(N+1)$ particle configurations that contribute to the process [CS97]; instead, here it is assumed that every subprocess is treated as a separate calculation. The factor $1/S$ is the BOSE symmetry factor which has to be included if the additional parton changes the multiplicity of identical particles; it is discussed in detail in [CS97].

The summation $\sum_{\{i,j\}=1}^{N+1}$ is over pairs of final state particles; for example the first sum in the case $N = 2$ would read

$$(396) \quad \sum_{\{i,j\}=1}^3 \sum_{\substack{k=1 \\ k \neq i,j}}^3 \mathcal{D}_{ij,k}(p_a, p_b; p_1, \dots, p_3) F_J^{(N)}(p_a, p_b; p_1, \dots, \tilde{p}_{ij}, \tilde{p}_k, \dots, p_3) =$$

$$\mathcal{D}_{12,3}(p_a, p_b; p_1, p_2, p_3) F_J^{(2)}(p_a, p_b; \tilde{p}_{12}, \tilde{p}_3)$$

$$+ \mathcal{D}_{13,2}(p_a, p_b; p_1, p_2, p_3) F_J^{(2)}(p_a, p_b; \tilde{p}_{13}, \tilde{p}_2)$$

$$+ \mathcal{D}_{23,1}(p_a, p_b; p_1, p_2, p_3) F_J^{(2)}(p_a, p_b; \tilde{p}_{23}, \tilde{p}_1)$$

The index structure of the dipoles denotes incoming particles with upper indices and final state particles with lower indices. The double index denotes the pair of partons that can become collinear, i.e. the *emitter*, the third index stands for the *spectator*. The momentum mapping from the $(N+1)$ to the N particle kinematics obeys momentum conservation and depends on the configuration, i.e. if the emitter and spectator are initial or final state partons.

Before the structure of the dipoles is discussed in detail for each case in the following sections the discussion of the partonic amplitude is continued. The last two terms in Equation (391) both have a $2 \rightarrow N$ kinematics. The virtual corrections plus the integrated subtraction terms are infrared finite in $n = 4$ dimensions,

$$(397) \quad \sigma_{ab}^{\text{NLO}\{N\}}(p_a, p_b) = \int d\Phi^{(N)}(Q) \left[\frac{d\sigma^{\mathcal{V}}}{d\Phi^{(N)}} + \int d\Phi^{(1)} \frac{d\sigma^{\mathcal{A}}}{d\Phi^{(N+1)}} \right]_{\varepsilon=0}.$$

The virtual correction is the interference term between the one-loop and the tree-level amplitude,

$$(398) \quad \frac{d\sigma^{\mathcal{V}}}{d\Phi^{(N)}} = \frac{1}{n_a n_b} \sum_{\lambda_i} F_J^{(N)}(p_1, \dots, p_N)$$

$$\times \langle c' | \mathcal{A}_{c'}^{\mathcal{V}}(p_a^{\lambda_a}, p_b^{\lambda_b}; p_1^{\lambda_1}, \dots, p_N^{\lambda_N})^* \mathcal{A}_c^{\mathcal{B}}(p_a^{\lambda_a}, p_b^{\lambda_b}; p_1^{\lambda_1}, \dots, p_N^{\lambda_N}) | c \rangle + \text{h.c.}$$

The integrated subtraction term is a tensor product of an insertion operator and the BORN level amplitude,

$$(399) \quad \int d\Phi^{(1)} \frac{d\sigma^{\mathcal{A}}}{d\Phi^{(N+1)}} = -\frac{\alpha_s}{2\pi} \frac{1}{\Gamma(1-\varepsilon)} \frac{1}{n_a n_b} F_J^{(N)}(p_1, \dots, p_N)$$

$$\times \sum_{\alpha \in \{a,b,1,\dots,N\}} \frac{1}{\mathbf{T}_\alpha^2} \mathcal{V}_\alpha(\varepsilon) \sum_{\substack{\beta \in \{a,b,1,\dots,N\} \\ \beta \neq \alpha}} \langle c' | \mathbf{T}_\alpha \cdot \mathbf{T}_\beta | c \rangle \left(\frac{4\pi\mu^2}{2p_\alpha \cdot p_\beta} \right)^\varepsilon$$

$$\times \sum_{\lambda_i} \mathcal{A}_{c'}^{\mathcal{B}}(p_a^{\lambda_a}, p_b^{\lambda_b}; p_1^{\lambda_1}, \dots, p_N^{\lambda_N})^* \mathcal{A}_c^{\mathcal{B}}(p_a^{\lambda_a}, p_b^{\lambda_b}; p_1^{\lambda_1}, \dots, p_N^{\lambda_N})$$

The colour operators \mathbf{T}_α are a $t_{\alpha'\alpha}^A$ in the case of a quark, $-t_{\alpha'\alpha}^A$ in the case of an antiquark and $f^{A\alpha'\alpha}$ in the case of a gluon and hence \mathbf{T}_α^2 is C_F for quarks and antiquarks

and C_A for gluons. The singular function $\mathcal{V}_\alpha(\varepsilon)$ is

$$(400) \quad \mathcal{V}_\alpha(\varepsilon) = \mathbf{T}_\alpha^2 \left(\frac{1}{\varepsilon^2} - \frac{\pi^2}{3} \right) + \gamma_\alpha \frac{1}{\varepsilon} + \gamma_\alpha + K_\alpha + \mathcal{O}(\varepsilon)$$

The constants γ_α and K_α depend on the flavour of the parton and are

$$(401) \quad \gamma_q = \gamma_{\bar{q}} = \frac{3}{2}C_F, \quad \gamma_g = \frac{11}{6}C_A - \frac{2}{3}T_R N_f,$$

and

$$(402) \quad K_q = K_{\bar{q}} = \left(\frac{7}{2} - \frac{\pi^2}{6} \right) C_F, \quad K_g = \left(\frac{67}{18} - \frac{\pi^2}{6} \right) C_A - \frac{10}{9}T_R N_f.$$

The last piece of Equation (391) contains the renormalisation scale dependent part of the subtraction terms and is free of singularities. It can be written as a convolution of the leading order matrix element with two colour-charge operators \mathbf{K} and \mathbf{P}

$$(403) \quad \begin{aligned} \sigma_{ab}^{\text{C}\{N\}}(p_a, p_b) &= \int_0^1 dx \int d\Phi^{(N)}(xp_a + p_b) F_J^{(N)}(xp_a, p_b; p_1, \dots, p_N) \\ &\times \frac{1}{n_a n_b} \sum_{\lambda_i} \mathcal{A}_{c'}^{\mathcal{B}}(xp_a^{\lambda_a}, p_b^{\lambda_b}; p_1^{\lambda_1}, \dots, p_N^{\lambda_N})^* \mathcal{A}_c^{\mathcal{B}}(xp_a^{\lambda_a}, p_b^{\lambda_b}; p_1^{\lambda_1}, \dots, p_N^{\lambda_N}) \\ &\times \sum_{a'} \langle c' | \left(\mathbf{K}^{a,a'}(x) + \mathbf{P}^{a,a'}(xp_a, x; \mu_F^2) \right) | c \rangle \\ &+ \int_0^1 dx \int d\Phi^{(N)}(p_a + xp_b) F_J^{(N)}(p_a, xp_b; p_1, \dots, p_N) \\ &\times \frac{1}{n_a n_b} \sum_{\lambda_i} \mathcal{A}_{c'}^{\mathcal{B}}(p_a^{\lambda_a}, xp_b^{\lambda_b}; p_1^{\lambda_1}, \dots, p_N^{\lambda_N})^* \mathcal{A}_c^{\mathcal{B}}(p_a^{\lambda_a}, xp_b^{\lambda_b}; p_1^{\lambda_1}, \dots, p_N^{\lambda_N}) \\ &\times \sum_{b'} \langle c' | \left(\mathbf{K}^{b,b'}(x) + \mathbf{P}^{b,b'}(xp_b, x; \mu_F^2) \right) | c \rangle. \end{aligned}$$

The sums over a' and b' run over all possible splittings aa' (bb' respectively) for the given initial state parton a (b resp.). The two operators $\mathbf{K}^{a,a'}$ and $\mathbf{P}^{a,a'}$ have the following structure in $\overline{\text{MS}}$ [CS97]:

$$\begin{aligned} \mathbf{K}^{a,a'}(x) &= \frac{\alpha_s}{2\pi} \left\{ \overline{K}^{aa'}(x) + \delta^{aa'} \sum_{i=1}^N \mathbf{T}_i \cdot \mathbf{T}_a \frac{\gamma_i}{\mathbf{T}_i^2} \left[\left(\frac{1}{1-x} \right)_+ + \delta(1-x) \right] \right. \\ &\quad \left. - \mathbf{T}_b \cdot \mathbf{T}_{a'} \frac{1}{\mathbf{T}_{a'}^2} \tilde{K}^{aa'}(x) \right\} \end{aligned}$$

with the plus distribution as defined in Equation (488), and

$$(404) \quad \begin{aligned} \mathbf{P}^{a,a'}(xp_a, p_b, p_1, \dots, p_N; x, \mu_F^2) &= \frac{\alpha_s}{2\pi} P^{aa'}(x) \\ &\times \frac{1}{\mathbf{T}_{a'}^2} \left[\sum_{i=1}^N \mathbf{T}_i \cdot \mathbf{T}_{a'} \ln \frac{\mu_F^2}{2xp_a p_i} + \mathbf{T}_b \cdot \mathbf{T}_{a'} \ln \frac{\mu_F^2}{2xp_a p_b} \right]. \end{aligned}$$

In the latter equation one has to insert the regularised ALTARELLI-PARISI splitting functions

$$(405a) \quad P^{qg}(x) = P^{\bar{q}g}(x) = C_F \frac{1 + (1-x)^2}{x},$$

$$(405b) \quad P^{gq}(x) = P^{g\bar{q}}(x) = T_R (x^2 + (1-x)^2),$$

$$(405c) \quad P^{qq}(x) = P^{\bar{q}\bar{q}}(x) = T_F \left(\frac{1+x^2}{1-x} \right)_+$$

and

$$(405d) \quad P^{gg}(x) = 2C_A \left[\left(\frac{1}{1-x} \right)_+ + \frac{1-x}{x} - 1 + x(1-x) \right] + \delta(1-x) \left[\frac{11}{6}C_A - \frac{2}{3}N_f T_R \right].$$

Equation (404) requires the integration kernels

$$(406a) \quad \bar{K}^{qg}(x) = \bar{K}^{\bar{q}g}(x) = P^{qg}(x) \ln \frac{1-x}{x} + C_F x,$$

$$(406b) \quad \bar{K}^{gq}(x) = \bar{K}^{g\bar{q}}(x) = P^{gq}(x) \ln \frac{1-x}{x} + T_R \cdot 2x(1-x),$$

$$(406c) \quad \bar{K}^{qq}(x) = \bar{K}^{\bar{q}\bar{q}}(x) = C_F \left[2 \left(\frac{\ln \left(\frac{1-x}{x} \right)}{1-x} \right)_+ - (1+x) \ln \frac{1-x}{x} + (1-x) \right] - \delta(1-x)(5 - \pi^2)C_F,$$

$$(406d) \quad \bar{K}^{q\bar{q}}(x) = \bar{K}^{\bar{q}q}(x) = 0 \quad \text{and}$$

$$(406e) \quad \bar{K}^{gg}(x) = 2C_A \left[\left(\frac{\ln \left(\frac{1-x}{x} \right)}{1-x} \right)_+ + \left(\frac{1-x}{x} - 1 + x(1-x) \right) \ln \frac{1-x}{x} \right] - \delta(1-x) \left[\left(\frac{50}{9} - \pi^2 \right) C_A - \frac{16}{9} T_R N_f \right].$$

Finally the terms $\tilde{K}^{aa'}$ are required,

$$(407a) \quad \tilde{K}^{qg}(x) = \tilde{K}^{\bar{q}g}(x) = P^{qg}(x) \ln(1-x),$$

$$(407b) \quad \tilde{K}^{gq}(x) = \tilde{K}^{g\bar{q}}(x) = P^{gq}(x) \ln(1-x),$$

$$(407c) \quad \tilde{K}^{qq}(x) = \tilde{K}^{\bar{q}\bar{q}}(x) = -C_F(1+x) \ln(1-x) + C_F \left[2 \left(\frac{\ln(1-x)}{1-x} \right)_+ - \frac{\pi^2}{3} \delta(1-x) \right],$$

$$(407d) \quad \tilde{K}^{gg} = 2C_A \left[\frac{1-x}{x} - 1 + x(1-x) \right] \ln(1-x) + C_A \left[2 \left(\frac{\ln(1-x)}{1-x} \right)_+ - \frac{\pi^2}{3} \delta(1-x) \right].$$

7.2. Final state emitter, final state spectator: $\mathcal{D}_{ij,k}$. In the case where both emitter and spectator are final state partons the following momentum mapping has to

be used:

$$(408a) \quad \tilde{p}_{ij} = p_i + p_j - \frac{y_{ij,k}}{1 - y_{ij,k}} p_k,$$

$$(408b) \quad \tilde{p}_k = \frac{1}{1 - y_{ij,k}} p_k,$$

with

$$(408c) \quad y_{ij,k} = \frac{p_i p_j}{p_i p_j + (p_i + p_j) p_k} \quad \text{and}$$

$$(408d) \quad \tilde{z}_i = \frac{p_i p_k}{(p_i + p_j) p_k}.$$

All other momenta remain unchanged, $\tilde{p}_n = p_n$. Along with \tilde{z}_i one defines \tilde{z}_j such that $\tilde{z}_j = 1 - \tilde{z}_i$.

The dipole term is

$$(409) \quad \mathcal{D}_{ij,k}(p_a, p_b; p_1, \dots, p_{N+1}) = -\frac{1}{2p_i \cdot p_j} \langle c' | \frac{\mathbf{T}_k \cdot \mathbf{T}_{(ij)}}{\mathbf{T}_{(ij)}^2} | c \rangle \\ \times \sum_{\lambda_i, \lambda'_j} \mathcal{A}_{c'}^{\mathcal{B}}(p_a^{\lambda_a}, p_b^{\lambda_b}; \tilde{p}_1^{\lambda_1}, \dots, \tilde{p}_N^{\lambda_N})^* \mathcal{A}_c^{\mathcal{B}}(p_a^{\lambda_a}, p_b^{\lambda_b}; \tilde{p}_1^{\lambda'_1}, \dots, \tilde{p}_N^{\lambda'_N}) V_{ij,k}^{\lambda, \lambda'},$$

and the operator for the three different splittings are

$$(410) \quad V_{ij,k}|_{i=q}^{j=g} = 8\pi\mu^{2\varepsilon}\alpha_s C_F \left[\frac{2}{1 - \tilde{z}_i(1 - y_{ij,k})} - (1 + \tilde{z}_i) - \varepsilon(1 - \tilde{z}_i) \right] \delta^{\lambda(ij)\lambda'_{(ij)}}$$

$$(411) \quad V_{ij,k}|_{i=q}^{j=\bar{q}} = 8\pi\mu^{2\varepsilon}\alpha_s T_R \left[-g^{\mu\nu} - \frac{2}{p_i \cdot p_j} (\tilde{z}_i p_i^\mu - \tilde{z}_j p_j^\mu)(\tilde{z}_i p_i^\nu - \tilde{z}_j p_j^\nu) \right]$$

and

$$(412) \quad V_{ij,k}|_{i=q}^{j=g} = 16\pi\mu^{2\varepsilon}\alpha_s C_A \left[-g^{\mu\nu} \left(\frac{1}{1 - \tilde{z}_i(1 - y_{ij,k})} + \frac{1}{1 - \tilde{z}_j(1 - y_{ij,k})} - 2 \right) \right. \\ \left. + (1 - \varepsilon) \frac{1}{p_i \cdot p_j} (\tilde{z}_i p_i^\mu - \tilde{z}_j p_j^\mu)(\tilde{z}_i p_i^\nu - \tilde{z}_j p_j^\nu) \right].$$

Here, μ and ν denote the spin indices of the gluon (ij) in \mathcal{A} and \mathcal{A}^* respectively. The operators are orthogonal in all other spin indices, i.e. include implicit factors $\delta^{\lambda_n \lambda'_n}$ for $n \neq (ij)$.

7.3. Final state emitter, initial state spectator: \mathcal{D}_{ij}^a . The second case one has to consider is when the collinear singularity stems from final state partons but the spectator is in the initial state. The appropriate momentum mapping is given below:

$$(413a) \quad \tilde{p}_{ij} = p_i + p_j - (1 - x_{ij,a}) p_a,$$

$$(413b) \quad \tilde{p}_a = x_{ij,a} p_a,$$

with

$$(413c) \quad x_{ij,a} = \frac{(p_i + p_j)p_a - p_i p_j}{(p_i + p_j)p_a} \quad \text{and}$$

$$(413d) \quad \tilde{z}_i = \frac{p_i p_a}{(p_i + p_j)p_a}.$$

All other momenta remain unchanged, $\tilde{p}_n = p_n$. Along with \tilde{z}_i one defines \tilde{z}_j such that $\tilde{z}_j = 1 - \tilde{z}_i$.

The dipole term is

$$(414) \quad \mathcal{D}_{ij}^a(p_a, p_b; p_1, \dots, p_{N+1}) = -\frac{1}{2p_i \cdot p_j} \frac{1}{x_{ij,a}} \langle c' | \frac{\mathbf{T}_a \cdot \mathbf{T}_{(ij)}}{\mathbf{T}_{(ij)}^2} | c \rangle \\ \times \sum_{\lambda_i, \lambda'_j} \mathcal{A}_{c'}^{\mathcal{B}}(\tilde{p}_a^{\lambda_a}, p_b^{\lambda_b}; \tilde{p}_1^{\lambda_1}, \dots, \tilde{p}_N^{\lambda_N})^* \mathcal{A}_c^{\mathcal{B}}(\tilde{p}_a^{\lambda_a}, p_b^{\lambda_b}; \tilde{p}_1^{\lambda'_1}, \dots, \tilde{p}_N^{\lambda'_N}) V_{ij}^{a \lambda, \lambda'},$$

and one obtains the operator

$$(415) \quad V_{ij}^a|_{i=q}^{j=g} = 8\pi\mu^{2\varepsilon}\alpha_s C_F \left[\frac{2}{1 - \tilde{z}_i + (1 - x_{ij,a})} - (1 + \tilde{z}_i) - \varepsilon(1 - \tilde{z}_i) \right] \delta^{\lambda_{(ij)} \lambda'_{(ij)}}$$

for the quark-gluon splitting,

$$(416) \quad V_{ij}^a|_{i=q}^{j=\bar{q}} = 8\pi\mu^{2\varepsilon}\alpha_s T_R \left[-g^{\mu\nu} - \frac{2}{p_i \cdot p_j} (\tilde{z}_i p_i^\mu - \tilde{z}_j p_j^\mu)(\tilde{z}_i p_i^\nu - \tilde{z}_j p_j^\nu) \right]$$

in the case of gluon-quark splitting and

$$(417) \quad V_{ij}^a|_{i=g}^{j=g} = 16\pi\mu^{2\varepsilon}\alpha_s C_A \left[-g^{\mu\nu} \left(\frac{1}{1 - \tilde{z}_i(1 - y_{ij,k})} + \frac{1}{1 - \tilde{z}_j(1 - y_{ij,k})} - 2 \right) \right. \\ \left. + (1 - \varepsilon) \frac{1}{p_i \cdot p_j} (\tilde{z}_i p_i^\mu - \tilde{z}_j p_j^\mu)(\tilde{z}_i p_i^\nu - \tilde{z}_j p_j^\nu) \right]$$

for gluon-gluon splitting.

The spin correlations and the indices μ and ν are the same as in Section 7.2.

7.4. Initial state emitter, final state spectator: \mathcal{D}_k^{ai} . The reverse case of the previous one is the situation where the singularity is in the initial state but the spectator is a final state parton. Here, one uses the momentum mapping

$$(418a) \quad \tilde{p}_{ai} = x_{ik,a} p_a,$$

$$(418b) \quad \tilde{p}_k = p_k + p_i - (1 - x_{ik,a}) p_a,$$

with

$$(418c) \quad x_{ik,a} = \frac{(p_i + p_k)p_a - p_i p_k}{(p_i + p_k)p_a} \quad \text{and}$$

$$(418d) \quad u_i = \frac{p_i p_a}{(p_i + p_k)p_a}.$$

All other momenta remain unchanged, $\tilde{p}_n = p_n$.

The dipole term is

$$(419) \quad \mathcal{D}_k^{ai}(p_a, p_b; p_1, \dots, p_{N+1}) = -\frac{1}{2p_a \cdot p_i} \frac{1}{x_{ik,a}} \langle c' | \frac{\mathbf{T}_k \cdot \mathbf{T}_{(ai)}}{\mathbf{T}_{(ai)}^2} | c \rangle \\ \times \sum_{\lambda_i, \lambda'_j} \mathcal{A}_{c'}^{\mathcal{B}}(\tilde{p}_{ai}^{\lambda_a}, p_b^{\lambda_b}; \tilde{p}_1^{\lambda_1}, \dots, \tilde{p}_N^{\lambda_N})^* \mathcal{A}_c^{\mathcal{B}}(\tilde{p}_{ai}^{\lambda_a}, p_b^{\lambda_b}; \tilde{p}_1^{\lambda'_1}, \dots, \tilde{p}_N^{\lambda'_N}) V_k^{ai \lambda, \lambda'},$$

and one obtains the operator V_k^{ai} for the three different splittings,

$$(420) \quad V_k^{ai} \Big|_{a=g}^{i=g} = 8\pi\mu^{2\varepsilon} \alpha_s C_F \left[\frac{2}{1 - x_{ik,a} + u_i} - (1 + \tilde{x}_{ik,a}) - \varepsilon(1 - \tilde{x}_{ik,a}) \right] \delta^{\lambda_{(ai)} \lambda'_{(ai)}},$$

$$(421) \quad V_k^{ai} \Big|_{a=g}^{i=\bar{q}} = 8\pi\mu^{2\varepsilon} \alpha_s T_R [(1 - \varepsilon) - 2x_{ik,a}(1 - x_{ik,a})] \delta^{\lambda_{(ai)} \lambda'_{(ai)}},$$

$$(422) \quad V_k^{ai} \Big|_{a=q}^{i=q} = 8\pi\mu^{2\varepsilon} \alpha_s C_F \\ \times \left[-g^{\mu\nu} x_{ik,a} + \frac{1 - x_{ik,a}}{x_{ik,a}} \frac{2u_i(1 - u_i)}{p_i \cdot p_k} \left(\frac{p_i^\mu}{u_i} - \frac{p_k^\mu}{1 - u_i} \right) \left(\frac{p_i^\nu}{u_i} - \frac{p_k^\nu}{1 - u_i} \right) \right]$$

and

$$(423) \quad V_k^{ai} \Big|_{a=g}^{i=g} = 16\pi\mu^{2\varepsilon} \alpha_s C_A \left[-g^{\mu\nu} \left(\frac{1}{1 - x_{ik,a} + u_i} - 1 + x_{ik,a}(1 - x_{ik,a}) \right) \right. \\ \left. + (1 - \varepsilon) \frac{1 - x_{ik,a}}{x_{ik,a}} \frac{u_i(1 - u_i)}{p_i \cdot p_k} \left(\frac{p_i^\mu}{u_i} - \frac{p_k^\mu}{1 - u_i} \right) \left(\frac{p_i^\nu}{u_i} - \frac{p_k^\nu}{1 - u_i} \right) \right].$$

The spin correlations and the indices μ and ν are the same as in Section 7.2.

7.5. Initial state emitter, initial state spectator: $\mathcal{D}^{ai,b}$. The last case to be considered for our purpose is the situation with an initial state singularity and an initial state spectator. In this case the momentum mapping involves all final state particles, not only the QCD partons; it is

$$(424a) \quad \tilde{p}_{ai} = x_{i,ab} p_a,$$

$$(424b) \quad \tilde{p}_b = p_b,$$

$$(424c) \quad \tilde{p}_j = p_j - \frac{2p_j \cdot (K + \tilde{K})}{(K + \tilde{K})^2} (K + \tilde{K}) + \frac{2p_j \cdot K}{K^2} \tilde{K}$$

with

$$(424d) \quad x_{i,ab} = \frac{p_a p_b - p_i(p_a + p_b)}{p_a p_b},$$

$$(424e) \quad K = p_a + p_b - p_i \quad \text{and}$$

$$(424f) \quad \tilde{K} = \tilde{p}_{ai} + p_b.$$

The dipole for this case is

$$(425) \quad \mathcal{D}^{ai,b}(p_a, p_b; p_1, \dots, p_{N+1}) = -\frac{1}{2p_a \cdot p_i} \frac{1}{x_{i,ab}} \langle c' | \frac{\mathbf{T}_b \cdot \mathbf{T}_{(ai)}}{\mathbf{T}_{(ai)}^2} | c \rangle \\ \times \sum_{\lambda_i, \lambda'_j} \mathcal{A}_{c'}^{\mathcal{B}}(\tilde{p}_{ai}^{\lambda_a}, p_b^{\lambda_b}; \tilde{p}_1^{\lambda_1}, \dots, \tilde{p}_N^{\lambda_N})^* \mathcal{A}_c^{\mathcal{B}}(\tilde{p}_{ai}^{\lambda_a}, p_b^{\lambda_b}; \tilde{p}_1^{\lambda'_1}, \dots, \tilde{p}_N^{\lambda'_N}) V^{ai,b\lambda,\lambda'}$$

The splitting operators are

$$(426) \quad V^{ai,b} \Big|_{a=q}^{i=g} = 8\pi\mu^{2\varepsilon} \alpha_s C_F \left[\frac{2}{1-x_{i,ab}} - (1+x_{i,ab}) - \varepsilon(1-x_{i,ab}) \right] \delta^{\lambda_{(ai)}\lambda'_{(ai)}},$$

$$(427) \quad V^{ai,b} \Big|_{a=g}^{i=\bar{q}} = 8\pi\mu^{2\varepsilon} \alpha_s T_R [(1-\varepsilon) - 2x_{i,ab}(1-x_{i,ab})] \delta^{\lambda_{(ai)}\lambda'_{(ai)}},$$

and for the gluon induced cases

$$(428) \quad V^{ai,b} \Big|_{a=q}^{i=q} = 8\pi\mu^{2\varepsilon} \alpha_s C_F \\ \times \left[-g^{\mu\nu} x_{i,ab} + \frac{1-x_{i,ab}}{x_{i,ab}} \frac{2p_a \cdot p_b}{(p_i \cdot p_a)(p_i \cdot p_b)} \left(p_i^\mu - \frac{p_i p_a}{p_a p_b} p_b^\mu \right) \left(p_i^\nu - \frac{p_i p_a}{p_a p_b} p_b^\nu \right) \right]$$

and

$$(429) \quad V^{ai,b} \Big|_{a=g}^{i=g} = 16\pi\mu^{2\varepsilon} \alpha_s C_A \left[-g^{\mu\nu} \left(\frac{x_{i,ab}}{1-x_{i,ab}} + x_{i,ab}(1-x_{i,ab}) \right) \right. \\ \left. + (1-\varepsilon) \frac{1-x_{i,ab}}{x_{i,ab}} \frac{p_a \cdot p_b}{(p_i \cdot p_a)(p_i \cdot p_b)} \left(p_i^\mu - \frac{p_i p_a}{p_a p_b} p_b^\mu \right) \left(p_i^\nu - \frac{p_i p_a}{p_a p_b} p_b^\nu \right) \right].$$

The spin correlations and the indices μ and ν are the same as in Section 7.2.

7.6. Counterterms for the Six-Quark Amplitude. For the amplitude $u(p_a) + \bar{u}(p_b) \rightarrow d(p_1) + \bar{d}(p_2) + b(p_3) + \bar{b}(p_4)$ a convenient colour basis is expressed in terms of KRONECKER deltas, because the colour structure of any diagram can be reduced to this basis using Equation (43). Explicitly, one basis choice is

$$(430) \quad \begin{array}{lll} |1\rangle & = & \delta_{i_a}^{j_b} \delta_{i_2}^{j_1} \delta_{i_4}^{j_3} \\ |4\rangle & = & \delta_{i_4}^{j_b} \delta_{i_2}^{j_1} \delta_{i_a}^{j_3} \end{array} \quad \begin{array}{lll} |2\rangle & = & \delta_{i_a}^{j_b} \delta_{i_4}^{j_1} \delta_{i_2}^{j_3} \\ |5\rangle & = & \delta_{i_4}^{j_b} \delta_{i_a}^{j_1} \delta_{i_2}^{j_3} \end{array} \quad \begin{array}{lll} |3\rangle & = & \delta_{i_2}^{j_b} \delta_{i_4}^{j_1} \delta_{i_a}^{j_3} \\ |6\rangle & = & \delta_{i_2}^{j_b} \delta_{i_a}^{j_1} \delta_{i_4}^{j_3} \end{array}$$

In this basis the colour correlation matrix has the following form

$$(431) \quad \langle c|c' \rangle = \begin{pmatrix} N_C^3 & N_C^2 & N_C & N_C^2 & N_C & N_C^2 \\ N_C^2 & N_C^3 & N_C^2 & N_C & N_C^2 & N_C \\ N_C & N_C^2 & N_C^3 & N_C^2 & N_C & N_C^2 \\ N_C^2 & N_C & N_C^2 & N_C^3 & N_C^2 & N_C \\ N_C & N_C^2 & N_C & N_C^2 & N_C^3 & N_C^2 \\ N_C^2 & N_C & N_C^2 & N_C & N_C^2 & N_C^3 \end{pmatrix}$$

Similarly, one obtains the colour correlations for the dipoles; as an example $\mathbf{T}_{(ai)} \cdot \mathbf{T}_3$ has been chosen²⁶,

$$(432) \quad \langle c | \frac{\mathbf{T}_{(ai)} \cdot \mathbf{T}_3}{\mathbf{T}_{(ai)}^2} | c' \rangle = \frac{1}{C_F} \langle c | (-t_{c_a c'_a}^A) t_{c_3 c'_3}^A | c' \rangle = -\frac{T_R}{C_F} \left(\langle c | \delta_{c_a}^{c'_a} \delta_{c_3}^{c'_3} | c' \rangle - \frac{\langle c | c' \rangle}{N_C} \right)$$

where Equation (43) has been used to reduce the product of generators; the explicit matrix in this case is

$$(433) \quad \langle c | \frac{\mathbf{T}_{(ai)} \cdot \mathbf{T}_3}{\mathbf{T}_{(ai)}^2} | c' \rangle = - \begin{pmatrix} 0 & 0 & N_C & N_C^2 & N_C & 0 \\ 0 & 0 & N_C^2 & N_C & 0 & N_C \\ N_C & N_C^2 & N_C^3 & N_C^2 & N_C & N_C^2 \\ N_C^2 & N_C & N_C^2 & N_C^3 & N_C^2 & N_C \\ N_C & 0 & N_C & N_C^2 & 0 & 0 \\ 0 & N_C & N_C^2 & N_C & 0 & 0 \end{pmatrix}$$

For the real emission one has to consider the process with an additional gluon in the final state, $u(p_a) + \bar{u}(p_b) \rightarrow d(p_1) + \bar{d}(p_2) + b(p_3) + \bar{b}(p_4) + g(p_5)$. The only dipoles that can be produced with the BORN level matrix element are those where a (anti-)quark splits into a gluon plus (anti-)quark. The subtraction term therefore is as follows:

$$(434) \quad \frac{d\sigma^A}{d\Phi^{(5)}} = \frac{1}{2N_C} \frac{1}{2N_C} \sum_{\{\mathcal{D}\}} F_J^{(4)}(\{\tilde{p}\}) \mathcal{D}$$

where the sum over all dipole runs over

$$(435) \quad \{\mathcal{D}\} = \{\mathcal{D}_{15,2}, \mathcal{D}_{15,3}, \mathcal{D}_{15,4}, \mathcal{D}_{15}^a, \mathcal{D}_{15}^b, \mathcal{D}_{25,1}, \mathcal{D}_{25,3}, \mathcal{D}_{25,4}, \mathcal{D}_{25}^a, \mathcal{D}_{25}^b, \\ \mathcal{D}_{35,1}, \mathcal{D}_{35,2}, \mathcal{D}_{35,4}, \mathcal{D}_{35}^a, \mathcal{D}_{35}^b, \mathcal{D}_{45,1}, \mathcal{D}_{45,2}, \mathcal{D}_{45,3}, \mathcal{D}_{45}^a, \mathcal{D}_{45}^b, \\ \mathcal{D}_1^{a5}, \mathcal{D}_2^{a5}, \mathcal{D}_3^{a5}, \mathcal{D}_4^{a5}, \mathcal{D}_1^{b5}, \mathcal{D}_2^{b5}, \mathcal{D}_3^{b5}, \mathcal{D}_4^{b5}, \mathcal{D}^{a5,b}, \mathcal{D}^{b5,a}\}.$$

The term $\sigma_{ab}^{C\{N\}}$ for this amplitude is

$$(436) \quad \sigma_{ab}^{C\{N\}}(p_a, p_b) = \int_0^1 dx \int d\Phi^{(4)}(xp_a + p_b) F_J^{(4)}(xp_a, p_b; p_1, \dots, p_4) \\ \times \frac{1}{(2N_C)^2} \sum_{\lambda_i} \mathcal{A}_{c'}^{\mathcal{B}}(xp_a^{\lambda_a}, p_b^{\lambda_b}; p_1^{\lambda_1}, \dots, p_4^{\lambda_4})^* \mathcal{A}_c^{\mathcal{B}}(xp_a^{\lambda_a}, p_b^{\lambda_b}; p_1^{\lambda_1}, \dots, p_4^{\lambda_4}) \\ \times \langle c' | (\mathbf{K}^{q,q}(x) + \mathbf{P}^{q,q}(xp_a, x; \mu_F^2)) | c \rangle \\ + \int_0^1 dx \int d\Phi^{(4)}(p_a + xp_b) F_J^{(4)}(p_a, xp_b; p_1, \dots, p_4) \\ \times \frac{1}{n_a n_b} \sum_{\lambda_i} \mathcal{A}_{c'}^{\mathcal{B}}(p_a^{\lambda_a}, xp_b^{\lambda_b}; p_1^{\lambda_1}, \dots, p_4^{\lambda_4})^* \mathcal{A}_c^{\mathcal{B}}(p_a^{\lambda_a}, xp_b^{\lambda_b}; p_1^{\lambda_1}, \dots, p_4^{\lambda_4}) \\ \times \langle c' | (\mathbf{K}^{\bar{q},\bar{q}}(x) + \mathbf{P}^{\bar{q},\bar{q}}(xp_b, x; \mu_F^2)) | c \rangle.$$

²⁶Note that the extra minus comes from the convention for an initial state quark $\mathbf{T}_{ai} = -t_{i_a j_a}^A$

7.7. Counterterms for the Two-Gluon plus Four-Quark Amplitude. The process $g(p_a) + g(p_b) \rightarrow d(p_1) + \bar{d}(p_2) + b(p_3) + \bar{b}(p_4)$ can be projected onto the colour basis

$$\begin{aligned}
 (437) \quad |1\rangle &= t_{i_2 j_1}^A t_{i_4 j_3}^B & |2\rangle &= t_{i_2 j_1}^B t_{i_4 j_3}^A & |3\rangle &= t_{i_4 j_1}^A t_{i_2 j_3}^B \\
 |4\rangle &= t_{i_4 j_1}^B t_{i_2 j_3}^A & |5\rangle &= t_{i_2 j'}^A t_{j' j_1}^B \delta_{i_4}^{j_3} & |6\rangle &= t_{i_2 j'}^B t_{j' j_1}^A \delta_{i_4}^{j_3} \\
 |7\rangle &= t_{i_4 j'}^A t_{j' j_1}^B \delta_{i_2}^{j_3} & |8\rangle &= t_{i_4 j'}^B t_{j' j_1}^A \delta_{i_2}^{j_3} & |9\rangle &= t_{i_2 j'}^A t_{j' j_3}^B \delta_{i_4}^{j_1} \\
 |10\rangle &= t_{i_2 j'}^B t_{j' j_3}^A \delta_{i_4}^{j_1} & |11\rangle &= t_{i_4 j'}^A t_{j' j_3}^B \delta_{i_2}^{j_1} & |12\rangle &= t_{i_4 j'}^B t_{j' j_3}^A \delta_{i_2}^{j_1} \\
 |13\rangle &= t_{i' j'}^A t_{j' i'}^B \delta_{i_2}^{j_1} \delta_{i_4}^{j_3} & |14\rangle &= t_{i' j'}^B t_{j' i'}^A \delta_{i_4}^{j_1} \delta_{i_2}^{j_3}
 \end{aligned}$$

where for $N_C = 3$ one vector can be eliminated by the relation

$$(438) \quad |14\rangle - |13\rangle + |12\rangle + |11\rangle - |10\rangle - |9\rangle - |8\rangle - |7\rangle + |6\rangle + |5\rangle - |4\rangle - |3\rangle + |2\rangle + |1\rangle = 0$$

which reflects the fact that an antisymmetrisation over more than N_C fundamental indices of an $SU(N)$ -tensor is zero.

The counterterms are as in the previous section, with the only difference that the flavours $a = g$, $b = g$ have to be replaced in all formulæ.

7.8. Outlook and Improvements. Implementations of the dipole subtraction show that the time which is spent on the computation of the subtraction terms is comparable to the computational cost of the real emission matrix element itself. This drawback has been improved by NAGY [Nag03] in the following way: the subtraction term σ^A is only relevant at the border of the phase-space, where collinear and soft divergences can appear. A new parameter $0 < \alpha \leq 1$ separates the possibly divergent region from the unproblematic bulk of the phase space; $\alpha = 1$ corresponds to the full dipole subtraction as presented in [CS97]. The dipoles are restricted to the critical phase space by the modification

$$(439a) \quad \mathcal{D}_{ij,k} \rightarrow \mathcal{D}_{ij,k} \cdot \Theta(y_{ij,k} < \alpha),$$

$$(439b) \quad \mathcal{D}_k^{ai} \rightarrow \mathcal{D}_k^{ai} \cdot \Theta(u_i < \alpha),$$

$$(439c) \quad \mathcal{D}_{ij}^a \rightarrow \mathcal{D}_{ij}^a \cdot \Theta(1 - x_{ij,a} < \alpha),$$

$$(439d) \quad \mathcal{D}^{ai,b} \rightarrow \mathcal{D}^{ai,b} \cdot \Theta(\tilde{v}_i < \alpha).$$

A new parameter has been introduced for the dipole $\mathcal{D}^{ai,b}$, $\tilde{v}_i = p_a \cdot p_i / p_a \cdot p_b$. The modification of the dipoles induces a change also in the integrated dipoles. Here only the constant K_i has to be replaced by

$$(440) \quad K_i \rightarrow K_i(\alpha) = K_i - \mathbf{T}_i^2 \ln^2(\alpha) + \gamma_i \cdot (\alpha - 1 - \ln \alpha).$$

Further modifications have to be taken into account for the \mathbf{K} and \mathbf{P} operators; the reader is referred to Equations (13)–(17) in the original work [Nag03].

8. Phase Space Integration and Monte-Carlo Techniques

8.1. Introduction. So far the discussion was focused on the computation of matrix elements. However, for a complete calculation one also needs to perform the

phase-space integral for the final state particles. The N -particle phase-space is defined as [Wei00]

$$(441) \quad d\Phi^{(N)}(Q; p_1, \dots, p_N) = \prod_{j=1}^N \frac{d^4 p_j}{(2\pi)^3} \Theta(p_j^0) \delta(p_j^2 - m_j^2) \cdot (2\pi)^4 \delta^{(4)} \left(Q - \sum_{i=1}^N p_i \right) =$$

$$\prod_{j=1}^N \frac{d^3 \vec{p}_j}{(2\pi)^3 \cdot 2\omega_j} \cdot (2\pi)^4 \delta^{(4)} \left(Q - \sum_{i=1}^N p_i \right)$$

where $\omega_j = \sqrt{p_j^2 - m_j^2}$. This phase space is $(3N - 4)$ dimensional; for non-trivial physical processes these integrals are difficult to be done analytically and can classical adaptive methods cannot solve the integral in an efficient manner. Furthermore, the constraints on the phase-space imposed by experimental cuts render a analytic treatment of the integrals impossible. Instead, Monte-Carlo methods are used [HH65, Wei00]. For classical methods, e.g. the GAUSSIAN quadrature the error bound drops like $\mathcal{O}(n^{-2/d})$ where n denotes the number of evaluations of the integrand. In Monte Carlo methods the behaviour of the error $\mathcal{O}(1/\sqrt{n})$ is constant in the number of dimensions and therefore outperforms the classical methods for higher-dimensional integrals.

8.2. Monte-Carlo Integration. The basic idea behind Monte Carlo integration is to evaluate the integrand function f in n randomly chosen points $\vec{x}^{(j)}$ to obtain an estimator for the exact integral

$$(442) \quad I = \int_0^1 d\vec{x} f(\vec{x}) = \int_0^1 dx_1 \cdots \int_0^1 dx_d f(x_1, \dots, x_d) \approx E = \frac{1}{n} \sum_{j=1}^n f(x_1^{(j)}, \dots, x_d^{(j)}).$$

The $\vec{x}^{(j)}$ are chosen according to a uniform distribution in the hypercube $0 \leq x_i^{(j)} \leq 1$. The restriction to the interval $[0; 1]$ can always be overcome by a variable transformation.

The statistical error can be obtained by integrating out all random variables,

$$(443) \quad \int_0^1 d\vec{x}^{(1)} \int_0^1 d\vec{x}^{(2)} \cdots \int_0^1 d\vec{x}^{(n)} \left(\frac{1}{n} \sum_{j=1}^n f(\vec{x}^{(j)}) - I \right)^2 = \frac{\sigma^2(f)}{n},$$

where the variance of the the function f has been introduced,

$$(444) \quad \sigma^2(f) = \int_0^1 d\vec{x} (f(\vec{x}) - I)^2.$$

From the central limit theorem one can conclude that the estimate of the integral lies in the interval [Wei00]

$$(445) \quad \lim_{n \rightarrow \infty} \text{Prob} \left(-a \frac{\sigma(f)}{\sqrt{n}} \leq \frac{1}{n} \sum_{j=1}^n f(\vec{x}^{(j)}) - I \leq b \frac{\sigma(f)}{\sqrt{n}} \right) = \frac{1}{\sqrt{2\pi}} \int_{-a}^b dt e^{-\frac{t^2}{2}}.$$

The exact knowledge of $\sigma(f)$ would render a Monte Carlo integration unnecessary and is usually not available. Therefore, in practical applications one estimates the error by

Monte Carlo techniques, too,

$$(446) \quad \sigma^2(f) \approx S \equiv \frac{1}{n-1} \sum_{j=1}^n \left(f(\vec{x}^{(j)}) - E \right)^2.$$

Here, E is the estimator as defined in Equation (442).

In the following two methods are discussed which can be used to reduce the variance $\sigma^2(f)$ and therefore for a reduction of the error, *stratified sampling* and *importance sampling*. A combination of these two ideas leads to an adaptive algorithm for Monte Carlo integration, *VEGAS*, which closes the discussion of Monte Carlo techniques. In Section 8.4 I introduce a method that uses importance sampling for the integration of the virtual contribution of NLO cross-sections. This method has been successfully applied in the calculation of the process $u\bar{u} \rightarrow b\bar{b}b\bar{b}$, results of which are presented in Chapter 4.

Stratified sampling uses the simple fact that the integration region can be split into disjoint subsets

$$(447) \quad [0; 1]^d = \biguplus_{\nu=1}^k M_\nu.$$

The volume of each subset is

$$(448) \quad \text{vol}(M_\nu) = \int_0^1 d^d \vec{x} \, \Theta(\vec{x} \in M_\nu)$$

and therefore $\sum_{\nu=1}^k \text{vol}(M_\nu) = 1$. If in each region the Monte Carlo estimator $E = \sum_{\nu=1}^k E_\nu$ is evaluated with N_ν points, $\sum_{\nu=1}^k N_\nu = N$,

$$(449) \quad E_\nu = \frac{\text{vol}(M_\nu)}{N_\nu} \sum_{j=1}^{N_\nu} f(\vec{x}^{(\nu;j)}), \quad \vec{x}^{(\nu;j)} \in M_\nu$$

the new error estimate is

$$(450) \quad \sum_{\nu=1}^k \text{vol}(M_\nu)^2 \frac{\sigma^2(f)|_{M_\nu}}{N_\nu}$$

with the variance restricted on the subspace M_ν

$$(451) \quad \sigma^2(f)|_{M_\nu} = \frac{1}{\text{vol}(M_\nu)} \int_0^1 d^d \vec{x} (f(\vec{x})\Theta(\vec{x} \in M_\nu) - I|_{M_\nu})^2$$

and

$$(452) \quad I|_{M_\nu} = \frac{1}{\text{vol}(M_\nu)} \int_0^1 d^d \vec{x} f(\vec{x}).$$

For a given partition $\{M_\nu\}$ of the hypercube $[0; 1]^d$ the error is minimised for the choice

$$(453) \quad \frac{N_\mu}{N} = \frac{\text{vol}(M_\mu) \sigma^2(f)|_{M_\mu}}{\sum_{\nu=1}^k \text{vol}(M_\nu) \sigma^2(f)|_{M_\nu}}.$$

A second useful technique is *importance sampling*, which corresponds to a variable transformation in usual integration,

$$(454) \quad \int_0^1 d^d \vec{x} f(\vec{x}) = \int_0^1 d^d \vec{x} \frac{f(\vec{x})}{p(\vec{x})} p(\vec{x}).$$

If $p(\vec{x})$ is positive and normalised such that

$$(455) \quad \int_0^1 d^d \vec{x} p(\vec{x}) = 1$$

then $p(\vec{x})$ can be interpreted as the density of the probability distribution $P(\vec{x})$,

$$(456) \quad p(\vec{x}) = \frac{\partial^d}{\partial x_1 \cdots \partial x_d} P(\vec{x}).$$

The Monte Carlo estimator can be replaced by

$$(457) \quad E = \frac{1}{N} \sum_{j=1}^n \frac{f(\vec{x}^{(j)})}{p(\vec{x}^{(j)})}$$

and the points $\vec{x}^{(j)}$ are chosen according to the probability distribution $P(\vec{x})$. The statistical error is $\sigma(f/p)/\sqrt{n}$; if f and p are very similar the ratio f/p becomes flat and hence the error decreases.

In the VEGAS algorithm [Lep78], one combines the above ideas in the following way: the probability density is approximated by a grid

$$(458) \quad p(\vec{x}) = \prod_{j=1}^d p_j(x_j) \quad \text{with } p_j(x_j) = \frac{1}{k_j} \sum_{i=1}^{k_j} \frac{\Theta(x_{i-1,j} \leq x_j < x_{i,j})}{x_{i,j} - x_{i-1,j}}$$

The grid is separated at points $0 = x_{0,j} < x_{1,j} < \dots < x_{k_j,j} = 1$ and is adjusted step-wise such that each bin contributes

$$(459) \quad \frac{1}{\prod_{j=1}^d k_j} \int_0^1 d^d \vec{x} |f(\vec{x})|.$$

A sequence of m adaption steps leads to the estimates $E_{(1)}, \dots, E_{(m)}$ and estimates for the variance $S_{(1)}, \dots, S_{(m)}$. If the number of points in step j is $N_{(j)}$ one obtains a combined result

$$(460) \quad E_{\text{combined}} = \sum_{j=1}^m \frac{N_{(j)} E_{(j)}}{S_{(j)}^2} \bigg/ \sum_{i=1}^m \frac{N_{(i)}}{S_{(i)}^2}$$

One also can check the consistency of the estimators using χ^2 per degree of freedom,

$$(461) \quad \chi^2/\text{d.o.f.} = \frac{1}{m-1} \sum_{j=1}^m \frac{(E_{(j)} - E)^2}{S_{(j)}^2}.$$

8.3. Phase Space mapping: RAMBO. Although nowadays many different and optimised methods are available to map the hypercube $[0; 1]^{4N}$ to the phase space $d\Phi^{(N)}$, here I will only focus on the RAMBO [KSE86]; a broader overview over different phase space mappings is given for example in [Wei00].

In the first step of the RAMBO algorithm, one generates a set of N lightlike vectors q_i with isotropic angular distribution and energy distribution $E e^{-E} dE$. The vector

$q_i^\mu = E_i(1, \cos \varphi_i \sin \theta_i, \sin \varphi_i \sin \theta_i, \cos \theta_i)$ is generated from four uniformly distributed random numbers $u_{i1} \dots u_{i4}$ in the hypercube $(0; 1]^4$ with the transformation

$$(462a) \quad \cos \theta_i = 2u_{i1} - 1,$$

$$(462b) \quad \varphi_i = 2\pi u_{i2},$$

$$(462c) \quad E_i = -\ln(u_{i3}u_{i4}).$$

To obtain physical momenta that obey momentum conservation $\tilde{Q} = \sum_{j=1}^n p_j^\mu$ for a time like vector $\tilde{Q} = (Q^0, 0, 0, 0)$ in a second step, one has to apply the LORENTZ transformation $p_i^\mu = \Lambda_\nu^\mu q_i^\nu$,

$$(463) \quad \Lambda_\nu^\mu = x \left(\frac{\gamma}{\vec{b}} \middle| \frac{\vec{b}^\top}{\mathbb{I} + a \vec{b} \vec{b}^\top} \right)$$

parametrised by

$$(464) \quad \vec{b} = -\frac{1}{\sqrt{v^2}} \vec{v}, \quad \text{with } v^\mu = \sum_{j=1}^N q_j^\mu,$$

$$(465) \quad \gamma = \sqrt{1 + |\vec{b}|^2},$$

$$(466) \quad a = \frac{1}{1 + \gamma} \quad \text{and}$$

$$(467) \quad x = \sqrt{\frac{\tilde{Q}^2}{v^2}}.$$

One can show [KSE86, Wei00] that from the transformation each event obtains the weight

$$(468) \quad w = w_0 = (2\pi)^{4-3N} \left(\frac{\pi}{2}\right)^{N-1} \frac{(Q^2)^{N-2}}{\Gamma(N)\Gamma(N-1)}.$$

In order to obtain momenta k_i for massive particles from the momenta p_i as defined above, one applies a second transformation

$$(469) \quad k_i^0 = \sqrt{m_i^2 + \xi^2 (p_i^0)^2}, \quad \vec{k}_i = \xi \vec{p}_i,$$

where the parameter ξ is a solution of the equation

$$(470) \quad \sqrt{\tilde{Q}^2} = \sum_{j=1}^N \sqrt{m_j^2 + \xi^2 (p_j^0)^2}.$$

Each event obtains a new weight $w = w_0 w_m$, where w_m is

$$(471) \quad w_m = (\tilde{Q}^2)^{2-N} \left(\sum_{j=1}^N |\vec{k}_j|^2 \right)^{2N-3} \left(\prod_{j=1}^N \frac{|\vec{k}_j|}{k_j^0} \right) / \left(\sum_{j=1}^N \frac{|\vec{k}_j|^2}{k_j^0} \right)$$

8.4. Integration of NLO Amplitudes. In this section I present a method which is well suited for an efficient implementation of an event generator at one-loop level. [B⁺08b] Traditionally, one uses an adaptive Monte Carlo program such as VEGAS and call it with the differential cross-section $d\sigma^\nu$ in order to obtain the virtual corrections σ^ν to the inclusive cross-section.

Working with the virtual correction already in the initialisation of the integrator has two disadvantages: the virtual corrections are computationally much more expensive than the LO matrix element and hence one adds to the run time of the integration. Secondly, the integrator is likely to adapt to integrable singularities in the phase space which destabilises the adaption process.

The method presented below avoids part of the computational cost using the LO matrix element for the initialisation steps and calling the virtual corrections only on a set of phase-space points which have been obtained from the integration of the LO cross-section, thus also avoiding destabilisation of the adaption phase of the integrator.

An observable for a collider can be defined as the integral²⁷

$$(472) \quad \langle O \rangle = \int_0^1 dx_1 \int_0^1 dx_2 f_a(x_1) f_b(x_2) \int d\Phi^{(N)}(x_1 P_1 + x_2 P_2; p_1, \dots, p_N) \\ \times \frac{d\sigma_{ab}(x_1 P_1, x_2 P_2; p_1, \dots, p_N)}{d\Phi^{(N)}} O(x_1 P_1, x_2 P_2; p_1, \dots, p_N) \\ \approx \frac{1}{n} \sum_{j=1}^n f_a(x_1^{(j)}) f_b(x_2^{(j)}) \frac{d\sigma_{ab}(x_1^{(j)} P_1, x_2^{(j)} P_2; p_1^{(j)}, \dots, p_N^{(j)})}{d\Phi^{(N)}} O(x_1^{(j)} P_1, x_2^{(j)} P_2; p_1^{(j)}, \dots, p_N^{(j)})$$

At LO one has $d\sigma_{ab} = d\sigma_{ab}^B$ and $\sigma_{ab} = \langle 1 \rangle$. Most LO event generators are capable of producing *unweighted* events, i.e. from all events $e_{(j)} = (x_1^{(j)}, x_2^{(j)}; p_1^{(j)}, \dots, p_N^{(j)})$ a subset U is chosen such that for a large number of events

$$(473) \quad \langle O \rangle = \frac{\sigma_{a,b}^B}{|U|} \sum_{e_{(j)} \in U} O(x_1^{(j)} P_1, x_2^{(j)} P_2; p_1^{(j)}, \dots, p_N^{(j)}).$$

The right hand corresponds to a Monte Carlo estimator using importance sampling with the probability density

$$(474) \quad p(e_{(j)}) = \frac{1}{\sigma_{a,b}^B} f_a(x_1^{(j)}) f_b(x_2^{(j)}) \frac{d\sigma_{ab}(x_1^{(j)} P_1, x_2^{(j)} P_2; p_1^{(j)}, \dots, p_N^{(j)})}{d\Phi^{(N)}}$$

One can carry this idea of importance sampling further and evaluate the one-loop corrections to the BORN process using the estimate

$$(475) \quad \langle O \rangle^\nu = \langle O \cdot K \rangle = \frac{\sigma_{a,b}^B}{|U|} \sum_{e_{(j)} \in U} O(e_{(j)}) K(e_{(j)}),$$

where the local K -factor is defined as

$$(476) \quad K(e_{(j)}) = \frac{d\sigma^\nu(e_{(j)})}{d\sigma^B(e_{(j)})}.$$

²⁷The presence of real corrections is not important for this discussion because their contribution can be computed by standard techniques.

for a phase-space point $e_{(j)}$. The advantage is that an adaptive Monte Carlo program is trained — i.e. the grid is optimised in the case of VEGAS — according to the BORN level matrix element; therefore the initialisation is very fast and robust, as explained above. As this method is well defined as an application of importance sampling, one can calculate S/\sqrt{N} as an estimate of the error introduced by the integration over the unweighted events. Our experience with the $u\bar{u} \rightarrow b\bar{b}b\bar{b}$ shows that this contribution to the total error is comparable with the error on the LO matrix element, which is shown in Chapter 4.

CHAPTER 4

Virtual NLO Corrections for $u\bar{u} \rightarrow b\bar{b}b\bar{b}$

*However beautiful the strategy, you
should occasionally look at the results.*
— WINSTON CHURCHILL

Introduction

In the previous chapter all theoretical foundations necessary for a computation of NLO matrix elements have been presented, many of which relate directly to algorithms suitable for computer algebra systems. An overview over the implementation of a program for such a computation is given in Appendix E. One of the main ideas behind [BGH⁺05] is the freedom of branching between numerical evaluation and algebraic reduction of the amplitude for different sets of basis functions: in the fully numerical approach the form factors $A_{j_1 \dots j_r}^{N,r}$, $B_{j_1, \dots, j_{r-2}}^{N,r}$ and $C_{j_1 \dots j_{r-4}}^{N,r}$ are implemented in a numerical library and only a minimal set of algebraic simplifications is carried out in order to bring the expression into a form suitable for compilation with **Fortran**. The other possibility of an evaluation is the reduction of the form factors down to scalar integrals. Here one has the choice between the two function sets $\mathcal{I}_{\mathcal{N}}$ and $\mathcal{I}_{\mathcal{S}}$ as specified in (330). Having chosen the latter one introduces inverse GRAM determinants which have to cancel algebraically in order to guarantee a numerically stable evaluation of the expression. The results below which are given for the virtual corrections have been obtained with the numerical implementation of the reduction algorithm. An implementation of the algebraic reduction has provided an independent check to verify the correctness of the program.

As an application, we have calculated the NLO corrections to the process $u\bar{u} \rightarrow b\bar{b}b\bar{b}$ in massless QCD. Continuing from the previous chapter, again the focus is on the virtual corrections. The real corrections are obtained using **Whizard** [Kil01, RG] but are not included in the results shown below. For the IR subtraction terms we have used CATANI-SEYMOUR dipole subtraction [CS97] with the modifications as suggested in [Nag03]. In our integration we have set the cut off for the dipoles to $\alpha = 0.1$.

All data sets are generated with the following cuts, which are chosen to agree with the study of [D⁺00], to which the process $u\bar{u} \rightarrow b\bar{b}b\bar{b}$ is an important background. In particular, these cuts are

- a p_T cut of $p_T > 25$ GeV,
- a rapidity cut of $|\eta| < 2.5$ and
- a separation cut of $\Delta R > 0.4$.

Unless stated otherwise, the factorisation scale μ_F and the renormalisation scale μ_R are chosen as the average transverse momentum of the final state partons,

$$(477) \quad \mu_F = \mu_R = \sum_{i=1}^4 \frac{p_{T,i}}{4}.$$

For the Parton Distribution Functions (PDFs) we have used the set CTEQ 6.5 [T⁺07].

1. Performance and Accuracy

The Monte Carlo integration has been carried out on the Edinburgh Computing and Data Facility (ECDF)¹ using the method described in Section 8.4 of Chapter 3. The implementation of the matrix element is available in double precision and quadruple precision; a performance of 8.9s (17.6s) per phase-space point has been achieved for a single node² in double (quadruple) precision.

The reason to have an implementation in two different precisions is to reduce and to quantify the error on the result due to numerical instabilities: in some phase space regions our amplitude representation induces large terms cancelling against each other, which in a numerical implementation leads to a loss of significant digits. Typically, for those points one observes large ratios between NLO and LO result, which is referred to as *local K-factor*, or an incomplete cancellation of the pole parts of the amplitude. The histograms in Figure 1 are generated for 200.000 phase-space points. The tail of each distribution stretching towards large values of the respective quantity is reduced by an evaluation in higher precision, indicating that these quantities can be used to single out points which cause numerical problems. However, these are only indicators but neither necessary nor sufficient conditions for numerical instabilities.

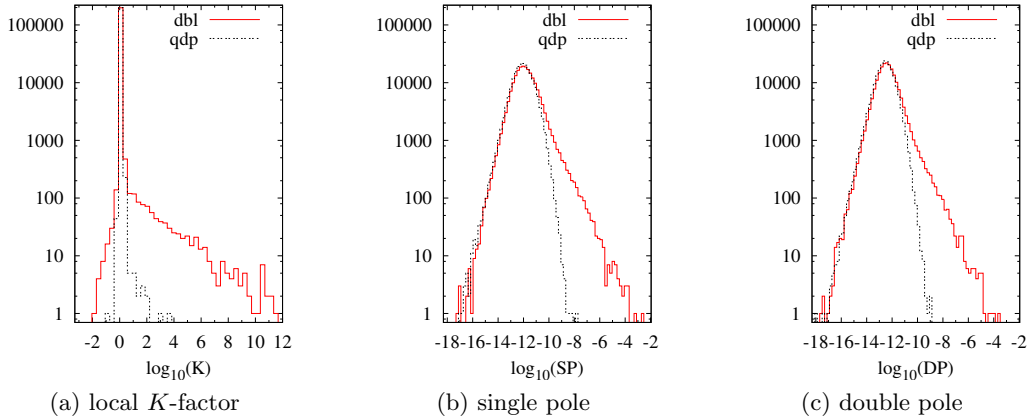


Figure 1: Distributions for double and quadruple precision obtained from 200.000 randomly generated phase space points. Left: the local K -factor. Middle: the single pole of the squared NLO matrix element normalised by the square of the LO matrix element. Right: as middle, but for the double pole.

¹See Section 6.7 of Appendix E

²Intel Xeon 5450 quad-core 3 GHz

In order to enjoy the benefits of the improved stability of an evaluation in quadruple precision and the speed of the calculation in double precision, we investigated different criteria applied for each phase-space point, such that

- the point is calculated in double precision if it passes the test,
- the point is re-evaluated in higher precision if the test fails,
- the outcome of the test only depends on the double precision result.

The above motivation has lead to the comparison of three different criteria. The first test uses the local K -factor as defined in Equation (476),

$$K(e_{(j)}) = \frac{d\sigma^{\mathcal{V}}(e_{(j)})}{d\sigma^{\mathcal{B}}(e_{(j)})};$$

the other two tests compare the residual value of the single (resp. double) pole of the local K -factor, which in an evaluation with arbitrary precision would be zero³. If the considered value is larger than a given, fixed cut-off the test fails and the evaluation is repeated in higher precision.

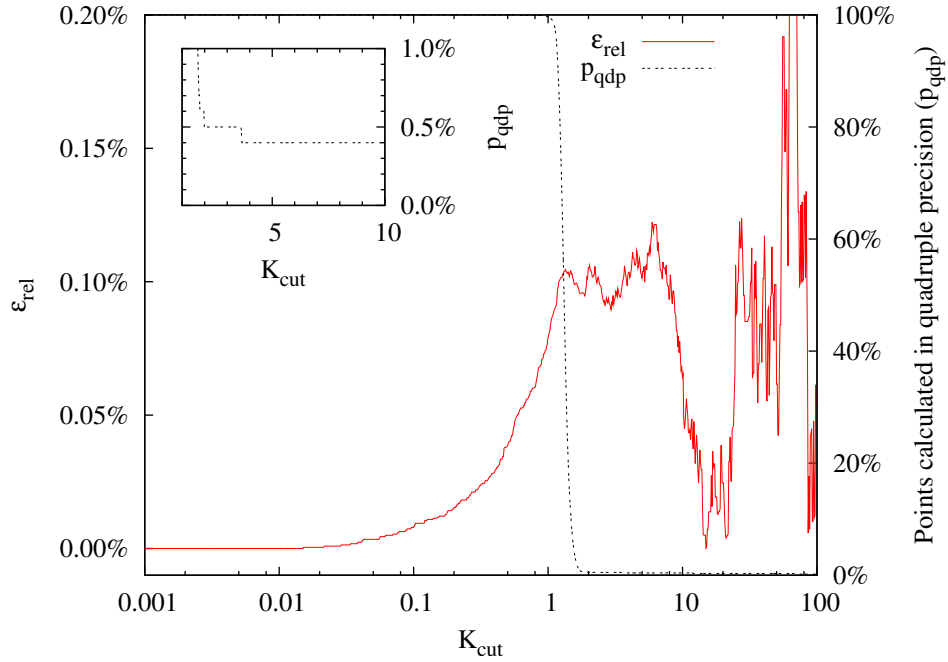


Figure 2: Relative error $\varepsilon_{\text{rel}} = \frac{|\sigma(K_{\text{cut}}) - \sigma(0)|}{\sigma(0)}$ of the integral over a sample of 200.000 random points. For each phase-space point the local K -factor has been calculated in double precision (K_{dbl}); if $|K_{\text{dbl}}| \geq K_{\text{cut}}$ the K -factor evaluated in quadruple precision (K_{qdp}) entered the result, otherwise K_{dbl} has been used. The second curve shows the percentage of points p_{qdp} required in quadruple precision to evaluate $\sigma(K_{\text{cut}})$. The figure has been produced from 1.000 different values of K_{cut} , distributed linearly in $\log(K_{\text{cut}})$. The inlay shows p_{qdp} for the region between $2 \leq K_{\text{cut}} \leq 10$.

³The cancellation of the poles is also influenced by the precision of the kinematics as an input parameter, which in our calculation is fixed to be double precision.

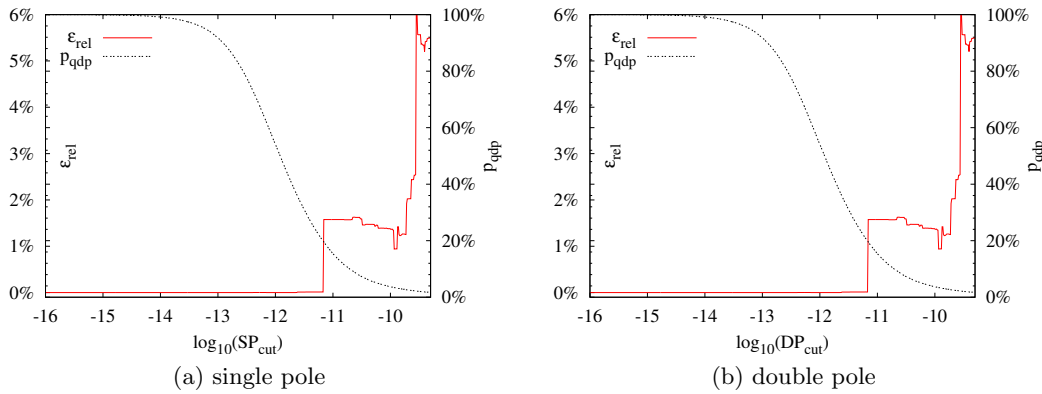


Figure 3: Relative error $\varepsilon_{\text{rel}} = \frac{|\sigma(P_{\text{cut}}) - \sigma(0)|}{\sigma(0)}$ of the integral over a sample of 200.000 random points. The procedure is the same as in Figure 2 but instead of K_{cut} the single (resp. double) pole of the K -factor, $P_{\text{cut}} = \{SP_{\text{cut}}, DP_{\text{cut}}\}$ respectively, have been used as the criterion for an evaluation with higher precision.

Figures 2 and 3 show the relative errors on the inclusive Monte Carlo integral obtained from 200.000 phase space points for different values of the cut-off parameters. In figure 2 we vary the value of K_{cut} and re-evaluate phase-space points $e_{(j)}$, where $K(e_{(j)}) \geq K_{\text{cut}}$. For values of $K_{\text{cut}} \lesssim 10$ the relative error on the Monte Carlo estimate as opposed to a complete evaluation in quadruple precision remains small ($\varepsilon \lesssim 0.1\%$). On the other hand, the number of points to be calculated in quadruple precision drops below 0.5% around $K_{\text{cut}} \approx 1.5$, and hence moderate values of K_{cut} ($2 \leq K_{\text{cut}} \leq 10$) yield an estimate that is within an error of $\mathcal{O}(0.1\%)$ compared to the result obtained in quadruple precision with a performance close to the speed of a calculation in double precision.

The authors of [GZ08] propose to use the correlation between the accuracy with which the poles in $\varepsilon = (4 - n)/2$ cancel in order to obtain an estimate for the stability of the numerical evaluation of a phase space point. In Figure 3 a similar method as in Figure 2 has been used to obtain estimates for the error on a Monte Carlo integral over 200.000 points: instead of the local K -factor, the pole-parts of the squared NLO matrix element normalised by the square of the LO matrix element have been used as a cut-off parameter to switch between double precision and quadruple precision. However, for the $u\bar{u} \rightarrow b\bar{b}b\bar{b}$ amplitude we observe an identification of unstable points which is worse than in the case where the local K -factor has been used as a discriminant. In order to obtain a relative error of less than 0.1% one has to evaluate $\mathcal{O}(20\%)$ of the phase space points in higher precision. The results are very similar for the single pole (Figure 3 (a)) and the double pole (Figure 3 (b)).

As an estimate of the error on the NLO results we consider the sum of three contributions:

$K \cdot \delta\sigma_{\text{LO}}$	is the propagation of the error on σ_{LO} introduced by the Monte Carlo integration of the leading order result.
$\frac{S}{\sqrt{N}}$	estimates the error resulting from the integration of the NLO matrix element, where N is the number of unweighted events used for the integration and S is the estimate of the standard deviation as defined in Equation (446).
ε_{rel}	as obtained from Figure 2 is added to the error to account for the limited numerical precision. In all our calculations we choose $K_{\text{cut}} = 4.0$ and $\varepsilon_{\text{rel}} = 0.1\%$.

Table 1 shows the error contributions for two integrations of the virtual part of the inclusive cross-section. The errors in both cases are very small; in the larger sample of 10^6 phase-space points both the error induced by the integration of the LO part and the error from the integration of the NLO matrix element are comparable.

N	100,000	1,000,000
$K \cdot \delta\sigma_{\text{LO}}$	0.71%	0.58%
S/\sqrt{N}	2.79%	0.49%
ε_{rel}	0.10%	0.10%
total error	3.59%	1.17%

Table 1: Relative error contributions to the virtual corrections of the inclusive cross-section for $u\bar{u} \rightarrow b\bar{b}b\bar{b}$ at NLO. Each result is based on an independent sample of N events with a p_T cut of 25 GeV, a rapidity cut of $|\eta| < 2.5$ and a separation cut $\Delta R > 0.4$ applied. The scales are chosen as $\mu_F = \mu_R = \sum p_T/4$ and CTEQ6.5 PDFs [T⁺07] have been used.

We have varied the renormalisation scale μ_R and the factorisation scale μ_F in an interval from $1/8$ to 8 times of their central value $\mu_0 = \sum_{i=1}^4 p_T^{(i)}/4$ to study the influence of the scale choice on the result. The NLO corrections in this calculation consist of the virtual corrections and the insertion operator $\langle I(\varepsilon) \rangle$; this subset of terms ensures that all poles cancel and the results presented are IR finite. The real corrections together with the dipoles and the subtraction term $\sigma^{C\{N\}}$ as described in Section 7 of Chapter 3 need to be added to obtain the full NLO corrections.

The result for the inclusive cross-section is shown in Figure 4 for the case where both scales are varied in parallel and the case of antiparallel (antipodal) scale variation. Both graphs show a plateau region for $2 \lesssim \xi \lesssim 4$. In the region around $\xi \approx 1$ one expects the real emission to significantly change the result and hence we eschew a interpretation of the data in this region until the NLO corrections are complete.

2. Exclusive Observables

In this section we study distributions of exclusive observables, which are relevant for example in MSSM Higgs boson searches in the $b\bar{b}b\bar{b}$ channel at the LHC [D⁺00, Mah01, DGV95].

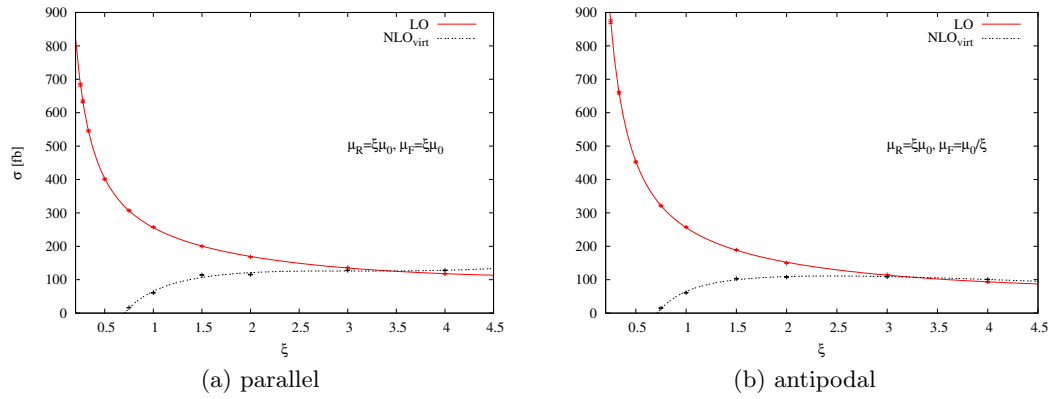


Figure 4: Scale dependence of the virtual corrections. The two plots compare the LO with the NLO result of the inclusive cross-section for different choices of the scales μ_R and μ_F . The NLO graph contains the contributions $\sigma^{\text{NLO}_{\text{virt}}} = \sigma^{\mathcal{B}} + \sigma^{\mathcal{V}} + \langle I(\varepsilon) \rangle$, where $\langle I(\varepsilon) \rangle$ is the sum of the integrated dipoles. Each data point is generated from a Monte Carlo integral over 10^5 phase-space points. In the left graph the scales have been varied in parallel, $\mu_F = \mu_R = \xi\mu_0$. The plot on the right shows the antipodal variation, $\mu_F = \mu_0/\xi$, $\mu_R = \xi\mu_0$, where μ_0 is the average p_T of the four jets.

Figure 5 shows the distribution of the transverse momentum p_T of each jet, where the jets are p_T -ordered ($p_T^{\text{1st}} \geq p_T^{\text{2nd}} \geq p_T^{\text{3rd}} \geq p_T^{\text{4th}}$). The reader be reminded that the histograms only contain a subset of the full NLO correction. The results are obtained from 10^6 phase space points and only show small fluctuations, confirming our earlier estimates of the statistical error. The distributions of the pseudorapidity η ,

$$(478) \quad \eta(\vec{p}) = -\ln \tan(\theta_p/2),$$

where θ_p is the angle between the momentum \vec{p} and the beam axis, look very similar for all four (p_T -ordered) jets. Figure 6 shows the η -distribution of the hardest jet within the applied cuts, $|\eta| < 2.5$; the interval has been divided into 100 bins.

Two important discrimination criteria between signal and background for HIGGS boson searches at the LHC in the four- b channel are the distributions of the invariant mass of the four- b and the two- b systems. The transverse mass of a particle of momentum p is $m_T^2(p) = m^2 + p_T^2$ and for a system of particles we define

$$(479) \quad m_T(bbbb) = m_T(p_1) + m_T(p_2) + m_T(p_3) + m_T(p_4),$$

$$(480) \quad m_T(bb) = m_T(p_i) + m_T(p_j), \quad i \neq j.$$

Figure 7a shows the distribution of the transverse mass for the two-jet systems, where all six possible ways of choosing i and j have been taken into account, which explains that the total cross-section is enhanced by a factor of six. In Figure 7b the transverse mass of the four-jet system, $m_T(bbbb)$ is shown. Both histograms have been produced from a sample of 10^6 phase-space points.

It should be pointed out that other observables can be obtained easily with our approach as one stores a set of weighted events both for the LO and NLO part of the amplitude. These event files are independent of the observable and have to be created only once.

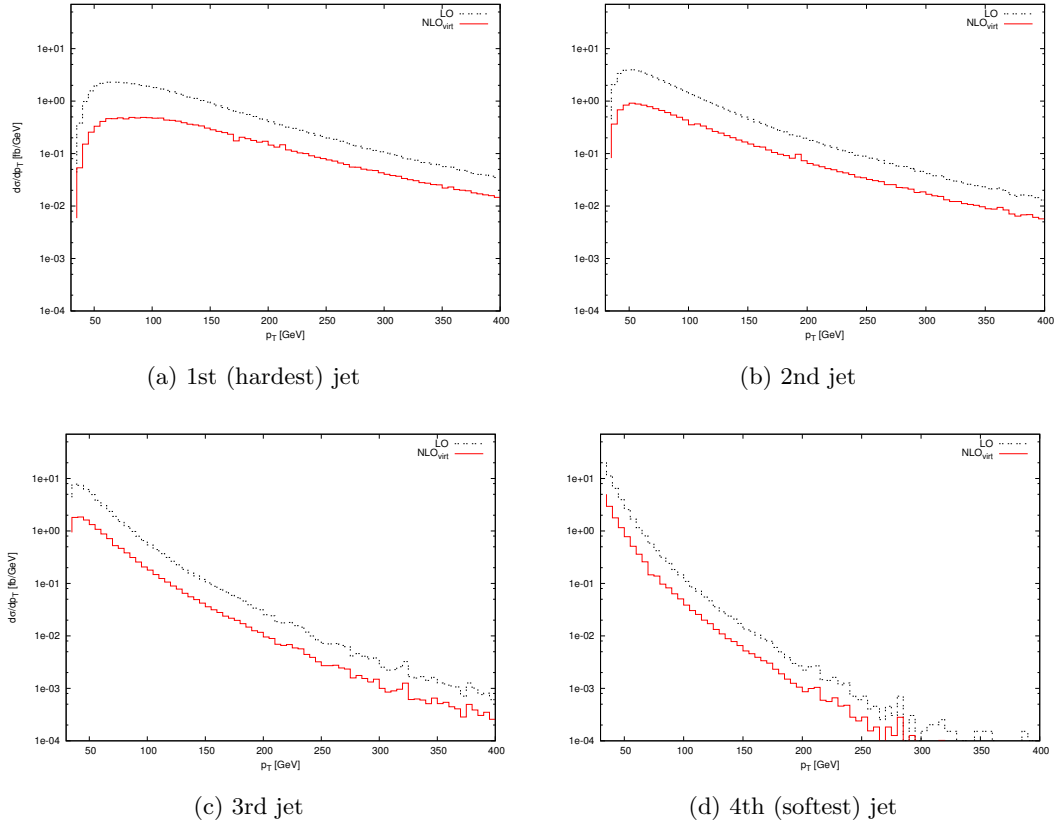


Figure 5: Transverse momentum (p_T) distributions of the four b -jets. After the jets are ordered by their p_T , the p_T values of the hardest jets, second hardest etc are distributed on the individual histograms. The distributions are based on a sample of 10^6 events and the p_T region separated into slices of 5 GeV. The curve for NLO_{virt} consists of the contributions $\sigma^{\mathcal{B}} + \sigma^{\mathcal{V}} + \langle I(\varepsilon) \rangle$.

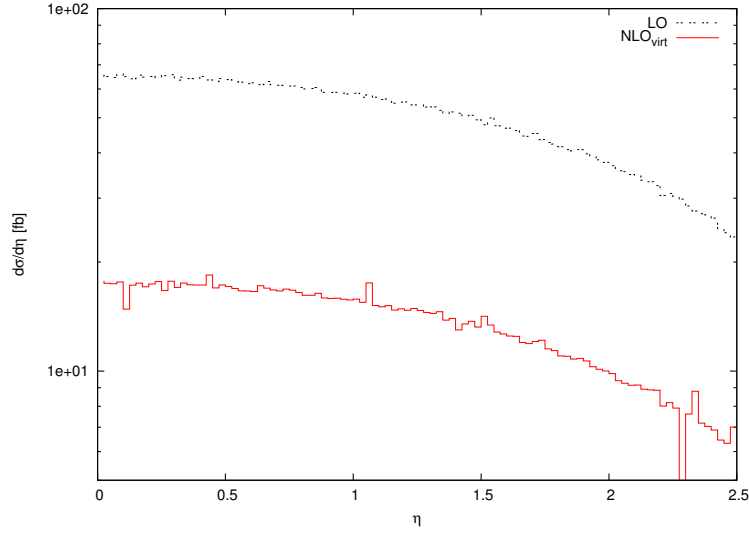


Figure 6: Rapidity distribution of the hardest of the four b -jets. This distribution has been produced from 10^6 phase-space points, where in every point the pseudorapidity η of the jet of highest p_T has been used for the histogram. The curve for NLO_{virt} consists of the contributions $\sigma^{\mathcal{B}} + \sigma^{\mathcal{V}} + \langle I(\varepsilon) \rangle$.

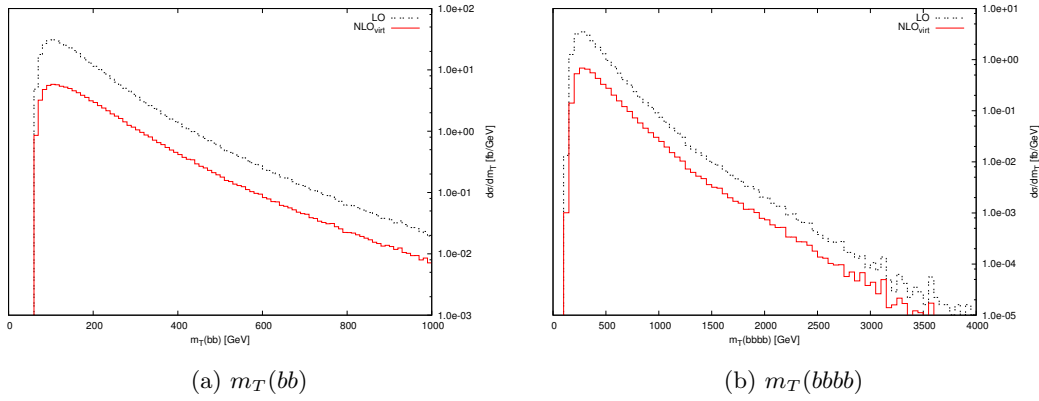


Figure 7: Invariant transverse mass m_T of the two- and four- b jet systems. Histogram (a), on the left, shows the distribution of m_T for the two-jet systems. The histogram takes into account all six possibilities of choosing a pair of b -jets, not distinguishing between b and \bar{b} . Figure (b), on the right, shows the transverse mass of the four-jet system. In both cases NLO_{virt} denotes the combination $\sigma^{\mathcal{B}} + \sigma^{\mathcal{V}} + \langle I(\varepsilon) \rangle$.

CHAPTER 5

Conclusion

*One never notices what has been done;
one can only see what remains to be done*
— MARIE CURIE

1. Summary

The LHC is of outstanding importance for the next decade of particle physics. For the first time a collider experiment can access the energies of electroweak symmetry breaking directly and thus almost certainly answer the question if the SM is an adequate description of elementary particle physics at this energy scale. The precision that will be achieved by the experiment, however, must be met by the phenomenological predictions for the SM or any model describing BSM physics and I have motivated earlier that this precision goal implies that for many processes QCD predictions must be made with at least one-loop accuracy [(NLO/ML)08].

In this work I presented and implemented an algorithm for the calculation of the virtual corrections of processes with many particles in the final state. The virtual contributions currently form the bottleneck of most cross-section calculations at NLO; while for the BORN level and the real emission contributions one can rely on automated tools, the computation of the virtual corrections very often remains highly customised and process specific. The LHC's demand for NLO predictions motivates the automation of one-loop calculations, especially for the case of QCD corrections.

As a possible solution I presented an algorithm based on the calculation of FEYNMAN diagrams in which the method of spinor helicity projections is used to obtain compact results. Different approaches for the treatment of the $SU(N)$ colour algebra have been presented and compared. For the calculation of the tensor integrals, arising from the momentum integration of a virtual particle, a reduction algorithm has been discussed which projects the integrals on to a basis of form factors, which then can be evaluated numerically [BGH⁺05, BGH⁺08]. The integration of the differential NLO cross-section has been improved by a method that avoids the destabilisation of adaptive Monte Carlo programs in their initialisation phase.

The algorithm outlined above has been implemented for massless particles and has been used to compute the virtual corrections for the process $u\bar{u} \rightarrow b\bar{b}b\bar{b}$ in the massless limit. The results indicate that our method is well suited for the computation of QCD processes with up to four final state particles at NLO.

2. Outlook

One of the disadvantages of FEYNMAN diagram based methods is the factorial growth of the number of diagrams as one increases the number of external particles in a process. This drawback is avoided by alternative constructions of QCD tree-level amplitudes [CSW04, PT86, BCF05, BCFW05] combined with the observation that one-loop amplitudes to a large extent are defined by their analytical properties [BDDK94, BDDK95], having triggered the development of *unitarity based methods* for the calculation of NLO matrix elements [B⁺08a, GZ08, OPP08].

This calculation demonstrates, however, that processes with four-particle final states can be dealt with in an efficient manner by our method and it can be anticipated that it will provide a tool for many processes becoming relevant in the near future.

In order to provide a precision prediction for the QCD corrections to $pp \rightarrow b\bar{b}b\bar{b}$ some work beyond the scope of this thesis remains to be done. The calculation of the real corrections for the process $u\bar{u} \rightarrow b\bar{b}b\bar{b}$ is currently in progress and the calculation of the amplitude $gg \rightarrow b\bar{b}b\bar{b}$ is under investigation. The modifications for the latter case turn out to be straight forward due to the genericity in the design of the implementation. An extension to massive amplitudes and non-QCD particles is currently under consideration. The extension to masses in internal propagators is relevant for many processes with vector bosons or top quarks in the final state, such as $VVb\bar{b}$, $VV + 2\text{jets}$ or $VVV + \text{jet}$, where V represents either a W^\pm or a Z boson, or, for example, $t\bar{t}b\bar{b}$ ¹ and $t\bar{t} + 2\text{jets}$. All of these processes are motivated either by SM HIGGS boson searches or BSM physics [(NLO/ML)08]; in the near future the LHC experiment will release its first results and the above cross-sections will be required as an input to the analysis of the data. Along with the LHC the particle physics community has set up a large scale computing infrastructure, the Grid [B⁺b]. The program described in Appendix E is well suited and, in fact, has been designed for a distributed computing environment like the Grid. Hence, the chosen approach has the capabilities to lead into an automatic tool for the computation of virtual corrections at one-loop, complementing existing tools for tree-level calculations.

¹The process $pp \rightarrow t\bar{t}b\bar{b}$ is currently being calculated by the authors of [BDDP08]

APPENDIX A

Distributions

I consider that I understand an equation when I can predict the properties of its solutions, without actually solving it.

— PAUL ADRIEN MAURICE DIRAC

Introduction

For a general introduction to generalised functions the reader is referred to mathematical standard text books such as [Vla02]. For this work it is sufficient to define distributions by their action on test functions under integration. Let $G(x)$ be a distribution and $f(x)$ be a smooth, continuous test function. The distribution $G(x)$ defines an integral transform

$$(481) \quad F(y) = \int_{-\infty}^{\infty} dx G(x-y) f(x)$$

for all values of y where the integral converges. In many practical applications one is only interested in the integral

$$(482) \quad F(0) = \int_{-\infty}^{\infty} dx G(x) f(x).$$

Another way of defining distributions is by a sequence of ordinary functions $G_{\epsilon}(x)$ with the property

$$(483) \quad F(y) = \lim_{\epsilon \rightarrow 0} \int_{-\infty}^{\infty} dx G_{\epsilon}(x-y) f(x) = \int_{-\infty}^{\infty} dx G(x-y) f(x).$$

1. The δ -Distribution

One of the most commonly used distributions is the δ -distribution. It is defined by

$$(484) \quad f(y) = \int_{-\infty}^{\infty} dx \delta(x-y) f(x).$$

It can be represented as the limit $\epsilon \rightarrow 0$ of the sequence of functions

$$(485) \quad \delta_{\epsilon}(x) = \frac{1}{\epsilon\sqrt{\pi}} e^{-\frac{x^2}{\epsilon^2}}$$

or by its FOURIER transform

$$(486) \quad \delta(x) = \frac{1}{2\pi} \int_{-\infty}^{\infty} dk e^{ikx}$$

A useful identity for the δ -distribution is

$$(487) \quad \delta(g(x)) = \sum_i \frac{1}{|g'(x_i)|} \delta(x - x_i),$$

where x_i are all roots of $g(x_i) = 0$.

2. The Plus Distribution

The plus distribution $(\cdot)_+$ is defined as

$$(488) \quad F = \int_0^1 dx (g(x))_+ f(x) = \int_0^1 dx (f(x)g(x) - f(1)g(x))$$

where the test function f is a regular function and g is singular at $x = 1$. Typically these singular functions are $g(x) = 1/(1-x)$ or $g(x) = \ln(1-x)/(1-x)$.

Many authors also use $g(x) = 1/x$. Then it is implied that in Equation (488) one replaces $f(1)$ by $f(0)$.

APPENDIX B

The Moore-Penrose Inverse

We in science are spoiled by the success of mathematics. Mathematics is the study of problems so simple that they have good solutions.
— WHITFIELD DIFFIE

The pseudoinverse \tilde{M} of an arbitrary, real matrix M has to satisfy¹

$$(489a) \quad M\tilde{M}M = M,$$

$$(489b) \quad \tilde{M}M\tilde{M} = \tilde{M},$$

$$(489c) \quad (\tilde{M}M)^\top = \tilde{M}M \quad \text{and}$$

$$(489d) \quad (M\tilde{M})^\top = M\tilde{M}.$$

These properties ensure the following

Theorem 5. *Let $M \in \mathbb{R}^{m \times n}$ be an arbitrary matrix and \tilde{M} its MOORE-PENROSE pseudoinverse. The linear equation $Mb = v$ has a solution, if and only if $M\tilde{M}v = v$, and the solution $b(u) = \tilde{M}v + (\mathbb{I} - \tilde{M}M)u$ is the most general solution, where $u \in \mathbb{R}^n$ is an arbitrary vector that parametrises the homogeneous part of the solution.*

It is trivially shown that the condition $M\tilde{M}v = v$ is sufficient for $b(u)$ to be a solution of the linear system. Let b' another solution to the system, i.e. $Mb' = v$; then $b' = \tilde{M}Mb' + (\mathbb{I} - \tilde{M}M)b' = \tilde{M}v + (\mathbb{I} - \tilde{M}M)b' = b(b')$. This proves the generality of $b(u)$. To prove the other direction, we assume b_0 to be a solution of the linear equation, and hence $y = Mb_0 = M\tilde{M}Mb_0 = M\tilde{M}y$, and everything is proved.

For a symmetric squared matrix $M \in \mathbb{R}^{N \times N}$ of rank r the pseudoinverse is unique, and for $r = N$ it is identical with the inverse M^{-1} . This is easily shown using that for any symmetric matrix we find an orthogonal transformation matrix U such that

$$UMU^\top = \text{diag}(\lambda_1, \dots, \lambda_r, \underbrace{0, \dots, 0}_{N-r}), \quad \lambda_i \neq 0, i \in \{1, \dots, r\}.$$

The pseudoinverse then is constructed as

$$\tilde{M} = U^\top \text{diag}(\lambda_1^{-1}, \dots, \lambda_r^{-1}, \underbrace{0, \dots, 0}_{N-r})U.$$

¹Since S is real I will use S^\top instead of S^\dagger .

APPENDIX C

Loop Integrals

The traditional mathematician recognizes and appreciates mathematical elegance when he sees it. I propose to go one step further, and to consider elegance an essential ingredient of mathematics: if it is clumsy, it is not mathematics. — EDSGER DIJKSTRA

In this appendix I describe the procedure of transforming loop integrals into FEYNMAN parameter in more detail than I did in the chapters before. This part of the calculation is also described in many textbooks about particle physics, as for example in [PS95], but some proofs that contribute to the understanding of the underlying maths are usually left out.

In the Section 1 I establish basic facts about the Γ and B -function which are essential for the introduction of FEYNMAN parameters. The basic relation is

$$(490) \quad \frac{1}{\prod_{k=1}^n A_k^{\alpha_k}} = \int_0^1 d^n z \delta_z \frac{\prod_{k=1}^n z_k^{\alpha_k-1}}{(\sum_{k=1}^n A_k z_k)^\alpha} \frac{\Gamma(\alpha)}{\prod_{k=1}^n \Gamma(\alpha_k)}$$

for general complex¹ α_k and α , where $\alpha = \sum_{k=1}^n \alpha_k$. As a direct corollary one can rewrite equation (214) for non-integer exponents. Other than most text books, which, if at all, prove Equation (490) by induction I derive this formula by showing its equivalence to SCHWINGER parameters, which are more convenient to make the connection from the axiomatic introduction of loop integrals in Section 2.

At that point one is ready to go through the remaining steps, the WICK rotation and the integration of d -dimensional spherical coordinates, the FEYNMAN parametrisation and finally the expansion in ε , which are explained in Section 3.

1. Mathematical Prerequisites

1.1. The Gamma-Function. In this chapter I follow closely chapter 11 of [BF74]. The authors give the theorems about the Γ -function in form of exercises to the reader.

The definition of $\Gamma(t)$ is given via

$$(491) \quad \Gamma(t) = \int_0^\infty x^{t-1} e^{-x} dx, \quad t > 0$$

¹In fact for $\Re(\alpha_k) > 0$

By direct calculation one finds

$$(492) \quad \Gamma(1) = 1,$$

and we will later see that this normalisation defines the Γ -function together with the two properties in the following

Lemma 1. *The Γ -function has the following two properties:*

- (1) $\Gamma(t+1) = t\Gamma(t)$ and
- (2) $\frac{d^2}{dt^2} \ln \Gamma(t) > 0$ for all $t > 0$.

The first property is shown by integration by parts of (491). The second property is equivalent to

$$(493) \quad \begin{vmatrix} \Gamma(t) & \Gamma'(t) \\ \Gamma'(t) & \Gamma''(t) \end{vmatrix} > 0.$$

This can also be interpreted as the condition that the equation

$$(494) \quad \varphi_t(\lambda) \equiv \lambda^2 \Gamma(t) + 2\lambda \Gamma'(t) + \Gamma''(t) = 0$$

has no real roots λ . We can calculate

$$(495) \quad \frac{d^n}{dt^n} \Gamma(t) = \int (\ln x)^n x^{t-1} e^{-x} dx$$

directly and hence find

$$(496) \quad \varphi_t(\lambda) = \int (\lambda + \ln x)^2 x^{t-1} e^{-x} dx > 0 \quad \forall \lambda \in \mathbb{R}. \quad \square$$

These properties allow to extend the definition of $\Gamma(t)$ to all non-integer negative values of t by the recursive definition

$$(497) \quad \Gamma(t) \equiv \frac{\Gamma(t+1)}{t}, \quad \forall t \in \mathbb{R}^- - \{0, -1, -2, \dots\}.$$

From this definition one also finds that $\Gamma(t)$ has single Poles at all negative integer numbers where the residue is

$$(498) \quad \text{Res}_{z=-n} \Gamma(z) = \frac{(-1)^n}{n!}, \quad n = 0, 1, 2, \dots$$

The following lemma prepares the theorem about the uniqueness of the Γ -function.

Lemma 2. *Let $g(t)$ be a differentiable function defined for $t > 0$ which obeys the conditions*

- (1) $g(t+1) - g(t) = \frac{1}{t}$ and
- (2) $g'(t) \geq 0$.

There is a $c \in \mathbb{R}$ such that

$$g(t) = c - \frac{1}{t} + \sum_{k=1}^{\infty} \left(\frac{1}{k} - \frac{1}{k+t} \right).$$

If one constructs the function

$$p(t) \equiv g(t) + \frac{1}{t} - \sum_{k=1}^{\infty} \left(\frac{1}{k} - \frac{1}{k+t} \right)$$

one can use condition (1) to prove that $p(t+1) = p(t)$. If $p(t)$ is not constant then there is a $t_0 \in (t; t+1)$ such that $p(t_0) \neq p(t)$, and hence either $p(t_0) - p(t)$ or $p(t+1) - p(t_0)$ must be negative. According to the mean value theorem there lies a point t_1 between t and t_0 (t_0 and $t+1$ respectively) where $(t_0 - t) \cdot p'(t_1) = p(t_0) - p(t)$ or $(t+1 - t_0) \cdot p'(t_1) = p(t+1) - p(t_0)$ respectively and hence we can find a positive number ϵ such that $p'(t_1) = -\epsilon$. Plugging in the definition of $p(t)$ one obtains

$$(499) \quad \sum_{k=0}^{\infty} \frac{1}{(k+t_1)^2} - \epsilon = g'(t_1).$$

The series $\sum (1/k^2)$ converges which means that for any given ϵ one can find an $N = N(\epsilon)$ such that

$$(500) \quad \epsilon > \sum_{k=N}^{\infty} \frac{1}{k^2} = \sum_{k=0}^{\infty} \frac{1}{(k+N)^2}.$$

Choosing $t > N$ which also means $t_1 > t > N$ one has

$$(501) \quad \sum_{k=0}^{\infty} \frac{1}{(k+t_1)^2} < \sum_{k=0}^{\infty} \frac{1}{(k+N)^2} < \epsilon \Rightarrow g'(t_1) < 0,$$

which is in contradiction to the assumptions and one must conclude that $p'(t) = 0$ for all $t > 0$, or equally $p(t) = c$. \square

Corollary 1. *Let $h(t)$ be a double-differentiable function that is defined for $t > 0$ and fulfils*

- (1) $h(t+1) - h(t) = \ln(t)$ and
- (2) $h''(t) \geq 0$.

Two functions obeying (1) and (2) differ by only a additive constant.

Clearly $h'(t) = g(t)$ conforms with the assumptions of Lemma 2 and therefore $h(t)$ must be an antiderivative of $g(t)$,

$$(502) \quad h(t) = c - Ct - \ln t - \sum_{k=1}^{\infty} \left(\ln\left(1 + \frac{t}{k}\right) - \frac{t}{k} \right),$$

however, (1) requires C to be fixed as

$$(503) \quad C = \lim_{N \rightarrow \infty} \left(\sum_{k=1}^N \frac{1}{k} - \ln N \right) \equiv \gamma_E. \square$$

Theorem 6. *Given a double differentiable function $f(t)$ that is defined for $t > 0$ and fulfils*

- (1) $f(t+1) = tf(t)$ and
 - (2) $f(t)f''(t) - (f'(t))^2 \leq 0$. Then there is a $c \in \mathbb{R}$ such that
- $$(504) \quad f(t) = c\Gamma(t).$$

The theorem is a direct consequence of the fact that both, $\ln f(t)$ and $\ln \Gamma(t)$ fulfil the assumptions of Corollary 1. Therefore

$$(505) \quad \ln f(t) = c + \ln \Gamma(t),$$

and by exponentiation everything is proved. \square

Taking the explicit form of $h(t)$ from (502), the normalisation $\Gamma(1) = 1$ leads to $\Gamma'(1) = -C = -\gamma_E$, which is usually referred to as EULER's constant. This leads to the expansion of the Γ -function for small values ε ,

$$(506) \quad \Gamma(\varepsilon) = \frac{1}{\varepsilon} \Gamma(1 + \varepsilon) = \frac{1}{\varepsilon} (\Gamma(1) + \varepsilon \Gamma'(1) + \mathcal{O}(\varepsilon^2)) = \frac{1}{\varepsilon} - \gamma_E + \mathcal{O}(\varepsilon)$$

Some integrals, however, require to take also higher order terms into account. Therefore we need the values of higher derivatives of the Gamma function, i.e. $\Gamma'(1)$, $\Gamma''(1)$ and so on. A convenient notation can be achieved by introducing the digamma and polygamma functions [EM04],

$$(507) \quad \Psi(q) = \frac{d}{dq} \ln \Gamma(q) \quad \text{and}$$

$$(508) \quad \Psi^{(m)}(q) = \frac{d^m}{dq^m} \Psi(q) \quad \text{respectively.}$$

These functions are directly related to the HURWITZ zeta function

$$(509) \quad \zeta(z, q) = \sum_{n=0}^{\infty} \frac{1}{(q+n)^z}$$

which is a generalisation of the RIEMANN zeta function

$$(510) \quad \zeta(z) = \zeta(z, 1) = \sum_{n=1}^{\infty} \frac{1}{n^z}.$$

By inductions one can show that

$$(511) \quad \left(\frac{\partial}{\partial q} \right)^m \zeta(z, q) = (-1)^m (z)_m \zeta(z + m, q)$$

with the POCHHAMMER symbol

$$(512) \quad (z)_m \equiv \frac{\Gamma(z+m)}{\Gamma(z)} = (z+m-1)(z+m-2) \cdots (z+1)z.$$

As a direct consequence for $m > 0$ one obtains

$$(513) \quad \Psi^{(m)}(q) = (-1)^{m+1} m! \zeta(m+1, q).$$

On the other hand $\Psi^{(m)}(q)$ is related to the derivatives of the Gamma function. For the first two derivatives we get

$$(514) \quad \Psi^{(1)}(q) = \frac{\Gamma'(q)}{\Gamma(q)} \quad \text{and}$$

$$(515) \quad \Psi^{(2)}(q) = \frac{\Gamma''(q)\Gamma(q) - (\Gamma'(q))^2}{(\Gamma(q))^2}.$$

Evaluating the second equation at $q = 1$ leads to

$$(516) \quad \Psi^{(2)}(1) = \zeta(2) = \frac{\pi^2}{6} = \Gamma''(1) - \gamma_E^2.$$

Therefore one can extend the expansion of the Gamma function to the required accuracy,

$$(517) \quad \Gamma(1 + \varepsilon) = 1 - \gamma_E \varepsilon + \left(\frac{\pi^2}{12} + \frac{\gamma_E^2}{2} \right) \varepsilon^2 + \mathcal{O}(\varepsilon^3)$$

1.2. The Beta-Function. The Beta function is closely related to the previously discussed Gamma function; in the literature these function often share the common notation of EULER integrals of first respective second kind. In this section I will prove the relation

$$(518) \quad B(s, t) \equiv \int_0^\infty dx \frac{x^{s-1}}{(1+x)^{s+t}} = \int_0^1 dy y^{s-1} (1-y)^{t-1} = \frac{\Gamma(s)\Gamma(t)}{\Gamma(s+t)}, \quad \text{Re}(s), \text{Re}(t) > 0.$$

We first prove

$$(519) \quad \int_0^\infty dx \frac{x^{s-1}}{(1+x)^{s+t}} = \frac{\Gamma(s)\Gamma(t)}{\Gamma(s+t)}.$$

By the substitution $y = 1/x$ one can show directly that $B(s, t) = B(t, s)$, integration by part proves $(s+t)B(s, t+1) = tB(s, t)$. With

$$(520) \quad f_s(t) \equiv B(s, t)\Gamma(s+t)$$

one can use Theorem 6 to show that $f_s(t) = g(s)\Gamma(t)$ for some function $g(s)$. To determine g we evaluate the integral

$$(521) \quad g(s) = f_s(1) = \Gamma(s+1) \int_0^\infty dx \frac{1}{(1+x)^{s+1}} = \Gamma(s).$$

Therefore we find

$$(522) \quad B(s, t) = \frac{\Gamma(s)\Gamma(t)}{\Gamma(s+t)}.$$

To show that the two integrals in (518) are the same one would carry out the substitution $y = x/(x+1)$.

1.3. Some Useful Relations. The different representations of Beta- and Gamma functions are important to establish relations for products and series of Gamma functions.

The following relations can be used for the integration of the dipoles in [CS97],

$$(523) \quad \sum_{\nu=0}^{\infty} \frac{\Gamma(a+\nu)}{\Gamma(b+\nu)} = \frac{\Gamma(b-a-1)\Gamma(a)}{\Gamma(b-a)\Gamma(b-1)}.$$

The proof is as follows:

$$\begin{aligned}
 (524) \quad \sum_{\nu=0}^{\infty} \frac{\Gamma(a+\nu)}{\Gamma(b+\nu)} &= \frac{1}{\Gamma(b-a)} \sum_{\nu=0}^{\infty} B(a+\nu, b-a) = \\
 &= \frac{1}{\Gamma(b-a)} \sum_{\nu=0}^{\infty} \int_0^1 dt t^{a-1+\nu} (1-t)^{b-a-1} = \\
 &= \frac{1}{\Gamma(b-a)} \int_0^1 dt t^{a-1} (1-t)^{b-a-1} \sum_{\nu=0}^{\infty} t^{\nu} = \\
 &= \frac{1}{\Gamma(b-a)} \int_0^1 dt t^{a-1} \frac{(1-t)^{b-a-1}}{(1-t)} = \frac{B(a, b-a-1)}{\Gamma(b-a)}.
 \end{aligned}$$

As an example this can be applied to the integral

$$\begin{aligned}
 &\int_0^1 dz z^{-\varepsilon} (1-z)^{-\varepsilon} \int_0^1 dy y^{-1-\varepsilon} (1-y)^{1-2\varepsilon} \frac{2}{1-z(1-y)} = \\
 &= 2 \int_0^1 dz z^{-\varepsilon} (1-z)^{-\varepsilon} \int_0^1 dy y^{-1-\varepsilon} (1-y)^{1-2\varepsilon} \sum_{\nu=0}^{\infty} z^{\nu} (1-y)^{\nu} = \\
 &= 2 \sum_{\nu=0}^{\infty} B(1-\varepsilon+\nu, 1-\varepsilon) B(2-2\varepsilon+\nu, -\varepsilon) = \\
 &= 2 \sum_{\nu=0}^{\infty} \frac{\Gamma(1-\varepsilon+\nu)\Gamma(1-\varepsilon)}{\Gamma(2-2\varepsilon+\nu)} \frac{\Gamma(2-2\varepsilon+\nu)\Gamma(-\varepsilon)}{\Gamma(2-3\varepsilon+\nu)} = \\
 &= 2\Gamma(-\varepsilon)\Gamma(1-\varepsilon) \sum_{\nu=0}^{\infty} \frac{\Gamma(1-\varepsilon+\nu)}{\Gamma(2-3\varepsilon+\nu)} = \\
 &= 2\Gamma(-\varepsilon)\Gamma(1-\varepsilon) \frac{\Gamma(1-\varepsilon)\Gamma(-2\varepsilon)}{\Gamma(1-2\varepsilon)\Gamma(1-3\varepsilon)} = \\
 &= 2B(1-\varepsilon, -2\varepsilon)B(1-\varepsilon, -\varepsilon).
 \end{aligned}$$

2. An Axiomatic Approach

The introduction of dimensional regularisation arises from the observation that many of the loop integrals that diverge in four dimensions become convergent in a space with other than four dimensions. To take a smooth limit to four dimensions, starting from a dimensionality where the integral is well behaved, involves the concept of non-integer dimensions: The dimension is defined to be a complex parameter d , and the divergence of the integral shows up in poles for certain integer values of d , as we will see later. However, an integral in non-integer dimensions can only be defined on an infinite dimensional vector space; It is the definition of the integral that carries the parameter d , not the space it acts on. To make sure we get the right results back in four dimensions we require the integration to have certain properties. [Wil73]

Given a linear space V with a HERMITIAN form $p \cdot q \in \mathbb{R}$ for all $p, q \in V$ such that the four dimensional MINKOWSKI space \mathcal{M} is a subspace of V and the dot-product on \mathcal{M}

is the restriction of \cdot on \mathcal{M} . For any complex d we introduce the functional

$$(525) \quad \int_{k \in V} d^d_k f(k)$$

on LORENTZ covariant functions $f : V \rightarrow \mathbb{C}$, i.e. $f(k) = \tilde{f}(k^2, k \cdot q_1, k \cdot q_2, \dots, k \cdot q_N)$ where $k, q_1, \dots, q_N \in V$. The following properties uniquely define the integration

Linearity: For any two complex numbers a and b and functions f and g

$$\int_{k \in V} d^d_k (af(k) + bg(k)) = a \int_{k \in V} d^d_k f(k) + b \int_{k \in V} d^d_k g(k),$$

Translation Invariance: For any vector $q \in V$

$$\int_{k \in V} d^d_k f(k + q) = \int_{k \in V} d^d_k f(k),$$

Scaling: For any complex number s

$$\int_{k \in V} d^d_k f(sk) = s^{-d} \int_{k \in V} d^d_k f(k),$$

Normalisation:

$$\int_{k \in V} d^d_k e^{-k^2} = \pi^{d/2}.$$

To prove this one can use a generating function $f(k) = e^{-sk^2 + k \cdot p}$ for a complex parameter s and a vector $p \in V$. We can solve the integral over f by just using the above conditions:

$$(527) \quad \begin{aligned} \int_{k \in V} d^d_k e^{-sk^2 + k \cdot p} &= \int_{k \in V} d^d_k e^{-s(k - p/(2s))^2 - p^2/(4s^2)} = \\ &= \int_{k \in V} d^d_k e^{-s(k - p/(2s))^2 - p^2/(4s)} = s^{-d} e^{-p^2/(4s)} \int_{k \in V} d^d_k e^{-k^2} = s^{-d} e^{-p^2/(4s)} \pi^{d/2}. \end{aligned}$$

To be formally correct one had to show that this $f(k)$ indeed generates all functions one wants to address. Apparently one can generate all functions that have power series expansions in k^2 and $k \cdot p_i$. We can set $p = \sum_i 1^n s_i p_i$ to find

$$(528) \quad (k^2)^j = \left(-\frac{\partial}{\partial s} \right)^j e^{-sk^2 + s_1 k \cdot p_1 + s_2 k \cdot p_2 + \dots s_n k \cdot p_n} \Big|_{s, s_1, \dots, s_n=0} \quad \text{and}$$

$$(529) \quad (k \cdot p_l)^j = \left(\frac{\partial}{\partial s_l} \right)^j e^{-sk^2 + s_1 k \cdot p_1 + s_2 k \cdot p_2 + \dots s_n k \cdot p_n} \Big|_{s, s_1, \dots, s_n=0}.$$

In loop calculation we have to deal with functions that arise from products of propagators,

$$(530) \quad \frac{1}{A_1^{\alpha_1} A_2^{\alpha_2} \dots A_N^{\alpha_N}},$$

where A_j is of the form $A_j = [(k + r_j)^2 - m_j^2 + i\delta]$ and $\Re(\alpha_j) > 0$ for all $j \in \{1 \dots N\}$. SCHWINGER noticed that one can achieve the above exponential form by introducing an extra parameter for each propagator,

$$(531) \quad \frac{1}{A_j^{\alpha_j}} = \frac{1}{\Gamma(\alpha_j)} \int_0^\infty dt_j t_j^{\alpha_j-1} e^{-t_j A_j},$$

where the condition $\Re(A_j) > 0$ must hold². Finally, for expression (530) one can write

$$(532) \quad \frac{1}{A_1^{\alpha_1} A_2^{\alpha_2} \cdots A_N^{\alpha_N}} = \frac{1}{\Gamma(\alpha_1) \cdots \Gamma(\alpha_N)} \int_0^\infty \left(\prod_{j=1}^N dt_j t_j^{\alpha_j-1} \right) e^{-\sum_{\nu=1}^N t_\nu A_\nu}$$

2.1. Feynman Parameters. Although the SCHWINGER parametrisation is well suited to show the soundness of dimensional regularisation and the existence of the loop integrals in a mathematical sense, for actual loop calculations very often another parametrisation is more convenient.

In this section I introduce FEYNMAN parameters starting from Equation (532) and hence I show both the equivalence of both parametrisation and the validity of Equation (490).

One can introduce a new parameter $t = \sum_{j=1}^N t_j$ and substitute $t_j = tz_j$ in (532),

$$(533) \quad \frac{\Gamma(\alpha_1)\Gamma(\alpha_2)\cdots\Gamma(\alpha_N)}{A_1^{\alpha_1}A_2^{\alpha_2}\cdots A_N^{\alpha_N}} = \int_0^\infty dt t^\alpha \int_0^\infty \left(\prod_{j=1}^N dz_j z_j^{\alpha_j-1} \right) t^{\alpha-n} e^{-t \sum_{\nu=1}^N z_\nu A_\nu} \delta\left(t - t \sum_{\nu=1}^N z_\nu\right),$$

where $\alpha = \sum_{j=1}^N \alpha_j$. Using the homogeneity of the δ -function we can now carry out the t -integration by reversing SCHWINGER's trick (531),

$$(534) \quad \int_0^\infty dt t^{\alpha-1} \int_0^\infty \left(\prod_{j=1}^N dz_j z_j^{\alpha_j-1} \right) e^{-t \sum_{\nu=1}^N z_\nu A_\nu} \delta\left(1 - \sum_{\nu=1}^N z_\nu\right) = \Gamma(\alpha) \int_0^\infty dz_1 \cdots dz_N \delta\left(1 - \sum_{j=1}^N z_j\right) \frac{\prod_{j=1}^N z_j^{\alpha_j-1}}{\left(\sum_{j=1}^N z_j A_j\right)^\alpha}.$$

With the earlier definitions (206b) and (206c) the FEYNMAN parameters are

$$(535) \quad \frac{1}{\prod_{j=1}^N A_j^{\alpha_j}} = \frac{\Gamma(\alpha)}{\prod_{j=1}^N \Gamma(\alpha_j)} \int_0^1 d^N z \delta_z \frac{\prod_{j=1}^N z_j^{\alpha_j-1}}{\left(\sum_{j=1}^N z_j A_j\right)^\alpha}.$$

3. Evaluation of Loop Integrals

In the following section I show the omitted steps which are necessary to solve integrals (204). As a first step in Chapter 3, Section 1.4 we introduced a FEYNMAN parametrisation by using (490) with $A_j = (q_j^2 - m_j^2 + i\delta)$ and their exponents being 1, which finally led to (207). It was shown that the tensor structure $\hat{k}^\mu \hat{k}^\nu \dots$ always leads

²To formally achieve this for propagators $[(k+p)^2 - m^2 + i\delta]$ one can carry out a WICK rotation first to ensure $(k+p)^2 \geq 0$ and do the rest of the calculation for $m^2 < 0$. Analytically continuation allows to get a result for real masses after the integration has been carried out.

to a factor $(\hat{k}^2)^l$ in the numerator for some positive, integer l . The integral we started from hence is split up into a sum of integrals of the form

$$(536) \quad I_N^{d,\alpha,l}(l_1, \dots, l_N; S) = \Gamma(N) \int_0^N dz \delta_z \int \frac{d^4 \hat{k}}{i\pi^2} \frac{d^{d-4} \bar{k}}{\pi^{d/2-2}} \frac{(\bar{k}^2)^\alpha (\hat{k}^2)^l \prod_{\nu=1}^N z_\nu^{l_\nu}}{\left[\hat{k}^2 + \bar{k}^2 + \frac{1}{2} z^\top S z + i\delta \right]^N}$$

To carry out any further integration steps it is much easier to analytically continue the integral to EUCLIDEAN space. This can be achieved by what is known as a WICK rotation: The variable \hat{k}_0 can be extended from the real axis into the complex plane, and the integration contour can be closed at infinity in the first and third quadrant following the imaginary axis in between (see fig. 1). Since the poles of the integrand lie in the other quadrants, the integral over the closed contour has to vanish. The curved pieces of the contour do not contribute and hence we can replace the integration over the real axis by the integration over the imaginary axis, which after substituting $ik_0 = K_0$

$$(537) \quad \int_{-\infty}^{\infty} d\hat{k}_0 f(k_0^2 - \vec{k}^2) = - \int_{i\infty}^{-i\infty} d\hat{k}_0 f(k_0^2 - \vec{k}^2) = i \int_{-\infty}^{\infty} dK_0 f(-K_0^2 - \vec{k}^2)$$

can be reinterpreted as an integration over one component of a vector $K = (K_0, \vec{k})$ in a EUCLIDEAN vector space with a positive definite inner product.

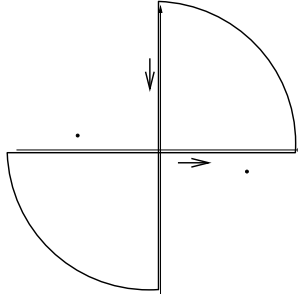


Figure 1: The integration contour in the complex \hat{k}^0 -plane that is used for the WICK rotation. The poles of the propagators, which lie outside the enclosed region, are indicated by dots.

After this step the integral has the form³

$$(538) \quad I_N^{d,\alpha,l}(l_1, \dots, l_N; S) = (-1)^{N+\alpha+l} \Gamma(N) \int_0^N dz \delta_z \int \frac{d^4 K}{\pi^2} \frac{d^{d-4} \bar{k}}{\pi^{d/2-2}} \frac{(K^2)^\alpha |\hat{k}^2|^l \prod_{\nu=1}^N z_\nu^{l_\nu}}{\left[K^2 + |\bar{k}^2| - \frac{1}{2} z^\top S z - i\delta \right]^N}$$

For both parts of the momentum integral the integration can be done in spherical coordinates. Here we use the axiom that the angular integration in d dimensions is the surface of the d -dimensional unit sphere,

$$(539) \quad \Omega_d = \frac{2\pi^{d/2}}{\Gamma(d/2)},$$

³Note that the notation earlier has been defined such that \bar{k}^2 is negative.

and hence we get

$$(540) \quad I_N^{d,\alpha,l}(l_1, \dots, l_N; S) = (-1)^{N+\alpha+l} \frac{4\Gamma(N)}{\Gamma(d/2-2)} \int_0^1 d^N z \delta_z \int_0^\infty \int_0^\infty d\kappa d\rho \, \kappa^3 \rho^{d-5} \frac{\rho^{2\alpha} \kappa^{2l} \prod_{\nu=1}^N z_\nu^{l_\nu}}{[\kappa^2 + \rho^2 - \frac{1}{2} z^\top S z - i\delta]^N}$$

The integrals over κ and ρ can be identified as Beta functions (see (518)) and hence we obtain the desired form of the integral,

$$(541) \quad I_N^{d,\alpha,l}(l_1, \dots, l_N; S) = (-1)^{N+\alpha+l} \Gamma(l+2) \frac{\Gamma(\frac{d}{2}-2+\alpha)}{\Gamma(\frac{d}{2}-2)} \Gamma(N - \frac{d}{2} - l - \alpha) \int_0^1 d^N z \delta_z \frac{\prod_{\nu=1}^N z_\nu^{l_\nu}}{[-\frac{1}{2} z^\top S z - i\delta]^{N-d/2-l-\alpha}},$$

which then can be reinterpreted as

$$(542) \quad I_N^{d,\alpha,l}(S; l_1, \dots, l_N) = (-1)^{\alpha+l} \frac{\Gamma(l+2)}{\Gamma(2)} \frac{\Gamma(\frac{d}{2}-2+\alpha)}{\Gamma(\frac{d}{2}-2)} I_N^{d+2\alpha+2l}(l_1, \dots, l_N; S),$$

where

$$(543) \quad I_N^d(l_1, \dots, l_N; S) = (-1)^N \Gamma(N - \frac{d}{2}) \int_0^1 d^N z \delta_z \frac{\prod_{\nu=1}^N z_\nu^{l_\nu}}{[-\frac{1}{2} z^\top S z - i\delta]^{N-d/2}}.$$

APPENDIX D

Integral Tables

Consider the postage stamp, its usefulness consists in the ability to stick to one thing till it gets there. — JOHN BILLINGS

1. Conventions

There is a set of conventions in the notation of loop integrals due to the fact, that many factors are common to most elementary integrals. One ubiquitous factor is

$$(544) \quad r_\Gamma \equiv \frac{\Gamma(1+\varepsilon)\Gamma(1-\varepsilon)^2}{\Gamma(1-2\varepsilon)}.$$

The expansion of r_Γ is

$$(545) \quad r_\Gamma = 1 - \gamma_E \varepsilon + \left(\frac{\gamma_E^2}{2} - \frac{\pi^2}{12} \right) \varepsilon^2 + \mathcal{O}(\varepsilon^3),$$

where $\gamma_E = -\Gamma'(1)$. Together with¹

$$(546) \quad (4\pi\mu^2)^{2-n/2} = (\mu^2)^\varepsilon (1 + \varepsilon \ln(4\pi) + \mathcal{O}(\varepsilon^2))$$

this factor constitutes the UV subtraction $\Delta \equiv 1/\varepsilon - \gamma_E + \ln(4\pi)$ in the $\overline{\text{MS}}$ scheme,

$$(547) \quad (4\pi\mu^2)^\varepsilon \frac{r_\Gamma}{\varepsilon} = (\mu^2)^\varepsilon (\Delta + \mathcal{O}(\varepsilon))$$

The factor of $(\mu^2)^\varepsilon$ fixes the dimension of expressions of the form

$$(548) \quad \ln(-s - i\delta) \equiv \ln\left(\frac{-s - i\delta}{\mu^2}\right).$$

For double poles it is convenient to also pull out a factor of $e^{-\varepsilon\gamma_E}$ which then allows for the simple result

$$(549) \quad \frac{r_\Gamma}{\varepsilon^2} = e^{-\varepsilon\gamma_E} \left(\frac{1}{\varepsilon^2} - \frac{\pi^2}{12} + \mathcal{O}(\varepsilon) \right).$$

¹See Section 1.4

In many cases it is convenient to express the loop integrals in terms of the functions (see [BGH⁺05])

$$(550a) \quad H_0(x, \alpha) = \frac{(-x - i\delta)^\alpha}{(\mu^2)^{-\varepsilon} x},$$

$$(550b) \quad H_1(x, y, \alpha) = \frac{1}{(x - y)} \left(x H_0(x, \alpha) - \frac{\alpha}{0 + \alpha} y H_0(y, \alpha) \right) \quad \text{and}$$

$$(550c) \quad H_{N+1}(x, y, \alpha) = \frac{1}{(x - y)} \left(\frac{N}{N + \alpha} x H_N(x, y, \alpha) - \frac{\alpha}{N + \alpha} y H_0(y, \alpha) \right), \quad N > 1.$$

Using the fact that

$$(551) \quad r_\Gamma = \frac{1}{\Gamma(1 - \varepsilon)} (1 + \mathcal{O}(\varepsilon^3))$$

the epsilon expansions of simple cross-section in QCD are very often found in a form like

$$(552) \quad \frac{C_{F\alpha_s}}{2\pi} \left(\frac{4\pi\mu^2}{Q^2} \right)^\varepsilon \frac{1}{\Gamma(1 - \varepsilon)} \left(\frac{A}{\varepsilon^2} + \frac{B}{\varepsilon} + C + D\pi^2 + \mathcal{O}(\varepsilon) \right) \dots,$$

where A , B , C and D are complex numbers.

2. Relations for One- and Two-Point Functions

The scalar tadpole function can be evaluated directly,

$$(553) \quad I_1^n(m^2) = m^2(m^2 - i\delta)^{-\varepsilon} \frac{1}{\varepsilon} \frac{1}{1 - \varepsilon} \Gamma(1 + \varepsilon) = m^2 [\Delta - \ln(m^2 - i\delta) - 1] + \mathcal{O}(\varepsilon)$$

The scalar two-point function in n dimensions can be expressed as

$$(554) \quad I_2^n(S) = I_2^n(s; m_1^2, m_2^2) = \Delta - \int_0^1 dz \ln(-sz(1 - z) + m_1^2 z + m_2^2(1 - z) - i\delta) + \mathcal{O}(\varepsilon).$$

all other one- and two-point functions can be expressed in terms of that function. The underlying S -matrix for $N = 2$ is parametrised as

$$(555) \quad S = \begin{pmatrix} -2m_1^2 & s - m_1^2 - m_2^2 \\ s - m_1^2 - m_2^2 & -2m_2^2 \end{pmatrix}.$$

For the one-point functions $I_1^d(m^2)$ the underlying S -matrix is $S = (-2m^2)$.

$$(556a) \quad I_2^n(l_0, l_1; S) = -S_{l_0 l_1}^{-1} I_2^{n+2}(S) - b_{l_0} I_2^{n+2}(l_1; S) + \sum_{k \in S_\#} S_{l_0 k}^{-1} I_1^{n+2}(S^{\{k\}})$$

$$(556b) \quad I_2^{n+2}(l_0; S) = \frac{b_{l_0}}{B} I_2^{n+2}(S) + \sum_{k \in S_\#} \left(S_{l_0 k}^{-1} - \frac{b_{l_0} b_k}{B} \right) I_1^{n+2}(S^{\{k\}})$$

$$(556c) \quad I_2^n(l_0; S) = \frac{b_{l_0}}{B} I_2^n(S) + \sum_{k \in S_\#} \left(S_{l_0 k}^{-1} - \frac{b_{l_0} b_k}{B} \right) I_1^n(S^{\{k\}})$$

$$(556d) \quad I_2^{n+2}(S) = \frac{1}{B(n-1)} \left[I_2^n(S) - \sum_{k \in S_\#} b_k I_1^n(S^{\{k\}}) \right]$$

$$(556e) \quad I_1^{n+2}(m^2) = \frac{m^4}{4} \left(I_2^n(0; 0, m^2) + \frac{1}{2} \right)$$

$$(556f) \quad I_1^n(m^2) = m^2 I_2^n(0; 0, m^2)$$

3. Massless Two- and Three-Point Integrals

The easiest case is given when all propagators are massless because then the S -matrix takes a very simple form. The massless tadpole vanishes identically in dimensional regularisation. The S -matrix is

$$(557) \quad S = \begin{pmatrix} 0 & s \\ s & 0 \end{pmatrix},$$

and the two-point integral reads as follows,

$$(558) \quad I_2^d(S) = \Gamma(2 - d/2) \int_0^1 dz [(-s - i\delta)z(1 - z)]^{d/2-2} = \Gamma(2 - d/2) \frac{\Gamma(d/2 - 1)^2}{\Gamma(d - 2)} s H_0(s, d/2 - 2),$$

which in the case $d = n = 4 - 2\varepsilon$ becomes

$$(559) \quad I_2^n(S) = \frac{r_\Gamma}{\varepsilon} \frac{1}{(1 - 2\varepsilon)} s H_0(s, -\varepsilon).$$

Hence, the expansion of $I_2^n(S)$ is

$$(560) \quad I_2^n(S) = \Delta - \ln(-s - i\delta) + 2 + \mathcal{O}(\varepsilon).$$

Similarly the other relevant two-point integrals are calculated,

$$(561) \quad I_2^{n+2}(S) = -\frac{r_\Gamma}{\varepsilon} \frac{1-\varepsilon}{(1-2\varepsilon)_3} s H_0(s, 1-\varepsilon) = \frac{s}{2(3-2\varepsilon)} I_2^n(S),$$

$$(562) \quad I_2^n(l; S) = \frac{r_\Gamma}{\varepsilon} \frac{1}{2(1-2\varepsilon)} s H_0(s, -\varepsilon) = \frac{1}{2} I_2^n(S),$$

$$(563) \quad I_2^n(l, l; S) = -\frac{r_\Gamma}{\varepsilon^2} \frac{2-\varepsilon}{2(3-2\varepsilon)(1-2\varepsilon)} s H_0(s, -\varepsilon) = \frac{2-\varepsilon}{2(3-2\varepsilon)} I_2^n(S),$$

$$(564) \quad I_2^n(1, 2; S) = \frac{r_\Gamma}{\varepsilon} \frac{(1-\varepsilon)^2}{(1-2\varepsilon)_3} s H_0(s, -\varepsilon) = \frac{1-\varepsilon}{2(3-2\varepsilon)} I_2^n(S),$$

$$(565) \quad I_2^{n+1}(S) = \varepsilon I_2^{n+2}(S) = \frac{s}{6} + \mathcal{O}(\varepsilon).$$

For the case of three-point function one has to distinguish the cases when $\det S$ vanishes, i.e. if one or two scales vanish. Explicit formulæ are given for the case when for

$$(566) \quad S = \begin{pmatrix} 0 & s & u \\ s & 0 & t \\ u & t & 0 \end{pmatrix}$$

one or two of the variables vanish. Below I restrict to the cases $u = 0$ and $t = u = 0$. For all three variables non-vanishing the usual reduction formula applies.

$$(567) \quad I_3^n(S_{t=u=0}) = \frac{r_\Gamma}{\varepsilon^2} H_0(s, -\varepsilon)$$

$$(568) \quad I_3^n(1; S_{t=u=0}) = I_3^n(2; S_{t=u=0}) = -\frac{r_\Gamma}{\varepsilon} \frac{1}{1-2\varepsilon} H_0(s, -\varepsilon)$$

$$(569) \quad I_3^n(3; S_{t=u=0}) = \frac{r_\Gamma}{\varepsilon^2} \frac{1}{1-2\varepsilon} H_0(s, -\varepsilon)$$

$$(570) \quad I_3^n(1, 1; S_{t=u=0}) = I_3^n(2, 2; t = u = 0) = -\frac{r_\Gamma}{\varepsilon} \frac{1}{2(1-2\varepsilon)} H_0(s, -\varepsilon)$$

$$(571) \quad I_3^n(1, 2; S_{t=u=0}) = I_3^n(2, 2; t = u = 0) = r_\Gamma \frac{1}{2(1-\varepsilon)(1-2\varepsilon)} H_0(s, -\varepsilon)$$

$$(572) \quad I_3^{n+2}(S_{t=u=0}) = \frac{r_\Gamma}{\varepsilon} \frac{1}{2(1-\varepsilon)(1-2\varepsilon)} H_0(s, 1-\varepsilon)$$

A full list of the three-point functions which are used in our tensor reduction for massless internal propagators are in [BGH⁺05]. A more general review on one-loop integrals with a compilation of the relevant formulæ can be found in [EZ08].

4. Polynomial Loop Integrals

In this appendix I present explicit expressions for the integrals of type,

$$(573) \quad \varepsilon I_N^{n-4+2N}(l_1, \dots, l_r; S) = (-1)^N P_N(l_1, \dots, l_r),$$

$$(574) \quad \varepsilon I_N^{n-4+2(N+1)}(l_1, \dots, l_r; S) = \frac{(-1)^N}{2} \sum_{j_1, j_2=1}^N S_{j_1 j_2} P_N(j_1, j_2, l_1, \dots, l_r),$$

which are introduced in section 1.5. The list includes those integrals that can arise in calculations using FEYNMAN gauge. Formula for $\eta > 1$ and larger numbers of FEYNMAN

parameters in the numerator can be derived using (220). Unless stated differently, all expressions are given up to order $\mathcal{O}(\varepsilon)$.

$$(575a) \quad \varepsilon I_N^{n-4+2N}(S) = \frac{(-1)^N}{(N-1)!}$$

$$(575b) \quad \varepsilon I_N^{n-4+2N}(l_1; S) = \frac{(-1)^N}{N!}$$

$$(575c) \quad \varepsilon I_N^{n-4+2N}(l_1, l_2; S) = \frac{(-1)^N}{(N+1)!} (1 + \delta_{l_1 l_2})$$

$$(575d) \quad \varepsilon I_N^{n-4+2N}(l_1, l_2, l_3; S) = \frac{(-1)^N}{(N+2)!} \\ \times (1 + \delta_{l_1 l_2} + \delta_{l_1 l_3} + \delta_{l_2 l_3} + 2\delta_{l_1 l_2} \delta_{l_2 l_3})$$

$$(575e) \quad \varepsilon I_N^{n-4+2N}(l_1, l_2, l_3, l_4; S) = \frac{(-1)^N}{(N+3)!} \\ \times (\delta_{l_1 l_2} (6\delta_{l_1 l_3} \delta_{l_2 l_4} + 2\delta_{l_1 l_3} + 2\delta_{l_2 l_4} + \delta_{l_3 l_4}) \\ + 2\delta_{l_3 l_4} (\delta_{l_1 l_3} + \delta_{l_2 l_4}) + \delta_{l_1 l_3} \delta_{l_2 l_4} + \delta_{l_1 l_4} \delta_{l_2 l_3} \\ + \delta_{l_1 l_2} + \delta_{l_1 l_3} + \delta_{l_1 l_4} + \delta_{l_2 l_3} + \delta_{l_2 l_4} + \delta_{l_3 l_4} + 1)$$

$$(575f) \quad \varepsilon I_N^{n-4+2(N+1)}(S) = \frac{(-1)^N}{2(N+1)!} \left(\sum_{j_1, j_2=1}^N S_{j_1 j_2} + \text{tr}\{S\} \right)$$

$$(575g) \quad \varepsilon I_N^{n-4+2(N+1)}(l_1; S) = \frac{(-1)^N}{2(N+2)!} \sum_{j_1, j_2=1}^N S_{j_1 j_2} (1 + \delta_{j_1 j_2}) \\ \times (1 + \delta_{l_1 j_1} + \delta_{l_1 j_2})$$

$$(575h) \quad \varepsilon I_N^{n-4+2(N+1)}(l_1, l_2; S) = \frac{(-1)^N}{2(N+3)!} \sum_{j_1, j_2=1}^N S_{j_1 j_2} \\ \times (\delta_{j_1 j_2} (6\delta_{j_1 l_1} \delta_{j_2 l_2} + 2\delta_{j_1 l_1} + 2\delta_{j_2 l_2} + \delta_{l_1 l_2}) \\ + 2\delta_{l_1 l_2} (\delta_{j_1 l_1} + \delta_{j_2 l_2}) + \delta_{j_1 l_1} \delta_{j_2 l_2} + \delta_{j_1 l_2} \delta_{j_2 l_1} \\ + \delta_{j_1 j_2} + \delta_{j_1 l_1} + \delta_{j_1 l_2} + \delta_{j_2 l_1} + \delta_{j_2 l_2} + \delta_{l_1 l_2} + 1)$$

The corresponding integrals in n dimensions are, by applying (209):

$$(576a) \quad I_N^{n, N-2}(S) = -\frac{1}{(N-1)(N-2)}$$

$$(576b) \quad I_N^{n, N-1}(S) = \frac{1}{2(N+1)N(N-1)} \left(\sum_{j_1, j_2=1}^N S_{j_1 j_2} + \text{tr}\{S\} \right)$$

$$(576c) \quad I_2^{n, 1}(S) = \frac{1}{12} (2\Delta_{12}^2 - 6(m_1^2 + m_2^2))$$

$$(576d) \quad \varepsilon I_2^n(S) = 1$$

$$(576e) \quad \varepsilon I_1^n(S) = -\frac{1}{2} S_{11}$$

$$(576f) \quad I_N^{n,N-2;\mu}(a; S) = \frac{1}{N(N-1)(N-2)} \sum_{j=1}^N \Delta_{ja}^\mu$$

$$(576g) \quad I_N^{n,N-1;\mu}(a; S) = -\frac{(N-2)!}{2(N+2)!} \sum_{j=1}^N \Delta_{ja}^\mu \\ \times \left(\sum_{j_1, j_2=1}^N S_{j_1 j_2} + \text{tr}\{S\} + 2 \sum_{l=1}^N S_{jl} + S_{jj} \right)$$

$$(576h) \quad \varepsilon I_2^{n;\mu}(a; S) = -\frac{1}{2} \sum_{j=1}^N \Delta_{ja}^\mu$$

$$(576i) \quad \varepsilon I_3^{n;\mu\nu}(a_1, a_2; S) = \frac{g^{\mu\nu}}{4}$$

$$(576j) \quad I_4^{n,1;\mu\nu}(a_1, a_2; S) = -\frac{1}{12} g^{\mu\nu}$$

APPENDIX E

Implementation of Amplitude Computations

The practical scientist is trying to solve tomorrow's problem with yesterday's computer; the computer scientist, we think, often has it the other way around.
— PRESS ET AL.^a

^aNumerical Recipes in C, 1992

Introduction

This chapter describes the implementation of cross-section calculations based on the strategy explained in the main part of this thesis. This code has been successfully tested for the $u\bar{u} \rightarrow b\bar{b}b\bar{b}$ amplitude, results of which are presented in 4.

One of the main technical challenges of an amplitude calculation in QCD at NLO precision is the computation of the virtual corrections due to the number of terms involved during the reduction of the diagrams. The size of the expressions makes the calculation computationally expensive already prior to the numerical evaluation and gives rise to a high consumption of resources, not only with respect to computing time but also memory allocation in order to store intermediate results. This high demand also addresses the software used for the computation as most of the standard software like computer algebra systems and compilers are not prepared to handle huge amounts of data. An implementation of a NLO calculation with many external particles therefore has to address the resource usage under different viewpoints. From the theoretical, mathematical side one has to choose a representation of the expression that avoids producing unnecessarily large amounts of terms. As a more technical issue one has to provide means to make the required computing resources accessible; this includes the choice of software capable of dealing with large amounts of data on the one hand and parallel and distributed computing techniques on the other hand.

Furthermore, general software design goals must be borne in mind [Bug94]. Two of the major aims for my project are *reusability* and *extensibility*; the importance of these design attributes can be seen from decomposing the process of matrix element evaluations. The major part of a calculation is process independent, like the evaluation of colour and DIRAC traces or the reduction and evaluation of FEYNMAN parameter integrals. Process and model dependencies only enter through few parameters like the number of ingoing and outgoing particles together with their masses, through the FEYNMAN rules and in the graph generation. These dependencies can be separated through *modularity* from an invariant, reusable application core which can serve as a general purpose tool. Once these criteria are met one is in the position to release

the code to a broader public. However, this step involves the necessity of *usability*, *maintainability* and *portability*. Although from a first look it seems as if these design metrics have to be considered only on a very late stage of the development process, it should be clear that their early disesteem most likely entails rewriting large parts of the code.

Literate Programming. Literate programming has been developed by KNUTH in the 1980s [Knu84, Knu92]. This concept describes the combination of computer programs and type setting in a way that from a common source both, a compilable program and a high quality document can be obtained. Rather than decorating a source code with comments literate programming understands a program as part of the document that describes the program. A computer program is organised in little chunks of which the order in the document does not necessarily correspond to the order in the final program code.

The original version of WEB implemented two tool, **weave** translates the WEB document into T_EX, **tangle** extracts the program fragment from the WEB document and generates the program code.

Here I give an overview overview over the literate programming tool **nuweb** [BRM]. Its main design goals are simplicity and language independence. Instead of two separate tools as in the case of **weave** and **tangle**, **nuweb** consists of a single command line tool that produces both program and documentation in one go. In the following, a simple example shall explain the main features and advantages of literate programming.

The example shows a FORM-program which generates a colour basis for a given partonic process. To calculate the colour basis for the process $gg \rightarrow q\bar{q}q\bar{q}$ one would specify

```

⟨Process Specification 1⟩ ≡
    Local colour =
        #call insertgluons(2)
        #call insertquarks(2)
        ;◇
Macro referenced in 2.
```

The above paragraph has been created with the **nuweb** commands

```

1 The example shows a \form-program ... one would specify
2 @d Process Specification
3 @{@_Local@_ colour =
4     @_call@_ insertgluons(2)
5     @_call@_ insertquarks(2)
6     ;@|
7 colour @}

```

Line 1 contains ordinary L^AT_EX text; line 2 introduces a macro called *Process Specification*. All **nuweb** markup start with an at (@) sign. Lines 3–7 contain a *scrap*, i.e. a short piece of embedded program code. Scraps usually are delimited by a pair of @{ and @}.

Since **nuweb** does not support automatic syntax highlighting it gives the user the opportunity to format the code using the directive **@_**, which formats the text in between in bold font; the formatting does not affect the generated source code.

The above example contains another **nuweb** instruction: the character sequence **@|** introduces a list of identifiers that are defined in the according scrap¹ for which an entry in the list of identifiers is generated. **nuweb** automatically creates a list of user-defined identifiers using the **@u** instruction (see Section 7.3), and similarly a list of macros with the **@m** command (see Section 7.2) and with the **@f** instruction a list of files (see Section 7.1).

The creation of output files for program code is initiated by the **@o** command². The next definition shows the overall structure of the program file **colour.frm**. The declaration section is terminated by the module separator **.global** and contains the definition of all relevant symbols, functions and procedures. In the second paragraph of the program the expression is transformed and the third paragraph prints the expression term by term.

```
"colour.frm" 2 ≡

  ⟨Symbol Definitions 3⟩
    ⟨Procedure definition insertquarks 4⟩
    ⟨Procedure definition insertgluons 6⟩
    ⟨Procedure definition stripcoeff 7⟩
  .global

  ⟨Process Specification 1⟩
  ⟨Perform Insertions 8⟩
  ⟨Simplify Result 12⟩

  # $num = 1;
  Print "color%$=%T", $num;
  $num = $num + 1;
  .end
  ◇
```

The above scrap has been generated by the following piece of **nuweb** code:

```
1 @o colour.frm
2 @{@<Symbol Definitions@>
3 @<Procedure definition \texttt{insertquarks}@>
4 ...
5 # $num = 1;
6 @_Print@_ "color%$=%T", $num;
7 $num = $num + 1;
```

¹It is irrelevant if the identifiers actually appear in this scrap

²Both the commands **@d** and **@o** have a capitalised variant (**@D** and **@O** resp.) which generate long scraps, i.e. the program fragments may span over several pages. However, for readability it is recommended that each scrap consists of up to 12 lines.

```

8 .@_end@_
9 @| $num@}

```

Macros are referenced by putting their names inside angle brackets `@<...@>`. Macros can be referenced before they are defined, i.e. the order of the macro definitions in the document is irrelevant. The above example also shows that macro names can contain virtually any L^AT_EX commands.

Lines 5–7 show how in FORM one can enumerate all terms in an expression by using dollar-variables and the `Print` command. Line 5 defines the dollar variable `$num` when the preprocessor runs, i.e. before the module is executed. Then for every term in the expression lines 6 and 7 are invoked. The format sequence `$$` prints out the first dollar variable from the list after the format string which is the number of the current term and the sequence `%T` prints the current term. Finally, line 7 increases the counter before the next term is processed.

This concludes the discussion of the main features of `nuweb` which are necessary for the understanding of the code and for the understanding of the main concepts of Literate Programming. A complete documentation of `nuweb` can be found in [BRM]. The rest of this section is concerned with the description of the main part of the FORM-program.

The symbol `x` is used as a pattern to represent arbitrary symbolic expressions. The functions `insertgluon`, `insertq` and `insertt` act on an expression like differential operators as explained below. The function `delta(i,j)` stands for a quark line δ_i^j and `t(i,j,g)` for a generator t_{ij}^g . The result is expressed in terms of the commuting functions `line(i,g1,...,gn,j)` which represents the product of generators $t_{ij_1}^{g_1} t_{j_1 j_2}^{g_2} \cdots t_{j_n j}^{g_n}$ and `tr` for traces of products of generators. Indices i_1, i_2, \dots are used for quarks, j_1, j_2, \dots for antiquarks and g_1, g_2, \dots for gluons; for quarks and antiquarks also the two sets `quarks` and `aquarks` are defined.

⟨Symbol Definitions 3⟩ ≡

```

Symbol x;
Functions insertgluon, delta, t, insertq, insertt;
CFunctions tr(cyclic), line;
Autodeclare Indices i, j, g;

Set quarks: i1, ..., i10;
Set aquarks: j1, ..., j10;◇

```

Macro referenced in 2.

The procedure `insertquarks(N)` generates a basis for N quark-antiquark pairs. If $N = 0$ a closed quark line `delta(i1,i1)` is inserted as a seed for the insertion of the gluons. Otherwise, by the product of two ε -tensors an antisymmetriser over all quark lines is generated.

```

⟨ Procedure definition insertquarks 4 ⟩ ≡
  #procedure insertquarks(N)
    #if 'N'>0
      e_(i1, ..., i'N') * e_(j1, ..., j'N')
    #else
      delta(i1,i1)
    #endif
  #endprocedure◇
Macro referenced in 2.

```

After contracting the pair of ε -tensors this antisymmetriser is turned into a symmetriser by discarding the signs.

```

⟨ Build Symmetriser 5 ⟩ ≡
  Contract;
  #call stripcoeff(insertgluon,d_,delta)
  .sort
  ◇
Macro referenced in 8.

```

For each of the N gluon the procedure `insertgluons(N)` multiplies the expression by an `insertgluon`-operator.

```

⟨ Procedure definition insertgluons 6 ⟩ ≡
  #procedure insertgluons(N)
    #do i=1,'N'
      insertgluon(g'i') *
    #enddo
  #endprocedure◇
Macro referenced in 2.

```

The program does not attempt to generate each basis vector in colour space exactly once; it only ensures that each vector is generated with a positive coefficient. Therefore, the procedure `stripcoeff` strips off all coefficients of the symbols which are given as arguments.

The implementation works as follows: The symbols in the argument list `?f` are bracketed off and all remaining factors are collected as arguments of the built-in function `dum_`. Then all occurrences of the function `dum_` are replaced by 1, i.e. the factors in the arguments are discarded.

```

⟨ Procedure definition stripcoeff 7 ⟩ ≡
  #procedure stripcoeff(?f)
    Bracket '?f';
  .sort
    Collect dum_;
    Id dum_(x?) = 1;
  #endprocedure◇
Macro referenced in 2.

```

In order to insert the gluons first all quark lines are cut in all possible ways; then for each generated pair of cuts a generator t_{ij}^g is inserted in all possible ways.

```

⟨ Perform Insertions 8 ⟩ ≡
  ⟨ Build Symmetriser 5 ⟩
  ⟨ Insert a pair of cuts 9 ⟩
  ⟨ Cut quark-lines 10 ⟩
  ⟨ Insert  $t_{ij}^g$  11 ⟩◇

```

Macro referenced in 2.

Since the program works with operators the commuting function `d_` has to be replaced by a non-commuting function `delta`. Then for each gluon a pair of dummy indices is introduced.

```

⟨ Insert a pair of cuts 9 ⟩ ≡
  Id d_(i1?quarks, i2?aquarks) = delta(i1, i2);
  Repeat;
    Id Once insertgluon(g?) = insertq(i0, ia) * insertt(i0, ia, g);
    Sum i0, ia;
  EndRepeat;◇

```

Macro referenced in 8.

There are three replacements for the insertion of the cuts: first, all `inserttt`-operators are permuted to the left such that the `insertq`-operators can act on the quark-lines `delta`. The second replacement implements the commutation relation

$$(577) \quad [\text{insertq}(i, j), \delta_{i'}^{j'}] = \delta_i^{j'} \delta_{i'}^j.$$

If a `insertq` stands to the right of the terms the according term is discarded by the third replacement.

```

⟨ Cut quark-lines 10 ⟩ ≡
  Repeat Id insertq(?any1) * insertt(?any2) =
    insertt(?any2) * insertq(?any1);
  Repeat Id insertq(i0?, ia?) * delta(i1?, i2?) =
    + delta(i1, ia) * delta(i0, i2)
    + delta(i1, i2) * insertq(i0, ia);
  Id insertq(?any) = 0;◇

```

Macro referenced in 8.

Similar to the previous set of rewriting rules the insertion of the generators again cuts the diagram in all possible ways and then fills generators into the gaps. It should be noted that here it is necessary to also consider insertions to the left and to the right of existing generators. The commutation relations in this case are

$$(578) \quad [\text{insertt}(j, i, g), \delta_{i'}^{j'}] = \delta_{i'}^j t_{ij'}^g + \delta_i^{j'} t_{i'j}^g \quad \text{and}$$

$$(579) \quad [\text{insertt}(j, i, g), t_{i'j'}^{g'}] = t_{i'j}^g t_{ij'}^{g'} + t_{i'j}^{g'} t_{ij}^g.$$

```

⟨ Insert  $t_{ij}^g$ , 11 ⟩ ≡
  Repeat;
    Id insertt(i0?, ia?, g?) * delta(i1?, i2?) =
      + delta(i1, i0) * t(ia, i2, g)
      + t(i1, i0, g) * delta(ia, i2)
      + delta(i1, i2) * insertt(i0, ia, g);
    Id insertt(i0?, ia?, g) * t(i1?, i2?, g0?) =
      + t(i1, i0, g) * t(ia, i2, g0)
      + t(i1, i0, g0) * t(ia, i2, g)
      + t(i1, i2, g0) * insertt(i0, ia, g);
  EndRepeat;
  Id insertt(?any) = 0;◇
Macro referenced in 8.

```

The last step consists of the simplification of the result: all dummy indices are contracted, traces of one or zero generators are replaced. Finally the numerical coefficients are stripped off.

```

⟨ Simplify Result 12 ⟩ ≡
  Id delta(i1?, i2?) = line(i1, i2);
  Id t(i1?, i2?, g?) = line(i1, i2, g);
  Repeat Id line(i1?, i2?, ?head) * line(i2?, i3?, ?tail) =
    line(i1, i3, ?head, ?tail);
  Id line(i1?, i1?, ?tail) = tr(?tail);

  Id tr(g?) = 0;
  Id tr() = 1;
  #call stripcoeff(line,tr)◇
Macro referenced in 2.

```

The order of the vectors in the result depends on the internal term ordering of the FORM implementation. The output of the program for the considered process $gg \rightarrow q\bar{q}q\bar{q}$ might look like the following:

```

color1=tr(g1,g2)*line(i1,j1)*line(i2,j2)
color2=tr(g1,g2)*line(i1,j2)*line(i2,j1)
color3=line(i1,j1)*line(i2,j2,g1,g2)
color4=line(i1,j1)*line(i2,j2,g2,g1)
color5=line(i1,j1,g1)*line(i2,j2,g2)
color6=line(i1,j1,g1,g2)*line(i2,j2)
color7=line(i1,j1,g2)*line(i2,j2,g1)
color8=line(i1,j1,g2,g1)*line(i2,j2)
color9=line(i1,j2)*line(i2,j1,g1,g2)
color10=line(i1,j2)*line(i2,j1,g2,g1)
color11=line(i1,j2,g1)*line(i2,j1,g2)
color12=line(i1,j2,g1,g2)*line(i2,j1)
color13=line(i1,j2,g2)*line(i2,j1,g1)
color14=line(i1,j2,g2,g1)*line(i2,j1)

```

The occurrence of 14 basis vectors confirms Equation (59). The program has been tested for all configurations of Table 1 with up to six gluons.

Programming with Contracts. The concept of *Programming by Contract* has been proposed by BERTRAND MEYER [Mey92a, MM92] and implemented in the programming language Eiffel [Mey92b]. Since then the concept has been adapted in other languages either by direct integration into the language definition or by additional libraries and tools such as preprocessors. Programming by contract incorporates three types of contracts between the caller of a method and the class that implements the method: *preconditions* are checked before a method is invoked, *postconditions* are checked after a method returns from execution and *class invariants* are checked before and after each call to a public method of a class.

In this work I use the programming language Python [vRD] with the additional package `contract` [Way]. This combination allows to specify contracts inside the interface documentation of Python classes.

As an example below are shown parts of the implementation of the implementation of a class for permutations.

```

1  import contract
2
3  class Permutation:
4      """
5          Implements permutations...
6
7          Internally, the permutations are stored in cycle representation
8          with all cycles of length 1 omitted.
9
10         inv:
11             all(len(c) > 1 for c in self.cycles)
12         """
13
14         def isIdentity(self):
15             return len(self.cycles) == 0
16
17         def inverse(self):
18             """
19                 Computes the inverse of this permutation
20
21                 post[]:
22                     (self * __return__).isIdentity()
23             """
24             ...
25
26 contract.checkmod(__name__)

```

Lines 10 and 11 define a class invariant which checks that no cycles of length one are stored. As usual in Python, indentation is meaningful also within the contracts, i.e. the invariant spans over all subsequent indented lines following line 10. Since the invariant

is checked before and after all methods, in `isIdentity` one can rely on assertion that the identity is the only permutation with no cycles of length larger than one³.

Lines 21–22 define a postcondition for the calculation of the inverse element of a permutation. The square brackets after the keyword `post` contain a list of variables that may be modified by the method. The empty list asserts that the method does not modify its environment at all. The postcondition itself specifies the defining equation for the inverse element, $gg^{-1} = \text{id}$.

The last line `contract.checkmod(__name__)` is necessary to activate the module `contract`, i.e. to parse the comments for the keywords `inv`, `pre` and `post` and wrap the methods inside new methods of the following format

```
def wrapper(...):
    check class invariants
    check preconditions
    __old__ = save old values
    __return__ = call original method
    check postconditions
    return __return__
```

The object `__old__` is created to allow the access to the old values of global variables where methods modify their environment. An example taken from the documentation of the package `contract` shows its use in a function that sorts a list in-place:

```
1 def sort(a):
2     """Sort a list.
3
4     pre: isinstance(a, type(list))
5     post[a]:
6         # array size is unchanged
7         len(a) == len(__old__.a)
8
9         # array is ordered
10        forall([a[i] >= a[i-1] for i in range(1, len(a))])
11
12        # all the old elements are still in the array
13        forall(__old__.a, lambda e: __old__.a.count(e) == a.count(e))
14    """
15    ...
```

The term *Programming by Contract* for this programming concept can be explained by having contracts between the caller of a method and the class as the two different parties of the contract. Both parties have benefits and obligations. The class, as an obligation, has to ensure that the postconditions of each method hold; its benefit from the contract is, that it can rely on the preconditions to be true. The converse is true for the caller: it can rely on the postconditions to be true and is obliged to ensure the

³All cycles have to be disjoint which is not checked here to maintain the simplicity of the example.

preconditions of the methods it calls. For the class invariants all obligations remain within the class. However, both the class and the caller then can rely on the class invariants. The example of the permutation showed that this can sometimes lead to more efficient implementations. If the contracts are kept very tight they can be used as a tool of software verification and one, in principle could prove the correctness of a program. In practise, however, very often the challenge is to find and implement the correct pre- and postconditions which are appropriate to ensure program correctness and at the same time are sufficiently fast to test them for non-trivial examples.

Program Correctness. In the previous two sections I have discussed two methods which help to write correct programs: A good documentation as provided through Literate Programming helps to structure the program and allows the reader to understand the program bit by bit. Programming by Contract if implemented thoroughly leads to clear interfaces between the components of a program and very often also helps to debug the single components.

Another technique which originates in *Extreme Programming* is the idea of *Test-driven Development* [Bec94, Bec02]. The programmer writes a test-case for every class or module. In the original model⁴ a test-case is a class with at least three methods: `setUp()` generates the data for the test-case to act on, `run()` runs the test on the generated data and `tearDown()` deallocates any resources held by the test-class. This model has been adapted e.g. by the JUnit [BG98] testing framework for the programming language Java [GJSB05] and similarly by the module `unittest` [Pur] in Python. A slightly different approach has been implemented by the `doctest` module [Lan08] which allows the programmer to place simple tests directly inside the documentation of a Python program; these tests at the same time serve as examples about the usage of the corresponding function, method or class. As an example we have another look at the function `sort` that has been used in the previous section about Programming by Contract.

```

1  def sort(a):
2      """Sort a list.
3
4      pre: isinstance(a, type(list))
5      post[a]:
6          # array size is unchanged
7          len(a) == len(__old__a)
8          ...
9
10     examples:
11         >>> a = [5, 1, 3, 4, 2]
12         >>> sort(a)
13         >>> print a
14         [1, 2, 3, 4, 5]
15     """
16     ...

```

⁴The concept was first discussed for the language Smalltalk.


```

17 import doctest
18 doctest.testmod()

```

Lines 11–14 contain the test for the function `sort`; commands for tests are marked as documentation lines that start with the characters `>>>` and are terminated by a blank line or the end of the documentation string. The tests are checked by printing out values which then are compared textually to the expected output (line 14). For more involved tests the `unittest` module is recommended where the setup of the data for the test is separated from the test itself.

Although these techniques and concepts already detect many of the possible errors there are also cases where even more checks are needed. Especially for complicated amplitude calculations in particle physics an established method is the implementation of an alternative, redundant computation of the amplitude by a second programmer. It is important that no untested code is shared between the programmers, and even for trusted parts of the code and third party contributions it is helpful to have alternative implementations. For the $u\bar{u} \rightarrow b\bar{b}s\bar{s}$ amplitude we produced two independent implementations that also differed in the reduction method. Table 1 summarises the differences between the two implementations. The numerical values of each FEYNMAN diagram for different phase space points have been compiled by a script for all helicities and colour structures and provided a regular and automated test tool during the code development.

	Implementation A	Implementation B
Diagram Generation	QGraf	Mathematica/FeynArts
Simplification	FORM	FORM and Maple TM
Representation	numerical	analytic
	form factors	basis integrals
Numerical Evaluation	Fortran90	Maple TM

Table 1: Comparison of two alternative implementations of the $u\bar{u} \rightarrow b\bar{b}s\bar{s}$ amplitude. As many aspects as possible have been chosen differently to ensure an effective error detection.

1. Overview

This section provides an overview over the interplay of the components of the amplitude calculation before in the following section the single program parts, each of which stand for a phase in the generation of a Fortran90 code for the efficient numerical computation of the amplitude. Figure 1 shows the main components and their interactions: the user specifies the process through the control files. The diagram generator QGraf reads in a command file (`qgraf.born`, `qgraf.virt`) which has to be provided for each of the subprocesses. A Python script (`golem.py`) is invoked and calls QGraf [Nog93] and FORM [Ver00, Ver02] automatically with the correct parameters in order to generate Fortran files for each diagram and the required helicity projections.

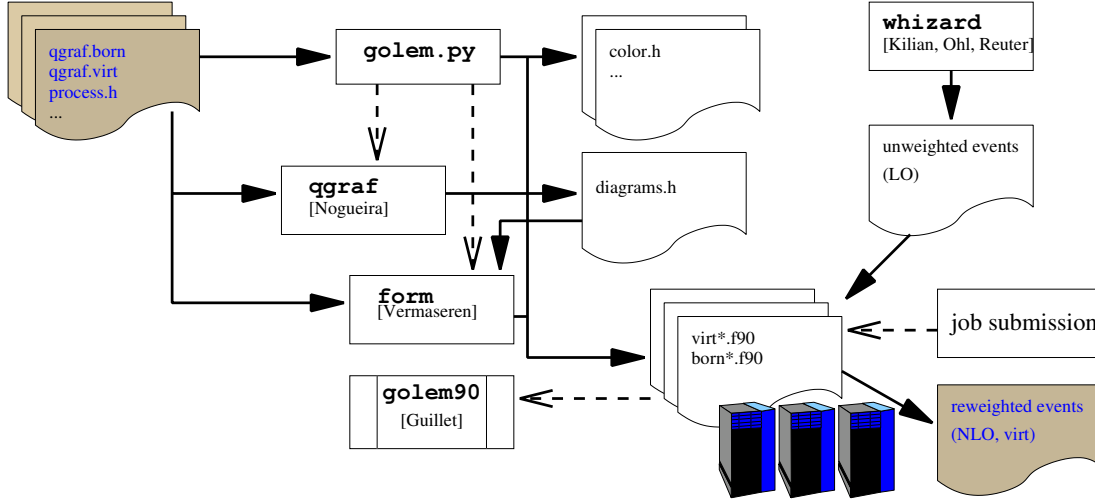


Figure 1: Interplay between the components of the amplitude computation in the implementation as described in this work. Straight arrows denote data flow, dashed arrows stand for control flow in the sense of a call graph.

The output of QGraf (`diagrams.h`) contains all diagrams as FORM expressions and is processed by some FORM program (`preprocess.frm`). It generates a Fortran90 module for each diagram in every helicity projection⁵; the FEYNMAN diagrams are represented as a product of DIRAC traces and form factors as specified by Equation (283). A typical piece of code would look like the following, which is the representation of the all-plus helicity projection of the diagram shown in Figure 2:

```

1 module      virt167_63
2   ! ... module imports ...
3   use virt_ff
4   use virt_tr
5   implicit none
6 contains
7 function      virt167h63(vecs) result(res)
8   implicit none
9   ! ... variable declarations ...
10  props = y12**2*y123*y56
11  prefactor = 1/(braket(-k4,1,k1,-1))/(braket(-k6,1,k1,-1))/(braket(k1&
12    & ,-1,-k3,1))/(braket(k1,-1,-k5,1))/(braket(k1,1,k4,-1))/(braket(&
13    & k4,-1,k2,1))*g**6
14  prefactor = prefactor / props
15  basis1(1) = 1.0_ki/72.0_ki != dF**(-2)*TR**3
16  ! ... basis(2) .. basis(5) ...
17  basis1(6) = - 1.0_ki/24.0_ki != -dF**(-1)*TR**3
18  result1 = - 32*i_fff48*tr4*tr16 - 32*i_fff48*tr4*tr15 - 32*i_fff48*&
19    & tr4*tr2*tr17 - 32*i_fff48*tr4*tr2*tr57 - 32*i_fff48*tr4*tr56 - &

```

⁵The user specifies which helicity projections are calculated directly and how to obtain the remaining ones by parity transformation.

```

20      & 32*i_ff48*tr4*tr55 - 16*i_ff47*tr28*tr30 - 16*i_ff47*tr46*&
21      & tr30 - 16*i_ff47*tr6*tr28*tr1 - 16*i_ff47*tr6*tr46*tr1 - 16*i_&
22      & ff47*tr4*tr6*tr30 - 16*i_ff47*tr4*tr6**2*tr1 + 32*i_eps*ff48*&
23      & tr4*tr16 + 32*i_eps*ff48*tr4*tr15 + 32*i_eps*ff48*tr4*tr2*tr17&
24      & + 32*i_eps*ff48*tr4*tr2*tr57 + 32*i_eps*ff48*tr4*tr56 + 32*i_&
25      & eps*ff48*tr4*tr55
26      do i = 1, 6
27          res(i) = result1 * basis1(i)
28          res(i) = res(i) * prefactor
29      end do
30 end function virt167h63
31 end module virt167_63

```

The traces are computed once for each helicity in the module `virt_tr` and then recycled across all diagrams. The form factors are the same for all helicities and are calculated once per phase space point in the module `virt_ff`. The files `virt_tr.f90`, `virt_ff.f90` and a interface for the summing all diagrams and producing the squared matrix element including the IR and UV subtractions are generated by the script `golem.py`. So far everything is automated up to the point where the user is left with a function `evaluate_me2(vecs, alphas)` that returns the matrix element squared for a given kinematics and a given value of α_s . The form factors are calculated by the `golem90` library. The relevant piece of the file `virt_ff.f90` for the above diagram looks as follows

```

1  subroutine init_ff(vecs)
2      ! ... other topologies ...
3      call allocation_s(6)
4      call yvariables(k1,k2,k3,k4,k5,k6)
5      ! ... initialize S ...
6      call allocate_cache(6)
7      ff47 = a22(2,6,(/1,3,4,5/))
8      ff1749 = a42(1,6,(/2,3/))
9      ff48 = b22(/1,3,4,5/)
10     ff1753 = b42(/2,3/)
11     ! ...
12     call clear_cache()
13     call deallocation_s()
14     ! ... other topologies ...
15 end subroutine init_ff

```

The `golem90` library uses a caching mechanism because many of the form factors are calculated recursively; lines 14 and 20 ensure that this cache is set up correctly. The notation of the form factors is very mnemonic, e.g. $a42(1,6,(/2,3/)) = A_{1,6}^{4,2}(S^{\{2,3\}})$.

The integrator that uses the matrix element is handwritten. Automatising at that point is only of limited benefit since the code very much depends on the observable the user wants to calculate.

2. Diagram Generation

In the chosen approach which is based on FEYNMAN diagrams one of the first step in order to calculate an amplitude at the given order in perturbation theory is the generation of all contributing FEYNMAN graphs. The diagram generator **QGraf** [Nog93] is a fast and robust option which is easy to configure through model files to determine the particle content and the interactions of the physical model and through style files which control the translation of the diagrams into formulæ or programs.

For the calculation of the processes $u\bar{u} \rightarrow b\bar{b}s\bar{s}$ and $gg \rightarrow b\bar{b}s\bar{s}$ a model file for SM-QCD has been implemented.

```

smqcd.model
[ model = 'Standard Model QCD' ]
[ fmrules = 'smqcd' ]
% Propagators:
[U, antiU,          -; PFUN='QuarkPropagator', FLAVOUR='1',
                     CHARGE=('+2/3', '-2/3'),
                     MASS=('emu', 'emu'),
                     IFUN=('u', 'vBAR'), OFUN=('uBAR', 'v')]
[D, antiD,          -; PFUN='QuarkPropagator', FLAVOUR='2',
                     CHARGE=('1/3', '-1/3'),
                     MASS=('emd', 'emd'),
                     IFUN=('u', 'vBAR'), OFUN=('uBAR', 'v')]
...
[Ghost, antiGhost, -; PFUN='GhostPropagator', FLAVOUR='0',
                     CHARGE=('0', '0'),
                     MASS=('0', '0'),
                     IFUN=('ERR', 'ERR'), OFUN=('ERR', 'ERR')]
[glue, glue,        +; PFUN='GluonPropagator', FLAVOUR='0',
                     CHARGE=('0'),
                     MASS=('0'),
                     IFUN=('pol'), OFUN=('polCONJ')]

% Vertices:
[glue, glue, glue;   VFUN='ThreeGluonVertex']
[glue, glue, glue, glue; VFUN='FourGluonVertex' ]
[antiU, U, glue;     VFUN='GluonQuarkVertex']
[antiD, D, glue;     VFUN='GluonQuarkVertex']
...
[antiGhost, Ghost, glue; VFUN='GluonGhostVertex']

```

Propagators have the format [$\langle\text{field}_1\rangle$, $\langle\text{field}_2\rangle$, $\langle\text{sign}\rangle$; $\langle\text{option}, \dots\rangle$; the $\langle\text{sign}\rangle$ is the sign from the commutation relations of that field, i.e. a minus for fermions and a plus for bosons. The options after the semi-colon are user-defined functions. In this model file PFUN has been used as the propagator function which is used in the output, IFUN and OFUN are the names of the functions for in- and outgoing legs. The electric charge CHARGE is not used in the current implementation but one can use it to extend the model file for the inclusion of Quantum Electrodynamics (QED) into future calculations. Similarly the masses of the particles are provided by the field MASS but

are set to zero later in the calculation. Vertices have a similar syntax: the interacting fields are given before the semi-colon and can have a set of parameters after that. The only parameter for the vertices is **VFUN**, the function that is used for a vertex in the output.

This model file also defines two constants **model**, which is a description of the model, and **fmrules**. The latter is used to include a corresponding **FORM** file in the algebraic reduction that will plug in the **FEYNMAN** rules for the symbolic names given in **PFUN**, **IFUN**, **OFUN** and **VFUN**.

The user selects a process by specifying the external particles in a command file together with selection criteria for the diagrams. The command file for the one-loop corrections to $u\bar{u} \rightarrow b\bar{b}s\bar{s}$ is given below. This file has to be called **qgraf.dat** and must reside in the directory from which **QGraf** is called.

```

1  output = 'diagrams.h' ;
2  style  = 'form/form.sty' ;
3  model  = 'form/smqcd.model' ;
4
5  in      = U[k1], antiU[k2] ;
6  out     = B[k3], antiB[k4], S[k5], antiS[k6] ;
7  loops   = 1 ;
8  loop_momentum = p ;
9
10 options= onshell, notadpole ;
11 % no top loops:
12 true = chord [ T, 0, 0 ] ;

```

Lines 1–8 are obligatory; lines 1–3 specify the output, style and model file respectively. The parameters **in** and **out** list the in- and out-going particles, where the names are the ⟨field⟩ names in the model file; in square brackets the user can add the names of the momenta of these particles. For the one-loop correction **loops** is set to one, for the tree-level amplitude one would have a zero in its place. The value of the variable **loop_momentum** prefixes the loop momenta; as only up to one-loop corrections are considered here the only loop momentum is **p1**. The **FORM** code assumes that the external momenta are called k_1, \dots, k_n , and the loop momentum must be called **p1** (see line 9).

In the optional section of the command file, here lines 10–12, restrictions can be applied to the diagram generation. The option **onshell** discards all diagrams that have a self-energy insertion on an external leg, **notadpole** suppresses the generation of tadpole graphs; both diagram types are zero in our renormalisation scheme for massless particles and can be safely discarded.

Line 12 is to be understood as follows: **QGraf** should only include⁶ diagrams which have exactly zero top-propagators running in a loop. Since no top-quarks are in the initial or in the final state this corresponds to excluding all top-loops.

⁶exclude, if **true** was replaced by **false**.

The operator `chord[<field>, <min>, <max>]` tests if a diagram contains at least $\langle \min \rangle$ but at most $\langle \max \rangle$ propagators of a field $\langle \text{field} \rangle$ that belong to loops. The opposite is the operator `bridge` that tests for propagators *not* belonging to loops.

The code below shows the expression which is created for the diagram in Figure 2.

```

1  *----- Diagram 167 -----
2  *--#[ d167:
3  *
4  Local 'DIAGRAM'167 =
5  - 1 *
6  u(1, 1, k1, emu, i2r2) *
7  vBAR(1, 2, k2, emu, i2r1) *
8  uBAR(2, 1, k3, emb, i4r1) *
9  v(2, 2, k4, emb, i3r2) *
10 uBAR(3, 3, k5, ems, i1r1) *
11 v(3, 4, k6, ems, i1r2) *
12 GluonQuarkVertex(iVERT1,
13   QuarkPropagator(3, iPROP{2*6+(-6)}, -k5, ems, i0r0, i1r1),
14   QuarkPropagator(3, iPROP{2*6+(-8)}, -k6, ems, i0r0, i1r2),
15   GluonPropagator(0, iPROP{2*6+(1)}, k5+k6, 0, i3r3, i1r3)) *
16 GluonQuarkVertex(iVERT2,
17   QuarkPropagator(1, iPROP{2*6+(-3)}, k2, emu, i0r0, i2r1),
18   QuarkPropagator(1, iPROP{2*6+(-1)}, k1, emu, i0r0, i2r2),
19   GluonPropagator(0, iPROP{2*6+(2)}, -k1-k2, 0, i5r3, i2r3)) *
20 GluonQuarkVertex(iVERT3,
21   QuarkPropagator(2, iPROP{2*6+(3)}, k4+k5+k6, emb, i4r2, i3r1),
22   QuarkPropagator(2, iPROP{2*6+(-4)}, -k4, emb, i0r0, i3r2),
23   GluonPropagator(0, iPROP{2*6+(1)}, -k5-k6, 0, i1r3, i3r3)) *
24 GluonQuarkVertex(iVERT4,
25   QuarkPropagator(2, iPROP{2*6+(-2)}, -k3, emb, i0r0, i4r1),
26   QuarkPropagator(2, iPROP{2*6+(3)}, -k4-k5-k6, emb, i3r1, i4r2),
27   GluonPropagator(0, iPROP{2*6+(4)}, k1+k2, 0, i6r3, i4r3)) *
28 GluonQuarkVertex(iVERT5,
29   QuarkPropagator(1, iPROP{2*6+(6)}, -p1, emu, i6r2, i5r1),
30   QuarkPropagator(1, iPROP{2*6+(5)}, p1-k1-k2, emu, i6r1, i5r2),
31   GluonPropagator(0, iPROP{2*6+(2)}, k1+k2, 0, i2r3, i5r3)) *
32 GluonQuarkVertex(iVERT6,
33   QuarkPropagator(1, iPROP{2*6+(5)}, -p1+k1+k2, emu, i5r2, i6r1),
34   QuarkPropagator(1, iPROP{2*6+(6)}, p1, emu, i5r1, i6r2),
35   GluonPropagator(0, iPROP{2*6+(4)}, -k1-k2, 0, i4r3, i6r3)) *
36 GluonPropagator(0, iPROP{2*6+(1)}, k5+k6, 0, i3r3, i1r3) *
37 GluonPropagator(0, iPROP{2*6+(2)}, -k1-k2, 0, i5r3, i2r3) *
38 QuarkPropagator(2, iPROP{2*6+(3)}, -k4-k5-k6, emb, i3r1, i4r2) *
39 GluonPropagator(0, iPROP{2*6+(4)}, k1+k2, 0, i6r3, i4r3) *
40 QuarkPropagator(1, iPROP{2*6+(5)}, p1-k1-k2, emu, i6r1, i5r2) *
41 QuarkPropagator(1, iPROP{2*6+(6)}, p1, emu, i5r1, i6r2)
42 ;
43 #ifndef 'LOOPS'

```

```

44     #define LOOPS "1"
45     #define LEGS "6"
46 #endif
47 *--#] d167:

```

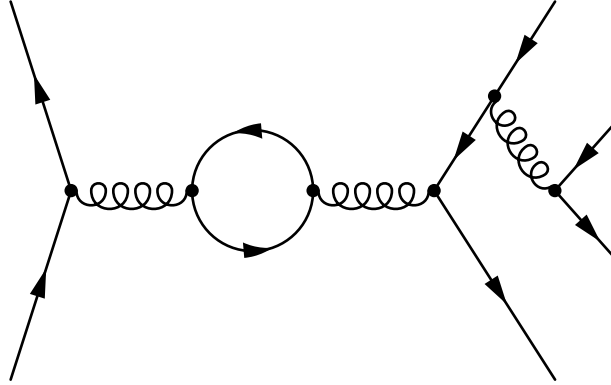


Figure 2: FEYNMAN diagram which illustrates the expression `d167` described in the text. The vertices v_i correspond to `iVERTi` in the expression.

These expressions form the input of the FORM program described in Section 5. The comments of the form `*--#[d167:` and `*--#] d167:` have a special meaning in FORM: they form a so-called *fold* and can be addressed in an `#include` statement to only include the lines that are enclosed by these two lines. This feature is later used to process one diagram at a time.

3. Automatic Code Generation

One of the aims of this project, besides the calculation of cross-sections for the LHC was the automatising of NLO calculations in general. An important part of this endeavour is the automatic code generation not only for the FEYNMAN diagrams but also for most of the auxiliary parts of the code. Section 5 will show an approach using FORM to generate Fortran90 files for each diagram. That FORM program also generates a Python file for each diagram containing information about its topology and all quantities which are to be managed by a global cache, such as the form factors of the tensor integrals and the spinor traces.

A full description of the program `golem.py` would certainly go beyond the scope of this thesis and only be of limited value for the reader. Therefore only selected algorithms and concepts are presented in the following sections. Some of the algorithms are valid for massless internal particles only.

3.1. Mandelstam Variables. In Section 4.2 of Chapter 3 it has been shown that all dot-products of two external momenta $k_i \cdot k_j$, with $1 \leq i, j \leq N$ can be expressed by a canonical set of MANDELSTAM variables which correspond to partitions of the set $\{1, \dots, N\}$ into two subsets. In principle this can be worked out once and for all for each value of N ; it is, however, quite easy to automate the generation of these

variables and the according equations to translate between MANDELSTAM variables and dot-products.

The function `sections` creates a list of all partitions of a set `mom` of momenta into two subsets. The partition is canonicalised and labelled according to the rules given in Chapter 3, Section 4.2. The function `section_name(i, j, n, prefix)` creates the according names, e.g. `section_name(2, 4, 6, "s")` would give `s23` whereas `section_name(4, 2, 6, "s")` returns `s4561`.

```

1 def sections(mom, prefix):
2     n = len(mom)
3     result = []
4     for i in range(1, n):
5         for j in range(0, i):
6             sets = [mom[j:i], mom[i:n] + mom[0:j]]
7             if len(sets[0]) <= len(sets[1]):
8                 result.append([section_name(j, i, n, prefix),
9                               sets[0], sets[1]])
10            else:
11                result.append([section_name(i, j, n, prefix),
12                              sets[1], sets[0]])
13    return result

```

The implementation ensures by the way the loops are nested that in the case where both sets of the partition have equal length the one starting with the lower index is chosen. In the case of four external legs the following output can be expected:

```

>>> lst = golem.sections(["k1", "k2", "k3", "k4"], 4, "s")
>>> print lst
[['s1', ['k1'], ['k2', 'k3', 'k4']], ['s12', ['k1', 'k2'], ['k3', 'k4']],
['s2', ['k2'], ['k3', 'k4', 'k1']], ['s4', ['k4'], ['k1', 'k2', 'k3']],
['s23', ['k2', 'k3'], ['k4', 'k1']], ['s3', ['k3'], ['k4', 'k1', 'k2']]]

```

It should be noted that the second element of each sublist contains the range of momenta that define the name of the MANDELSTAM variable and the third element contains the remaining momenta. Given this table it is easy to produce code to compute the MANDELSTAM variables numerically, as the following example shows:

```

>>> for line in lst:
...     print "%s = square(%s)" % (line[0], "+".join(line[1]))
s1 = square(k1)
s12 = square(k1+k2)
...
s3 = square(k3)

```

The reverse replacement, i.e. replacing dot products in favour of MANDELSTAM variables can be achieved using Equation (335). A practical implementation of this equation requires some extra care for the case $k_i \cdot k_j$ when $|i - j| \leq 1$. One can search for the

according lists of momenta by the second and third elements of each entry in `lst` to reproduce the canonical names of the MANDELSTAM variables.

3.2. Heuristic Optimisation for Dirac Traces. The two most time consuming parts in the calculation of NLO matrix elements in our case are the calculation of the form factors and the calculation of the spinor traces. Therefore one tries to reduce the amount of computing time especially for these two topics. All form factors are extracted from the amplitude and identified if they appear in more than one diagram such that they are calculated only once.

For the calculation of the DIRAC traces one has to choose between different approaches: at the one end of the spectrum one could expand out all traces to MANDELSTAM variables and ε -tensors. This leads to huge expressions for the FEYNMAN diagrams and one faces technical problems when compiling the resulting **Fortran** files. On the other end of the spectrum one can evaluate all traces numerically. The resulting expressions for the FEYNMAN diagrams become extremely compact but one is left with a large number of different traces that have to be evaluated. A set of identities that reduce the number of traces without increasing the number of terms is the following, where Γ stands for a product of DIRAC matrices:

$$(580a) \quad \text{tr}^\pm \{ \Gamma \not{k}_i \not{k}_i \} \rightarrow k_i^2 \text{tr}^\pm \{ \Gamma \}$$

$$(580b) \quad \text{tr}^- \{ \not{k} \Gamma \} \rightarrow \text{tr}^+ \{ \Gamma \not{k} \}$$

$$(580c) \quad \text{tr}^\pm \{ \gamma_{a_1}^{\mu_1} \gamma_{a_2}^{\mu_2} \dots \gamma_{a_n}^{\mu_n} \} = \text{tr}^\pm \{ \gamma_{a_n}^{\mu_n} \dots \gamma_{a_2}^{\mu_2} \gamma_{a_1}^{\mu_1} \}$$

$$(580d) \quad \text{tr}^\pm \{ \gamma_{a_1}^{\mu_1} \gamma_{a_2}^{\mu_2} \Gamma \} = \text{tr}^\pm \{ \Gamma \gamma_{a_1}^{\mu_1} \gamma_{a_2}^{\mu_2} \}$$

It is also advisable to include the rule

$$(581) \quad \text{tr} \{ \Gamma \} \rightarrow \text{tr}^+ \{ \Gamma \} + \text{tr}^- \{ \Gamma \}$$

although it doubles the number of terms in the expression. For a lightlike vector k and an odd number of DIRAC matrices in $\Gamma^{(1)}$ one can use the additional relation

$$(582) \quad \text{tr}^\pm \{ \not{k} \Gamma^{(1)} \not{k} \Gamma^{(2)} \} \rightarrow \text{tr}^\pm \{ \not{k} \Gamma^{(1)} \} \text{tr}^\pm \{ \not{k} \Gamma^{(2)} \}.$$

Using the above set of replacements one can decrease the number of traces that have to be computed already dramatically; in the case of $u\bar{u} \rightarrow b\bar{b}d\bar{d}$ at NLO roughly 90% of the trace calculations could be saved compared to the case where no standardisation was applied. In addition momentum conservation $k_N \rightarrow k_1 + \dots + k_{N-1}$ leads to an additional relation. It depends on the process how much can be gained by this replacement for one increases the number of terms on average by $(N - 2)$ for the massless case but at the same time one reduces the number of different traces to be calculated.

The implementation uses external channels [TV07] to establish a bi-directional communication between **FORM** and the **Python** program `golem.py` which generates the according replacement rules on the fly for each spinor trace. On the invocation of **FORM** a pair of pipes is generated using **Python**'s command `os.pipe()`. A minimal version of a pipe communicating with **form** is given below:

```

1 class FormPipe:
2     def __init__(self, formfile):
```

```

3      (r1, w1) = os.pipe()
4      (r2, w2) = os.pipe()
5      self._fds = [r1, w1, r2, w2]
6      args = ["form", "-pipe", "%d,%d" % (r1, w2), formfile]
7      self._proc = subprocess.Popen(args)
8      self._in = r2
9      self._out = w1
10     self._pid = os.getpid()
11     self._formPID = self.readLine().strip('\r\n')
12     self.write("%s,%d\n" % (self._formPID, self._pid))

```

The last line is part of the protocol as defined in [TV07].

The methods for communicating with the pipe simply act on the file descriptors `self._in` and `self._out`. The method `readLine` is for convenience; one has to be careful not to read ahead because communication through pipes is blocking and one easily creates a deadlock situation where both processes wait for each other ad infinitum.

```

1  def write(self, str):
2      os.write(self._out, str)
3      return self
4  def read(self, count=1):
5      return os.read(self._in, count)
6  def close(self):
7      for fd in self._fds:
8          os.close(fd)
9      self._fds = []
10 def readLine(self):
11     s = os.read(self._in, 1)
12     result = ""
13     while len(s) == 1 and s != "\n":
14         result += s
15         s = os.read(self._in, 1)
16     result += s
17     return result

```

3.3. Colour Correlation Matrices. Since the treatment of the colour algebra is not a computational issue for the processes that were addressed in this work the implementation uses the most simple colour basis rather than the most efficient one: all gluons in colour space are projected on a quark-antiquark pair as described in Section 1.3 of Chapter 2. A basis is generated by all possible ways connecting the quark with the antiquark lines. An efficient non-recursive algorithm for generating all permutations is the JOHNSON-TROTTER algorithm [Tro62, Joh63].

The projection of the gluons on to quark pairs as in Equation (53),

$$(583) \quad \text{gluon line} \rightarrow \frac{1}{\sqrt{T_R}} \text{quark loop with gluon line},$$

also requires a change of the rules for the insertion of a generator in the CATANI-SEYMOUR dipole subtraction [CS97, CDST02]. In the usual graphical notation the insertion operator becomes

(584)

$$\text{gluon line with generator} \rightarrow \frac{1}{\sqrt{T_R}} \text{quark loop with generator} = \frac{1}{\sqrt{T_R}} \left(\text{diagram 1} - \text{diagram 2} \right)$$

The current implementation automatises the whole colour algebra including the generation of the insertion operators for the infrared regularisation⁷ as defined in [CS97].

4. Translation of Tensor Integrals into Form Factors

This section describes a program that generates rewriting rules for a FORM program to translate from tensor integrals into a form factor representation according to Equation (283).

The program assumes that tensor integrals are denoted as

$$(585) \quad I_N^{d; \mu_1 \mu_2 \dots \mu_R}(a_1, a_2, \dots, a_R; S) = \text{TI}(d, N, R, r_{a_1}, \mu_1, r_{a_2}, \mu_2, \dots, r_{a_R}, \mu_R).$$

The information about the matrix S is to be kept elsewhere. The program is written in Java and implemented as a class called `FormFactory`.⁸ The program expects three arguments which are the numbers N and R of Equation (585) and the name of the output file as the third argument.

```
import java.io.*;
public class FormFactory {
    public static void main(String[] args) throws IOException {
        if(args.length == 3) {
            try {
                int legs = Integer.parseInt(args[0]);
                int rank = Integer.parseInt(args[1]);
                new FormFactory(legs, rank, args[2]);
            } catch(NumberFormatException ex) {
                System.err.println("Invalid numeric argument");
            }
        } else
            System.err.println("usage: java FormFactory <legs> <rank> <file name>");
    }
}
```

⁷for massless partons only

⁸All comments have been stripped from the printed version of the program and some of the methods which are very similar to each other have been left out.

```

    } // static method main

    // ... other methods ...

} // class FormFactory

```

The constructor serves as the main program. It opens the output file and writes to it the left hand side and, depending on the number of legs and the rank of the integral, the according terms of the right hand side: the B and C terms are only written if the number of legs is smaller than 6;

```

public FormFactory(int legs, int rank, String filename) throws IOException {
    FileOutputStream theFile = new FileOutputStream(filename);
    PrintStream out = new PrintStream(theFile);

    this.generateLHS(legs, rank, out);
    this.generateFormFactorA(legs, rank, out);
    if(legs < 6) {
        if(rank >= 2)
            this.generateFormFactorB(legs, rank, out);
        if(rank >= 4)
            this.generateFormFactorC(legs, rank, out);
    }
    out.println(";");
    theFile.close();
}

```

The generation of the left hand side of the replacement uses the triple-dot (“...”) operator of the FORM preprocessor rather than expanding out all arguments explicitly. The angle brackets hereby ensure that both arguments, q_1 and i_1 are incremented simultaneously.

```

protected void generateLHS(int legs, int rank, PrintStream out) {
    out.print("id TI(" + legs + ", " + rank);
    switch(rank) {
    case 0: break;
    case 1: out.print(", q1?,i1?"); break;
    default:
        out.print(", <q1?,i1?>, ..., <q" + rank + "? ,i" + rank + "?>");
    }
    out.println(") =");
}

```

The method `complementSet` computes the set theoretic complement of a subset of $\{1, \dots, n\}$. The routine assumes that the parameter `set` is already in increasing order.

```

protected static int[] complementSet(int[] set, int n) {
    int i = 0;
    int size = n - set.length;

```

```

int[] result = new int[size];
for(int k = 1; k <= n; ++k) {
    if((i < set.length) && (set[i] == k)) ++i;
    else result[k - i - 1] = k;
}
return result;
}

```

Another combinatorial algorithm that is required for the generation of the translation formula enumerates all subsets of the set $\{1, \dots, n\}$ that have $m \leq n$ elements. The method `nextSelection` enumerates these subsets: the first time the method has to be invoked with the array $\{1, 2, \dots, m\}$, after that the method must be called with the previous value of `set`; the next subset in the sequence is written in-place to the argument `set`. If no more sets can be found the method returns `false`.

```

protected static boolean nextSelection(int[] set, int n) {
    int m = set.length;

    for(int i = m - 1; i >= 0; --i) {
        if(set[i] <= n - (m - i)) {
            for(int j = m - 1; j >= i; --j) {
                set[j] = set[i] + 1 + (j - i);
            } // for
            return true;
        } // if
    } // for
    return false;
}

```

All elements of the set $\{1, \dots, n\}^r$ are generated by the method `nextCombination`; the calling conventions are similar to the previous method. For the first call the argument `lst` must be initialized with $\{1, 1, \dots, 1\}$.

```

protected static boolean nextCombination(int[] lst, int n) {
    int m = lst.length;
    ++ lst[m - 1];
    for(int i = m - 1; i >= 0; --i) {
        if(lst[i] > n) {
            lst[i] = 1; if(i > 0) ++lst[i - 1];
        }
        else return true;
    } // for
    return false;
}

```

Before the generation of the actual terms in the rewriting rule is discussed two utility functions are introduced: the first one, `printSymmetricTensor` prints the expression $g^{i_1 i_2} g^{i_3 i_4} + g^{i_1 i_3} g^{i_2 i_4} + g^{i_1 i_4} g^{i_2 i_3}$ for a given set of indices $\{i_1, i_2, i_3, i_4\}$. The second method, `printDelta` generate the FORM equivalent of the vector $\Delta_{ij}^{\mu_j}$.

```

private void printSymmetricTensor(int[] G, PrintStream out) {
    out.print("(");
    out.print("gTensor(n,i" + G[0] + ",i" + G[1] + ")"); out.print("*");
    out.print("gTensor(n,i" + G[2] + ",i" + G[3] + ")"); out.print(" + ");
    out.print("gTensor(n,i" + G[0] + ",i" + G[2] + ")"); out.print("*");
    out.print("gTensor(n,i" + G[1] + ",i" + G[3] + ")"); out.print(" + ");
    out.print("gTensor(n,i" + G[0] + ",i" + G[3] + ")"); out.print("*");
    out.print("gTensor(n,i" + G[1] + ",i" + G[2] + ")");
    out.print(")");
}
private void printDelta(int i, int j, PrintStream out) {
    out.print("DELTA(r" + i + ",q" + j + ",i" + j + ")");
}

```

The form factors $A_{j_1, \dots, j_r}^{N,r}$ occur under a multiple sum over all j_i with a coefficient $[\Delta_{j_1} \cdots \Delta_{j_r}]_{a_1, \dots, a_r}^{\mu_1, \dots, \mu_r}$. To generate all terms an array $J[] = \{j_1, \dots, j_r\}$ is generated for each possible combination of values for the j_i using the method `nextCombination`. Only a single term is generated for the case $r = 0$, where the tensor in front of the form factor is 1.

```

protected void generateFormFactorA(int legs, int rank, PrintStream out) {
    if(rank > 0) {
        int[] J = new int[rank];
        for(int j = 0; j < rank; ++j) J[j] = 1;
        do {
            out.print("  + ");
            for(int j = 0; j < rank; ++j) {
                this.printDelta(J[j], j + 1, out); out.print(" * ");
            } // for
            out.print("a" + legs + "" + rank + "(");
            for(int j = 0; j < rank; ++j)
                out.print(Integer.toString(J[j]) + ",");
            out.println("'SNULL'");
        } while(nextCombination(J, legs));
    } else {
        out.print("  + ");
        out.println("a" + legs + "" + rank + "('SNULL')");
    } // if
}

```

The form factor $B_{j_1, \dots, j_{r-2}}^{N,r}$ has to take into account the symmetrization over the additional g^{**} . The array G is filled with all possible selections of two of the indices μ_1, \dots, μ_r using the method `nextSelection`. The remaining indices are selected by the method `complementSet` and distributed in the same manner as for the form factor A .

```

protected void generateFormFactorB(int legs, int rank, PrintStream out) {
    if(rank > 2) {
        int[] J = new int[rank - 2];
        int[] G = new int[2];
    }
}

```

```

    for(int j = 0; j < rank - 2; ++j) J[j] = 1;
    for(int j = 0; j < 2; ++j) G[j] = j + 1;
    do {
        int[] C = complementSet(G, legs);
        do {
            out.print("  + ");
            out.print("gTensor(n,i" + G[0] + ",i" + G[1] + ")");
            out.print(" * ");
            for(int j = 0; j < rank - 2; ++j) {
                this.printDelta(J[j], C[j], out); out.print(" * ");
            } // for
            out.print("b" + legs + "" + rank + "(");
            for(int j = 0; j < rank - 2; ++j)
                out.print(Integer.toString(J[j]) + ",");
            out.println("'SNULL'");
        } while(nextCombination(J, legs));
    } while(nextSelection(G, rank));
} else {
    out.print("  + "); out.print("gTensor(n, i1, i2) * ");
    out.println("b" + legs + "" + rank + "('SNULL')");
} // if
}

```

The overall structure of the method `generateFormFactorC` is the same as the previous ones. The additional symmetrisation over the two metric tensors $g^{\mu\nu}g^{\rho\sigma}$ is done explicitly by the method `printSymmetricTensor`.

```

protected void generateFormFactorC(int legs, int rank, PrintStream out) {
    int[] G = new int[4];
    for(int j = 0; j < 4; ++j) G[j] = j + 1;
    if(rank > 4) {
        int[] J = new int[rank - 4];
        for(int j = 0; j < rank - 4; ++j) J[j] = 1;
        do {
            int[] C = complementSet(G, legs);
            do {
                out.print("  + ");
                this.printSymmetricTensor(G, out);
                out.print(" * ");
                for(int j = 0; j < rank - 4; ++j) {
                    this.printDelta(J[j], C[j], out); out.print(" * ");
                } // for
                out.print("c" + legs + "" + rank + "(");
                for(int j = 0; j < rank - 4; ++j)
                    out.print(Integer.toString(J[j]) + ",");
                out.println("'SNULL'");
            } while(nextCombination(J, legs));
        } while(nextSelection(G, rank));
    } else {
        out.print("  + "); this.printSymmetricTensor(G, out);
    }
}

```

```

        out.print(" * "); out.println("c" + legs + "" + rank + "('SNULL')");
    } // if
}

```

This concludes the program; it should be straight forward to modify the program in order to suite different requirements if one uses another computer algebra program or prefers another programming language. One of the reasons for adding this program in the appendix is to give an unambiguous specification of the meaning of the brackets $[\dots]_{a_1 \dots a_r}^{\mu_1 \dots \mu_r}$.

5. Algebraic Simplification

Introduction. This section describes the FORM code that is used to generate Fortran90 files from the output of the diagram generator QGraf. The main goal of this code is to keep the output as compact as possible. The arguments in favour of this approach are shorter compilation times and robustness against failures during the translation when the requirements of the computer algebra program exceed the resources provided by the system. On the other hand, the code which is generated this way is generally slower than an equivalent output that has been achieved by more subtle simplification routines that take into account all possible cancellations. However, the latter approach usually requires a higher degree of process dependent fine-tuning and is therefore less suitable for the implementation of a general purpose tool.

The Computer Algebra System (CAS) FORM [Ver00, Ver02, VT06] in contrast to most general purpose CASs has originally been developed mainly as a pure term rewriting system with added capability to handle DIRAC traces and vectors and, more general, higher rank tensors. Expressions are represented as lists of terms, and the canonical form is the fully expanded representation. FORM programs are structured as a list of modules; each module is applied term by term, and only at the end of a module all terms are sorted and the expression is brought into canonical form again.

The major drawback of this restriction to local replacements is the incapability of having rewriting rules like $a + b \rightarrow c$ because that would require the inspection of more than one term at the same time. However, this is the price to pay for two of the main advantages of FORM: it can handle arbitrarily big expressions (limited only by the resources of the computer) and it is very fast for it avoids the complexity of AC-unification [KN92].

5.1. The Main Program. The FORM program for the algebraic simplification is not called directly by the user but is invoked by a Python program that coordinates the translation (see Section 3). Command line options are passed to the program through preprocessor definitions using the FORM command line parameter -D as follows:

```

form -D DIAG= $\langle diagram \rangle$  -D PREFIX= $\langle prefix \rangle$  -D HELICITY= $\langle helicity \rangle$ 
      preprocess.frm

```

The parameter $\langle diagram \rangle$ is the index of the diagram to be processed and corresponds to the labelling assigned by QGraf. The prefix usually is one of **born**, **virt** or **real**

and selects which part of the amplitude is calculated; this, however, is just a naming convention. The diagrams always are read from the current `diagrams.h` file and the program relies on the controlling `Python` program to set up the environment correctly. The parameter $\langle helicity \rangle$ is the binary encoding of the helicity to be calculated. In the massless case, where the helicities $\lambda_i = \pm 1$ this number is

$$(586) \quad \langle helicity \rangle = \sum_{i=1}^N \frac{\lambda_i + 1}{2} \cdot 2^{i-1}$$

Before the actual program starts it verifies that all three parameters are present.

$\langle \text{check command line arguments 13} \rangle \equiv$

```
#IfNDef 'DIAG'
    #Message "Please, run with -D DIAG=<diagram> from command line."
    #Terminate
#EndIf

#IfNDef 'PREFIX'
    #Message "Please, run with -D PREFIX=<fileprefix> from command line."
    #Terminate
#EndIf

#IfNDef 'HELICITY'
    #Message "Please, run with -D HELICITY=<helicity> from command line."
    #Terminate
#EndIf◇
```

Macro referenced in 23.

Before the program starts the actual simplification it checks for the consistency of the diagram number. The total number of diagrams for a subprocess is found in a fold called `#global` in the file `diagrams.h`.

$\langle \text{check bounds on diagram number 14} \rangle \equiv$

```
#Define DIAGRAM "diagram"
#include- diagrams.h #global
#If 'DIAG' > 'DIAGRAMCOUNT'
    #Message "DIAG ('DIAG') > DIAGRAMCOUNT ('DIAGRAMCOUNT')"
    #Terminate
#EndIf◇
```

Macro referenced in 24.

The program should also check if it has been called with external channels set up correctly:

$\langle \text{check communication channels 15} \rangle \equiv$

```
#IfnDef 'PIPES_'
    #Message "This program must be called from within GOLEM."
    #Terminate
```

```
#EndIf
#SetExternal 'PIPE1_'◇
```

Macro referenced in 23.

Before the program can read in the FEYNMAN diagram all occurring symbols need to be declared. Here, two classes of symbols are distinguished: symbols that appear only in the FEYNMAN rules are defined in the according file, e.g. `smqcd.h` for Standard Model QCD, generic symbols that appear during the simplification are defined in a file called `symbols.h`. At the end of that file there is a list of automatic declarations mainly for symbols that are used locally only.

```
"symbols.h" 16 ≡
  <define symbols for colour algebra 17>
  <define symbols for LORENTZ and DIRAC algebra 18>
  <define vectors 19>
  <define topological functions 20>
  <define auxiliary functions and symbols 21>
  <define form factors 22>
  Symbol g;

  AutoDeclare Indices i;
  AutoDeclare CFunctions ANY, TEMP;
  AutoDeclare Functions NCTEMP;
  AutoDeclare Symbols cc, color, ff, tr;
  AutoDeclare Vectors vec;◇
```

The symbol `g` stands for the coupling constant. Symbols starting with `ff` and `tr` represent form factors and traces respectively. The same symbols are used by the Python code that maintains a global list of both.

For the colour algebra the scalar objects $\mathbf{dF} \equiv N_C$, $\mathbf{dA} \equiv N_C^2 - 1$, $\mathbf{TR} \equiv 1/2$ and $\mathbf{CA} \equiv C_A$ are used. The generators are called `T` in the fundamental and `f` in the adjoint representation, $\mathbf{f(A,B,C)} \equiv f^{ABC}$ and $\mathbf{T(i,j,A)} \equiv t_{ij}^A$.

```
<define symbols for colour algebra 17> ≡
  Symbols dF, dA, TR, CA;
  CFunctions f, T;
  CFunction AdjointID(symmetric);
  CFunction FundamentalID(symmetric);◇
```

Macro referenced in 16.

For the LORENTZ algebra and DIRAC algebra the following conventions are used: the DIRAC matrices are called `gg`, $\mathbf{gg(i,j,mu)} \equiv (\gamma^\mu)_{ij}$ and the corresponding identity matrix is `gammaID`; γ_5 is `gamma5` which defines $\mathbf{hProjector(\pm 1)} \equiv (\mathbb{I} \pm \gamma_5)/2$.

Spinor objects are represented by $\mathbf{Spinor}(k_i, \pm 1) \equiv |k_i^\pm\rangle$, $\mathbf{AdjSpinor}(k_i, \pm 1) \equiv \langle k_i^\pm|$ and $\mathbf{SpinorLine}(k_i, \lambda_i, \mu_1, \mu_2, \dots, \mu_r, k_j, \lambda_j) \equiv \langle k_i^{\lambda_i} | \mu_1, \mu_2, \dots, \mu_r | k_j^{\lambda_j} \rangle$. The metric tensor is denoted by `gTensor`. The dimension of the MINKOWSKI space is $\mathbf{n} = 4 - 2 \cdot \mathbf{eps} = 4 + [-2\mathbf{eps}]$.

\langle define symbols for LORENTZ and DIRAC algebra 18 $\rangle \equiv$

```
CFunctions gg, gammaID(symmetric), gamma5, hProjector;
CFunctions Spinor, AdjSpinor;
CFunctions SpinorLine, SpinorTrace;
CFunction gTensor(symmetric);
Symbols n, eps, [-2eps];
◇
```

Macro referenced in 16.

The four-momenta used in the calculation are k_1, k_2, \dots for the external momenta and p_1 for the integration momentum. The translation of polarisation vectors into spinor helicity notation (see Equation (130)) makes it necessary to have additional gauge vectors which are called **qGauge1**, **qGauge2** and so on where the index denotes the corresponding particle (**k1**, **k2**, ... resp.).

\langle define vectors 19 $\rangle \equiv$

```
#define MAXLEGS "7"
Vectors k1, ..., k'MAXLEGS';
Vectors p1;
Vectors qGauge1, ..., qGauge'MAXLEGS';◇
```

Macro referenced in 16.

For the analysis of the topology of each diagram the function **edge** is introduced for each propagator, the function **node** for every vertex and later **circle** to indicate the loop in a one-loop diagram.

\langle define topological functions 20 $\rangle \equiv$

```
CFunctions node, edge(symmetric), circle(cyclic);◇
```

Macro referenced in 16.

The function **POW** denotes powers, $\text{POW}(a, b) = a^b$; this is especially useful to treat denominators as $\text{POW}(\dots, -1)$. Spinor products are represented as $\langle p_{\lambda_1} | q_{\lambda_2} \rangle = \text{braket}(p, \lambda_1, q, \lambda_2)$. The function **MOMENTUM** prevents momenta from automatic contraction which is desired at several places in the program. Propagators are translated into $1/(q^2 - m^2) = \text{PROP}(q, m)$. For the translation of the tensor integrals into form factors at an intermediate step the function **TI** is introduced to represent a tensor integral. Its arguments are

$$(587) \quad I_N^{n; \mu_1 \mu_2 \dots \mu_r}(a_1, a_2, \dots, a_r; S) = \text{TI}(N, r, r_{a_1}, \mu_1, r_{a_2}, \mu_2, \dots, r_{a_r}, \mu_r).$$

The functions **PREFACTOR** and **COLORBASIS** are used to separate parts of the expression into the argument of the according function. The difference vectors $\Delta_{ij}^\mu = r_i^\mu - r_j^\mu$ are encoded into the function $\text{DELTA}(i, j, \mu)$. The symbol **SNULL** represents an empty list of pinches of the S -matrix.

\langle define auxiliary functions and symbols 21 $\rangle \equiv$

```

CFunction POW, brakel;
CFunctions MOMENTUM, PROP;
CFunctions TI;
CFunctions PREFACTOR, COLORBASIS;
CFunction DELTA;

#define SNULL "nullarray"
Symbol 'SNULL';◇

```

Macro referenced in 16.

The following list defines all integral form factors that can appear during the reduction, up to six-point function and tensor rank six.

⟨define form factors 22⟩ ≡

```

CFunctions
  a10, a20, a30, a40, a50, a60, a11, a21, a31,
  a41, a51, a61, a22, a32, a42, a52, a62, a33,
  a43, a53, a63, a44, a54, a64, a55, a65, a66;
CFunctions
  b10, b20, b30, b40, b50, b11, b21, b31, b41, b51,
  b22, b32, b42, b52, b33, b43, b53, b44, b54, b55;
CFunctions
  c10, c20, c30, c40, c50, c11, c21, c31, c41, c51,
  c22, c32, c42, c52, c33, c43, c53, c44, c54, c55;
Set FormFactors:
  a10, a20, a30, a40, a50, a60, a11, a21, a31, a41,
  a51, a61, a22, a32, a42, a52, a62, a33, a43, a53,
  a63, a44, a54, a64, a55, a65, a66, b10, b20, b30,
  b40, b50, b11, b21, b31, b41, b51, b22, b32, b42,
  b52, b33, b43, b53, b44, b54, b55, c10, c20, c30,
  c40, c50, c11, c21, c31, c41, c51, c22, c32, c42,
  c52, c33, c43, c53, c44, c54, c55;◇

```

Macro referenced in 16.

The structure of the main program follows below. After the program has checked the parameters and defined all symbols the main part of the program simplifies the expression for one diagram at the specified helicity and writes out a **Fortran90** program.

"preprocess.frm" 23 ≡

```

#-
#:Workspace 10M
On ShortStatistics;
Off Statistics;

⟨check communication channels 15⟩
⟨check command line arguments 13⟩
#Define OUT "'PREFIX' 'DIAG' _ 'HELICITY' .f90"

⟨read libraries and configuration 24⟩

```

```

    < determine the helicities of the external particles 25 >
    < define procedures 61 >
    .sort
    < simplification algorithm 53 >
    < output section 54 >
    #ToExternal "DONE\n"
    .end◇

```

The main program finishes with notifying the `Python` program about its termination through sending a line containing the word “DONE” through the external channels.

The first file that needs to be included is the file `symbols.h` which has been explained above. The file `'PREFIX'-color.h` is automatically generated by the `Python` program `golem.py` and provides information about the colour basis. The file `diagrams.h` which is generated by `QGraf` contains a variable `THEORY` in its global section; this specifies the file that must be used to translate the `FEYNMAN` rules into a theory-independent expression. The file `kin'LEGS'.h` defines the `MANDELSTAM` variables according to the number of external particles, which is stored in the variable `LEGS`.

< read libraries and configuration 24 > ≡

```

#Include- symbols.h
    < check bounds on diagram number 14 >
#Include- 'PREFIX'-color.h
#Include- 'THEORY'.h
#Include- diagrams.h #d'DIAG'
.sort
#Include- kin'LEGS'.h
#Include- process.h◇

```

Macro referenced in 23.

It should be noted that the order of the include statements matters in the sense that some files depend on the information supplied by other files such as the number of external particles.

The helicities of the external particles are encoded in an integer number in binary. If $\lambda_i = \pm 1$ is the helicity of the particle associated with the momentum k_i then this number is

$$\sum_{i=1}^N \left(\frac{\lambda_i + 1}{2} \right) \cdot 2^{i-1}.$$

In the program the variables `HELi` = λ_i are used.

< determine the helicities of the external particles 25 > ≡

```

#Define HEL " 'HELICITY' "
#Do i=1, 'LEGS'
    #Define HEL 'i' "{2*('HEL'%2)-1}"
    #Redefine HEL "{ 'HEL'/2 }"
#EndDo
#UnDefine HEL◇

```

Macro referenced in 23.

5.2. Simplification Algorithm.

5.2.1. *Topological Analysis.* Rather than the process $1 + 2 \rightarrow 3 + 4 + \dots + N$ we consider $1 + 2 + \dots + N \rightarrow 0$ by crossing all outgoing legs to the initial state.

\langle make all momenta ingoing 26 $\rangle \equiv$

```
#Do i=3,'LEGS'
  Multiply replace_(k'i', vec'i');
  Multiply replace_(vec'i', -k'i');
#EndDo◇
```

Macro referenced in 53.

For one-loop diagrams we introduce $r_i = k_1 + \dots + k_i$, $q_i = p + r_i$, where p is the integration momentum, and $\Delta_{ij} = \text{Dix}j = r_i - r_j$. The procedure `IntroduceRMomenta` replaces the sums of momenta by the abbreviations r_i , q_i and Δ_{ij} . The `Argument` statement is necessary in order to replace the momenta inside function arguments, too.

\langle introduce momenta q_i and r_i for one-loop processes 27 $\rangle \equiv$

```
#If 'LOOPS' == 1
  .sort
  Vectors q1, ..., q'$loopsiz';
  Vectors r1, ..., r'$loopsiz';
  #Do i=1,{'$loopsiz'-1}
    #Do j={'i'+1}, '$loopsiz'
      Vector D'i'x'j';
    #EndDo
  #EndDo
  Set qSET: q1, ..., q'$loopsiz';
  Set rSET: r1, ..., r'$loopsiz';

  #Call IntroduceRMomenta()
  Argument VertexFunction;
  #Call IntroduceRMomenta()
  EndArgument;
#EndIf◇
```

Macro referenced in 53.

The procedure `TopologyInfo` determines the loop size, the pinched propagators and the permutation of the external legs. This information is passed to the `Python` program through the external channels.

\langle determine graph topology 28 $\rangle \equiv$

```
#Call TopologyInfo()
#ToExternal "LO 'LOOPS'\n"
#ToExternal "LE 'LEGS'\n"
```

```

#ToExternal "PE 'LEGPERMUTATION'\n"
#ToExternal "PI 'PINCHES'\n"
#If ('LOOPS' == 1)
    #ToExternal "LS '$loopsizes'\n"
#Else
    #ToExternal "LS 0\n"
#EndIf◇

```

Macro referenced in 53.

5.2.2. *Colour Algebra.* For an efficient evaluation of the diagram one has to avoid multiple reevaluation of the same expressions. Therefore linear combinations of colour basis elements are grouped together such that different colour structures only arise from the four-gluon vertices where colour and spin information does not factorise. The FEYNMAN rules are constructed such that each different colour factor is labelled by a function ANYCS(...) with a unique argument. If no four-gluon vertex is in the diagram the factor ANYCS(1) ensures that the algorithm still works as desired and exactly one colour structure is built.

In order to label the colour structures by an increasing index one can make use of FORM's capability of interacting between the preprocessor and the compiled program using dollar-variables. The preprocessor variable `cs` is reset to zero every time the first `Id` statement finds the pattern on its left-hand-side; the argument of the function `TEMPCS` that matches is written to the dollar variable `$cs`.

⟨find next colour structure 29⟩ ≡

```

Id IfMatch->cstruelab'$dummy' TEMPCS(cc?$cs) = TEMPCS(cc);
Goto csfalselab'$dummy';
Label cstruelab'$dummy';
ReDefine cs, "0";
Label csfalselab'$dummy';◇

```

Macro referenced in 31.

After a `.sort` the preprocessor comes back into action and increases the counter in case of a match, i.e. when `cs` is zero at this point. The second `Id` statement uses the content of `$cs` to identify all occurrences of that colour structure and labels it by the function `TEMPKIN` with the counter as an argument.

⟨actual replacement of colour structure 30⟩ ≡

```

#$dummy = {'$dummy'+1};
#If 'cs' == 0
    #$counter = {'$counter'+1};
    Id TEMPCS($cs) = TEMPKIN('$counter');
#EndIf◇

```

Macro referenced in 31.

When eventually no more terms match the variable `cs` is not reset anymore and the loop terminates.

$\langle \text{label colour structures 31} \rangle \equiv$

```

#$dummy = 0;
#$counter = 0;
#Do cs=1,1
   $\langle \text{find next colour structure 29} \rangle$ 
.sort
   $\langle \text{actual replacement of colour structure 30} \rangle$ 
.sort
#EndDo◇

```

Macro referenced in 32.

Finally, the expression holding the entire FEYNMAN diagram is discarded in favour of the expressions `struct‘i’` that hold the single colour structures.

$\langle \text{split into colour structures 32} \rangle \equiv$

```

Multiply ANYCS(1);
Id ANYCS(?all) = TEMPSC(ANYCS(?all));
ChainIn TEMPSC;
Repeat Id TEMPSC(cc0?, cc1?, ?tail) = TEMPSC(cc0*cc1, ?tail);
.sort
 $\langle \text{label colour structures 31} \rangle$ 
Bracket TEMPKIN;
.sort
#Do i=1,$counter'
  Local struct‘i’ = ‘DIAGRAM’‘DIAG’[TEMPKIN(‘i’)] * TEMPKIN(‘i’);
#EndDo
.sort
Drop ‘DIAGRAM’‘DIAG’;◇

```

Macro referenced in 53.

To project on the colour basis elements first all products of KRONECKER deltas (here: `FundamentalID`) are replaced by symbolic names (`color1`, `color2`, ...).

The steps it takes to create a colour vector are the following. One starts from an expression like

$$\sum_{i=1}^{\text{NUMCS}} c_i \cdot \text{color}i.$$

The `Collect` statement puts the whole expression into the argument of a function; the function argument is then copied `NUMCS` times, and in each copy one of the basis elements is set to one. All remaining colour basis elements are replaced by zero. Finally, the function `COLORBASIS` contains the arguments `COLORBASIS(c1, c2, ..., cNUMCS)`.

$\langle \text{create colour vector 33} \rangle \equiv$

```

AntiBracket T, f, dF, dA, TR, color1, ..., color‘NUMCS’;
.sort
Collect TEMPcolor;
Normalize TEMPcolor;

```



```

Id TEMPCOLOR(cc0?) = COLORBASIS(cc0 * replace_(color1,1)
#Do c=2,'NUMCS'
    , cc0 * replace_(color'c',1)
#EndDo
);
#Do c=1,'NUMCS'
    Multiply replace_(color'c',0);
#EndDo◇

```

Macro referenced in 34.

The elements of the colour vectors for each colour structure are read into dollar variables `$basis'i'x'c'` for each colour structure `i` and the basis element `c`.

$\langle \text{project on colour basis 34} \rangle \equiv$

```

#Call colorstructures()
Id POW(TR, -1/2)^2 = 1/TR;
#Do k=1,10
    Sum i'k'r1, i'k'r2, i'k'r3,i'k'r4;
#EndDo
 $\langle \text{create colour vector 33} \rangle$ 
#Do i=1,'$counter'
    #Do c=1,'NUMCS'
         $\$basis'i'x'c' = 0;$ 
        Id TEMPKIN('i') * COLORBASIS(cc?$basis'i'x'c', ?tail) =
            TEMPKIN('i') * COLORBASIS(?tail);
    #EndDo
#EndDo
Id TEMPKIN(cc?) * COLORBASIS = 1;
.sort◇

```

Macro referenced in 53.

One of the last steps of the program is to evaluate the colour vector numerically by plugging in $N_C = 3$.

$\langle \text{evaluate colour vector numerically 35} \rangle \equiv$

```

#Do i=1,'$counter'
    #Do c=1,'NUMCS'
        Local basis'i'x'c' = $basis'i'x'c';
    #EndDo
#EndDo
Id dA = 8;
Id dF = 3;
Id 1/dF = 1/3;
Id TR = 1/2;◇

```

Macro referenced in 53.

5.2.3. *Integration.* Although in the current implementation all internal masses are expected to be zero they are already written to dollar variables. Once a massive implementation is being developed this information needs to be provided to the `Golem90` library in order to set up the correct S -matrix.

$\langle \text{read propagator masses 36} \rangle \equiv$

```
#Do i=1, '$loopsz'
  #mass'i' = 0;
  Id PROP(-q'i', cc?) = PROP(q'i', cc);
  Id PROP(-q'i', 0) = PROP(q'i', 0);
  Id PROP(q'i', cc?mass'i') = 1;
  Id PROP(q'i', 0) = 1;
#EndDo◇
```

Macro referenced in 39.

The numerator of each tensor integral is written into a temporary function; the arguments are pairs of momenta and indices (r_i, μ) for each q_i^μ in the numerator. for each such pair one power of the symbol `ccCOUNT` is multiplied to the corresponding term. Since the variable `$rank` is determined for each term, together with the `If`-statement one calculates the maximal rank that occurs in this diagram in the variable `$maxrank`. The imaginary i in front of the function `TI` ensures that the definition of the tensor integral is the same as in Equation (204).

$\langle \text{construct tensor integral 37} \rangle \equiv$

```
Multiply TEMP;
  Id MOMENTUM(n, vec?qSET?rSET, iMU?) = TEMP(vec, iMU) * ccCOUNT;
  ChainIn TEMP;
  Id ccCOUNT^n?$rank = 1;
  If($rank > $maxrank);
    $maxrank = $rank;
  EndIf;
  Id TEMP(?all) = i_ * TI('$loopsz', nargs_(?all)/2, ?all);◇
```

Macro referenced in 39.

The rewriting rules for the translation of tensor integrals into form factors are automatically generated by a `Java` program which is explained in Section 4. The one-point form factors are replaced by zero as only massless integrals are considered. This needs to be changed for a massive calculation and ideally be implemented in the `Golem90` library.

$\langle \text{introduce form factors 38} \rangle \equiv$

```
#Do r=0, '$maxrank'
  #Include- ff-'$loopsz'-'r'.h
#EndDo
  Id a10(?all) = 0;
  Id a11(?all) = 0;◇
```

Macro referenced in 39.

In a last step the notation is changed from the function `DELTA` to the vectors $D^i x^j$.

$\langle \text{perform integration 39} \rangle \equiv$

```

#$maxrank = 0;
#$rank = 0;
Id MOMENTUM(n, -vec?qSET, iMU?) = - MOMENTUM(n, vec, iMU);
⟨read propagator masses 36⟩
⟨construct tensor integral 37⟩
.sort
⟨introduce form factors 38⟩
Id DELTA(vec?, vec?, iMU?) = 0;
#Do i=1,{'$loopsz'-1}
    #Do j={'i'+1},'$loopsz'
        Id DELTA(r'i', r'j', iMU?) = MOMENTUM(4, D'i'x'j', iMU);
        Id DELTA(r'j', r'i', iMU?) = -MOMENTUM(4, D'i'x'j', iMU);
    #EndDo
#EndDo◇

```

Macro referenced in 53.

5.2.4. *SO(N) Algebra*. After integration many simplifications can be made to the LORENTZ algebra since all $n \neq 4$ dimensional vectors have been eliminated during integration. All momenta and metric tensors are contracted as far as possible.

⟨carry out LORENTZ algebra 40⟩ ≡

```

Id gTensor(n, i1?, i1?) = 4 - 2 * eps;
Argument MOMENTUM;
#Call kinematics()
EndArgument;
Id MOMENTUM(n, iNU?, iMU?) = MOMENTUM(4, iNU, iMU);
Repeat Id gTensor(n, iMU?, iNU?) * MOMENTUM(4, vec?, iMU?) =
    MOMENTUM(4, vec, iNU);
Repeat Id gTensor(n, iMU?, iNU?) * SpinorTrace(?head, gg(n, iMU?), ?tail) =
    SpinorTrace(?head, gg(n, iNU), ?tail);
Repeat Id MOMENTUM(4, vec?, iMU?) * SpinorTrace(?head, gg(n, iMU?), ?tail) =
    SpinorTrace(?head, gg(4, vec), ?tail);
Id MOMENTUM(4, vec1?, iMU?) * MOMENTUM(4, vec2?, iMU?) = vec1.vec2;
#Call kinematics()
Argument SpinorTrace;
    Id vec? = gg(4, vec);
EndArgument;◇

```

Macro referenced in 53.

Although no n -dimensional vectors remain after integration one still has to deal with n -dimensional DIRAC matrices unless one decides to work in the DR scheme. The code below implements the commutator according to the 'tHo scheme,

$$(588) \quad (\hat{\gamma}^\mu + \bar{\gamma}^\mu)\gamma_5 = \gamma_5(-\hat{\gamma}^\mu + \bar{\gamma}^\mu)$$

and follows largely the Algorithms 5 and 6.

⟨ n -dimensional spinor algebra 41⟩ ≡

```

Normalize SpinorTrace;
Repeat Id SpinorTrace(?head, gg(n, iMU?), ?tail) =

```

```

    SpinorTrace(?head, gg(4, iMU), ?tail) +
    SpinorTrace(?head, gg([-2eps], iMU), ?tail);
⟨move  $\bar{\gamma}^\mu$  right 42⟩
⟨split traces 43⟩
⟨evaluate  $(n-4)$ -dimensional traces 44⟩
.sort

* Get rid of the gTensors:
Repeat Id gTensor([-2eps], i1?, i2?) * gTensor([-2eps], i2?, i3?) =
    gTensor([-2eps], i1, i3);

Id gTensor([-2eps], i1?, i1?) = -2 * eps;
Id gTensor([-2eps], i1?, i2?) * SpinorTrace(?head, gg(4, i2?), ?tail) = 0;
◇

```

Macro referenced in 53.

In order to split the traces into a 4-dimensional trace and a $(n-4)$ -dimensional one all $\bar{\gamma}^\mu$ are shuffled to the right according to the commutation rules.

⟨move $\bar{\gamma}^\mu$ right 42⟩ \equiv

```

Repeat;
  Id SpinorTrace(?head gg([-2eps], iMU?), gg(4, ?any), ?tail) =
    -SpinorTrace(?head, gg(4, ?any), gg([-2eps], iMU), ?tail);
  Id SpinorTrace(?head gg([-2eps], iMU?), hProjector(cc0?), ?tail) =
    SpinorTrace(?head hProjector(cc0), gg([-2eps], iMU), ?tail);
  Id SpinorTrace(?head gg(4, ?any), hProjector(cc0?), ?tail) =
    SpinorTrace(?head hProjector(-cc0), gg(4, ?any), ?tail);
  Id SpinorTrace(hProjector(cc0?), hProjector(cc0?), ?tail) =
    SpinorTrace(hProjector(cc0), ?tail);
  Id SpinorTrace(hProjector(1), hProjector(-1), ?tail) = 0;
  Id SpinorTrace(hProjector(-1), hProjector(1), ?tail) = 0;
EndRepeat;◇

```

Macro referenced in 41.

For the splitting three cases have to be considered for technical reasons: the first $(n-4)$ -dimensional matrix being adjacent to a 4-dimensional DIRAC matrix, being adjacent to a projector and finally being the first matrix in the trace. The function **TEMPTRACE** carries the number of DIRAC matrices as the first argument. The splitting into two traces is based on Equation (184).

⟨split traces 43⟩ \equiv

```

  Id SpinorTrace(?head, gg(4, ?any), gg([-2eps], iNU?), ?tail) =
    SpinorTrace(?head, gg(4, ?any)) *
    TEMPTTRACE(nargs_(?tail) + 1, gg([-2eps], iNU), ?tail);
  Id SpinorTrace(hProjector(cc0?), gg([-2eps], iNU?), ?tail) =
    4 * (1/2) * TEMPTTRACE(nargs_(?tail) + 1, gg([-2eps], iNU), ?tail);
  Id SpinorTrace(gg([-2eps], iNU?), ?tail) =
    4 * TEMPTTRACE(nargs_(?tail) + 1, gg([-2eps], iNU), ?tail);◇

```

Macro referenced in 41.

The $(n-4)$ dimensional trace can be evaluated by the usual rules. In fact Equation (188) is sufficient for a reduction of the traces, as has been shown earlier. The algorithm below implements this equation. The initial replacement $\text{gg}([-2\text{eps}], \text{iMU?}) \rightarrow \text{iMU}$ starts the loop over the sum of all swaps in Equation (188). For traces of length 4 and below explicit formulæ are used for efficiency.

$\langle \text{evaluate } (n-4)\text{-dimensional traces 44} \rangle \equiv$

```

Id TEMPTRACE(cc0?odd_, ?tail) = 0;
Repeat;
  Id TEMPTRACE(cc0?{>4}, gg([-2eps], iMU?), ?tail) =
    TEMPTRACE(cc0, iMU, ?tail);
  Repeat Id TEMPTRACE(cc0?{>4}, ?head, iMU?,
    gg([-2eps], iNU?), ?tail) =
    gTensor([-2eps], iMU, iNU) * TEMPTRACE(cc0 - 2, ?head, ?tail)
    - TEMPTRACE(cc0, ?head, gg([-2eps], iNU), iMU ?tail);
  Id TEMPTRACE(cc0?{>4}, ?head, iMU?) = 0;
EndRepeat;
Id TEMPTRACE(2, gg([-2eps], i1?), gg([-2eps], i2?)) =
  gTensor([-2eps], i1, i2);
Id TEMPTRACE(4, gg([-2eps], i1?), gg([-2eps], i2?),
  gg([-2eps], i3?), gg([-2eps], i4?)) =
  + gTensor([-2eps], i1, i2) * gTensor([-2eps], i3, i4)
  - gTensor([-2eps], i1, i3) * gTensor([-2eps], i2, i4)
  + gTensor([-2eps], i1, i4) * gTensor([-2eps], i2, i3);◇

```

Macro referenced in 41.

The only remaining LORENTZ indices in the expression are those connecting DIRAC matrices in the traces. In Section 1 of Chapter 1 it has been shown that the CHISHOLM identities can be used to achieve an index-free expression. The procedure **hProjectorSimplify** needs to be invoked repeatedly to restore the canonical order of the trace, i.e. to shuffle all helicity projectors to the left after one of the CHISHOLM identities has been applied. The **Bracket** statement allows for a more efficient evaluation since only the relevant factors of each term are considered in the replacements and the overall number of terms can be temporarily reduced, since **FORM** groups terms with the same spinor traces into one bracket.

The last four replacements carry out immediate simplifications and bring the traces into a standard form which is used later: the first argument of each trace is a number $\{\pm 1, 0\}$ that either represents the projector or the identity matrix.

$\langle \text{eliminate LORENTZ indices 45} \rangle \equiv$

```

Repeat Id SpinorTrace(?head, gg(4, i1?), ?tail) =
  SpinorTrace(?head, i1, ?tail);
Bracket SpinorTrace;
.sort;
Keep Brackets;
#Call hProjectorSimplify()

```

```

Repeat;
  < deal with situation tr{... $\gamma^\mu$ ... $\gamma_\mu$ ...} 46 >
  < deal with situation tr{... $\gamma^\mu$ ...} tr{... $\gamma_\mu$ ...} 47 >
  #Call hProjectorSimplify()
Endrepeat;
Id SpinorTrace() = 4;
Id SpinorTrace(hProjector(cc0?)) = 2;
Id SpinorTrace(hProjector(cc0?), ?tail) = SpinorTrace(cc0, ?tail);
Id SpinorTrace(vec?, ?tail) = SpinorTrace(0, vec, ?tail);◇

```

Macro referenced in 53.

One possible contraction of LORENTZ indices is inside the same trace. In the first rule the part of the trace between the two contracted matrices is stored in the function `ANY0` together with the length of the strip. The second rule ensures that all projectors have been moved to the left properly. The remaining rules distinguish between the cases where the strip is of even or odd length according to Equations (192) and (194).

< deal with situation tr{... γ^μ ... γ_μ ...} 46 > \equiv

```

Id Once SpinorTrace(?head, i1?, ?mid, i1?, ?tail) =
  ANY0(nargs_(?mid), ?mid) * SpinorTrace(?head, ANY0, ?tail);
Id ANY0(?head, hProjector(cc0?), ?tail) = TEMPERRORTOKEN;
Id ANY0(cc0?odd_, ?mid) * SpinorTrace(?head, ANY0, ?tail) =
  - 2 * SpinorTrace(?head, reverse_(?mid), ?tail);
Id ANY0(cc0?even_, ?mid, vec?) * SpinorTrace(?head, ANY0, ?tail) =
  + 2 * SpinorTrace(?head, vec, ?mid, ?tail)
  + 2 * SpinorTrace(?head, reverse_(?mid), vec, ?tail);
Id ANY0(cc0?even_, ?mid, i1?) * SpinorTrace(?head, ANY0, ?tail) =
  + 2 * SpinorTrace(?head, i1, ?mid, ?tail)
  + 2 * SpinorTrace(?head, reverse_(?mid), i1, ?tail);
Id ANY0(0) * SpinorTrace(?head, ANY0, ?tail) =
  + 4 * SpinorTrace(?head, ?tail);◇

```

Macro referenced in 45.

The remaining case is the situation with a product of two traces connected by a LORENTZ contraction. Here Equation (195) applies.

< deal with situation tr{... γ^μ ...} tr{... γ_μ ...} 47 > \equiv

```

Id SpinorTrace(?h1, i1?, ?t1) * SpinorTrace(?h2, i1?, ?t2) =
  + 2 * SpinorTrace(?t2, ?h2, ?t1, ?h1)
  + 2 * SpinorTrace(?t2, ?h2, reverse_(?t1, ?h1));◇

```

Macro referenced in 45.

5.2.5. Subexpression Elimination. The following section describes the simplest form of an incomplete elimination of common subexpressions. In a first step all remaining propagators that are not part of the loop integral are stripped from the diagram and stored in a dollar variable.

```

⟨strip propagators 48⟩ ≡
    Argument POW;
    #Call kinematics()
EndArgument;
Id POW(cc0?, -1) = TEMP(cc0);
Multiply TEMP(1);
Repeat Id TEMP(cc0?) * TEMP(cc1?) = TEMP(cc0 * cc1);
Bracket TEMP;
.sort
#$props = 1;
Keep Brackets;Id TEMP(cc0?$props) = 1;
.sort◊

```

Macro referenced in 53.

In a next step all form factors are replaced by symbols. These symbols are generated by the Python program `golem.py` such that equivalent form factors have the same symbol across all diagrams.

Before the actual replacement all form factors are symmetrised over their indices which to minimise the number of different terms.

```

⟨symmetrise form factors 49⟩ ≡
    #Do r=2,{'$maxrank'}
        Symmetrize a['$loopsize','r', 1, ..., 'r'];
        #If ('r' > 2) && ('$loopsize' < 6)
            Symmetrize b['$loopsize','r', 1, ..., {'r'-2}];
        #EndIf
        #If ('r' > 4) && ('$loopsize' < 6)
            Symmetrize b['$loopsize','r', 1, ..., {'r'-4}];
        #EndIf
    #EndDo◊

```

Macro referenced in 50.

The procedure `recfind` builds all possible form factors and carries out the necessary steps for their replacement. All powers of ε higher than ε^2 are removed beforehand to avoid spurious calculations⁹

```

⟨replace form factors by symbols 50⟩ ≡

    ⟨symmetrise form factors 49⟩
    Id eps^n?{>=3} = 0;
    #Do r=0, '$maxrank'
        #Call recfind(a['$loopsize','r', '$loopsize', 'r'])
    #EndDo
    #If '$loopsize' < 6
        #Do r=2, '$maxrank'
            #Call recfind(b['$loopsize','r', '$loopsize', {'r'-2}])
        #EndDo
        #Do r=4, '$maxrank'
            #Call recfind(c['$loopsize','r', '$loopsize', {'r'-4}])
        #EndDo
    #EndIf◊

```

⁹The highest order of divergence in a form factor is ε^{-2} at one-loop.

Macro referenced in 53.

A similar strategy as for the form factors is pursued for the spinor traces. For each trace an expression is obtained from the Python program `golem.py` which consists of a polynomial of symbols representing canonical traces; therefore the `FromExternal` statement receives a replacement rule that replaces the trace which has been matched by the previous `Id` statement in the loop.

```

⟨replace spinor traces by constants 51⟩ ≡
  #$dummy = 0;
  #Define TREXP "ERR"
  #Do sp=1,1
    #$dummy = {'$dummy'+1};
    Id IfMatch->labsp'$dummy'
      SpinorTrace(cc?$spsign, ?tail$spmoms) = SpinorTrace(cc, ?tail);
    Goto labsp'$dummy'fail;
    Label labsp'$dummy';
    ReDefine sp, "0";
    Label labsp'$dummy'fail;
  .sort
  #If 'sp' == 0
    #ToExternal "TR '$spsign','$spmoms'\n"
    #FromExternal
    Id SpinorTrace('$spsign','$spmoms') = 'TREXP';
  #EndIf
  #EndDo◇
Macro referenced in 53.

```

5.2.6. *Summary.* Below the topics which have been discussed above are put in order. The procedure `FeynmanRules` is defined in a file `'THEORY'.h` and replaces the propagator- and vertex-functions and the external states by their actual representations according to the FEYNMAN rules. The procedure `masses` is defined in `process.h` and typically contains a statement to replace particle masses by zero, e.g. to use a massless approximation for the u , d and s quark one would define the procedure as follows:

```

#procedure masses()
  Multiply replace_(emu, 0, emd, 0, ems, 0);
#endprocedure

```

After splitting the expressions into the distinct colour structures the $SU(N)$ algebra is carried out by calling the procedure `sunsimplify`; then each colour structure is projected on the colour basis.

The spinor lines are completed to traces by insertions of appropriate ratios of the form

$$\langle k_{i,\pm} | \Gamma_{ij} | k_{j,\pm} \rangle = \langle k_{i,\pm} | \Gamma_{ij} | k_{j,\pm} \rangle \frac{\langle k_{j,\pm} | \not{n} | k_{i,\pm} \rangle}{\langle k_{j,\pm} | m_{\mp} \rangle \langle m_{\mp} | k_{i,\pm} \rangle} = \frac{\text{tr}^{\pm} \{ k_i \Gamma_{ij} k_j \not{n} \}}{\langle k_{j,\pm} | m_{\mp} \rangle \langle m_{\mp} | k_{i,\pm} \rangle}.$$

The brackets in the denominator are evaluated numerically and go into a global prefactor:

```

⟨strip global factor 52⟩ ≡

```



```

Id 1/braket(?all) = ANYBRAKET(?all);
AntiBracket ANYBRAKET, g;
.sort
Collect PREFACTOR;
Normalize PREFACTOR;
Id PREFACTOR(cc0?$prefactor) = 1;
.sort◊

```

Macro referenced in 53.

A call to the procedure **buildspinorlines** does the contractions of the form $|k_{\pm}\rangle \langle k_p m| = \Pi_{\pm} \not{k}$.

The integrals are translated into form factors after that step so that no n -dimensional vectors remain in the expression. All traces containing the $(n-4)$ -dimensional DIRAC matrices $\bar{\gamma}^{\mu}$ are carried out in the next step and all explicit appearances of LORENTZ indices are eliminated. Finally some of the subexpressions are replaced by symbols before the expression is written into a **Fortran** file.

\langle simplification algorithm 53 $\rangle \equiv$

```

 $\langle$  make all momenta ingoing 26  $\rangle$ 
   $\langle$  determine graph topology 28  $\rangle$ 
   $\langle$  introduce momenta  $q_i$  and  $r_i$  for one-loop processes 27  $\rangle$ 
  #Call FeynmanRules()
  #Call masses()
  #Call RemoveMetricTensors()
  .sort
   $\langle$  split into colour structures 32  $\rangle$ 
  #Call sunsimplify()
   $\langle$  project on colour basis 34  $\rangle$ 
  #Call spinorties()
   $\langle$  strip global factor 52  $\rangle$ 
  #Call buildspinorlines()
  .sort
  #If 'LOOPS' == 1
     $\langle$  perform integration 39  $\rangle$ 
  #EndIf
  Id PROP(vec?, cc?) = POW(vec.vec - cc^2, -1);
  Id PROP(vec?, 0) = POW(vec.vec, -1);
  .sort
   $\langle$  carry out LORENTZ algebra 40  $\rangle$ 
   $\langle$   $n$ -dimensional spinor algebra 41  $\rangle$ 
   $\langle$  eliminate LORENTZ indices 45  $\rangle$ 
  .sort
   $\langle$  strip propagators 48  $\rangle$ 
  #If ('LOOPS' == 1)
     $\langle$  replace form factors by symbols 50  $\rangle$ 
  #Else
    Id eps^n?{>0} = 0;
  #EndIf
   $\langle$  replace spinor traces by constants 51  $\rangle$ 
  .sort

```

⟨evaluate colour vector numerically 35⟩◇

Macro referenced in 23.

5.3. Generation of the Fortran File. In this section the output generated by the FORM program is described. FORM supports the programmer in generating files in other languages than FORM by providing the `Format` statement which sets the format of the output to the desired format. However, this format only applies to expressions; therefore the dollar variables `$prefactor` and `$props` are written to local expressions to allow FORM to take control over their format.

⟨output section 54⟩ ≡

```
#Define COUNTER "$counter"
#Define LOOPSIZE "$loopsize"
Format Fortran;
.sort
Local prefactor = '$prefactor';
Local props = '$props';
Id ANYBRACKET(?all) = 1/braket(?all);
.sort

#Write <'OUT'> "module      'PREFIX' 'DIAG' 'HELICITY'"
⟨write header of Fortran module 55⟩
#Write <'OUT'> "contains"
⟨write function for diagram 56⟩
#Write <'OUT'> "end module 'PREFIX' 'DIAG' 'HELICITY'"◇
```

Macro referenced in 23.

The header of the Fortran file contains also information about the file creation such as the FORM version and the creation date; this can be valuable if one tries to trace back which files are affected by problems in other components of the code. The rest of the header is the import of all relevant module files.

⟨write header of Fortran module 55⟩ ≡

```
#Write <'OUT'> "! Created by FORM 'VERSION_'.'SUBVERSION_'"
#Write <'OUT'> " 'NAMEVERSION_'"
#Write <'OUT'> "!          from file 'NAME_', 'DATE_'"
#Write <'OUT'> "!"
#Write <'OUT'> ""
#Write <'OUT'> "    use precision"
#Write <'OUT'> "    use form_factor_type"
#Write <'OUT'> "    use algebra"
#Write <'OUT'> "    use param"
#Write <'OUT'> "    use 'PREFIX'_tr"
#If 'LOOPS'==1
    #Write <'OUT'> "    use 'PREFIX'_ff"
#EndIf
#Write <'OUT'> "    use mandelstam'LEGS'"
#Write <'OUT'> "    implicit none"◇
```

Macro referenced in 54.

The second part of the output section writes a function that calculates a single diagram for the given helicity. After all variables are defined and initialised the colour vector is calculated; in the last section the expressions for each colour structure are printed out and all parts are summed up.

\langle write function for diagram 56 $\rangle \equiv$

```
#Write <'OUT'> "function      'PREFIX' 'DIAG' h 'HELICITY' (vecs) result(res)"
#Write <'OUT'> "    implicit none"
   $\langle$  write variable declarations 57  $\rangle$ 
   $\langle$  initialise local variables 59  $\rangle$ 
  .sort
   $\langle$  write colour vector 58  $\rangle$ 
   $\langle$  combine result 60  $\rangle$ 
#Write <'OUT'> "end function 'PREFIX' 'DIAG' h 'HELICITY'"
```

Macro referenced in 54.

The input to the function is a list of the four-vectors k_1, \dots, k_N in unphysical, i.e. all ingoing kinematics. As result the function returns a vector containing a form factor type for each colour basis element. The variables **props** and **prefactor** are the quantities which have been stripped off the expression earlier. The variables **result*i*** contain the coefficients of each colour structure and the variables **basis*i*** contain the associated colour vector.

\langle write variable declarations 57 $\rangle \equiv$

```
#Write <'OUT'> "    real(ki), dimension('LEGS',4), intent(in) :: vecs"
#Write <'OUT'> "    type(form_factor), dimension(1:'NUMCS') :: res"
#Write <'OUT'> "    integer :: i"
#Write <'OUT'> "    complex(ki) :: props, prefactor"
#Do i=1,'COUNTER'
  #Write <'OUT'> "    type(form_factor) :: result'i'"
  #Write <'OUT'> "    real(ki), dimension(1:'NUMCS') :: basis'i'"
#EndDo
#Write <'OUT'> "    real(ki), dimension(4) :: k1%"
#Do i=2,'LEGS'
  #Write <'OUT'> " ,k'i'%"
#EndDo
#Write <'OUT'> ""
```

Macro referenced in 56.

In order to keep the code human-readable all entries of the colour vectors are denoted both numerically and as a comment symbolically. After each colour vector the according coefficient is printed. The line **! VAR result'*i*'** is a sentinel for the **awk** script that postprocesses the output: if the format is set to produce **Fortran** code, **FORM** breaks each expression into chunks which are separated by the indicator "**_ = _**", where the underscores need to be replaced by the variable name. The reason for this is that most

Fortran compilers only allow a limited number of continuation lines. The comment line above instructs the awk script to set `result'i'` as the new variable name and replaces the sentinel sequence accordingly.¹⁰

⟨write colour vector 58⟩ ≡

```
#Do i=1,'COUNTER'
  #Do c=1,'NUMCS'
    #Write <'OUT'> "    basis'i'('c') = %$", $basis'i'x'c'
    #Write <'OUT'> "    basis'i'('c') = %E", basis'i'x'c'
  #EndDo
  #Write <'OUT'> "    ! VAR result'i'"
  #Write <'OUT'> "    result'i' = %E", struct'i'
#EndDo◇
```

Macro referenced in 56.

The code sets up variables k_i because the variable `LEGPERMUTATION` is given in that format. The subroutine `yvariables` globally defines symbols for the `MANDELSTAM` variables according to the current permutation of external legs.

⟨initialise local variables 59⟩ ≡

```
#Do i=1,'LEGS'
  #Write <'OUT'> "    k'i'(1:4)=vecs('i', 1:4)"
#EndDo
#Write <'OUT'> "    call yvariables('LEGPERMUTATION')"
.sort
#Write <'OUT'> "    ! VAR props"
#Write <'OUT'> "    props = %E", props
#Write <'OUT'> "    ! VAR prefactor"
#Write <'OUT'> "    prefactor = %E", prefactor
#Write <'OUT'> "    prefactor = prefactor / props"◇
```

Macro referenced in 56.

The last part of the function runs a loop over all colour structures to add up the results. In the very end the prefactor that is global to all terms is multiplied.

⟨combine result 60⟩ ≡

```
#Write <'OUT'> "    do i = 1, 'NUMCS'"
  #Write <'OUT'> "        res(i) = result1 * basis1(i)%"
  #Do i = 2,'COUNTER'
    #Write <'OUT'> "&"
    #Write <'OUT'> "        &          + result'i' * basis'i'(i)%"
  #EndDo
  #Write <'OUT'> ""
  #Write <'OUT'> "        res(i) = res(i) * prefactor"
  #Write <'OUT'> "    end do"◇
```

Macro referenced in 56.

¹⁰ At that point 'i' is already replaced by a number.

5.4. Subroutines. Subroutines — or procedures, as they are called in FORM — serve several purposes. One reason for using procedures is to structure the source code into smaller pieces that can be understood independently; in FORM one can write procedures into separate files which adds a physical structure to the code on top of the logical structure. In addition procedures can be parametrised and hence be reused in different places of the code. They also support recursion, a feature that has been used in the procedure `findff`, which together with `recfind` replaces the form factors.

`< define procedures 61 > ≡`

```

< define procedure TopologyInfo 62 >
  < define procedure IntroduceRMomenta 71 >
  < define procedure RemoveMetricTensors 74 >
  < define procedure recfind 75 >
  < define procedure kinematics 79 >
  < define procedure hProjectorSimplify 80 >
  < define procedure sunsimplify 87 > >

```

Macro referenced in 23.

5.4.1. *Determination of the Loop Topology.* In the massless case the S matrix is fully determined by two pieces of information: given any planar embedding of the FEYNMAN diagram into the two-dimensional drawing plane then the order in which the external lines are traversed when walking around the diagram defines a permutation of the symbols $\{k_1, \dots, k_N\}$. In an unpinched graph, i.e. a graph which contains a loop of size N this permutation is unique up to a cyclic permutation of the legs and a \mathbb{Z}_2 symmetry. These two symmetries define the freedom of choosing a starting point and the direction in which one starts the traversal. For a pinched graph, i.e. a graph of girth smaller than N , there are additional symmetries.

If π is the permutation denoting the order of the legs (“LEGPERMUTATION”) and in the pinched kinematics $r_{i+1} - r_i = k_{a_1} + \dots + k_{a_p}$ for some sequence a_1, \dots, a_p such that¹¹ $a_i = \pi(i_0 + i)$ then k_{a_2}, \dots, k_{a_p} are part of the pinch list, and the pinch list (“PINCHES”) is built by all those sequences for i running over all loop propagators. If the graph is tree level the permutation is fixed to be the identity and all legs are in the pinch list.

`< define procedure TopologyInfo 62 > ≡`

```

#Define LEGPERMUTATION ""
#Define PINCHES ""
#Procedure TopologyInfo()
  < introduce edge and node functions 63 >
  < remove node functions 64 >
  < collect momenta in the loop 65 >
  < determine $loopsz and  $r_i$  66 >
  .sort
  #If '$loopsz' > 1
    < calculate  $\Delta_{i,i+1}$  69 >
    < determine the permutation of the legs and the pinches 70 >
  #Else

```

¹¹As usual the indices have to be cyclically continued $i + N \equiv i$.

```

#ReDefine LEGPERMUTATION "k1"
#Do i=2,'LEGS'
  #ReDefine LEGPERMUTATION "'LEGPERMUTATION',k'i'"
#EndDo
#ReDefine PINCHES "'LEGPERMUTATION'"
#EndIf
#EndProcedure◇

```

Macro referenced in 61.

The code decorates any propagator function with a function called **edge** that contains the momentum and the indices denoting both ends of the propagator as parameters; all vertices, similarly are multiplied by a function called **node** that contains a index labelling the vertex and the indices of the according end-points of all adjacent propagators.

The program restricts the degree of the vertices to three and four, which can be changed if one needs to examine other quantum field theories that contain higher degree vertices.

(introduce **edge** and **node** functions 63) \equiv

```

Id ANY?PropagatorFunction
  (ccFlavour?, iPROP?, k1?, ccMass?, iFrom?, iTo?) =
  ANY(ccFlavour, iPROP, k1, ccMass, iFrom, iTo) *
  edge(k1, iFrom, iTo);

#Do deg=3,4
  id ANY?VertexFunction(iVertex?
  #Do i=1,'deg'
    , ANYP'i'?(ccFlavour'i?', iPROP'i?', k'i?', ccMass'i'?
    , iFrom'i?', iTo'i'?)
  #EndDo
  ) =
  ANY(iVertex
  #Do i=1,'deg'
    , ANYP'i'(ccFlavour'i', iPROP'i', k'i', ccMass'i'
    , iFrom'i', iTo'i')
  #EndDo
  ) * node(iVertex, iFrom1, ..., iFrom'deg');
#EndDo◇

```

Macro referenced in 62.

The functions **node** can be eliminated if the indices denoting the endpoints of each edge are replaced by the indices denoting the vertices themselves; the full information about the topology is still preserved.

(remove **node** functions 64) \equiv

```

Repeat Id node(iVertex?, ?mid, iFrom?, ?end) *
  edge(p1?, iFrom?, i2?) =
  node(iVertex, ?mid, iFrom, ?end) * edge(p1, iVertex, i2);
Repeat Id node(iVertex?, ?mid, iFrom?, ?end) *

```

```

edge(p1?, i1?, iFrom?) =
  node(iVertex, ?mid, iFrom, ?end) * edge(p1, i1, iVertex);
Id node(?all) = 1;◇

```

Macro referenced in 62.

The form of the expression which has just been achieved is now suited for the use with the **ReplaceLoop** statement. It scans the arguments of the **edge** functions for a closed loop of indices and replaces the list of remaining arguments, which in this case is a list of the momenta of the propagators in the loop, by the function **circle**. The important feature of the **ReplaceLoop** statement is that it preserves the order of the arguments; the function **circle** is defined as cycle-symmetric; to fix the starting point for counting the first argument is chosen to be **p1**. The function **node** is chosen instead of **circle** because of the symmetry of the **circle** function¹². The statement **SplitArg** allows to separate the $q_i = p + r_i$ into the pair (p, r_i) .

⟨collect momenta in the loop 65⟩ ≡

```

ReplaceLoop edge, arguments=3, loopsize=all, outfun=circle;
Id edge(k1?, iFrom?, iFrom?) = circle(k1);
Id edge(k1?, iFrom?, iTo?) = 1;
Id circle(p1, ?tail) = node(0, ?tail);
Id circle(-p1, ?tail) = node(0, ?tail);
Repeat;
  SplitArg (p1), node;
  Id node(?head, k1?, -p1, ?tail) = node(?head, -k1, ?tail);
  Id node(?head, k1?, p1, ?tail) = node(?head, k1, ?tail);
EndRepeat;◇

```

Macro referenced in 62.

The arguments of the function **node** are read into the dollar variables $\$r_i$. The size of the loop can easily be determined by counting the arguments using the built-in function **nargs_**. It should be noted that the vectors r_i are chosen such that $r_{\$loopsize} = 0$.

⟨determine \$loopsize and r_i 66⟩ ≡

```

Id node(?all) = node(nargs_(?all), ?all);
Id node(cc0?$loopsize, ?all) = node(?all);
.sort
Id node(cc0?$r'$loopsize'
  #Do i=1, {'$loopsize'-1}
    , k'i'?$r'i'
  #EndDo
) = 1;◇

```

Macro referenced in 62.

In the next scrap the program makes use of the fact that all external momenta are chosen to be ingoing. The main difficulty in determining the permutation of the external vectors and the pinch list is the ambiguity in the representation of a sum of external

¹² The function **circle** would “forget” about the earlier choice of a starting point.

vectors $v = k_{i_1} + \dots + k_{i_p}$: because of momentum conservation $z = k_1 + \dots + k_N = 0$ the vectors v and $(v \pm z)$ are the same. However, the program has to choose one of the three representations which ensures that one ends up with a list of all vectors.

The algorithm starts from a list of all $\Delta_{i,i+1}$ which is stored in the argument list of a function **TEMPLegs**.

$\langle \text{list all } \Delta_{i,i+1} \text{ 67} \rangle \equiv$

```
Multiply TEMPLegs(
    $r1 - $r'$loopsize'
    #Do i=2,'$loopsize'
        , $r{'i'} - $r{'i'-1}
    #EndDo
);◇
```

Macro referenced in 69.

Then each argument v in the list is replaced by a pair $(v \cdot \eta, v)$; after one substitutes $k_i \cdot \eta = 1$ the first entry in the pair becomes an integer number which counts the number of external vectors in the sum and is either positive if v is the list of vectors to be used in the permutation, or negative if instead the list is $(z - v)$.

$\langle \text{discriminate } v \text{ and } (v - z) \text{ 68} \rangle \equiv$

```
Repeat Id TEMPLegs(?head, p1?, ?tail) =
    TEMPLegs(?head, node(p1.vec, p1), ?tail);
Argument TEMPLegs;
Argument node;
    Id p1?{k1,...,k'LEGS'}.vec = 1;
EndArgument;
Id node(cc0?neg_, p1?) =
    node(-p1, 0, (k1 + ... + k'LEGS') + p1);
Id node(cc0?pos_, p1?) =
    node((k1 + ... + k'LEGS') - p1, 0, p1);
SplitArg node;
EndArgument;◇
```

Macro referenced in 69.

The function **TEMPLegs** is split into two lists **TEMPHeads** and **TEMPTails**, each containing either all v or all $(z - v)$.

$\langle \text{calculate } \Delta_{i,i+1} \text{ 69} \rangle \equiv$

```
 $\langle \text{list all } \Delta_{i,i+1} \text{ 67} \rangle$ 
 $\langle \text{discriminate } v \text{ and } (v - z) \text{ 68} \rangle$ 
Id TEMPLegs(?all) = TEMPHeads(?all) * TEMPTails(?all);
Repeat Id TEMPHeads(?a, node(?head, 0, ?tail), ?b) =
    TEMPHeads(?a, node(?head), ?b);
Repeat Id TEMPTails(?a, node(?head, 0, ?tail), ?b) =
    TEMPTails(?a, node(?tail), ?b);◇
```


Macro referenced in 62.

A priori it is not clear how the diagram generator chooses to denote the momenta in the graph. Therefore both choices, v and $(z - v)$ are considered as possibilities. In the end those lists are selected which have the right number of arguments, i.e. the list of legs must have 'LEGS' elements and the list of pinches ('LEGS' - \$loopsz).

\langle determine the permutation of the legs and the pinches 70 $\rangle \equiv$

```

Id TEMPHeads(?all) = TEMPLEgs(?all) * TEMPPinches(?all);
Id TEMPTails(?all) = TEMPLEgs(?all) * TEMPPinches(?all);
Repeat Id TEMPLEgs(?head, node(?all), ?tail) =
    TEMPLEgs(?head, ?all, ?tail);
Repeat Id TEMPPinches(?head, node(?pinches, p1?), ?tail) =
    TEMPPinches(?head, ?pinches, ?tail);
Id TEMPLEgs(p1?, ?all) = TEMPLEgs(nargs_(p1, ?all), p1, ?all);
Id TEMPPinches(p1?, ?all) = TEMPPinches(nargs_(p1, ?all), p1, ?all);
Id TEMPPinches() = TEMPPinches(0);
Id TEMPLEgs('LEGS', ?all$legperm) = 1;
Id TEMPLEgs(cc0?, ?all) = 1;
Id TEMPPinches({'LEGS'-'$loopsz'}, ?all$legpinches) = 1;
Id TEMPPinches(cc0?, ?all) = 1;
.sort
#ReDefine LEGPERMUTATION "$legperm"
#ReDefine PINCHES "$legpinches"◇

```

Macro referenced in 62.

5.4.2. *The procedure IntroduceRMomenta.* The procedure `IntroduceRMomenta` replaces sums of momenta that correspond to r_i or $\Delta_{ij} = (r_i - r_j)$ or $q_i = p + r_i$ by a single vector. These replacements are only done within propagators. The loop over Z ensures that different representations of the same sum of external vectors are caught by the same set of substitution rules.

\langle define procedure IntroduceRMomenta 71 $\rangle \equiv$

```

#Procedure IntroduceRMomenta()
     $\langle$  find  $q_i$  vectors 72  $\rangle$ 

    $zero = k1 + ... + k'LEGS';
    #Do Z={0, '$zero', -('$zero')}
         $\langle$  find  $r_i$  and  $\Delta_{ij}$  73  $\rangle$ 
    #EndDo
#EndProcedure◇

```

Macro referenced in 61.

The first set of replacements tries to match sums that correspond to the vectors q_i . Only the two cases stemming from different overall signs have to be considered.

\langle find q_i vectors 72 $\rangle \equiv$

```

#Do i=1, '$loopsz'
  Id ANYP?PropagatorFunction(ccFlavour?, iPROP?, p1 + ('$r'i'),
    ccMass?, iFrom?, iTo?) =
    ANYP(ccFlavour, iPROP, q'i', ccMass, iFrom, iTo);
  Id ANYP?PropagatorFunction(ccFlavour?, iPROP?, -p1 - ('$r'i'),
    ccMass?, iFrom?, iTo?) =
    ANYP(ccFlavour, iPROP, -q'i', ccMass, iFrom, iTo);
#EndDo

```

Macro referenced in 71.

The substitution set inside the loop over Z, which runs over three different notations of the zero vector, considers the patterns for Δ_{ij} and Δ_{ji} for $i < j$ only.

$\langle \text{find } r_i \text{ and } \Delta_{ij} \text{ 73} \rangle \equiv$

```

#Do i=1, {'$loopsz'-1}
  #Do j={'i'+1}, '$loopsz'
    Id ANYP?PropagatorFunction(ccFlavour?, iPROP?,
      ('Z') + ('$r'i') - ('$r'j'),
      ccMass?, iFrom?, iTo?) =
      ANYP(ccFlavour, iPROP, D'i'x'j', ccMass, iFrom, iTo);
    Id ANYP?PropagatorFunction(ccFlavour?, iPROP?,
      ('Z') + ('$r'j') - ('$r'i'),
      ccMass?, iFrom?, iTo?) =
      ANYP(ccFlavour, iPROP, -D'i'x'j', ccMass, iFrom, iTo);
  #EndDo
#EndDo

```

Macro referenced in 71.

5.4.3. *The procedure RemoveMetricTensors.* As the name suggests the procedure `RemoveMetricTensors` tries to replace all KRONECKER deltas and metric tensors that occur in the expression and do not require special treatment.

$\langle \text{define procedure RemoveMetricTensors 74} \rangle \equiv$

```

#Procedure RemoveMetricTensors()
  Repeat;
    Id gTensor(n, i1?, i2?) * gTensor(n, i2?, i3?) =
      gTensor(n, i1, i3);
    Id gTensor(n, i1?, i2?) * MOMENTUM(n, k1?, i1?) =
      MOMENTUM(n, k1, i2);
    Id gTensor(n, i1?, i2?) * gg(n, i1?, is1?, is2?) =
      gg(n, i2, is1, is2);
    Id AdjointID(iA?, iB?) * T(i1?, i2?, iA?) =
      T(i1, i2, iB);
    Id AdjointID(iA?, iE?) * f(iA?, iB?, iC?) =
      f(iE, iB, iC);
    Id FundamentalID(i1?, i3?) * T(i1?, i2?, iA?) =
      T(i3, i2, iA);
    Id FundamentalID(i2?, i3?) * T(i1?, i2?, iA?) =
      T(i1, i3, iA);

```

```

EndRepeat;
#EndProcedure◊

```

Macro referenced in 61.

5.4.4. *Replacement of the Form Factors.* The procedure `findff` that scans for all form factors that can occur in a certain diagram is probably the least transparent of the procedures in this program. For the understanding of the procedure it should be noted that variables such as `fffound` which are declared inside the procedure are in a local context.

The main program calls the procedure `recfind` with the name of a form factor, the loop size and the number of indices; a typical call would look like “`#call recfind(b53,5,1)`” because the form factor $B_j^{5,1}(S)$ has one index j and belongs to a topology of loop size 5. The procedure `recfind` then calls `recfind1` if the number of indices is larger than one; it calls directly to `findff` if there are no indices.

```

⟨define procedure recfind 75⟩ ≡

#Procedure recfind(name,l,counter)
  #If 'counter' > 0
    #Call recfind1('name','l','counter')
  #Else
    #Call findff('name')
  #EndIf
#EndProcedure
⟨define procedure recfind1 76⟩
⟨define procedure findff 77⟩◊

```

Macro referenced in 61.

The procedure `recfind1` adds an index to the argument list and decreases the parameter `counter` by one before it calls itself recursively; if the counter reaches zero the procedure `findff` is called to actually do the substitution.

```

⟨define procedure recfind1 76⟩ ≡

#Procedure recfind1(name,l,counter,?args)
  #Define newcounter "{ 'counter'-1 }"
  #If 'counter' > 0
    #Do i=1,'l'
      #Call recfind1('name','l','newcounter','i','?args')
    #EndDo
  #Else
    #Call findff('name','?args')
  #EndIf
#EndProcedure◊

```

Macro referenced in 75.

Finally, the procedure `findff` builds a rewriting rule for a given form factor `'name'('args')` by communicating with the programme `golem.py` to obtain a global symbol that represents its value in the given topology.

$\langle \text{define procedure findff 77} \rangle \equiv$

```

#$dummy = 0;
#Procedure findff(name,?args)
  #$dummy = {'$dummy'+1};
  #Define fffound "0"

  Id IfMatch->lab'$dummy' 'name'('args','SNULL') =
    'name'('args','SNULL');
  Goto lab'$dummy'fail;
  Label lab'$dummy';
    Redefine fffound, "1";
  Label lab'$dummy'fail;
  .sort
  #If 'ffffound'
    #ToExternal "FF 'args' 'name' \n"
    #FromExternal
  #EndIf
#EndProcedure◇

```

Macro referenced in 75.

5.4.5. *define procedure kinematics*. The procedure `kinematics` replaces dot-products between momenta by MANDELSTAM variables. As a first step it removes all momenta abbreviations by their representation in external momenta.

$\langle \text{eliminate } r_i \text{ and } \Delta_{ij} \text{ 78} \rangle \equiv$

```

#If 'LOOPS' == 1
  #Do i=1,{'$loopsz'-1}
    #Do j={'i'+1},'$loopsz'
      Id D'i'x'j' = r'i' - r'j';
    #EndDo
  #EndDo
  #Do i=1,{'$loopsz'}
    Id r'i' = '$r'i'';
  #EndDo
#EndIf◇

```

Macro referenced in 79.

Then the MANDELSTAM variables are plugged in and the on-shell conditions are applied.

$\langle \text{define procedure kinematics 79} \rangle \equiv$

```

#Procedure kinematics()
   $\langle \text{eliminate } r_i \text{ and } \Delta_{ij} \text{ 78} \rangle$ 
  #Call mandelstam('LEGPERMUTATION')
  #Call onshell()

```

#EndProcedure kinematics◇

Macro referenced in 61.

5.4.6. *The procedure hProjectorSimplify.* The procedure `hProjectorSimplify` orders a trace with respect to the helicity projectors Π_{\pm} it contains.

⟨define procedure `hProjectorSimplify` 80⟩ ≡

```
#Procedure hProjectorSimplify()
  ⟨shuffle projectors to the left 81⟩
  ⟨use projector properties 82⟩
#EndProcedure◇
```

Macro referenced in 61.

First the projectors are shuffled to the left of the trace. If a trace contains more than one projector this ensures that they are all adjacent to each other.

⟨shuffle projectors to the left 81⟩ ≡

```
Repeat;
  Repeat Id SpinorTrace(?head, vec?, hProjector(cc0?), ?tail) =
    SpinorTrace(?head, hProjector(-cc0), vec, ?tail);
  Id SpinorTrace(?head, iMu?, hProjector(cc0?), ?tail) =
    SpinorTrace(?head, hProjector(-cc0), iMu, ?tail);
EndRepeat;◇
```

Macro referenced in 80.

In a second step the idempotence and the orthogonality of the projectors are used to obtain a simplification.

⟨use projector properties 82⟩ ≡

```
Repeat Id SpinorTrace
  (hProjector(cc0?), hProjector(cc0?), ?tail) =
  SpinorTrace(hProjector(cc0), ?tail);
Id SpinorTrace(hProjector(+1), hProjector(-1), ?tail) = 0;
Id SpinorTrace(hProjector(-1), hProjector(+1), ?tail) = 0;◇
```

Macro referenced in 80.

5.4.7. *Procedure for the Colour Algebra.* The colour algebra is carried out in a very similar manner as described in algorithm 1. To speed the rewriting up the procedure brackets off all factors that do not contain colour information.

⟨separate colour factor for efficiency 83⟩ ≡

```
Bracket AdjointID, FundamentalID, T, f;
.sort
Collect ANYNonColor;
```

```

Bracket AdjointID, FundamentalID, T, f;
.sort;
Keep Brackets;◇

```

Macro referenced in 87.

In the next step equation (48) is exploited to eliminate all structure constants f^{ABC} . The expression $2l + e - 2$, where l is the number of loops and e is the number of legs counts the maximum number of structure constants that can occur in a diagram of that complexity.

⟨eliminate f^{ABD} 84⟩ ≡

```

#Do i=1, {2*‘LOOPS’+‘LEGS’-2}
  Id Once f(iADJ1?, iADJ2?, iADJ3?) =
    -i_ * 1/TR * (
      + T(i'i'T0, i'i'T1, iADJ1) *
        T(i'i'T1, i'i'T2, iADJ2) *
        T(i'i'T2, i'i'T0, iADJ3)
      - T(i'i'T0, i'i'T1, iADJ3) *
        T(i'i'T1, i'i'T2, iADJ2) *
        T(i'i'T2, i'i'T0, iADJ1)
    );
#EndDo◇

```

Macro referenced in 87.

All internal gluon lines are removed from the colour diagram using the completeness relation (43).

⟨completeness relation (43) 85⟩ ≡

```

Id T(i1?, i2?, iADJ?) * T(i3?, i4?, iADJ?) =
  TR * (
    FundamentalID(i1, i4) * FundamentalID(i2, i3)
    - 1/dF * FundamentalID(i1, i2) * FundamentalID(i3, i4)
  );◇

```

Macro referenced in 87.

What remains are contractions of KRONECKER deltas and possibly tadpole graphs, which can be reduced by the code below.

⟨contract colour deltas 86⟩ ≡

```

Repeat Id AdjointID(i1?, i2?) * AdjointID(i2?, i3?) =
  AdjointID(i1, i3);
Repeat Id FundamentalID(i1?, i2?) * FundamentalID(i2?, i3?) =
  FundamentalID(i1, i3);
Id AdjointID(iADJ1?, iADJ2?) * T(i1?, i2?, iADJ1?) =
  T(i1, i2, iADJ2);
Id FundamentalID(i1?, i3?) * T(i1?, i2?, iADJ1?) =
  T(i3, i2, iADJ1);
Id FundamentalID(i2?, i3?) * T(i1?, i2?, iADJ1?) =
  T(i1, i3, iADJ1);

```

```

Id AdjointID(iADJ1?, iADJ1?) = dA;
Id FundamentalID(iADJ1?, iADJ1?) = dF;
Id T(i1?, i1?, iADJ1?) = 0;◇

```

Macro referenced in 87.

It should be noted that the star-triangle relations and the reduction of the quadratic CASIMIR operators is not used explicitly, unlike stated in Algorithm 1 to maintain the simplicity of the resulting algorithm. The very last step just removes the function that has been introduced earlier for efficiency reasons.

⟨define procedure sunsimplify 87⟩ ≡

```

#Procedure sunsimplify
  ⟨separate colour factor for efficiency 83⟩
  ⟨eliminate  $f^{ABD}$  84⟩
  Repeat;
    ⟨completeness relation (43) 85⟩
    ⟨contract colour deltas 86⟩
  EndRepeat;
  .sort
    Id ANYNonColor(cc0?) = cc0;
  .sort
#EndProcedure◇

```

Macro referenced in 61.

6. Numerical Evaluation

6.1. Introduction. The numerical integration of a cross-section can be computationally very expensive when many particles are in the final state and the amplitude consists of millions of terms. The previous sections described how **Fortran90** [ISO90] code for the expression for an amplitude can be generated automatically at the one-loop level in a way that spurious calculations are kept to a minimum.

In this approach most steps are carried out numerically, and algebraic simplifications are done where necessary and where the simplification is immediate; lengthy simplifications where cancellations only happen in the very end have been avoided since the success of such calculations very often depends on human intervention at many steps and automation is only possible to a limited degree; conversely, a fully analytic calculation can lead to more compact expressions and to faster code.

In the rest of this section the calculation of the matrix element is considered only as far as the evaluation of the form factors goes. Apart from that it is considered as a black box that has been explained in the previous sections, and for the following discussion it is enough to assume the existence of the function `evaluate_me2(vecs, alphas)` that returns the squared matrix element including IR and UV counterterms and therefore returns a finite, real result.

Section 6.2 gives an overview over the structure of a phase space integrator that uses the reweighting procedure as described in Equations (475) and (475). Although **Fortran** is not famous for object-oriented design, Section 6.3 shows for the example of the form-factor type how **Fortran90** provides object-oriented principles, which have proved useful in the context of a direct translation from expression obtained from computer algebra programs into **Fortran** code. Section 6.4 introduces the **Golem90** library in detail with the focus on the calculation of the form factors. A short review of parallelisation methods and the description of ECDF, the cluster on which the calculations have been performed conclude this chapter.

6.2. Overview. In Section 8.4 of Chapter 3 I have introduce a method for integrating the NLO corrections of a process over a phase space. [B⁺08b]

This method has been implemented by reading unweighted LO events that have been created using **Whizard** [KOR07, MOR01, Kil01] and are stored in the **HepEvent** format [B⁺a]; to each of the events is attached the local K -factor as defined in Equation (??), which defines our reweighting procedure. Apart from the additional entry the output is still in **HepEvent** format to allow for an easy interchange with other packages; In the current version the analysis of the reweighted events is done with custom programmes.

6.3. Object-Oriented Design in Fortran90. Although **Fortran** is not renowned for its object-oriented capabilities it does support many of the language constructs one would expect from an object-oriented programming language. The authors of [DNS98] argue that “*Fortran 90 clearly has some language features which are useful for OOP (derived types, modules, generic interfaces), but clearly lacks some others (inheritance, run-time polymorphism)*” and give recipes how to emulate the latter features; thereby they extend the earlier work of [Dup94].

For the current implementation of the **Golem90** library certain object-oriented concepts are applied in representation of the form factors. The expansion of an arbitrary one-loop integral in dimensional regularisation starts at ε^{-2} , where the dimension is $d = 4 - 2\varepsilon$. Neglecting all positive powers of ε the integral can therefore be represented by three coefficients which are independent of ε ,

$$(589) \quad I(\{p_i\}) = \frac{A(\{p_i\})}{\varepsilon^2} + \frac{B(\{p_i\})}{\varepsilon} + C(\{p_i\}) + \mathcal{O}(\varepsilon).$$

This expansion can be directly mapped onto a derived type in **Fortran90**:

```

type form_factor
  complex(ki) :: a, b, c
end type form_factor

```

The parameter **ki** specifies the precision and is defined in another module. The interface to the routines implementing the form factors, e.g. the routine for the form factor $A_{j_1 j_2}^{3,2}(S)$ is declared below.

```

function a32

```

```

interface
  function      a32(j1,j2,S)
    integer, intent (in) :: j1,j2
    integer, intent (in), dimension(:) :: S
    type(form_factor) :: a32
  end function a32
end interface

```

The argument **S** is a list of pinches, i.e. the form factor $A_{j_1,j_2}^{3,2}(S^{1,2})$ translates to the function call `a32(j1,j2,(/1,2/))`. Up to this point the only advantage of a derived type over an array of complex numbers is the improved type safety. The main justification of using derived types in this example is the possibility of overloading operators. The reason is that the **Fortran** code is generated from a computer algebra program which should translate expressions like

$$2A_{4,3}^{3,2}(S^{\{1,2\}}) - 3\epsilon B^{3,2}(S^{\{1,2\}})$$

as straight-forward as possible both to keep the computer algebra code simple and to maintain the readability of the output; we aim for an output like `2*ff1-3*eps*ff2`, where `ff1` and `ff2` are defined as the above form factors `a32(4,3,(/1,2/))` and `b32((/1,2/))` respectively. The symbol `eps` is of the type `epsilon_type` which is defined below and represents positive powers of ϵ with an optional complex coefficient.

```

type epsilon_type
  complex(ki) :: coefficient
  integer :: power
end type epsilon_type

```

In order to allow the above expression in **Fortran90** one has to overload the according operators, which below is shown in two examples. For a fully working implementation all possible combination of operators and types that may appear in an expression have to be defined. One basic operation that has to be defined for the form factors is the addition of two form factors. In an **interface** declaration the operator `+` is overloaded by the function `add_ff_ff` which is defined later in the module.

```

interface operator(+)
  module procedure add_ff_ff
end interface
...
pure function add_ff_ff(ff1, ff2) result(r)
  type(form_factor), intent(in) :: ff1, ff2
  type(form_factor) :: r
  r%a = ff1%a + ff2%a
  r%b = ff1%b + ff2%b
  r%c = ff1%c + ff2%c
end function add_ff_ff

```

As a second example the multiplication of ε^n with a form factor is implemented.

```

type function mul_ff_eps
interface operator(*)
  module procedure mul_ff_eps
end interface
...
pure function mul_ff_eps(ff, x) result(r)
  type(epsilon_type), intent(in) :: x
  type(form_factor), intent(in) :: ff
  type(form_factor) :: r
  if (x%power >= 3) then
    r = 0.0_ki
  elseif (x%power == 2) then
    r%a = 0.0_ki
    r%b = 0.0_ki
    r%c = x%coefficient * r%a
  else
    r%a = 0.0_ki
    r%b = x%coefficient * ff%a
    r%c = x%coefficient * ff%b
  end if
end function mul_ff_eps

```

It should be noted that the above setup cannot evaluate an expression like $(\varepsilon + 2\varepsilon^2)B^{3,2}(S)$ although it is mathematically equivalent to its expanded form, unless one overloads the operator $+$ for the signature `(epsilon_type, epsilon_type)`. Therefore care has to be taken when the expression is generated by the computer algebra programme.

6.4. Tensor-Integrals in Golem90. Golem90 [BGH⁺08] is a Fortran90 library that defines an interface to the form factors that are defined through Equation (283). It maps the form factors $A_{j_1, \dots, j_r}^{N,r}(S)$, $B_{j_1, \dots, j_{r-2}}^{N,r}(S)$ and $C_{j_1, \dots, j_{r-4}}^{N,r}(S)$ onto functions $\mathbf{a}\langle N \rangle \langle r \rangle(j_1, \dots, j_r)$, $\mathbf{b}\langle N \rangle \langle r \rangle(j_1, \dots, j_{r-2})$ and $\mathbf{c}\langle N \rangle \langle r \rangle(j_1, \dots, j_{r-4})$ respectively. It should be noted, that the form factors $B^{6,r}$ and $C^{6,r}$ are not implemented. Instead, they are absorbed through relation (301).

As explained in Sections 2 and 3 of Chapter 3 it is always possible to reduce the tensor integrals down to an extended integral basis $\mathcal{I}_{\mathcal{N}}$ as defined in Equation (330a) without introducing inverse GRAM determinants. This basis contains integrals with non-trivial numerators; their evaluation allows for different methods. The phase space can be separated by a parameter Λ which discriminates

$$\begin{aligned}
 &\text{the bulk of the phase space where } \frac{\det G}{\det S} > \Lambda \\
 &\text{from the critical phase space where } \frac{\det G}{\det S} < \Lambda.
 \end{aligned}$$

In the bulk region one can use the equations given in Chapter 3, Section 3.5 and similar relations for the four-point functions in order to reduce the integral set $\mathcal{I}_{\mathcal{N}}$ to

the purely scalar integral set \mathcal{I}_S . In the critical phase space an analytic reduction would introduce numerical instabilities through inverse GRAM determinants. For many of the three-point functions integral-free representations can be found analytically without a reduction in the above sense. The remaining integrals in the **Golem90** library are solved by numerical integration.

6.5. Numerical Integration of the Basis Functions. As an example we shall consider the box-integrals in $n + 2$ and $n + 4$ dimensions,

$$(590) \quad I_4^{n+2} = \Gamma(1 + \varepsilon) \int_0^1 d^4 z \delta_z \frac{z_1^{\alpha_1} z_2^{\alpha_2} z_3^{\alpha_3} z_4^{\alpha_4}}{\left(-\frac{1}{2} z^\top S z - i\delta\right)^{1+\varepsilon}} \quad \text{and}$$

$$(591) \quad I_4^{n+4} = \frac{\Gamma(1 + \varepsilon)}{\varepsilon} \int_0^1 d^4 z \delta_z \frac{z_1^{\alpha_1} z_2^{\alpha_2} z_3^{\alpha_3} z_4^{\alpha_4}}{\left(-\frac{1}{2} z^\top S z - i\delta\right)^\varepsilon}.$$

As all propagators and k_1 are assumed to be massless, the matrix S reads

$$(592) \quad S = \begin{pmatrix} 0 & s_2 & s_{23} & 0 \\ s_2 & 0 & s_3 & s_{12} \\ s_{23} & s_3 & 0 & s_4 \\ 0 & s_{12} & s_4 & 0 \end{pmatrix}.$$

We are only interested in the ε expansion of the integrals and hence can write them as

$$(593) \quad I_4^{n+2} = \int_0^1 d^4 z \delta_z \frac{z_1^{\alpha_1} z_2^{\alpha_2} z_3^{\alpha_3} z_4^{\alpha_4}}{-\frac{1}{2} z^\top S z - i\delta} + \mathcal{O}(\varepsilon) \quad \text{and}$$

$$(594) \quad I_4^{n+4} = \frac{\Gamma(1 + \varepsilon)C}{\varepsilon} - \int_0^1 d^4 z \delta_z z_1^{\alpha_1} z_2^{\alpha_2} z_3^{\alpha_3} z_4^{\alpha_4} \ln \left(-\frac{1}{2} z^\top S z - i\delta \right) + \mathcal{O}(\varepsilon),$$

where the constant C can be derived from Equations (214) and (218),

$$(595) \quad C = P_{\alpha_1, \alpha_2, \alpha_3, \alpha_4} = \frac{\alpha_1! \alpha_2! \alpha_3! \alpha_4!}{(3 + \alpha_1 + \alpha_2 + \alpha_3 + \alpha_4)!}.$$

In the remaining integrals the δ -function can be eliminated by the transformation,

$$(596) \quad z = \begin{pmatrix} z_1 \\ z_2 \\ z_3 \\ z_4 \end{pmatrix} = w \cdot \begin{pmatrix} (1 - z) \\ xyz \\ xy(1 - z) \\ x(1 - y) \end{pmatrix}$$

that leads to the JACOBIAN factor $\mathcal{J} = -w^3 x^2 y$; the δ function becomes $\delta_z = \delta(1 - w)$. In terms of the new variables the denominators of Equation (590) and (591) factorise into

$$(597) \quad -\frac{1}{2} z^\top S z = -xy [a_1 xy + a_2 x + a_3],$$

with a_1 , a_2 and a_3 being quadratic polynomials in z . The integrals over x and y can be worked out analytically, in general leading to an integral like **[BGH⁺08]**

$$(598) \quad I = \int_0^1 dz \frac{f(z) \ln[f(z)] - g(z) \ln[g(z)]}{h(z)[f(z) - g(z)]}$$

with f , g and h being polynomials in z . This remaining integral is solved numerically by the GAUSS-KRONROD quadrature **[Kro64, Pat68]** after applying the contour deformation $z = u \pm u(1 - u)$, which avoids crossing the cut of the logarithms in I . **[BGH⁺08]**

6.6. Distributed and Parallel Computing. The problem of a Monte Carlo integration is very often described as *embarrassingly parallel*. This essentially means that the problem can be split into subprocesses which require no or virtually no communication. Such problems are very well suited for computation on clusters and have no need for specialised hardware. On the other hand the evaluation of each helicity amplitude can be split into the computation of single FEYNMAN diagrams. In this case the diagrams share a pool of data, i.e. form factors and spinor traces which have to be computed once per helicity amplitude, but do not modify any of the data. In this case it would be natural and desirable to distribute the amplitude calculation across multiple processors with shared memory. To achieve this second kind of parallelisation one can take advantage of nodes equipped with multiple cores.

6.6.1. Message Passing with MPI. A Monte Carlo integrator for our purpose can be split into two parts, a stochastic source of phase space points and an integrand function. In NLO calculations typically the generation of the phase space points is relatively cheap compared to the evaluation of the integrand.

Although Monte Carlo integration is an example where N processes can work in parallel with *no* communication at all there are two reasons why a message-passing implementation can be advantageous over the completely independent approach:

- Only one of the processes needs access to the storage device. Since the phase space points in our case were pregenerated and are stored in a file the integrator needs disk access both for reading and writing. Large numbers of parallel processes accessing the same disk at the same time, however, can destabilise the system and decrease the performance. Therefore the one-to- n topology as shown in Figure 3 has been used; the alternative of using the local disks of each nodes involves additional file transfers which can complicate the data handling unnecessarily.
- It cannot be guaranteed that a single evaluation of the integrand always takes the same time. At critical phase-space points the integrals can converge much slower than for the bulk of the phase space. The *Master* process in Figure 3 handles these situations dynamically and guarantees an optimal distribution of the workload such the idle time of the processors is minimised.

However, these benefits do not come for free. More care and effort by the programmer is required for the Message Passing Interface (MPI) implementation than for the sequential approach. A second drawback is the lower failure tolerance if one of the processes drops out.

6.6.2. Shared Memory Parallel Computing with *openMP*. Shared memory parallel programming comes into play when the parallel entities of a program need to update shared parts of the memory. It is typically easier to implement but errors due to improper synchronisation of the parallel threads are more likely. Most programming languages require the use of explicit multi-threading to make use of shared memory parallelism. In order to hide these technicalities from the programmer *openMP* has been introduced as a standard interface for parallelisation through multi-threading [DM98]. Rather than forcing the programmer to set up threads, *openMP* allows to place instructions to tell the compiler where parallelisation is possible and how to deal with global data regions.

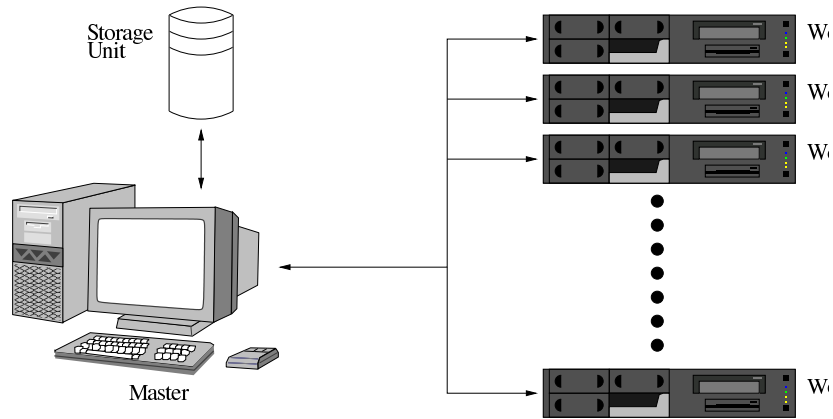


Figure 3: Monte Carlo integration on a cluster: the *Master* supplies each *Worker* with phase-space points and collects the results. In this scenario the *Master* is the only process that needs access to I/O devices.

The use of `openMP` has not been built into the current version of the code as the structure of the `Golem90` library makes heavy use of global but private variables. Therefore a parallelisation of the calculation of the form factors using `openMP` appears to be very difficult.

Applying `openMP` to other less time-consuming sections like the calculation of the spinor traces does not lead to significant improvements; when applied to rather inexpensive code fragments the overhead of creating threads even increases the run time and cannot be compensated for by distributing the workload to multiple processors.

6.7. The ECDF Cluster. The University of Edinburgh runs the Edinburgh Computing and Data Facility (ECDF), which has been used for the numerical integration of the cross section. Part of it is a cluster consisting of “128 worker nodes each with

two dual core CPUs, and 118 worker nodes each with two quad core CPUs, giving a total of 1456 cores. The worker nodes are interconnected by gigabit Ethernet networking.”¹³ Only part of the cluster has been used subject to availability, which usually was between 100 and 200 nodes.

The job submission is controlled by the Sun Grid Engine and message passing has been realised through the `openMPI` implementation. The source file have been compiled with the Intel `Fortran` compiler which optimises the code for the underlying architecture¹⁴.

7. Index of Literate Programs

7.1. Index of Output Files.

"colour.frm" Defined by 2.

"preprocess.frm" Defined by 23.

"symbols.h" Defined by 16.

7.2. Index of Macros.

- $\langle n\text{-dimensional spinor algebra 41} \rangle$ Referenced in 53.
- $\langle \text{Build Symmetriser 5} \rangle$ Referenced in 8.
- $\langle \text{Cut quark-lines 10} \rangle$ Referenced in 8.
- $\langle \text{Insert } t_{ij}^g \text{ 11} \rangle$ Referenced in 8.
- $\langle \text{Insert a pair of cuts 9} \rangle$ Referenced in 8.
- $\langle \text{Perform Insertions 8} \rangle$ Referenced in 2.
- $\langle \text{Procedure definition } \texttt{insertgluons} \text{ 6} \rangle$ Referenced in 2.
- $\langle \text{Procedure definition } \texttt{insertquarks} \text{ 4} \rangle$ Referenced in 2.
- $\langle \text{Procedure definition } \texttt{stripcoeff} \text{ 7} \rangle$ Referenced in 2.
- $\langle \text{Process Specification 1} \rangle$ Referenced in 2.
- $\langle \text{Simplify Result 12} \rangle$ Referenced in 2.
- $\langle \text{Symbol Definitions 3} \rangle$ Referenced in 2.
- $\langle \text{actual replacement of colour structure 30} \rangle$ Referenced in 31.
- $\langle \text{calculate } \Delta_{i,i+1} \text{ 69} \rangle$ Referenced in 62.
- $\langle \text{carry out LORENTZ algebra 40} \rangle$ Referenced in 53.
- $\langle \text{check bounds on diagram number 14} \rangle$ Referenced in 24.
- $\langle \text{check command line arguments 13} \rangle$ Referenced in 23.
- $\langle \text{check communication channels 15} \rangle$ Referenced in 23.
- $\langle \text{collect momenta in the loop 65} \rangle$ Referenced in 62.
- $\langle \text{combine result 60} \rangle$ Referenced in 56.
- $\langle \text{completeness relation (43) 85} \rangle$ Referenced in 87.
- $\langle \text{construct tensor integral 37} \rangle$ Referenced in 39.
- $\langle \text{contract colour deltas 86} \rangle$ Referenced in 87.
- $\langle \text{create colour vector 33} \rangle$ Referenced in 34.
- $\langle \text{deal with situation } \text{tr}\{\dots\gamma^\mu\dots\gamma_\mu\dots\} \text{ 46} \rangle$ Referenced in 45.
- $\langle \text{deal with situation } \text{tr}\{\dots\gamma^\mu\dots\}\text{tr}\{\dots\gamma_\mu\dots\} \text{ 47} \rangle$ Referenced in 45.
- $\langle \text{define auxiliary functions and symbols 21} \rangle$ Referenced in 16.
- $\langle \text{define form factors 22} \rangle$ Referenced in 16.
- $\langle \text{define procedure } \texttt{IntroduceRMomenta} \text{ 71} \rangle$ Referenced in 61.

¹³<http://www.is.ed.ac.uk/ecdf/eddie.shtml>, 6 August 2008

¹⁴Intel Xeon 5160, 3 GHz (dual core nodes) and Intel Xeon 5450, 3 GHz (quad core nodes)

- ⟨define procedure **RemoveMetricTensors** 74⟩ Referenced in 61.
- ⟨define procedure **TopologyInfo** 62⟩ Referenced in 61.
- ⟨define procedure **findff** 77⟩ Referenced in 75.
- ⟨define procedure **hProjectorSimplify** 80⟩ Referenced in 61.
- ⟨define procedure **kinematics** 79⟩ Referenced in 61.
- ⟨define procedure **recfind1** 76⟩ Referenced in 75.
- ⟨define procedure **recfind** 75⟩ Referenced in 61.
- ⟨define procedure **sunsimplify** 87⟩ Referenced in 61.
- ⟨define procedures 61⟩ Referenced in 23.
- ⟨define symbols for LORENTZ and DIRAC algebra 18⟩ Referenced in 16.
- ⟨define symbols for colour algebra 17⟩ Referenced in 16.
- ⟨define topological functions 20⟩ Referenced in 16.
- ⟨define vectors 19⟩ Referenced in 16.
- ⟨determine **\$loops** and r_i 66⟩ Referenced in 62.
- ⟨determine graph topology 28⟩ Referenced in 53.
- ⟨determine the helicities of the external particles 25⟩ Referenced in 23.
- ⟨determine the permutation of the legs and the pinches 70⟩ Referenced in 62.
- ⟨discriminate v and $(v - z)$ 68⟩ Referenced in 69.
- ⟨eliminate f^{ABD} 84⟩ Referenced in 87.
- ⟨eliminate r_i and Δ_{ij} 78⟩ Referenced in 79.
- ⟨eliminate LORENTZ indices 45⟩ Referenced in 53.
- ⟨evaluate $(n - 4)$ -dimensional traces 44⟩ Referenced in 41.
- ⟨evaluate colour vector numerically 35⟩ Referenced in 53.
- ⟨find q_i vectors 72⟩ Referenced in 71.
- ⟨find r_i and Δ_{ij} 73⟩ Referenced in 71.
- ⟨find next colour structure 29⟩ Referenced in 31.
- ⟨initialise local variables 59⟩ Referenced in 56.
- ⟨introduce **edge** and **node** functions 63⟩ Referenced in 62.
- ⟨introduce form factors 38⟩ Referenced in 39.
- ⟨introduce momenta q_i and r_i for one-loop processes 27⟩ Referenced in 53.
- ⟨label colour structures 31⟩ Referenced in 32.
- ⟨list all $\Delta_{i,i+1}$ 67⟩ Referenced in 69.
- ⟨make all momenta ingoing 26⟩ Referenced in 53.
- ⟨move $\bar{\gamma}^\mu$ right 42⟩ Referenced in 41.
- ⟨output section 54⟩ Referenced in 23.
- ⟨perform integration 39⟩ Referenced in 53.
- ⟨project on colour basis 34⟩ Referenced in 53.
- ⟨read libraries and configuration 24⟩ Referenced in 23.
- ⟨read propagator masses 36⟩ Referenced in 39.
- ⟨remove **node** functions 64⟩ Referenced in 62.
- ⟨replace form factors by symbols 50⟩ Referenced in 53.
- ⟨replace spinor traces by constants 51⟩ Referenced in 53.
- ⟨separate colour factor for efficiency 83⟩ Referenced in 87.
- ⟨shuffle projectors to the left 81⟩ Referenced in 80.
- ⟨simplification algorithm 53⟩ Referenced in 23.
- ⟨split into colour structures 32⟩ Referenced in 53.
- ⟨split traces 43⟩ Referenced in 41.
- ⟨strip global factor 52⟩ Referenced in 53.
- ⟨strip propagators 48⟩ Referenced in 53.
- ⟨symmetrise form factors 49⟩ Referenced in 50.
- ⟨use projector properties 82⟩ Referenced in 80.
- ⟨write colour vector 58⟩ Referenced in 56.
- ⟨write function for diagram 56⟩ Referenced in 54.
- ⟨write header of **Fortran** module 55⟩ Referenced in 54.

⟨ write variable declarations 57 ⟩ Referenced in 56.

7.3. Index of Identifiers.

$\$basis^*$: (34).
 $\$legperm$: 70.
 $\$legpinches$: 70.
 $\$loopsize$: 27, 28, 36, 37, 38, 39, 49, 50, 54, 62, 66, 67, 70, 72, 73, 78.
 $\$mass^*$: (36).
 $\$num$: 2.
 $\$prefactor$: 52, 54.
 $\$props$: 48, 54.
 $\$r^*$: (66).
AdjointID: 17, 74, 83, 86.
ANY*: (16).
ANYNonColor: 83, 87.
aquarks: 3, 9.
braket: 21, 52, 54.
CA: 17.
cc*: (16).
circle: 20, 65.
color*: (16).
COLORBASIS: 21, 33, 34.
colour: 1, 16, 31, 32, 34, 53, 56, 87.
COUNTER: 54, 57, 58, 60.
dA: 17, 33, 35, 86.
DELTA: 21, 39.
delta: 3, 4, 5, 9, 10, 11, 12.
dF: 17, 33, 35, 85, 86.
DIAG: 13, 14, 23, 24, 32, 54, 56.
DIAGRAMCOUNT: 14.
edge: 20, 62, 63, 64, 65.
f: 7, 17, 33, 74, 83, 84, 87.
ff*: (16).
findff: 75, 76, 77.
FormFactors: 22.
FundamentalID: 17, 74, 83, 85, 86.
g: 3, 6, 8, 9, 11, 12, 16, 52, 63.
g*: (3).
HEL*: (25).
HELICITY: 13, 23, 25, 54, 56.
hProjectorSimplify: 45, 61, 80.
i*: (3).
insertgluon: 3, 5, 6, 9.
insertgluons: 1, 2, 6.
insertq: 3, 9, 10.
insertquarks: 1, 2, 4.
inserttt: 3, 9, 10, 11.
IntroduceRMomenta: 27, 61, 71.
j*: (3).
kinematics: 40, 48, 61, 79.
k'i': 19, 26, 57, 59, 62, 63, 66.
LEGPERMUTATION: 28, 59, 62, 70, 79.

line: 3, 12, 13, 23.
 LOOPSIZE: 54.
 MAXLEGS: 19.
 MOMENTUM: 21, 37, 39, 40, 74.
 NCTEMP*: (16).
 node: 20, 62, 63, 64, 65, 66, 68, 69, 70.
 nullarray: 21.
 p1: 19, 64, 65, 68, 70, 72.
 PINCHES: 28, 62, 70.
 POW: 21, 34, 48, 53.
 PREFACTOR: 21, 52.
 prefactor: 52, 54, 57, 59, 60.
 PREFIX: 13, 23, 24, 54, 55, 56.
 PROP: 21, 36, 53.
 props: 48, 54, 57, 59.
 qGauge‘i’: (19).
 quarks: 3, 9.
 recfind: 50, 61, 75.
 recfind1: 75, 76.
 RemoveMetricTensors: 53, 61, 74.
 SNULL: 21, 77.
 stripcoeff: 2, 5, 7, 12.
 struct*: (32).
 sunsimplify: 53, 61, 87.
 T: 2, 17, 33, 74, 83, 84, 85, 86.
 t: 3, 11, 12.
 TEMP*: (16).
 TEMPHeads: 69, 70.
 TEMPLegs: 67, 68, 69, 70.
 TEMPTails: 69, 70.
 THEORY: 24.
 TI: 21, 37.
 TopologyInfo: 28, 61, 62.
 TR: 17, 33, 34, 35, 51, 84, 85.
 tr: 3, 12, 16, 45.
 tr*: (16).
 vec*: (16).

Acronyms

BSM	Beyond Standard Model
CAS	Computer Algebra System
CMS	Compact Muon Solenoid
DR	Dimensional Reduction
DReg	Dimensional Regularization
ECDF	Edinburgh Computing and Data Facility
$GL(N)$	General Linear Group
h.c.	hermitian conjugate
IR	infrared
LEP	Large Electron Positron Collider
LHC	Large Hadron Collider
LO	Leading Order
LSP	Lightest Supersymmetric Particle
LR	LITTLEWOOD-RICHARDSON
MPI	Message Passing Interface
MS	Minimal Subtraction
\overline{MS}	Modified Minimal Subtraction
MSSM	Minimal Supersymmetric Standard Model
NDR	Naïve Dimensional Reduction
NLO	Next to Leading Order
NNLO	Next to Next to Leading Order
OOP	Object Oriented Programming
PDF	Parton Distribution Function
QCD	Quantum Chromodynamics
QED	Quantum Electrodynamics
SHP	Spinor Helicity Projection
SM	Standard Model
$SL(N)$	Special Linear Group
$SO(N)$	Special Orthogonal Group
$Sp(N)$	Symplectic Group
$SU(N)$	Special Unitary Group
S_k	Symmetric Group
'tHo	'T HOOFT-VELTMAN
UV	ultraviolet
WvdW	WEYL-VAN DER WAERDEN

Bibliography

- [ADK⁺04] B. C. Allanach, A. Djouadi, J. L. Kneur, W. Porod and P. Slavich, *Precise determination of the neutral Higgs boson masses in the MSSM*, JHEP **09**, 044 (2004), [hep-ph/0406166](#), DOI 10.1088/1126-6708/2004/09/044.
- [ALEPH06] S. Schael et al. (ALEPH Collaboration), *Precision electroweak measurements on the Z resonance*, Phys. Rept. **427**, 257 (2006), [hep-ex/0509008](#), DOI 10.1016/j.physrep.2005.12.006.
- [ATL] ATLAS Collaboration, *ATLAS detector and physics performance. Technical design report. Vol. 2*, CERN-LHCC-99-15.
- [B⁺a] B. Bambah et al., *QCD GENERATORS FOR LEP*, Presented at the 2nd General Meeting of the LEP Physics Workshop 89, Geneva, May 8-9, 1989.
- [B⁺b] I. Bird et al., *LHC computing Grid. Technical design report*, <http://cdsweb.cern.ch/record/840543/files/lhcc-2005-024.pdf>, CERN-LHCC-2005-024.
- [B⁺06] C. Buttar et al., *Les Houches physics at TeV colliders 2005, standard model, QCD, EW, and Higgs working group: Summary report*, (2006), [hep-ph/0604120](#).
- [B⁺08a] C. F. Berger et al., *An Automated Implementation of On-Shell Methods for One-Loop Amplitudes*, Phys. Rev. **D78**, 036003 (2008), [0803.4180](#), DOI 10.1103/PhysRevD.78.036003.
- [B⁺08b] T. Binoth et al., *Precise predictions for LHC using a GOLEM*, (2008), [0807.0605](#).
- [Bar69] W. A. Bardeen, *Anomalous Ward identities in spinor field theories*, Phys. Rev. **184**, 1848–1857 (1969).
- [BCF05] R. Britto, F. Cachazo and B. Feng, *New recursion relations for tree amplitudes of gluons*, Nucl. Phys. **B715**, 499–522 (2005), [hep-th/0412308](#), DOI 10.1016/j.nuclphysb.2005.02.030.
- [BCFW05] R. Britto, F. Cachazo, B. Feng and E. Witten, *Direct proof of tree-level recursion relation in Yang-Mills theory*, Phys. Rev. Lett. **94**, 181602 (2005), [hep-th/0501052](#), DOI 10.1103/PhysRevLett.94.181602.
- [BDDK94] Z. Bern, L. J. Dixon, D. C. Dunbar and D. A. Kosower, *One loop n point gauge theory amplitudes, unitarity and collinear limits*, Nucl. Phys. **B425**, 217–260 (1994), [hep-ph/9403226](#), DOI 10.1016/0550-3213(94)90179-1.
- [BDDK95] Z. Bern, L. J. Dixon, D. C. Dunbar and D. A. Kosower, *Fusing gauge theory tree amplitudes into loop amplitudes*, Nucl. Phys. **B435**, 59–101 (1995), [hep-ph/9409265](#), DOI 10.1016/0550-3213(94)00488-Z.
- [BDDP08] A. Bredenstein, A. Denner, S. Dittmaier and S. Pozzorini, *NLO QCD corrections to $pp \rightarrow t\bar{t}b\bar{b}+X$ via quark anti-quark annihilation*, (2008), [0807.1453](#).
- [BDJ01a] M. Böhm, A. Denner and H. Joos, *Gauge Theories of the Strong and Electroweak Interaction*, Teubner, Stuttgart and Leipzig and Wiesbaden, 3rd edition, 2001.
- [BDJ01b] M. Böhm, A. Denner and H. Joos, *GAUGE THEORIES of the Strong and Electroweak Interaction*, B. G. Teubner, Stuttgart, Leipzig, Wiesbaden, 3rd edition, 2001.
- [BDK94] Z. Bern, L. J. Dixon and D. A. Kosower, *Dimensionally regulated pentagon integrals*, Nucl. Phys. **B412**, 751–816 (1994), [hep-ph/9306240](#).
- [Bec94] K. Beck, *Simple Smalltalk Testing*, Smalltalk Report **4**(2), 16–18 (October 1994), <http://www.xprogramming.com/testfram.htm>.
- [Bec02] K. Beck, *Test-driven development: By Example*, Addison-Wesley, Boston, 2002.
- [BF74] M. Barner and F. Flohr, *Analysis I*, Walter de Gruyter, Berlin and New York, 1974.
- [BG98] K. Beck and E. Gamma, *Test infected: Programmers love writing tests*, Java Report **3**(7), 37–50 (1998), <http://members.pingnet.ch/gamma/junit.htm>.
- [BG08] C. Bernicot and J.-P. Guillet, *Six-Photon Amplitudes in Scalar QED*, JHEP **01**, 059 (2008), [0711.4713](#), DOI 10.1088/1126-6708/2008/01/059.

- [BGH00] T. Binoth, J. P. Guillet and G. Heinrich, *Reduction formalism for dimensionally regulated one-loop N -point integrals*, Nucl. Phys. **B572**, 361–386 (2000), [hep-ph/9911342](#), DOI 10.1016/S0550-3213(00)00040-7.
- [BGH⁺05] T. Binoth, J. P. Guillet, G. Heinrich, E. Pilon and C. Schubert, *An algebraic / numerical formalism for one-loop multi-leg amplitudes*, (2005), [hep-ph/0504267](#).
- [BGH⁺08] T. Binoth, J. P. Guillet, G. Heinrich, E. Pilon and T. Reiter, *Golem95: a numerical program to calculate one-loop tensor integrals with up to six external legs*, (2008), 0810.0992.
- [BHS05] G. Bertone, D. Hooper and J. Silk, *Particle dark matter: Evidence, candidates and constraints*, Phys. Rept. **405**, 279–390 (2005), [hep-ph/0404175](#), DOI 10.1016/j.physrep.2004.08.031.
- [Bin05] T. Binoth, Standard Model QCD, Lecture at the SUPA Graduate School, 2005.
- [BJOZ07] G. Bozzi, B. Jäger, C. Oleari and D. Zeppenfeld, *Next-to-leading order QCD corrections to $W+Z$ and $W-Z$ production via vector-boson fusion*, Phys. Rev. **D75**, 073004 (2007), [hep-ph/0701105](#), DOI 10.1103/PhysRevD.75.073004.
- [BN37] F. Bloch and A. Nordsieck, *Note on the Radiation Field of the Electron*, Phys. Rev. **52**(2), 54–59 (Jul 1937), DOI 10.1103/PhysRev.52.54.
- [BP99] D. Bardin and G. Passarino, *The Standard Model in the Making*, Clearendon Press, Oxford, 1999.
- [BRM] P. Briggs, J. D. Ramsdell and M. W. Mengel, *Nuweb Version 1.0b1: A Simple Literate Programming Tool*, <http://nuweb.sourceforge.net/>.
- [Bug94] D. Bugden, *Software Design*, Addison-Wesley Publishing Company, Wokingham, England and Reading, Massachusetts et al., 1994.
- [CDD07] M. Ciccolini, A. Denner and S. Dittmaier, *Strong and electroweak corrections to the production of Higgs+2jets via weak interactions at the LHC*, Phys. Rev. Lett. **99**, 161803 (2007), 0707.0381, DOI 10.1103/PhysRevLett.99.161803.
- [CDD08] M. Ciccolini, A. Denner and S. Dittmaier, *Electroweak and QCD corrections to Higgs production via vector-boson fusion at the LHC*, Phys. Rev. **D77**, 013002 (2008), 0710.4749, DOI 10.1103/PhysRevD.77.013002.
- [CDST02] S. Catani, S. Dittmaier, M. H. Seymour and Z. Trocsanyi, *The dipole formalism for next-to-leading order QCD calculations with massive partons*, Nucl. Phys. **B627**, 189–265 (2002), [hep-ph/0201036](#).
- [CEZ06] J. M. Campbell, R. K. Ellis and G. Zanderighi, *Next-to-leading order Higgs + 2 jet production via gluon fusion*, JHEP **10**, 028 (2006), [hep-ph/0608194](#).
- [CKEZ07] J. M. Campbell, R. Keith Ellis and G. Zanderighi, *Next-to-leading order predictions for $WW + 1$ jet distributions at the LHC*, JHEP **12**, 056 (2007), 0710.1832, DOI 10.1088/1126-6708/2007/12/056.
- [CompHEP04] E. Boos et al. (CompHEP Collaboration), *CompHEP 4.4: Automatic computations from Lagrangians to events*, Nucl. Instrum. Meth. **A534**, 250–259 (2004), [hep-ph/0403113](#), DOI 10.1016/j.nima.2004.07.096.
- [CS97] S. Catani and M. H. Seymour, *A general algorithm for calculating jet cross sections in NLO QCD*, Nucl. Phys. **B485**, 291–419 (1997), [hep-ph/9605323](#).
- [CSW04] F. Cachazo, P. Svrcek and E. Witten, *MHV vertices and tree amplitudes in gauge theory*, JHEP **09**, 006 (2004), [hep-th/0403047](#), DOI 10.1088/1126-6708/2004/09/006.
- [Cut60] R. E. Cutkosky, *Singularities and discontinuities of Feynman amplitudes*, J. Math. Phys. **1**, 429–433 (1960).
- [Cvi08] P. Cvitanović, *Group Theory: Birdtracks, Lie's, and Exceptional Groups*, Princeton University Press, Princeton, 2008, <http://www.nbi.dk/GroupTheory/>.
- [D⁺00] A. Djouadi et al., *The Higgs working group: Summary report*, (2000), [hep-ph/0002258](#).
- [Dav91] A. I. Davydchev, *A Simple formula for reducing Feynman diagrams to scalar integrals*, Phys. Lett. **B263**, 107–111 (1991), DOI 10.1016/0370-2693(91)91715-8.
- [DD03] A. Denner and S. Dittmaier, *Reduction of one-loop tensor 5-point integrals*, Nucl. Phys. **B658**, 175–202 (2003), [hep-ph/0212259](#), DOI 10.1016/S0550-3213(03)00184-6.
- [DD06] A. Denner and S. Dittmaier, *Reduction schemes for one-loop tensor integrals*, Nucl. Phys. **B734**, 62–115 (2006), [hep-ph/0509141](#), DOI 10.1016/j.nuclphysb.2005.11.007.
- [DGH94] J. F. Donoghue, E. Golowich and B. R. Holstein, *Dynamics of the Standard Model*, Cambridge University Press, Cambridge and New York and Melbourne, 1994.

- [DGV95] J. Dai, J. F. Gunion and R. Vega, *LHC detection of neutral MSSM Higgs bosons via $g \rightarrow b$ anti- b $h \rightarrow b$ anti- b b anti- b* , Phys. Lett. **B345**, 29–35 (1995), [hep-ph/9403362](#), DOI 10.1016/0370-2693(94)01497-Z.
- [DGV96] J. Dai, J. F. Gunion and R. Vega, *Detection of neutral MSSM Higgs bosons in four- b final states at the Tevatron and the LHC: An update*, Phys. Lett. **B387**, 801–803 (1996), [hep-ph/9607379](#), DOI 10.1016/0370-2693(96)01096-9.
- [Dit99] S. Dittmaier, *Weyl-van-der-Waerden formalism for helicity amplitudes of massive particles*, Phys. Rev. **D59**, 016007 (1999), [hep-ph/9805445](#).
- [Dix96] L. J. Dixon, *Calculating scattering amplitudes efficiently*, (1996), [hep-ph/9601359](#).
- [Djo08] A. Djouadi, *The anatomy of electro-weak symmetry breaking. II: The Higgs bosons in the minimal supersymmetric model*, Phys. Rept. **459**, 1–241 (2008), [hep-ph/0503173](#), DOI 10.1016/j.physrep.2007.10.005.
- [DKP02] P. D. Draggotis, R. H. P. Kleiss and C. G. Papadopoulos, *Multi-jet production in hadron collisions*, Eur. Phys. J. **C24**, 447–458 (2002), [hep-ph/0202201](#).
- [DKU08] S. Dittmaier, S. Kallweit and P. Uwer, *NLO QCD corrections to WW+jet production at hadron colliders*, Phys. Rev. Lett. **100**, 062003 (2008), 0710.1577, DOI 10.1103/PhysRevLett.100.062003.
- [DM98] L. Dagum and R. Menon, *OpenMP: An Industry-Standard API for Shared-Memory Programming*, IEEE Comput. Sci. Eng. **5**(1), 46–55 (1998), DOI 10.1109/99.660313.
- [DNS98] V. K. Decyk, C. D. Norton and B. K. Szumansky, *How to support inheritance and run-time polymorphism in Fortran 90*, Comput. Phys. Commun. **115**(1), 9–17 (December 1998).
- [DONUT01] K. Kodama et al. (DONUT Collaboration), *Observation of tau-neutrino interactions*, Phys. Lett. **B504**, 218–224 (2001), [hep-ex/0012035](#), DOI 10.1016/S0370-2693(01)00307-0.
- [Dup94] B. J. Dupée, *Object oriented methods using Fortran 90*, SIGPLAN Fortran Forum **13**(1), 21–30 (1994), DOI <http://doi.acm.org/10.1145/191559.191563>.
- [EB64] F. Englert and R. Brout, *BROKEN SYMMETRY AND THE MASS OF GAUGE VECTOR MESONS*, Phys. Rev. Lett. **13**, 321–322 (1964), DOI 10.1103/PhysRevLett.13.321.
- [ECK03] H. Elvang, P. Cvitanovic and A. D. Kennedy, *Diagrammatic Young Projection Operators for $U(n)$* , (2003), [hep-th/0307186](#).
- [Eid04] S. Eidelman et al., *Review of Particle Physics*, Physics Letters B **592**, 1+ (2004), <http://pdg.lbl.gov>.
- [ELPW02] T. O. Eynck, E. Laenen, L. Phaf and S. Weinzierl, *Comparison of phase space slicing and dipole subtraction methods for $\gamma^* \rightarrow Q$ anti- Q* , Eur. Phys. J. **C23**, 259–266 (2002), [hep-ph/0109246](#), DOI 10.1007/s100520100868.
- [EM04] O. Espinosa and V. H. Moll, *A Generalized Polygamma Function*, Integral Transforms and Special Functions **15**(2), 101–116 (2004), DOI 10.1080/10652460310001600573.
- [ERT81] R. K. Ellis, D. A. Ross and A. E. Terrano, *The Perturbative Calculation of Jet Structure in e^+e^- Annihilation*, Nucl. Phys. **B178**, 421 (1981).
- [ESW96] R. K. Ellis, W. J. Stirling and B. R. Webber, *QCD and Collider Physics*, Cambridge University Press, Cambridge, 1996.
- [EWW] EWWG, Plots for Winter 2008, <http://lepewwg.web.cern.ch/LEPEWWG/plots/winter2008/>, accessed 25 August 2008.
- [EZ] R. K. Ellis and G. Zanderighi, <http://qcdloop.fnal.gov/>.
- [EZ08] R. K. Ellis and G. Zanderighi, *Scalar one-loop integrals for QCD*, JHEP **02**, 002 (2008), 0712.1851, DOI 10.1088/1126-6708/2008/02/002.
- [FF00] J. A. Fill and D. E. Fishkind, *The Moore–Penrose Generalized Inverse for Sums of Matrices*, SIAM Journal on Matrix Analysis and Applications **21**(2), 629–635 (2000), <http://citeseer.ist.psu.edu/fill98moorepenrose.html>.
- [FGG08] R. Frederix, T. Gehrmann and N. Greiner, *Automation of the Dipole Subtraction Method in MadGraph/MadEvent*, (2008), 0808.2128.
- [FGML73] H. Fritzsch, M. Gell-Mann and H. Leutwyler, *Advantages of the Color Octet Gluon Picture*, Phys. Lett. **B47**, 365–368 (1973), DOI 10.1016/0370-2693(73)90625-4.
- [FJT00] J. Fleischer, F. Jegerlehner and O. V. Tarasov, *Algebraic reduction of one-loop Feynman graph amplitudes*, Nucl. Phys. **B566**, 423–440 (2000), [hep-ph/9907327](#), DOI 10.1016/S0550-3213(99)00678-1.

- [Ful97] W. Fulton, *Young tableaux:with applications to representation theory and geometry*, Cambridge University Press, Cambridge, 1997.
- [GF64] B. A. Galler and M. J. Fisher, *An improved equivalence algorithm*, Commun. ACM **7**(5), 301–303 (1964), DOI <http://doi.acm.org/10.1145/364099.364331>.
- [GJSB05] J. Gosling, B. Joy, G. Steele and G. Bracha, *Java(TM) Language Specification*, Addison-Wesley, Upper Saddle River, NJ, 3rd edition, 2005.
- [GK08] T. Gleisberg and F. Krauss, *Automating dipole subtraction for QCD NLO calculations*, Eur. Phys. J. **C53**, 501–523 (2008), 0709.2881, DOI 10.1140/epjc/s10052-007-0495-0.
- [Gla61] S. L. Glashow, *Partial Symmetries of Weak Interactions*, Nucl. Phys. **22**, 579–588 (1961), DOI 10.1016/0029-5582(61)90469-2.
- [Gro07] A. Grozin, *Lectures on QED and QCD*, World Scientific Publishing, Singapore, 2007.
- [GZ08] W. T. Giele and G. Zanderighi, *On the Numerical Evaluation of One-Loop Amplitudes: the Gluonic Case*, (2008), 0805.2152.
- [Hab97] H. E. Haber, *Higgs Boson Masses and Couplings in the Minimal Supersymmetric Model*, volume 17 of *Directions in High Energy Physics*, pages 23–67, World Scientific, Singapore and New Jersey and London and Hong Kong, 1997.
- [Hah01] T. Hahn, *Generating Feynman diagrams and amplitudes with FeynArts 3*, Comput. Phys. Commun. **140**, 418–431 (2001), hep-ph/0012260, DOI 10.1016/S0010-4655(01)00290-9.
- [Hah05] T. Hahn, *New developments in FormCalc 4.1*, (2005), hep-ph/0506201.
- [HH65] J. Hammersley and D. Handscomb, *Monte Carlo Methods*, Methuen & Co Ltd, London, 1965.
- [HH91] H. E. Haber and R. Hempfling, *Can the mass of the lightest Higgs boson of the minimal supersymmetric model be larger than $m(Z)$?*, Phys. Rev. Lett. **66**, 1815–1818 (1991), DOI 10.1103/PhysRevLett.66.1815.
- [Hig64a] P. W. Higgs, *BROKEN SYMMETRIES AND THE MASSES OF GAUGE BOSONS*, Phys. Rev. Lett. **13**, 508–509 (1964), DOI 10.1103/PhysRevLett.13.508.
- [Hig64b] P. W. Higgs, *Broken symmetries, massless particles and gauge fields*, Phys. Lett. **12**, 132–133 (1964), DOI 10.1016/0031-9163(64)91136-9.
- [Hig66] P. W. Higgs, *Spontaneous Symmetry Breakdown Without Massless Bosons*, Phys. Rev. **145**, 1156–1163 (1966), DOI 10.1103/PhysRev.145.1156.
- [HK97] J. Hakkinen and H. Kharraziha, *Colour: A computer program for QCD colour factor calculations*, Comput. Phys. Commun. **100**, 311–321 (1997), hep-ph/9603229.
- [HO02] B. W. Harris and J. F. Owens, *The two cutoff phase space slicing method*, Phys. Rev. **D65**, 094032 (2002), hep-ph/0102128, DOI 10.1103/PhysRevD.65.094032.
- [HR06] T. Hahn and M. Rauch, *News from FormCalc and LoopTools*, Nucl. Phys. Proc. Suppl. **157**, 236–240 (2006), hep-ph/0601248, DOI 10.1016/j.nuclphysbps.2006.03.026.
- [HS81] H. V. Henderson and S. R. Searle, *On Deriving the Inverse of a Sum of Matrices*, SIAM Review **23:1**, 53–60 (1981).
- [HZ08] V. Hankele and D. Zeppenfeld, *QCD corrections to hadronic WWZ production with leptonic decays*, Phys. Lett. **B661**, 103–108 (2008), 0712.3544, DOI 10.1016/j.physletb.2008.02.014.
- [ISO90] ISO/IEC, *Information processing systems — Computer graphics — Programmer’s Hierarchical Interactive Graphics System (PHIGS)language bindings — Part 1: FORTRAN*, 1st edition, 1990, ISO/IEC 9593-1:1990.
- [Jeg01] F. Jegerlehner, *Facts of life with gamma(5)*, Eur. Phys. J. **C18**, 673–679 (2001), hep-th/0005255.
- [Joh63] S. M. Johnson, *Generation of Permutations by Adjacent Transposition*, Mathematics of Computation **17**(83), 282–285 (July 1963), <http://www.jstor.org/stable/2003846>.
- [JOZ06a] B. Jäger, C. Oleari and D. Zeppenfeld, *Next-to-leading order QCD corrections to $W+W$ -production via vector-boson fusion*, JHEP **07**, 015 (2006), hep-ph/0603177.
- [JOZ06b] B. Jäger, C. Oleari and D. Zeppenfeld, *Next-to-leading order QCD corrections to Z boson pair production via vector-boson fusion*, Phys. Rev. **D73**, 113006 (2006), hep-ph/0604200, DOI 10.1103/PhysRevD.73.113006.
- [JWW01] S. Jadach, B. F. L. Ward and Z. Waś, *Global positioning of spin GPS scheme for half-spin massive spinors*, Eur. Phys. J. **C22**, 423–430 (2001), hep-ph/9905452.
- [K⁺06] Y. Kurihara et al., *NLO-QCD calculation in GRACE*, Nucl. Phys. Proc. Suppl. **157**, 231–235 (2006), DOI 10.1016/j.nuclphysbps.2006.03.025.

- [KBR07] A. D. Kennedy, T. Binoth and T. Rippon, *Automating Renormalization of Quantum Field Theories*, (2007), 0712.1016.
- [Kil01] W. Kilian, *Whizard 1.0: A generic Monte-Carlo integration and event generation package for multi-particle processes*, January 2001, <http://www-flc.desy.de/lcnotes/>, LC-TOOL-2001-039.
- [Kin62] T. Kinoshita, *Mass singularities of Feynman amplitudes*, J. Math. Phys. **3**, 650–677 (1962).
- [KKS02] F. Krauss, R. Kuhn and G. Soff, *AMEGIC++ 1.0: A matrix element generator in C++*, JHEP **02**, 044 (2002), [hep-ph/0109036](http://arxiv.org/abs/hep-ph/0109036).
- [KN92] D. Kapur and P. Narendran, Double-exponential complexity of computing a complete set of AC-unifiers, in *Logic in Computer Science, 1992. LICS '92, Proceedings of the Seventh Annual IEEE Symposium*, pages 11–21, Santa Cruz, CA, USA, June 1992, DOI 10.1109/LICS.1992.185515.
- [Knu84] D. E. Knuth, *Literate Programming.*, Comput. J. **27**(2), 97–111 (1984).
- [Knu92] D. E. Knuth, *Literate Programming*, Center for the Study of Language and Information, Stanford, CA, 1992.
- [Knu97] D. E. Knuth, *The Art of Computer Programming: Fundamental Algorithms*, volume 1 of *The Art of Computer Programming*, Addison-Wesley, Reading, Massachusetts, 3rd edition, 1997, <http://www-cs-faculty.stanford.edu/~knuth/taocp.html>.
- [KOR07] W. Kilian, T. Ohl and J. Reuter, *WHIZARD: Simulating Multi-Particle Processes at LHC and ILC*, (2007), 0708.4233.
- [Kro64] A. S. Kronrod, *Integration with Control of Accuracy*, Soviet Physics Doklady **9**, 17 (July 1964).
- [Kro08] W. Krolkowski, *A Hidden Valley model of cold dark matter*, (2008), 0803.2977.
- [KS85] R. Kleiss and W. J. Stirling, *SPINOR TECHNIQUES FOR CALCULATING p anti- $p \rightarrow W^{+-} / Z^0 + JETS$* , Nucl. Phys. **B262**, 235–262 (1985).
- [KSE86] R. Kleiss, W. J. Stirling and S. D. Ellis, *A NEW MONTE CARLO TREATMENT OF MULTIPARTICLE PHASE SPACE AT HIGH-ENERGIES*, Comput. Phys. Commun. **40**, 359 (1986), DOI 10.1016/0010-4655(86)90119-0.
- [Lan59] L. D. Landau, *On analytic properties of vertex parts in quantum field theory*, Nucl. Phys. **13**, 181–192 (1959), DOI 10.1016/0029-5582(59)90154-3.
- [Lan08] O. Lang, *Doctest and unittest... now they'll be merrily together*, The Python Papers **3**(1) (2008), <http://ojs.pythonpapers.org/index.php/tpp/article/view/56>.
- [Lep78] G. P. Lepage, *A New Algorithm for Adaptive Multidimensional Integration*, J. Comput. Phys. **27**, 192 (1978), DOI 10.1016/0021-9991(78)90004-9.
- [(LHWG)03] R. Barate et al. (LEP Working Group for Higgs boson searches (LHWG) Collaboration), *Search for the standard model Higgs boson at LEP*, Phys. Lett. **B565**, 61–75 (2003), [hep-ex/0306033](http://arxiv.org/abs/hep-ex/0306033), DOI 10.1016/S0370-2693(03)00614-2.
- [LMP07] A. Lazopoulos, K. Melnikov and F. Petriello, *QCD corrections to tri-boson production*, Phys. Rev. **D76**, 014001 (2007), [hep-ph/0703273](http://arxiv.org/abs/hep-ph/0703273), DOI 10.1103/PhysRevD.76.014001.
- [LN64] T. D. Lee and M. Nauenberg, *Degenerate Systems and Mass Singularities*, Phys. Rev. **133**, B1549–B1562 (1964), DOI 10.1103/PhysRev.133.B1549.
- [LR34] D. E. Littlewood and A. R. Richardson, *Group characters and algebra*, Philosophical Transactions **A 233**, 99–141 (1934).
- [Mah01] K. Mahboubi, *ATLAS Level-1 Jet Trigger Rates and study of the ATLAS discovery potential of the neutral MSSM Higgs bosons in b -jet decay channels*, Doctor of natural sciences, Ruprecht-Karls-Universität Heidelberg, Heidelberg, 2001, HD-KIP-01-06.
- [Mel65] D. B. Melrose, *Reduction of Feynman diagrams*, Nuovo Cim. **40**, 181–213 (1965).
- [Mey92a] B. Meyer, *Applying “Design by Contract”*, Computer (IEEE) **25**, 40–51 (October 1992), <http://se.ethz.ch/~meyer/publications/computer/contract.pdf>.
- [Mey92b] B. Meyer, *Eiffel: the language*, Prentice-Hall, Inc., Upper Saddle River, NJ, USA, 1992.
- [MM92] D. Mandrioli and B. Meyer, editors, *Advances in object-oriented software engineering*, Prentice-Hall, Inc., Upper Saddle River, NJ, USA, 1992.
- [MMP⁺03] M. L. Mangano, M. Moretti, F. Piccinini, R. Pittau and A. D. Polosa, *ALPGEN, a generator for hard multiparton processes in hadronic collisions*, JHEP **07**, 001 (2003), [hep-ph/0206293](http://arxiv.org/abs/hep-ph/0206293).
- [Moh02] R. N. Mohapatra, *Unification and supersymmetry: the frontiers of quark-lepton physics*, Springer-Verlag, New York and Berlin, 3rd edition, 2002.

- [MOR01] M. Moretti, T. Ohl and J. Reuter, *O'Mega: An optimizing matrix element generator*, (2001), [hep-ph/0102195](#).
- [MPSW03] F. Maltoni, K. Paul, T. Stelzer and S. Willenbrock, *Color-flow decomposition of QCD amplitudes*, Phys. Rev. **D67**, 014026 (2003), [hep-ph/0209271](#).
- [MS03] F. Maltoni and T. Stelzer, *MadEvent: Automatic event generation with MadGraph*, JHEP **02**, 027 (2003), [hep-ph/0208156](#).
- [Mur38] F. D. Murnaghan, *The Theory of Group Representations*, The John Hopkins Press, Baltimore, 1938.
- [Mut87] T. Muta, *Foundations of quantum chromodynamics: an introduction to perturbative methods in gauge theories*, volume 5 of *Lecture Notes in Physics*, World Scientific Publishing, Singapore, 1st edition, 1987.
- [Nag03] Z. Nagy, *Next-to-leading order calculation of three-jet observables in hadron hadron collision*, Phys. Rev. **D68**, 094002 (2003), [hep-ph/0307268](#), DOI 10.1103/PhysRevD.68.094002.
- [Nan03] G. Nanava, *A Monte Carlo simulation of decays under the SANC project*, Nucl. Instrum. Meth. **A502**, 583–585 (2003).
- [(NLO/ML)08] Z. Bern et al. (NLO Multileg Working Group (NLO/ML) Collaboration), *The NLO multileg working group: summary report*, (2008), [0803.0494](#).
- [Nog93] P. Nogueira, *Automatic Feynman graph generation*, J. Comput. Phys. **105**, 279–289 (1993).
- [NW78] A. Nijjenhuis and H. S. Wilf, *Combinatorial algorithms for computers and calculators*, Academic Press, Inc., London, 2nd edition, 1978, First published in 1975 under title: Combinatorial algorithms.
- [Ohl95] T. Ohl, *Drawing Feynman diagrams with Latex and Metafont*, Comput. Phys. Commun. **90**, 340–354 (1995), [hep-ph/9505351](#), DOI 10.1016/0010-4655(95)90137-S.
- [OPP08] G. Ossola, C. G. Papadopoulos and R. Pittau, *CutTools: a program implementing the OPP reduction method to compute one-loop amplitudes*, JHEP **03**, 042 (2008), [0711.3596](#), DOI 10.1088/1126-6708/2008/03/042.
- [OYY91] Y. Okada, M. Yamaguchi and T. Yanagida, *Upper bound of the lightest Higgs boson mass in the minimal supersymmetric standard model*, Prog. Theor. Phys. **85**, 1–6 (1991), DOI 10.1143/PTP.85.1.
- [Pat68] T. N. L. Patterson, *On Some Gauss and Lobatto Based Integration Formulae*, Mathematics of Computation **22**(104), 877–886 and s32–s36 (1968), <http://www.jstor.org/stable/2004589>.
- [(PDG)08] C. Amsler et al. (Particle Data Group (PDG) Collaboration), *Review of particle physics*, Phys. Lett. **B667**, 1 (2008), DOI 10.1016/j.physletb.2008.07.018.
- [Pit97] R. Pittau, *A simple method for multi-leg loop calculations*, Comput. Phys. Commun. **104**, 23–36 (1997), [hep-ph/9607309](#).
- [PS95] M. E. Peskin and D. V. Schroeder, *An Introduction to Quantum Field Theory*, Westview Press, Boulder and Oxford, 1995.
- [PT86] S. J. Parke and T. R. Taylor, *An Amplitude for n Gluon Scattering*, Phys. Rev. Lett. **56**, 2459 (1986), DOI 10.1103/PhysRevLett.56.2459.
- [Pur] S. Purcell, *Python unit testing framework*, <http://pyunit.sourceforge.net/>, Accessed 9 September 2008.
- [PV79] G. Passarino and M. J. G. Veltman, *One Loop Corrections for e^+e^- Annihilation Into $\mu^+\mu^-$ in the Weinberg Model*, Nucl. Phys. **B160**, 151 (1979).
- [RG] J. Reuter and A. Guffanti, private communication, work in progress.
- [RWF97] E. Richter-Was and D. Froidevaux, *MSSM Higgs searches in multi-b-jet final states at the LHC*, Z. Phys. **C76**, 665–676 (1997), [hep-ph/9708455](#), DOI 10.1007/s002880050589.
- [Sag01] B. E. Sagan, *The symmetric group: representations, combinatorial algorithms, and symmetric functions*, Springer-Verlag, New York, 2001.
- [Sal] A. Salam, *Weak and Electromagnetic Interactions*, Originally printed in *Svartholm: Elementary Particle Theory, Proceedings Of The Nobel Symposium Held 1968 At Lerum, Sweden*, Stockholm 1968, 367–377.
- [SK08] G. Sanguinetti and S. Karg, *NLO QCD corrections to the production of a weak boson pair associated by a hard jet*, (2008), [0806.1394](#).
- [ST08] M. H. Seymour and C. Tevlin, *TeVJet: A general framework for the calculation of jet observables in NLO QCD*, (2008), [0803.2231](#).

-
- [SvN05] J. Smith and W. L. van Neerven, *The difference between n -dimensional regularization and n -dimensional reduction in QCD*, Eur. Phys. J. **C40**, 199–203 (2005), [hep-ph/0411357](#).
- [T⁺07] W. K. Tung et al., *Heavy quark mass effects in deep inelastic scattering and global QCD analysis*, JHEP **02**, 053 (2007), [hep-ph/0611254](#).
- [Tan90] H. Tanaka, *A METHOD FOR NUMERICAL CALCULATIONS OF HELICITY AMPLITUDES FOR PROCESSES INVOLVING MASSIVE FERMIONS*, Comput. Phys. Commun. **58**, 153–168 (1990).
- [tH74] G. 't Hooft, *A PLANAR DIAGRAM THEORY FOR STRONG INTERACTIONS*, Nucl. Phys. **B72**, 461 (1974).
- [tHV72] G. 't Hooft and M. J. G. Veltman, *Regularization and Renormalization of Gauge Fields*, Nucl. Phys. **B44**, 189–213 (1972).
- [Tro62] H. F. Trotter, *Algorithm 115: Perm*, Commun. ACM **5**(8), 434–435 (1962), DOI 10.1145/368637.368660.
- [TV07] M. Tentyukov and J. A. M. Vermaseren, *Extension of the functionality of the symbolic program FORM by external software*, Comput. Phys. Commun. **176**, 385–405 (2007), [cs/0604052](#), DOI 10.1016/j.cpc.2006.11.007.
- [UK97] F. E. Udwalla and R. E. Kalaba, *An alternative proof of the Greville formula*, J. Optim. Theory Appl. **94**(1), 23–28 (1997), DOI 10.1023/A:1022699317381.
- [Ver00] J. A. M. Vermaseren, *New features of FORM*, (2000), [math-ph/0010025](#).
- [Ver02] J. A. M. Vermaseren, *FORM, version 3.1: Reference manual*, 2002, <http://www.nikhef.nl/%7Eform/>.
- [Vla02] V. Vladimirov, *Methods of the Theory of Generalized Functions*, CRC Press, London and New York, 1st edition, 2002.
- [vNV84] W. L. van Neerven and J. A. M. Vermaseren, *THE ROLE OF THE FIVE POINT FUNCTION IN RADIATIVE CORRECTIONS TO TWO PHOTON PHYSICS*, Phys. Lett. **B142**, 80 (1984), DOI 10.1016/0370-2693(84)91140-7.
- [vRD] G. van Rossum and F. L. Drake, *Python Tutorial Release 2. 1.1*, citeseer.ist.psu.edu/rossum01python.html.
- [VT06] J. A. M. Vermaseren and M. Tentyukov, *What is new in FORM*, Nucl. Phys. Proc. Suppl. **160**, 38–43 (2006).
- [Wae32] B. L. v. d. Waerden, *Die gruppentheoretische Methode in der Quantenmechanik*, Springer, Berlin, 1932.
- [Way] T. Way, *PEP 316 – Programming by Contract for Python*, <http://www.python.org/dev/peps/pep-0316/>.
- [WB92] J. Wess and J. Bagger, *Supersymmetry and supergravity*, Princeton University Press, Princeton, New Jersey, 2nd edition, 1992.
- [Wei67] S. Weinberg, *A Model of Leptons*, Phys. Rev. Lett. **19**(21), 1264–1266 (Nov 1967), DOI 10.1103/PhysRevLett.19.1264.
- [Wei00] S. Weinzierl, *Introduction to Monte Carlo methods*, (2000), [hep-ph/0006269](#).
- [Wei06] S. Weinzierl, *Automated computation of spin- and colour-correlated Born matrix elements*, Eur. Phys. J. **C45**, 745–757 (2006), [hep-ph/0510157](#).
- [Wey31] H. Weyl, *Gruppentheorie und Quantenmechanik*, Hirzel, Leipzig, 2nd edition, 1931.
- [Wey39] H. Weyl, *The classical groups: their invariants and representations*, Princeton University Press, Princeton, NJ, 1939.
- [Wil73] K. G. Wilson, *Quantum field theory models in less than four-dimensions*, Phys. Rev. **D7**, 2911–2926 (1973).
- [WMAP03] D. N. Spergel et al. (WMAP Collaboration), *First Year Wilkinson Microwave Anisotropy Probe (WMAP) Observations: Determination of Cosmological Parameters*, Astrophys. J. Suppl. **148**, 175 (2003), [astro-ph/0302209](#).
- [Wom] J. Womersley, *The LHC physics program*, To be published in the proceedings of 20th International Workshop on Fundamental Problems of High-Energy Physics and Field Theory, Protvino, Russia, 24–26 Jun 1997.
- [XZC87] Z. Xu, D.-H. Zhang and L. Chang, *Helicity Amplitudes for Multiple Bremsstrahlung in Massless Non-Abelian Gauge Theories*, Nucl. Phys. **B291**, 392–428 (1987).
- [Y⁺00] F. Yuasa et al., *Automatic computation of cross sections in HEP: Status of GRACE system*, Prog. Theor. Phys. Suppl. **138**, 18–23 (2000), [hep-ph/0007053](#).
- [ZS98] A. Zoghbi and I. Stojmenović, *Fast Algorithms for Generating Integer Partitions*, Intern. J. Computer Math. **70**, 319–332 (1998).

Acknowledgements

I want to thank my supervisors Thomas Binoth and Tony Kennedy for their support and guidance during my postgraduate studies. Parts of the results of this work were achieved through the support of the **Golem** collaboration: Jean-Philippe Guillet took the main responsibility for the **Golem90** library, Alberto Guffanti and Jürgen Reuter calculated the real emission contribution of the $u\bar{u} \rightarrow b\bar{b}b\bar{b}$ amplitude and the generated the LO event files which served as an input for my integrated results.

Part of my research was accomplished at the LAPPTH in Annecy, the Fermilab in Batavia and the GGI in Florence; I wish to thank all three hosts for inviting me to their institutes, which offered an inspiring environment and great hospitality. I also want to thank the Scottish Universities Physics Alliance who founded my research through a studentship.

This work has made use of the resources provided by the Edinburgh Computing and Data Facility (ECDF)¹⁵. The ECDF is partially supported by the eDIKT initiative¹⁶.

The FEYNMAN diagrams in this thesis have been drawn using the **FeynMF** package [Ohl95].

¹⁵<http://www.ecdf.ed.ac.uk/>

¹⁶<http://www.edikt.org>

Index

- Smatrix, 17
- $(k)_n$, *see also* POCHHAMMER symbol
- Δ , **137**
- Δ_{ij}^μ , 62
- $F_J^{(N)}$, *see also* measurement function
- Ω_d , 94, **135**
- Π_\pm , **44**
- S_{ij} , **62**
- \mathcal{S}_k , *see also* symmetric group
- $c_{\mu\nu}^\lambda$, *see also* LITTLEWOOD-RICHARDSON coefficient
- δ_z , **63**, 68, 134
- f^λ , **32**
- γ_5 , 56–57
- γ_E , 56, **137**
- h_{ij} , *see also* hook number
- λ/μ , *see also* YOUNG tableau, skew
- $|p_\pm\rangle$, $\langle p_\pm|$, $\langle pq\rangle$, **44**
- q_i^μ , 61
- $[qp]$, 44
- r_Γ , **137**
- r_i^μ , 61
- $\text{sh}(Y)$, 31
- $\text{tr}^\pm\{\dots\}$, 45
- antisymmetriser, **30**
- ballot sequence, *see also* lattice word
- CHISHOLM identity, 58–59
- completeness relation, 24, 25
- conjugacy class, 28
- contract, programming by, 149
- cycle notation (permutations), **27**
- defining representation, *see also* representation
- dimensional regularisation, 56
 - axioms, 132–133
- double parton scattering, 76
- double-line notation, 22
- FEYNMAN
 - parameter, 79, 84, 127, **134**
 - rules, *see also* QCD, FEYNMAN rules
- FIERZ identity, 47
- GARNIR
 - relation, 34
- Gauge
 - axial, 92
- gauge
 - axial gauge fixing term, 11
 - covariant gauge fixing term, 11
 - FEYNMAN gauge, 11
- Generating function, 133
- GORDON identity, 47
- GRAM, 70–71
 - determinant, 61
 - matrix, **70**
- group algebra, 30
- group module, 29
- HIGGS mechanism, 1–2
- 'T HOOFT-VELTMAN
 - algebra, 56
 - scheme, 58
- hook number, 32
- Importance sampling, **109**
- integer partition, 28
- K -factor
 - local, **111**, 114
- LANDAU
 - pole, 13
- lattice word, 39
- Literate programming, 144
- literate programming, 144
- LITTLEWOOD-RICHARDSON
 - coefficient, 39
 - rule, 39
- MANDELSTAM variable, 85
- measurement function, 89
- MOORE-PENROSE pseudoinverse, **125**
- $\overline{\text{MS}}$, 56
- PENROSE pseudoinverse, *see also* MOORE-PENROSE pseudoinverse
- permutation
 - cycle notation, **27**
- POCHHAMMER
 - symbol, **130**
- polarisation vector

- for massive gauge bosons, 49
 - for massless gauge bosons, 47
- Pseudo-inverse, *see also* MOORE-PENROSE
 - pseudoinverse
- pseudorapidity, 118
- QCD, 10–13
 - FEYNMAN rules, 11
 - LAGRANGian density, 10
 - running coupling constant, 12
- RAMBO, 109–110
- recoupling relation, 24
- regularisation schemes, comparison, 61
- representation
 - defining, 30
 - $GL(N)$, 36–37
 - regular, 30
- Scattering matrix, 17
- SCHWINGER
 - parametrisation, **133**
- six- j symbol, 24
- spinor
 - helicity projection, 44
 - massive, 48
- Spinor helicity projections, 45
- standard model, 1–3
 - minimal supersymmetric, 4–5
- star-triangle relation, 20, **25**
- Stratified sampling, **108**
- SUDAKOV parametrisation, 92
- symmetric group, 27
- symmetriser, **30**
- Tableau, *see also* YOUNG tableau
- test-driven development, 152
- three- j symbol, 24
- transposition, 29
- unit test, *see also* test-driven development
- unweighted event, 111
- VEGAS, **109**
- WEYL-VAN DER WAERDEN representation, 22, **52**
- WICK rotation, **135**
- WICK rotation, 134
- YAMANOUCHI word, *see also* lattice word
- YOUNG
 - diagram, **29**
 - diagram, transposed, **29**
 - natural representation, **31**
 - projector, **32**
 - tableau, **31**
 - semi-standard, 32
 - skew, 39